The emergence of cooperation in spatial evolutionary games played on graphs

Mattie Susan Landman

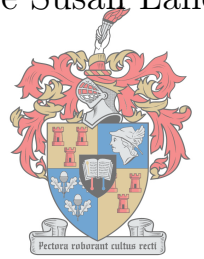

UNIVERSITEIT
iYUNIVESITHI
STELLENBOSCH
UNIVERSITY

Thesis presented in partial fulfilment of the requirements for the degree of
Master of (Industrial) Engineering
in the Faculty of Engineering at Stellenbosch University

Supervisor: Prof JH van Vuuren

December 2018

Declaration

By submitting this thesis electronically, I declare that the entirety of the work contained therein is my own, original work, that I am the sole author thereof (save to the extent explicitly otherwise stated), that reproduction and publication thereof by Stellenbosch University will not infringe any third party rights and that I have not previously in its entirety or in part submitted it for obtaining any qualification.

Date: December 2018

Abstract

The principle of cooperation pervades our society and the natural habitat in which we function. In the classic Darwinian framework of evolution, however, individuals rather tend to compete with one another because of a perceived fitness advantage, while cooperation requires altruistic behaviour. Hence, the emergence of cooperation is paradoxical. This leads to the following interesting question: How can cooperation emerge in a world of egoists without the interference of central authority?

In game theory, the well-known prisoner's dilemma is often employed as a simplified hypothetical context in which to study cooperation and the factors that enable its persistence. Past studies have shown that cooperation may be a viable strategy if the prisoner's dilemma is placed within an evolutionary framework. In evolutionary game theory, games are repeated and players with bounded rationality and limited knowledge of these games are given the opportunity to learn and adapt their strategies iteratively. In such a context, one mechanism that enables the persistence of cooperation is the structure of interaction between players.

A mathematical framework is proposed in this thesis for the prisoner's dilemma within an evolutionary game theoretic context, called the *Evolutionary Spatial Prisoner's Dilemma* (ESPD). This game is analysed on relatively simple graph structures in order to investigate the effect of various spatial player arrangements on the emergence of persistent cooperation.

More specifically, analytical means (void computer aid) are employed to establish conditions for, and the likelihood of, persistent cooperation among players of the ESPD on a circulant graph, a natural extension of a cycle for which an analysis of the ESPD has already been analysed. The objective is to determine how the extension of each player's cyclic neighbourhood affects the likelihood of persistent cooperation when players are arranged in a cyclic topology. It is found that as players extend the sizes of their neighbourhoods from two to four players, the probability of the emergence of persistent cooperation decreases.

A further analysis is carried out (this time with the aid of a computer) to investigate the conditions for, and the likelihood of, persistent cooperation in the ESPD on small toroidal grid graphs. The objective of this second analysis is to determine how the order of the underlying graph affects the likelihood of persist cooperation. It is found that for certain (pay-off value) parameter combinations, the probability of cooperation persisting increases as the order of the underlying graph increases, while for other parameter combinations this probability decreases.

Uittreksel

Die beginsel van samewerking deurgrond ons samelewing en die natuurlike habitat waarin ons funksioneer. In die klassieke evolusie-raamwerk van Darwin is individue egter eerder geneig om weens 'n oënskynlike fiksheidsvoordeel met mekaar te kompeteer, terwyl samewerking altruïstiese gedrag vereis. Daarom is die ontstaan van samewerking paradoksaal. Dit lei tot die volgende interessante vraag: Hoe kan samewerking in 'n wêreld van egoïste sonder die inmenging van 'n sentrale gesag ontstaan?

In speleteorie word die bekende gevangene se dilemma dikwels as 'n vereenvoudigde hipotetiese konteks gebruik om samewerking te bestudeer en die faktore wat die voortbestaan daarvan moontlik maak. Vorige studies het getoon dat samewerking 'n lewensvatbare strategie kan wees as die gevangene se dilemma in 'n evolusionêre raamwerk geplaas word. In evolusionêre speleteorie word spele herhaal en spelers met beperkte rasionaliteit en beperkte kennis van hierdie spele kry die geleentheid om strategieë iteratief te leer en aan te pas. In só 'n konteks is een meganisme wat die voortbestaan van samewerking moontlik maak, die struktuur van interaksie tussen spelers.

'n Wiskundige raamwerk word in hierdie tesis vir die gevangene se dilemma in 'n evolusionêre spelteoretiese konteks, bekend as die *Evolusionêre Ruimtelike Gevangene se Dilemma* (ERGD), daargestel. Hierdie spel word op relatief eenvoudige grafiekstrukture ontleed om die effek van verskillende ruimtelike speler-rangskikkings op die ontstaan van volgehoue samewerking te ondersoek.

In die besonder word analitiese tegnieke (sonder die gebruik van 'n rekenaar) ingespan om toestande vir en die waarskynlikheid van volgehoue samewerking tussen spelers van die ERGD op 'n sikulant-grafiek te bepaal, 'n natuurlike veralgemening van 'n siklus waarvoor 'n analise van die ERGD reeds uitgevoer is. Die doel is om te bepaal hoe die uitbreiding van elke speler se sikliese omgewing die waarskynlikheid van volgehoue samewerking beïnvloed wanneer spelers in 'n sikliese topologie gerangskik word. Daar word bevind dat soos spelers die groottes van hul omgewings van twee tot vier spelers uitbrei, die waarskynlikheid van die ontstaan van volgehoue samewerking verminder.

'n Verdere analise word uitgevoer (hierdie keer met behulp van 'n rekenaar) om die toestande vir en die waarskynlikheid van volgehoue samewerking in die ERGD op 'n klein toroidale roostergrafiek te ondersoek. Die doel van hierdie tweede analise is om vas te stel hoe die orde van die onderliggende grafiek die waarskynlikheid van volgehoue samewerking beïnvloed. Daar word bevind dat vir sekere (uitbetalingswaarde) parameterkombinasies, die waarskynlikheid van voortgesette samewerking toeneem namate die orde van die onderliggende grafiek toeneem, terwyl vir ander parameterkombinasies hierdie waarskynlikheid afneem.

Acknowledgements

The author wishes to acknowledge the following people and institutions for their various contributions towards the completion of this work:

- I wish to thank Prof Jan van Vuuren for his support and exceptional guidance throughout the project. I truly admire his patience, precision and unwavering effort to ensure that work of a high standard is delivered. Furthermore, his insight and passion for knowledge which are not confined to the field of this thesis is admirable.
- I wish to thank Dr Alewyn Burger for his time and advice in constructing the algorithms presented in this thesis.
- I wish to thank the SUnORE research group for their financial support in the form of a bursary as well as computer facilities and office space.
- I wish to thank my fellow SUnORE research group members for their continual assistance and support. I appreciate the experiences shared through many enjoyable social events.
- Finally, I wish to extend my deepest gratitude to my family and friends for their love, support, interest and prayers especially during the last few months.

Table of Contents

List of Acronyms

ESPD: Evolutionary spatial prisoner's dilemma

ESS: Evolutionary stable strategy

PD: Prisoner's dilemma

List of Figures

List of Tables

List of Algorithms

CHAPTER 1

Introduction

Contents

"The only thing that will redeem mankind is cooperation." — Bertrand Russel

1.1 Background

Not even Sherlock Holmes could have foreseen the mysterious events of Christmas eve 1914 — German and British soldiers meeting one another in the spirit of cooperation. During this historic event known as the *Christmas Truce*, roughly 100 000 soldiers, fighting in the western front-line trenches, exchanged seasonal greetings and sang Christmas carols together. In some areas, soldiers ventured into no man's land to exchange food, cigarettes and souvenirs with British and German soldiers alike. Accounts of the truce even describe football matches being played. The truce was not ubiquitous as fighting continued in many other sectors of the front-line. After the Christmas Truce, the High Commands on both sides attempted to prohibit further fraternisation during the war. Despite this, several incidents where soldiers deliberately ceased fire to repair trenches and gather dead soldiers continued to take place [1].

Cooperation is formally defined as the process by which groups of organisms work or act together in pursuit of a common or mutual benefit, as opposed to competing for selfish benefit. The words of Charles Darwin, in his *Descent of man* [12], reveal the significant affect of man's capacity to cooperate: "The small strength and speed of man, his want of natural weapons, are more than counterbalanced by his social qualities, which lead him to give and receive aid from his fellow-man." To Darwin, this ability to cooperate was man's competitive advantage in the survival of the fittest.

The emergence of cooperation may seem intuitive when it benefits all individuals involved in a direct manner. This natural intuition does not, however, extend to the case in which benefits are experienced in an indirect manner or when a greater benefit can be achieved through its exploitation, such as the example of the Christmas Truce during the First World War, which has baffled many philosophers and scientists. In the classical Darwinian framework, the emergence

and persistence of cooperation is paradoxical as cooperators have to succeed in the struggle for survival with defectors who, by definition, have a certain fitness advantage. Because of this paradoxical quality, the emergence and persistence of cooperation attracts attention when it occurs. Consequently, the question of interest becomes: Under what conditions will cooperation emerge in a world of egoists without central authority? A review of the related literature reveals that five main theories have been proposed in response to this question, namely the theories of *kin selection*, *direct reciprocity*, *indirect reciprocity*, *group selection* and *network reciprocity* [49].

Kin selection [23] is based on the idea that cooperation can emerge if the donor and recipient of an altruistic act are genetically related. More specifically, the cooperative behaviour is the consequence of a "selfish gene." The theory of *direct reciprocity* [70] assumes that encounters between individuals are repeated and individuals adopt the thinking strategy "if I cooperate now, you may cooperate later." Similarly, the theory of *indirect reciprocity* [54] is built upon the notion that observed acts of cooperation are discussed and stored within subsets of a population (likened to a collective memory). Consequently, helpful individuals are labelled accordingly and are thus more likely to receive help in the future. *Group selection* [69] employs the idea that competition is not between individuals but rather between groups. A population will therefore contain subsets of cooperators who then inherently compete against each other. The theory of *network reciprocity* [57] assumes that the structure of a population allows certain individuals to interact more often than others, thereby accepting responsibility for affecting the evolutionary and ecological dynamics of the population and allowing clusters of cooperation to form. Within the context of this thesis, network reciprocity is employed as underlying theory in order to study the emergence and persistence of cooperation from a mathematical perspective.

The mathematical analysis of the emergence and persistence of cooperation takes place in this thesis within a spatio-temporal framework and is the product of a synthesis between the fields of game theory and graph theory. Game theory is "the study of mathematical models of conflict and cooperation between intelligent rational decision-makers"[44], while graph theory facilitates a study of the mathematical structures when modelling pairwise relations between objects. Consequently, the evolution of cooperation is investigated in this thesis through the study of games on graphs. More specifically, an adaptation of the well-known classical *prisoner's dilemma* (PD) within game theory is adopted as the modelling paradigm in this thesis. Because an underlying population topology is assumed in combination with an ability of individuals to learn and adapt their strategies within the context of the PD, the particular game considered in this thesis is the *evolutionary spatial prisoner's dilemma* (ESPD).

A review of the academic literature reveals that the majority of research on the evolution of cooperation that employs the study of games on graphs has been conducted in a simulation environment. This general use of simulation modelling makes sense as it is the most intuitive approach when analysing the evolution of cooperation for a case-specific population structure. A more fundamental approach is, however, adopted in this thesis by studying the evolution of cooperation analytically on basic graph structures in order to contribute towards a general understanding of the effect that spatial factors have on the emergence and persistence of cooperation.

1.2 Problem description

In this thesis, the effect of the structure of the underlying topology of the ESPD on the evolution of cooperation is considered. More specifically, the two main research questions are:

1. In what manner does the size of every individual's neighbourhood (*i.e.* the number of game

interactions in which every individual partakes) affect the emergence and persistence of cooperation within a population?

2. In what manner does the order of the underlying graph affect the probability of emergence of persistent cooperation within a population?

The first research question is analysed in the context of the ESPD with an underlying cyclic topology. The second is analysed in the context of both the ESPD with an underlying cyclic topology and the ESPD with toroidal grids as underlying topology.

In order to analyse the emergence and persistence of cooperation, each case is studied analytically in two main stages: The strategy configurations that the players of a game can exhibit are first enumerated, after which a characterisation and enumeration follow of all states that allow for cooperation to persist. This allows for the estimation of the likelihood of the emergence of persistent cooperation.

1.3 Thesis scope

The scope of this thesis is limited to the modelling of pairwise cooperation in the context of the PD. This well-known analogy employed to investigate the likelihood of the emergence of persistent cooperation is well-suited to the purpose of this thesis. More specifically, the analogy represents a very basic form of interaction between two entities within which cooperation may manifest itself. The simplified type of interaction is fitting of the manner in which the fundamental dynamics underlying the mechanisms of cooperation are investigated in this thesis. Furthermore, the PD is contextualised in a spatio-temporal framework known as the ESPD. Only instances of the ESPD with isomorphic interaction and updating structures, as well as deterministic updating rules, are considered. On a more practical note, the work presented in this thesis builds upon the work of Burger *et al.* [10, 11] and Van der Merwe [72].

As a fundamental understanding of the influence of spatial structure on the evolution of cooperation is pursued in this thesis, only analytical techniques (*i.e.* excluding simulation modelling) are employed in investigations of the game dynamics of the ESPD. Nowak [54] remarked "Games on graphs are easy to study by computer simulations, but they are difficult to analyse mathematically because of the enormous number of possible configurations." Due to the complexity of the analysis, the thesis is limited to the study of two relatively simple underlying graph topologies:

The *ESPD with the circulant $C_n\langle 1, 2\rangle$ as underlying graph.* The game dynamics of the ESPD with the cycle C_n of order n as underlying graph has previously been studied by Burger *et al.* [10]. The extension of each player's cyclic neighbourhood from size two to four is considered in this thesis when players are still arranged according to a cyclic topology.

The *ESPD with the toroidal grid as underlying graph.* Only *small* toroidal grid graphs (of dimensions at most 6×6) are considered in this thesis.

No other underlying graph topologies are considered in this thesis due to time and space constraints. It is, however, anticipated that the modelling framework adopted and techniques employed may be applicable to the analysis of other underlying graph topologies.

1.4 Research objectives

The following six objectives are pursued in this thesis:

I To *conduct* a thorough survey of the literature related to the ESPD on various underlying graph structures.

II To *establish* a mathematical model capable of capturing the emergence and persistence of cooperation on various small, relatively simple, underlying graph structures.

III To analyse the likelihood that cooperation will persist in the long run in the ESPD with the circulant $C_n\langle 1, 2\rangle$ as underlying graph.

IV To compare the results obtained in pursuit of Objective III with the likelihood that cooperation will persist in the ESPD with a cycle as underlying graph, as reviewed from the literature.

V To *analyse* the likelihood that cooperation will persist in the long run in the ESPD with a small toroidal grid structure as underlying graph.

VI To *recommend* sensible follow-up work related to the work of this thesis which may be pursued in future.

1.5 Thesis organisation

Apart from this introductory chapter, this thesis contains a further six chapters, a bibliography and four appendices. Chapter 2 is devoted to a review of certain mathematical prerequisites for following the arguments presented later in this thesis. First basic graph theoretic notions are reviewed, and this is followed by a discussion on basic group theoretic notions.

The third chapter of this thesis is devoted to a brief review of the literature related to the ESPD. The chapter opens with a review of central notions in classical game theory, and this is followed by a brief history of developments in the field. Important concepts and terminology related to the analysis of games are then presented. This is followed by the brief review of well-known variations of two-person symmetric games and strategies that determine their game dynamics. The focus of the chapter then shifts to evolutionary game theory where important concepts and developments within that particular field are presented. A particular emphasis is placed on the literature related to spatial evolutionary games and the various methods that have been adopted in the literature to analyse the evolution of cooperation in that context, either adopting a numerical approach, an analytical approach or other less conventional approaches.

In the fourth chapter, a mathematical framework for modelling games on graphs is established. This includes the various rules which govern the dynamics of the ESPD. The notion of a state graph is then introduced as a visual representation tool of game dynamics. The construction of a pay-off parameter phase plane is finally described in order to allow for the identification of the various parameter regions which may lead to fundamentally different game dynamics.

The effect of players extending their cyclic neighbourhoods when arranged according to a cyclic topology on the game dynamics of the ESPD is investigated in Chapter 5. A brief overview of the analysis of the ESPD game dynamics with a cycle as underlying graph is first reviewed from the literature. Analytical means (void computer aid) are then employed to analyse the dynamics of the ESPD with the circulant $C_n\langle 1, 2\rangle$ as underlying graph. This entails a characterisation and

an enumeration of the possible equilibrium states of the ESPD, followed by an investigation into the likelihood of the emergence of persistent cooperation. The analysis is only fully presented for a single phase plane parameter region (but the entire analysis for the remaining parameter regions can be found in the first three appendices). The chapter closes with a comparison of the analyses of the game dynamics of the ESPD with a cycle as underlying graph with that of the ESPD with the circulant as underlying graph, in order to determine the effect of players extending their cyclic neighbourhoods on the evolution of cooperation.

The dynamics of the ESPD with a small toroidal grid as underlying graph is investigated in Chapter 6. Analytical means together with computer aid are employed throughout the chapter. The chapter opens with a mathematical motivation for the need of computer aid due to the inherent combinatorial explosion in the analysis. Because of this inherent combinatorial complexity, a new analysis visualisation tool, called the equilibrium state diagram, is proposed to replace the state graph for larger toroidal grid dimensions during analyses of ESPD game dynamics. Various algorithms are proposed (and their implementation discussed) for the construction of the equilibrium state diagrams. Equilibrium state diagrams are then computed for the ESPD with the eleven underlying toroidal grids of dimensions 2×6, 3×3, 3×4, 3×5, 3×6, 4×4, 4×5, 4×6, 5×5, 5×6 and 6×6. Only the equilibrium state diagram for a validation case (the ESPD on a 3×3 toroidal grid graph, previously analysed by Van der Merwe [72]) is presented in the chapter, while the remaining equilibrium state diagrams are presented in the fourth appendix. In each case, the number of components in the equilibrium state diagrams are enumerated, and this is followed by an investigation of the likelihood of persistent cooperation emerging. A collective analysis of the ability of a small toroidal grid to facilitate the emergence of persistent cooperation in the ESPD is finally presented.

The contributions of the thesis are summarised in Chapter 7, and this summary is followed by an appraisal of these contributions. Possible avenues for future research related to the work presented in this thesis are finally suggested.

CHAPTER 2

Mathematical prerequisites

Contents

The first section of this chapter is devoted to a review of basic notions from the realm of graph theory. The second section contains a brief review of various basic notions from the realm of group theory, with particular emphasis on the Cauchy-Frobenius lemma which is used extensively for enumeration purposes later in this thesis.

2.1 Graph theoretic prerequisites

This section contains descriptions of basic notions in graph theory that are required for an understanding of the work presented later in this thesis. The definitions and terminology adopted conform to those in [26], unless otherwise stated.

2.1.1 A graph and its properties

A *graph* G is a finite, non-empty *vertex set* $V(G)$ together with a finite, possibly empty *edge set* $E(G)$, where each edge is a set of (unordered) pairs from $V(G)$. The number of vertices in a graph G is called its *order* and is denoted by $n(G)$, whereas the number of edges in G is called its *size* and is denoted by $m(G)$. Therefore, $n(G) = |V(G)|$ and $m(G) = |E(G)|$. The standard form of graphical representation of a graph is illustrated in Figure 2.1(a); each vertex is represented by a point and each edge by a line or curve.

Two vertices u and v are *adjacent* if they are joined by an edge $e = \{u, v\}$. In this case, the vertex u is *incident* with the edge e, and similarly for v and e. Two distinct edges, e_1 and e_2 are *adjacent* if they are incident with a common vertex.

The *complement* $\overline{G}$ of a graph G is a graph with vertex set $V(\overline{G}) = V(G)$ and for which the edge set $E(\overline{G})$ contains all two-element subsets $\{u, v\}$ from $V(G)$ that are not contained in $E(G)$. The complement of the graph $G_{2.1}$ in Figure 2.1(a) is shown in Figure 2.1(b). A graph H is a *subgraph* of a graph G if $V(H) \subseteq V(G)$ and $E(H) \subseteq E(G)$. A *spanning subgraph* of G is a subgraph of G which contains all the vertices in $V(G)$.

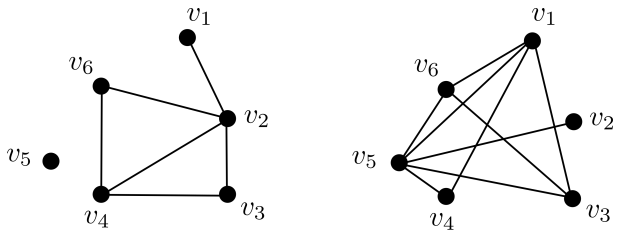

(a) $G_{2.1}$ (b) $\overline{G}_{2.1}$

FIGURE 2.1: *A graph $G_{2.1}$ and its complement $\overline{G}_{2.1}$.*

The *degree* of a vertex v is the number of vertices adjacent to it, denoted by $d(v)$. The minimum and maximum degree over all the vertices in a graph G is denoted by $\delta(G)$ and $\Delta(G)$, respectively. The parity of the degree of a vertex determines whether it is *odd* or *even*. The *open neighbourhood* $N(v)$ of a vertex v is the set of vertices adjacent to v, defined by $N(v) = \{u \in V(G) \mid uv \in E(G)\}$. The *closed neighbourhood* of a vertex v is its open neighbourhood set together with the vertex v itself, denoted by $N[v] = N(v) \cup \{v\}$. Therefore, the size of the open neighbourhood of a vertex is its degree. To elucidate, consider the vertex v_3 in the graph $G_{2.1}$ of Figure 2.1(a). Its open neighbourhood is $N(v_3) = \{v_2, v_4\}$ and hence its degree is $d(v_3) = 2$, while its closed neighbourhood is $N[v_3] = \{v_2, v_3, v_4\}$.

The *degree distribution* $P(k)$ of a graph is a function indicating the probability that a randomly selected vertex of the graph has the degree k. The graph $G_{2.1}$, for example, has degree distribution

$$P(k) = \begin{cases} \frac{1}{6} & \text{if } k = 0 \\ \frac{1}{6} & \text{if } k = 1 \\ \frac{2}{6} & \text{if } k = 2 \\ \frac{1}{6} & \text{if } k = 3 \\ \frac{1}{6} & \text{if } k = 4. \end{cases}$$

An *edge-weighted graph* is a graph G in which each edge e is assigned a positive real number, called the weight of e and denoted by $w(e)$. Similarly, a *vertex-weighted graph* is a graph in which each vertex v is assigned a weight, denoted by $w(v)$. Examples of an edge-weighted graph and a vertex-weighted graph are shown in Figure 2.2.

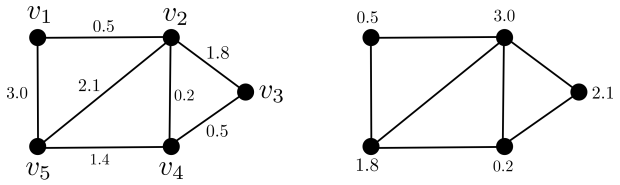

(a) $G_{2.2}$ (b) $G_{2.3}$

FIGURE 2.2: *(a) An edge-weighted graph $G_{2.2}$ and (b) a vertex-weighted graph $G_{2.3}$.*

The *cartesian product* $G = G_1 \times G_2$[1] of two graphs G_1 and G_2 is a graph with vertex set $V(G) = V(G_1) \times V(G_2)$ in which the vertex set (u_1, u_2) is adjacent to (v_1, v_2) if and only if

[1]The cartesian product of two graphs G_1 and G_2 is also commonly denoted by $G_1 \square G_2$. In this thesis, however, the older notation $G_1 \times G_2$ is adopted.

either $u_1 = v_1$ and $u_2v_2 \in E(G_2)$, or $u_2 = v_2$ and $u_1v_1 \in E(G_1)$. An example of the cartesian product of two graphs is illustrated graphically in Figure 2.3.

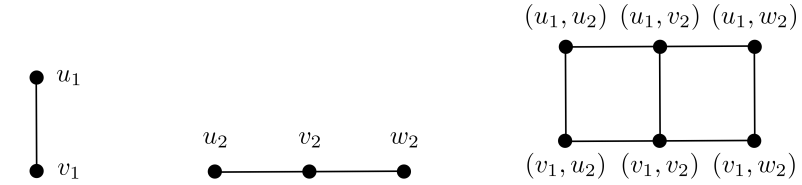

(a) $G_{2.4}$ (b) $G_{2.5}$ (c) $G_{2.4} \times G_{2.5}$

FIGURE 2.3: *The cartesian product of two graphs $G_{2.4}$ and $G_{2.5}$.*

2.1.2 Connectivity

A v_0-v_n *walk* in a graph G is an alternating sequence of vertices and edges $v_0, e_1, v_1, e_2, \ldots, v_{n-1}, e_n, v_n$ beginning with the vertex v_0 and ending with vertex v_n, such that $e_i = v_{i-1}v_i \in E(G)$ for all $i = 1, \ldots, n$. A walk is *even* if its length is even, or else it is *odd*. Edges and vertices may be repeated in a walk. The number of (not necessarily distinct) edges in a walk is called the *length* of the walk. If $v_0 = v_n$, then the walk is *closed*; otherwise it is *open*. A *trail* is a walk in which no edges are repeated, while a *path* is a walk in which no vertices are repeated. A cycle is a closed path containing at least three vertices. A graph is called *acyclic* if it contains no cycles as subgraphs. In the case of an edge-weighted graph, however, the length of a walk, path or trail is the sum of the edge weights in the corresponding walk, path or trail.

A graph G is *connected* if there exists a path between every pair of its vertices. A graph that is not connected is called *disconnected*. A disconnected graph consists of maximal connected subgraphs, called *components*. The number of components of G is denoted by $k(G)$. A connected graph G has a single component, and so $k(G) = 1$ in this case. The distance $d(u, v)$ between two vertices u and v in a connected graph is the length of the shortest u-v path in the graph.

2.1.3 Digraphs, multigraphs and pseudographs

A directed graph, or *digraph*, D is a graph in which each edge is directed from one vertex to another. Such directed edges are called *arcs*. A digraph therefore consists of a vertex set $V(D)$ and an arc set $E(D)$ containing *ordered* pairs of vertices. The order of D is $|V(D)|$, while its size is $|E(D)|$. An arc (u, v) is represented graphically by means of an arrow, with its tail at the vertex u and its head at the vertex v. The *outdegree* $\mathrm{od}(v)$ of a vertex v is the number of tails incident with the vertex, while the *indegree* $\mathrm{id}(v)$ of a vertex v is the number of heads incident with the vertex. The *degree* of a vertex in a digraph is the sum of its outdegree and its indegree, *i.e.* $d(v) = \mathrm{od}(v) + \mathrm{id}(v)$.

Each digraph D is associated with an *underlying graph*. The associated underlying graph is obtained by removing the directions of all the arcs from the digraph, as well as all multiple edges that may thus arise between pairs of vertices. A digraph and its underlying graph therefore have the same vertex set. An example of a digraph together with its associated underlying graph is shown in Figure 2.4.

A digraph D is *symmetric* if, for every arc (u, v) in D, the arc (v, u) is also present in D. A digraph D is *asymmetric* if, for every arc (u, v) in D, there is no arc (v, u) in D. The digraph

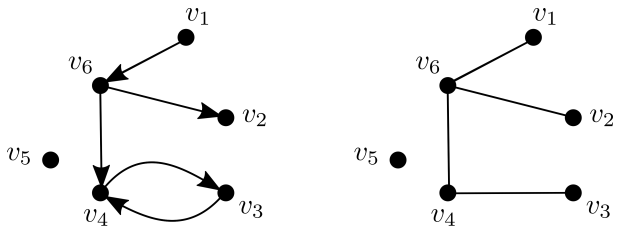

(a) $D_{2.1}$ (b) $G_{2.6}$

FIGURE 2.4: *(a) A digraph $D_{2.1}$ and (b) its associated underlying graph $G_{2.6}$.*

$D_{2.1}$ in Figure 2.4 is therefore neither symmetric nor asymmetric.

A *multigraph* is graph in which there is more than one edge between some pair of vertices. The various edges that join the same pair of vertices are called *parallel edges*. An edge that joins a vertex to itself is called a *loop*. A *pseudograph* is a graph containing at least one loop. If a graph contains both parallel edges and loops it is both a multigraph and a pseudograph. A pseudodigraph is a pseudograph in which the edges are directed. Examples of a multigraph, a pseudograph and a pseudodigraph are shown in Figure 2.5.

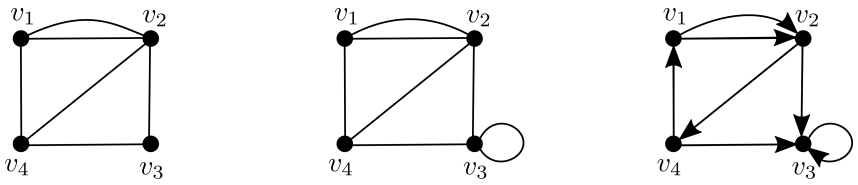

(a) $G_{2.7}$ (b) $G_{2.8}$ (c) $D_{2.2}$

FIGURE 2.5: *(a) A multigraph $G_{2.7}$, (b) a pseudograph $G_{2.8}$ and (c) a pseudodigraph $D_{2.2}$.*

A digraph D of order n can be represented in terms of an $n \times n$ *adjacency matrix* $\boldsymbol{A}$ in which the entry in row i and column j is $A_{ij} = 1$ if (v_i, v_j) is an element of $E(D)$, or $A_{ij} = 0$ otherwise. The adjacency matrix can then be used to calculate various metrics of the degree of connectivity of the digraph. Two of these measures are used extensively throughout this thesis. First, in order to enumerate the walks of a certain length within a digraph, the following theorem (whose proof can be found in [65, Theorem 4.7.1] may be used.

Theorem 1. *Let $\boldsymbol{A}$ be the $n \times n$ adjacency matrix of a digraph D of order n with vertex set $V(D) = \{v_1, \ldots, v_n\}$. Then the entry in row i and column j of the matrix power $\boldsymbol{A}^k$ is the number of v_i-v_j walks of length k in D.*

The following extension of Theorem 1 allows for the enumeration of the closed walks of a certain length within a digraph. The proof of this extension can be found in [65, Theorem 4.7.3].

Theorem 2. *Let $\boldsymbol{A}$ be the adjacency matrix of a digraph D and let $C_D(k)$ be the number of closed walks of length k in D. Then*

$$\sum_{k \geq 1} C_D(k) x^k = \frac{-xQ'(x)}{Q(x)},$$

where $Q(x) = \det(\boldsymbol{I} - x\boldsymbol{A})$.

2.1.4 Trees

A *tree* is a connected graph which contains no cycles, while a *forest* is a graph without cycles. Each component of a forest is therefore a tree. A *directed tree* is a digraph for which the underlying graph is a tree. A *rooted tree* is a directed tree in which one vertex is designated the *root* and which has the property that there exists a unique (directed) path from the root to each vertex in a rooted tree [26]. A vertex of degree one in a tree is called a *leaf*.

An example of a rooted tree is illustrated graphically in Figure 2.6. The vertex set of the tree has been partitioned into levels. The number of each level corresponds to the distance from the root of the tree to each vertex in the level. The *height* of the tree is the largest numbered level of the tree and hence the longest distance between the root and a vertex in the tree. The height of the rooted tree $T_{2.1}$ in Figure 2.6 is $h = 4$.

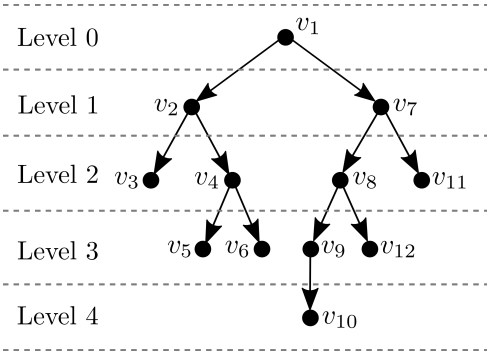

FIGURE 2.6: *Graphical representation of a rooted tree* $T_{2.1}$.

If T is a rooted tree and $u, v \in V(T)$, then v is called the *parent* of u if there exists an arc from v to u in T. In that case, u is then called a *child* of v. A vertex u is a *descendant* of a vertex v if there exists a directed v-u path in T. In such a case, u is called an *ancestor* of v in T. To elucidate, consider the rooted tree $T_{2.1}$ in Figure 2.6. In this case, v_1 is the parent of v_2, while v_2 is a child of v_1. Furthermore, v_2 is an ancestor of v_6, which is one of its descendants.

2.1.5 Isomorphisms

Two graphs G_1 and G_2 are *isomorphic* if they have the same order and there exists a permutation ϕ from $V(G_1)$ onto $V(G_2)$, such that $uv \in E(G_1)$ if and only if $\phi(u)\phi(v) \in E(G_2)$. An isomorphism between two graphs G_1 and G_2 is denoted by $G_1 \simeq G_2$. If there is no isomorphism between two graphs G_1 and G_2, then this fact is denoted by $G_1 \ncong G_2$. An isomorphism between a graph G and itself is called an *automorphism* of G. A *vertex-transitive* graph is a graph G in which, for any two vertices $v_1, v_2 \in V(G)$, there exists an automorphism ϕ of G such that $\phi(v_1) = v_2$. The notion of graph isomorphism is illustrated in Figure 2.7.

2.1.6 Special graphs

The most common graphs used to model games on graphs are reviewed in this section. Emphasis is placed on the classes of graphs that are central to the work presented later in this thesis, which are the circulant graphs and grid graphs.

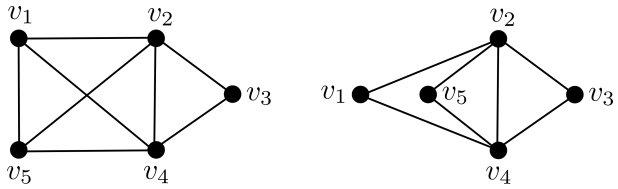

(a) $G_{2.9}$ (b) $G_{2.10}$

FIGURE 2.7: *(a) A graph $G_{2.9}$ and (b) a graph $G_{2.10}$ isomorphic to $G_{2.9}$.*

A *path* graph P_n is a graph of order $n \geq 2$ whose vertices can be listed as $v_1, v_2, \ldots, v_n$ in such a manner that each edge of the graph has the form $e_i = \{v_i, v_{i+1}\}$ for some $i \in \{1, \ldots, n-1\}$. Each path therefore contains two terminal vertices (leaves) of degree one and $n-2$ vertices of degree two. A *cycle* graph C_n is a graph of order n consisting of a single cycle. A cycle graph therefore contains n edges and every vertex has degree 2. Examples of path and cycle graphs are illustrated graphically in Figure 2.8.

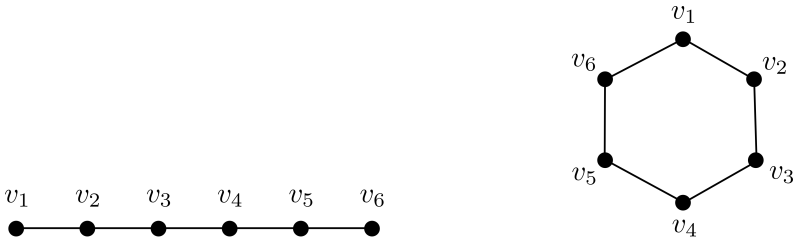

(a) P_6 (b) C_6

FIGURE 2.8: *(a) The path graph P_6 and (b) the cycle graph C_6.*

An *r-regular* graph is a graph G such that $d(v) = r$ for every vertex $v \in V(G)$. An example of a 3-regular graph $G_{2.11}$ is shown in Figure 2.9(a). A *complete* graph is a graph G in which every pair of distinct vertices is adjacent. A complete graph of order n is denoted by K_n. The complete graph K_6 is depicted in Figure 2.9(b). Note that each vertex in K_6 has degree 5. In general, K_n is an $(n-1)$-regular graph. An *empty* graph is a graph containing no edges. Such a graph of order n is denoted by $\overline{K}_n$. The graph $\overline{K}_6$ is illustrated graphically in Figure 2.9(c).

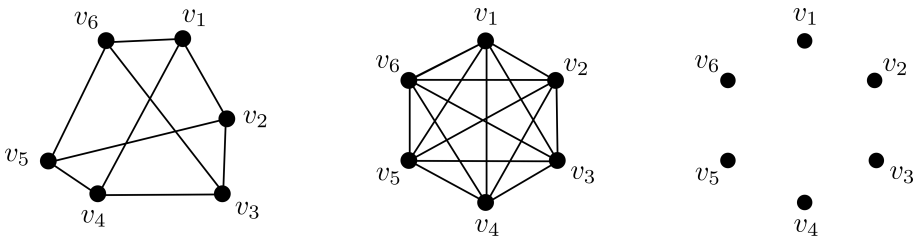

(a) $G_{2.11}$ (b) K_6 (c) $\overline{K}_6$

FIGURE 2.9: *(a) A 3-regular graph $G_{2.11}$, (b) the complete graph K_6 and (c) the empty graph $\overline{K}_6$.*

A *k-partite graph* is a graph whose vertex set can be partitioned into $k \geq 2$ disjoint subsets $V_1, \ldots, V_k$, called *partite sets*, so that no two vertices of the same partite set are adjacent. Such

a graph is denoted by $K_{n_1,\ldots,n_k}$ where $n_i = |V_i|$, for all $i \in \{1,\ldots,k\}$. If $k = 2$, the graph is called a *bipartite graph*. A *complete k-partite graph* is a k-partite graph in which each vertex in V_i is adjacent to *every* other vertex that is not in V_i, for all $i \in \{1,\ldots,k\}$. The complete bipartite graph $K_{3,5}$ is depicted in Figure 2.10(a). If all partite sets have equal size, ℓ (say), then the graph is called a *complete balanced k-partite graph* and is denoted by $K_{k\times\ell}$. The complete balanced 3-partite graph $K_{3\times3}$ is illustrated in Figure 2.10(b).

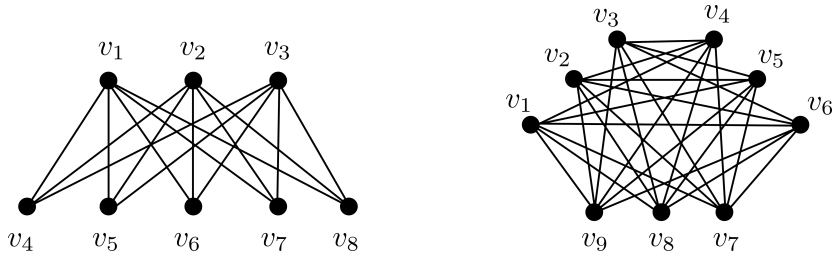

(a) $K_{3,5}$ (b) $K_{3\times3}$

FIGURE 2.10: *(a) The complete bipartite graph $K_{3,5}$ and (b) the complete balanced 3-partite graph $K_{3\times3}$.*

A *circulant* graph is a graph of order n in which the i^{th} vertex is adjacent to the $(i+j)^{th}$ and $(i-j)^{th}$ graph vertices for each j in a so-called *connection set*. A circulant graph of order n with connection set $\{j_1,\ldots,j_k\} \subseteq \{1,\ldots,\lfloor\frac{n}{2}\rfloor\}$ is denoted by $C_n\langle j_1,\ldots,j_k\rangle$.

An *elementary circulant*, is a circulant graph in which the connecting set contains only a single entry (*i.e.* $k = 1$). Otherwise, the circulant graph is called a *composite circulant*. A *singular circulant* is a circulant in which both n is even and the connection set contains the entry $j = \frac{n}{2}$. If n is even and the connection set does not contain $\frac{n}{2}$, or n is odd, then the circulant graph is called a *non-singular circulant*.

The elementary, singular circulant $C_8\langle4\rangle$ and the composite, singular circulant $C_8\langle1,3,4\rangle$ are illustrated graphically in Figures 2.11(a) and 2.11(b), respectively. Note that the cycle C_n is therefore isomorphic to the circulant $C_n\langle1\rangle$. The circulant $C_8\langle1\rangle \simeq C_8$ is illustrated graphically in Figure 2.11(c). The complete graph K_n is furthermore isomorphic to the circulant $C_n\langle1,\ldots,\lfloor\frac{n}{2}\rfloor\rangle$. The composite, non-singular circulant $C_n\langle1,2\rangle$ is considered extensively in this thesis and therefore the circulant $C_8\langle1,2\rangle$ is depicted in Figure 2.11(d).

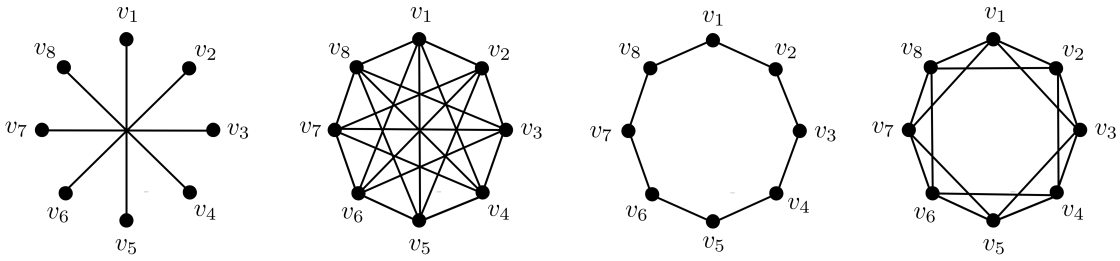

(a) $C_8\langle4\rangle$ (b) $C_8\langle1,3,4\rangle$ (c) $C_8\langle1\rangle$ (d) $C_8\langle1,2\rangle$

FIGURE 2.11: *Examples of circulant graphs of order 8. The circulant graphs in (a) and (c) are elementary, while the circulant graphs in (b) and (d) are composite. Furthermore, the circulant graphs in (a) and (b) are singular, while the circulant graphs in (c) and (d) are non-singular.*

A *lattice* is a regular grid-like structure which can be represented by an arrangement of points in a regular periodic pattern. The points of a lattice may be seen as representative of unit cells of various shapes, such as squares, rectangles or hexagons. A graph corresponding to a lattice structure can be constructed by placing a vertex in the centre of each unit cell, representing that unit cell. Two vertices are then adjacent in the graph representation if the corresponding unit cells share a common border. A lattice graph resulting from a square unit cell is shown in Figure 2.12(a). Similarly, the resulting triangular grid graph emanating from a hexagonal unit cell is shown in Figure 2.12(b).

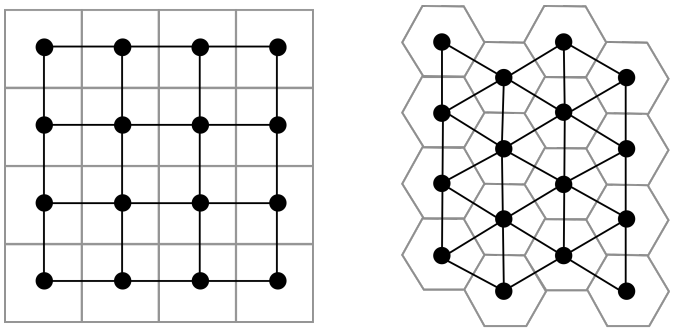

(a) (b)

FIGURE 2.12: *Examples of two lattice graphs. (a) A square grid graph over a square tiling landscape and (b) a triangular grid graph over a hexagonal tiling landscape.*

A lattice with vertices arranged in a rectangular array is often referred to as a *grid graph* or a *mesh*. Within this thesis, a grid graph is the main lattice structure analysed in the context of modelling games on graphs. More formally, a grid graph is the Cartesian product of a path graph of order n and a path graph of order m, denoted by $P_n \times P_m$. A path is therefore a grid graph of dimension $n \times 1$ while a grid of dimension 2×2 is a cycle of order 4. The vertices in a grid graph $P_n \times P_m$ may be associated with integer coordinates (x, y), where $x = \{1, \ldots, n\}$ and $y = \{1, \ldots, m\}$, and where two vertices are joined by an edge whenever the corresponding points are at a distance of one in $\mathbb{R}^2$. All grid graphs are also bipartite graphs. This can be verified by the fact that one can colour the vertices in a checkerboard fashion.

A grid graph can also be embedded on a torus. A toroidal grid can be constructed from a plane grid by "gluing" both pairs of opposite sides together without twisting. In this way an ordinary torus with a single "hole" results. An example of a grid and its corresponding toroidal embedding is shown in Figure 2.13. A toroidal grid graph is therefore often also referred to as a grid graph with wrapping. More formally, a toroidal grid graph is a Cartesian product of a cycle graph of order n and a cycle graph of order m, denoted by $C_n \times C_m$.

2.1.7 Complex graph types

Various complex graph topologies have been classified according to their characteristic *clustering coefficients* and *path lengths*. According to this classification, a graph can mainly be classified as either a homogeneous graph, a random graph, a scale-free network or a small-world network. These various graph models have received significant attention in the literature during attempts at modelling games on graphs and are reviewed briefly in this section. More specifically, the classification merits are outlined and each graph class is elucidated together with its associated properties.

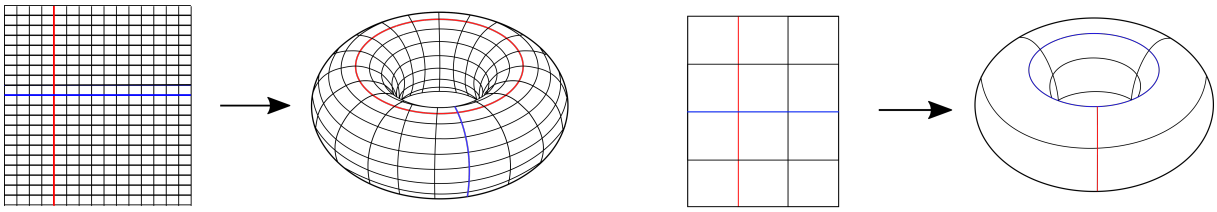

(a) $C_{20} \times C_{15}$ (b) $C_3 \times C_4$

FIGURE 2.13: *Examples of grid graphs and their embeddings on a torus. The red and blue lines are shown on both graph representations to elucidate the concept of wrapping that emerges from the initial plane embeddings.*

The *clustering coefficient* is a graph characteristic which measures the tendency of the vertices of the graph to cluster together. The *local clustering coefficient* $\mathcal{C}_v$ of a vertex v is the number of edges that occur between the vertices in the open neighbourhood of v, normalised by dividing by the maximum number of edges that can possibly exist between the vertices in its open neighbourhood [8]. That is,

$$\mathcal{C}_v = \frac{2|\{e_{uw} \mid v_u, v_w \in N_v,\ e_{uw} \in E(G)\}|}{d_v(d_v - 1)},$$

where d_v is the degree of the vertex v. The local clustering coefficient measures the ability of the neighbourhood of a vertex to form a complete subgraph. The *average clustering coefficient* $\overline{\mathcal{C}}_G$ of a graph G is obtained by averaging the *local clustering coefficients* of all its vertices [8]. That is,

$$\overline{\mathcal{C}}_G = \frac{1}{|V(G)|} \sum_{v \in V(G)} \mathcal{C}_v.$$

The *characteristic path length* $\mathcal{L}_G$ of a graph G is the average distance between pairs of vertices, taken over all vertex pairs in G.

The first complex graph type mentioned above was a *homogeneous graph*. A homogeneous graph is a graph which is regular or is very close to regular and therefore has a homogeneous degree distribution. The graph exhibits a low level of randomness (and the probability that any two randomly chosen vertices are adjacent is typically very low). Such a graph is characterised by long characteristic path lengths and high clustering coefficient values. Regular lattices, as well as trees, are examples of homogeneous graphs.

A *random graph*, also known as a *random ER (Erdos-Renyi) network*, is a graph constructed by starting with a disconnected set of vertices that are successively paired with a uniform probability. The degree distribution of such a graph follows the binomial distribution [5]. A random graph typically has a short characteristic path length and a small clustering coefficient.

Many real-world networks, especially social networks, exhibit some of the characteristics of *homogeneous graphs* and some of the characteristics of *random graphs*. Therefore, two alternative network models combining the properties of the aforementioned complex graph types have been developed, namely those of *small-world networks* and *scale-free networks*. These graph topologies have attracted a large amount of attention in the literature [15, 8, 77, 5].

A *small-world network* is formally defined as a graph whose geodesic distance (*i.e.* the minimum number of edges that must be traversed to travel from a starting vertex to a destination

vertex) between vertices increases at a rate slower than the logarithm of the number of vertices in the graph. Therefore, a small-world network is typically highly clustered, yet exhibits a small characteristic path length. A graph is considered a small-world network if its average clustering coefficient is significantly larger than that of a regular graph if both graphs were to contain the same vertex set. Small-world networks are structurally very close to many real-world social networks. This type of graph was introduced simultaneously with so-called *small-world phenomena*, popularly referred to as *six degrees of separation* (the property that in the social network of the world, any person is linked to any other person by an average of six intermediaries [5]).

A *scale-free network* is a connected graph whose degree distribution follows the power law $P(k) \sim k^{-\lambda}$, where $P(k)$ denotes the probability that a randomly selected vertex in the graph has degree k. The graph is called scale-free because zooming in on any part of the distribution does not affect its shape. A scale-free network can be constructed by progressively adding vertices to a graph with preferential attachment so that edges are constructed between newly added vertices and existing vertices with probabilities proportional to the number of edges incident with the existing vertices. Examples of scale-free networks include the topologies of web page inter-connection, the academic citation network and the power grid of the western United States [5].

2.2 Group theoretic prerequisites

A number of basic notions from group theory are reviewed in this section, so as to facilitate an understanding of the enumeration material presented in the remainder of this thesis. The primary sources of definitions and concepts in this section are [39, 65].

2.2.1 A group and its properties

A group is a set $\mathcal{G}$ together with a binary operation $\circ : \mathcal{G} \times \mathcal{G} \mapsto \mathcal{G}$ (*i.e.* the mapping of an ordered pair of elements of $\mathcal{G}$ to some other element in $\mathcal{G}$) that satisfies the following four axioms:

1. *The closure property:* $g_1 \circ g_2 \in \mathcal{G}$ for any pair $g_1, g_2 \in \mathcal{G}$;
2. *The associative property:* $g_1 \circ (g_2 \circ g_3) = (g_1 \circ g_2) \circ g_3$ for all $g_1, g_2, g_3 \in \mathcal{G}$;
3. *The existence of an identity element:* there exists a unique identity element $\iota \in \mathcal{G}$ such that $g \circ \iota = \iota \circ g = g$ for any $g \in \mathcal{G}$; and
4. *The existence of inverses:* for every element $g \in \mathcal{G}$ there exists a unique element of $\mathcal{G}$, denoted by g^{-1}, such that $g \circ g^{-1} = g^{-1} \circ g = \iota$.

The *order* of $\mathcal{G}$, denoted by $|\mathcal{G}|$, is the number of elements contained in $\mathcal{G}$. The order n of an element $g \in \mathcal{G}$ is the smallest natural number n for which $g^n = \iota$, if such a number exists[2]. If such a number does not exist, then g is said to have infinite order. From Lagrange's well known theorem (for which a proof can be found in [39, Corollary on p.78]) for a finite group g, the order of each element $g \in \mathcal{G}$ is a factor of $|\mathcal{G}|$.

[2]Here the notation g^n is shorthand for $g \circ g \circ g \circ \ldots \circ g$ (that is, the combination of $n-1$ instances of the binary operations $\circ$).

2.2.2 Symmetry groups and equivalence classes

The notion of symmetry groups and equivalence classes are described in this section within the context of two-dimensional euclidean geometry.

A *homomorphism* μ is a mapping from a group $\mathcal{G}$ to a group $\mathcal{G}'$ which transforms compositions into compositions. That is, for every pair of elements $g_1, g_2 \in \mathcal{G}$ there are associated elements $\mu(g_1), \mu(g_2) \in \mathcal{G}'$ such that $\mu(g_1 \circ g_2) = \mu(g_1) \circ \mu(g_2)$. A homomorphism therefore maps one group to another and preserves group structure (it may be thought of as the group analogy of a linear transformation on a vector space). A homomorphism which is a 1-1 mapping and in which $\mu(\mathcal{G}) = \mathcal{G}'$ is called an *isomorphism*. An isomorphism $\mu : \mathcal{G} \mapsto \mathcal{G}$ of a group $\mathcal{G}$ onto itself is called an *automorphism*. A special case of an isomorphism is an *isometry*, which is defined on a metric space[3] and preserves distances. That is, if μ is an isometry, then, $||\mu(\boldsymbol{v}_1) - \mu(\boldsymbol{v}_2)|| = ||\boldsymbol{v}_1 - \boldsymbol{v}_2||$ for all elements $\boldsymbol{v}_1, \boldsymbol{v}_2$ of a vector space, where $||\cdot||$ is a norm defined on the vector space.

In order to elucidate, various notations related to the most common forms of isomorphisms are briefly introduced. Let ρ denote clockwise rotation through 90° of a set of points in the plane about an axis O through the origin and orthogonally out of the plane. Then, $\rho^2 = \rho \circ \rho$ denotes rotation of the set through 180° about O, while $\rho^3 = \rho \circ \rho \circ \rho$ denotes rotation of the set through 270° about O. Furthermore, let σ denote reflection of a set of points in the plane about the x-axis of a cartesian system in the plane; that is, $\sigma((x, y)) = (x, -y)$ for any $(x, y) \in \mathbb{R}^2$. Finally, let ι be the identity mapping on the plane which maps each point of the plane to itself. Hence, $\sigma^2 = \sigma \circ \sigma = \iota$. Isomorphisms such as ρ, σ and ι may also be combined under the operation of composition. For example, for any point $P \in \mathbb{R}^2$, $\sigma\rho(P) = (\sigma \circ \rho)(P) = \sigma(\rho(P))$.

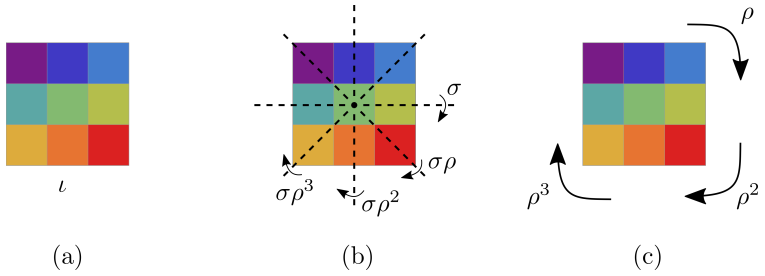

FIGURE 2.14: *The symmetry group of a square. (a) The identity symmetry, (b) reflection symmetries and (c) rotational symmetries.*

A *symmetry group* is a set of all the isomorphisms together with the binary operations of composition in which the elements of the set (on which the operations of the group are defined) remain invariant under the isomorphisms. By the definition of a group, any combination of two isomorphisms within a symmetry group, or an isomorphism and its inverse, results in another element of the symmetry group. To elucidate this concept, consider a square with its centre at the origin of $\mathbb{R}^2$ and corner points at $(-1, 1), (1, 1), (1, -1)$ and $(-1, -1)$. The square has eight isomorphisms under which it remains invariant: clockwise rotation by 90°, 180° or 270° about an axis O through the origin and orthogonal out of the plane, reflection about the x-axis, the y-axis and the two diagonal axes (within the plane) through the diagonally opposite corner points of the square, and the identity isomorphism which maps every point to itself. The symmetry group of a square is therefore the set of isomorphisms $\{\iota, \rho, \rho^2, \rho^3, \sigma, \sigma\rho, \sigma\rho^2, \sigma\rho^3\}$ together with the

[3] A metric space is a set equipped with a distance function defined on all pairs of elements of the set. Such a distance function d on a set X satisfies the following four properties: Non-negativity (denoted $d(x, y) \geq 0$ for all $x, y \in X$), symmetry (denoted $d(x, y) = d(y, x)$ for all $x, y \in X$), the triangle inequality (denoted $d(x, y) + d(y, z) \leq d(x, z)$ for all $x, y, z \in X$) and the identity of indiscernment (denoted $d(x, y) = 0$ if and only if $x = y$ for all $x, y \in X$).

binary operation of composition. These various isomorphisms are illustrated in Figure 2.14. In general, the *dihedral group* D_n is the symmetry group of a regular n-gon for some $n \geq 2$ and has $2n$ elements, namely $\{\iota, \rho, \rho^2, \ldots, \rho^{n-1}, \sigma, \sigma\rho, \sigma\rho^2, \ldots, \sigma\rho^{n-1}\}$. The symmetry group of a square is therefore denoted by D_4.

Let X be a set and let $\sim$ be an equivalence relation[4] defined on X. Then the equivalence class of an element $a \in X$ is the set $\{x \in X \mid x \sim a\}$ of elements which are equivalent to a. The collection of all equivalence classes of X forms a partition of X. Each equivalence class can be represented by one of its elements called the *canonical representative* or the *class representative*. In many enumerative analysis instances, an exclusive focus on the set of class representatives instead of considering the entire set X is without loss of generality. The considerable utility of this principle is exploited later in this thesis.

To elucidate the concepts of equivalence classes and of their class representatives, consider the set of all possible colourings of a 2×2 grid in two colours such that each grid cell is assigned exactly one of the colours, shown in Figure 2.15(a). A partition of this set into its equivalence classes is shown in Figure 2.15(b). Note that all the elements within an equivalence class can be formed by taking any element of the equivalence class, applying each of the isomorphisms of the symmetry group D_4 to this element and recording only the distinct[5] resulting states.

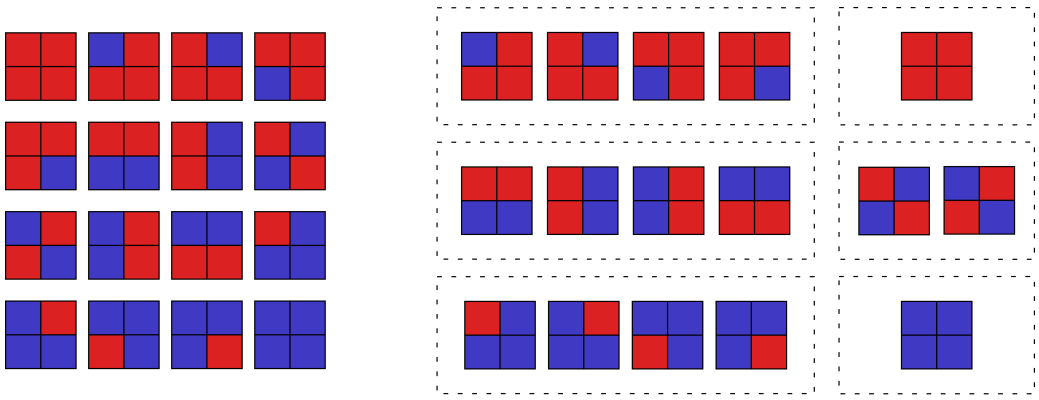

(a) (b)

FIGURE 2.15: *(a) The 16 ways in which a 2×2 grid can be coloured, using two colours, in such a manner that each grid cell is assigned exactly one of the colours, and (b) the resulting six equivalence classes of these colourings.*

The well-known Cauchy-Frobenius lemma may be used to enumerate the equivalence classes of a set. A proof of this result may be found in [39, Theorem on p.92].

Theorem 3. ***(Cauchy-Frobenius Lemma, also known as Burnside's Lemma)*** *If a group $\mathcal{G}$ acts on a set X, then the number of equivalence classes into which X can be partitioned by the action of $\mathcal{G}$ is*

$$\frac{1}{|\mathcal{G}|} \sum_{g \in \mathcal{G}} |F_g|,$$

where $F_g = \{x \in X \mid \pi_g(x) = x\}$ and π_g denotes the actions of the group element $g \in \mathcal{G}$.

[4] An equivalence relation $\sim$ on a set X is a subset of the cartesian product $X \times X$ that is reflexive (denoted $x \sim x$ for all $x \in X$), symmetric (denoted $x \sim y$ if $y \sim x$ for all $x, y \in X$) and transitive (denoted $x \sim y$ and $y \sim z$ imply $x \sim z$ for all $x, y, z \in X$).

[5] The descriptor *distinct* is used in this context to convey that the grid colouring appears different from a mere visual perspective.

In order to illustrate the application of the Cauchy-Frobenius Lemma, consider the number of essentially different[6] ways in which a 2×2 grid can be coloured with at most two colours. The six possible colourings are shown in Figure 2.16(b). Recall that a square has the symmetry group $D_4 = \{\iota, \rho, \rho^2, \rho^3, \sigma, \sigma\rho, \sigma\rho^2, \sigma\rho^3\}$. Applying the Cauchy-Frobenius Lemma, each isomorphism within the symmetry group has to be considered and the number of different colourings that yield an equivalent state when applying the isomorphism, enumerated. Consider first the identity isomorphism. Under this isomorphism all the possible colourings of a 2×2 grid will result in equivalent states, and so $|F_\iota| = 2^4$. Next, consider the isomorphism ρ which maps the first cell in Figure 2.16(a) to the second, the second cell to the fourth, the fourth cell to the third, and the third cell to the first. Hence, for an equivalent state to result under this isomorphism, all cells must have the same colour, and so $|F_\rho| = 2$. Now consider the isomorphism ρ^2. The positions of the first and fourth cells, as well as those of the second and third cells, are interchanged under this isomorphism, and so each pair must have the same colouring in order to yield an equivalent state under ρ^2. Hence, $|F_{\rho^2}| = 2^2$. The remaining isomorphisms within the symmetry group D_4 can be analysed in a similar fashion. Carrying out the analysis, it is readily found that $|F_\iota| = 2^4$, $|F_\rho| = 2$, $|F_{\rho^2}| = 2^2$, $|F_{\rho^3}| = 2$, $|F_\sigma| = 2^2$, $|F_{\sigma\rho}| = 2^2$, $|F_{\sigma\rho^2}| = 2^3$ and $|F_{\sigma\rho^3}| = 2^3$. According to the Cauchy-Frobenius Lemma, there are therefore $\frac{1}{8}(16+2+4+2+4+4+8+8) = 6$ essentially different ways of colouring a 2×2 grid with at most two colours.

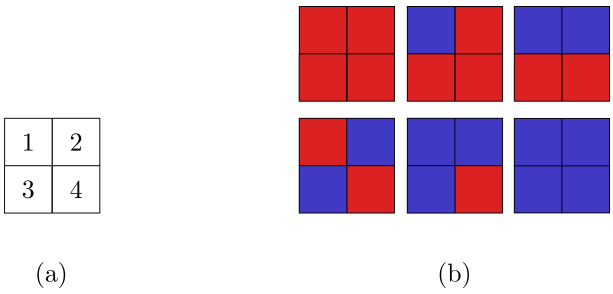

(a) (b)

FIGURE 2.16: *(a) A 2×2 grid with unit cells numbered $1, 2, 3$ and 4. (b) The six essentially different colourings of a 2×2 grid using at most two colours, which has D_4 as symmetry group.*

2.3 Chapter summary

In this chapter, various mathematical concepts were reviewed that are prerequisites for understanding the work documented later in this thesis. In §2.1, fundamental notions of graph theory were reviewed. In particular, the concepts of connectedness and graph isomorphisms were described. Various types of graphs were also reviewed with an emphasis on circulant and (toroidal) grid graphs. In §2.2 basic notions from group theory were reviewed. An emphasis was placed on the notion of an equivalence class and on the Cauchy-Frobenious lemma, which is a very useful tool in enumerative combinatorics.

[6]The descriptor *essentially different* is used in this context to convey grid colourings that are not isomorphic and therefore do not belong to the same equivalence class.

CHAPTER 3

Literature review

Contents

The literature related to classical and evolutionary game theory is reviewed in this chapter. Important concepts and terminology required for the definition, classification and analysis of games are also defined. This is followed by a brief background on various well-known two-player, two-strategy symmetric games as well as updating rules commonly applied within evolutionary games. Emphasis is finally placed on spatial evolutionary games, which is the main focus of this thesis.

3.1 Classical game theory

The concept of conflict is prevalent in society and nature. It is relatively easy to delineate the components of a conflicting situation: Several individuals making a series of decisions which leads to a possible outcome that each individual values differently. Conflict arises from the varied valuation of outcomes, and hence a collision of interests [71]. Although the notion of conflict has been present since the origin of man, a scientific approach to its analysis was only recently developed, as late as 1930, with the emergence of the field of *game theory*.

Game theory is a sub-discipline of operations research concerned with modelling and predicting the outcome from the interaction, known as a *game*, between rational decision makers, called *players* [16]. Each player selects a *strategy*, defining the player's choice of actions for any scenario within the game. The resulting interaction, and hence the outcome of the game, depends on all players' strategies, and each player is assigned a pay-off value accordingly. The goal of each player is to maximise its own expected pay-off value.

Game-theoretic insights have been found in various ancient records. For example, in two of Plato's texts, the *Laches* and the *Symposium* [9], the moral dilemma of a front-line solider in the Battle of Delium is recalled: A solider considers that his personal contribution is probabilistically

insignificant to the outcome of the battle and by fighting he runs the risk of being killed or injured. He is therefore better off running away. The dilemma is that if all soldiers acted within their best interest, then no men will remain to fight and the battle will be lost. This commentary affected the strategies of the Spanish conqueror Cortez [29]. When arriving in Mexico, he removed the risk that his troops may act in their own best interest and retreat by burning the ships on which they arrived. This episode gave rise to the modern saying "burning your ships."

Game theory is often applied in the fields of economics, the political sciences, tactical and strategic military science, computer science, engineering and evolutionary biology [19, 43, 56, 48, 13, 55]. In engineering, the interest in game theory is motivated by the possibility of designing large-scale systems that globally regulate their performance in a distributed and decentralised manner. Modelling a problem within a game-theoretic setting is particularly relevant to any practical application consisting of separate subsystems that compete for some limited resource.

3.1.1 A brief history of classical game theory

Originally, game theory focused on simplistic, strictly competitive games known as two-person zero-sum games [16]. This simplification was due to limitations in the mathematical framework available at the time, making the theory applicable only under special and limited conditions. Although this level of simplification may seem inappropriate for the more practical games encountered in economics and politics, it formed the cornerstone of general game theory.

The very first theorem of game theory, published in 1913, is Zermelo's Theorem [81]. Ernest Zermelo applied set theory in an analysis of the game of chess. He proved mathematically that chess is a strictly determined game[1], but was unable to determine its winning strategy. Zermelo also considered a wide class of parlour games including Checkers, Chinese Checkers and Go. He formulated what is now known as Zermelo's Theorem which applies to the following large class of games including the aforementioned parlour games: Two-person zero-sum games of perfect information[2] without stochastic strategic elements that contain a finite set of positions and an infinite sequences of moves. He proved that for these games it will never take more moves than there are positions available to a player to win the game if the player is in a *winning position*[3]. This theorem paved the way for more general results forming a foundation on which the field of game theory could be developed.

The foundations of game theory were laid by the mathematician and computer scientist John von Neumann in 1928, who is considered the 'father of game theory.' Although others preceeded him in formulating a theory of games, notably Emile Borel [36], it was Von Neumann who published the seminal paper *Zur Theorie der Gesellschaftsspiele* [74]. This paper provided a comprehensive and exact formalisation of important notions in game theory, as well as a formal proof of the Minimax Principle[4]. Von Neumann's original proof used Brouwer's fixed-point theorem on continuous mappings into compact convex sets to show that every two-person zero-sum game with finitely many pure strategies for each player is determined. The Minimax Principle became the cornerstone of game theory.

[1] A strictly determined game is a two-player zero-sum game where, if both players use pure strategies, then there is at least one Nash equilibrium [75].

[2] A sequential game has perfect information if each player participating in the game is perfectly informed of all events that previously occured, including the initialisation event [75].

[3] A winning position is formally defined as the non-emptiness of a certain set containing all possible sequences of moves that allow a player to win, independently of the moves of the opposing player [75].

[4] The Minimax Principle is a decision rule in which one minimises one's own maximum loss [53].

Von Neumann's paper was soon followed by a book titled *Theory of games and economic behaviour* [75], co-authored with economist Oskar Morgenstern in 1944. The book provided the climax of the pioneering period of game theory by providing a complete axiomatic utility theory, enabling game theory to be considered a formal mathematical discipline. Although the book was merely a review of previous work and contained no new results, it introduced the so-called *extensive form*[5] of a game, which was later reduced to the *normal form*[6] of a game by Kuhn [35]. It also allowed for the fundamental development of the concepts of *strategy*, the *strategic form* of a game, *mixed strategies* and *individual rationality*. The strategic form of a game, often represented as a pair of matrices for two-person games, is considered one of the most significant contributions to game theory. This foundational work also demonstrated the broad applications of game theory in economics and other well-known disciplines.

Another important milestone in the field of game theory occurred in 1950 when the American mathematician John Forbes Nash [47] developed a criterion for mutual consistency of players' strategies, known as a *Nash equilibrium*[7]. A Nash equilibrium may be seen as an extension of Von Neumann's minimax solution for n-player, non-zero-sum games. In zero-sum games, a minimax solution is the same as a Nash-equilibrium. Nash further proved the existence of at least one Nash equilibrium in each non-cooperative game. One of the most intriguing aspects of a Nash equilibrium is that it is not necessarily efficient in terms of aggregated social welfare.

Game theoretic research rapidly expanded after 1950. Al Tucker [45] formulated the PD, and the concept and analysis of repeated games emerged thereafter [23, 70, 76, 3]. A large amount of experimentation was also conducted by notable mathematicians, such as Merril Flood and Melvin Dresher, as part of RAND Corporation's investigation into game theory [59]. RAND pursued this investigation because of game theory's potential application to global nuclear strategy formation [59].

The field also found particular application to philosophy and the political sciences during this time. In 1954, the first paper was published on the use of game theoretic concepts to determine the power of the members of the United Nations Security Council [62]. This work further facilitated the game-theoretic modelling of situations related to elections, legislature, politics of interest groups, lobbies and bargaining, among others [21, 2, 43].

In 1973, two works pioneered the application of game theory to evolutionary biology. The first was British evolutionary biologist John Maynard Smith's and American geneticist George Price's paper titled *The logic of animal conflict* [42]. This paper introduced the concept of an *evolutionarily stable strategy*[8]. It also inspired further research which was summarised by Maynard Smith a decade later in his book *Evolution and the theory of games* [40]. The second was the American political scientist Robert Axelrod's book *The evolution of cooperation* [3], which explains, from a game-theoretic point of view, how cooperation may emerge, supporting the theory of biological evolution. The emergence of cooperation was previously perplexing as it appeared to oppose the Darwanistic framework of natural selection in which selfish individuals are favoured.

[5]The extensive form of game is an explicit representation of a number of key aspects, like the sequence of a player's possible moves, choices and potential pay-off values at every decision point. It is often represented graphically in the form of a decision tree [75].

[6]The normal form of a game is the representation of a game by means of a matrix [35].

[7]A Nash equilibrium of a game is a state of strategies from which no player has a unilateral incentive to deviate by choosing another strategy [47].

[8]An evolutionary stable strategy is a strategy which, if adopted by a population, cannot be invaded by a mutant strategy that is initially rare [42].

Utility maximising rationality has been observed to reflect the behaviour of animals better than that of humans [16]. An experiment involving probability matching was performed in which the subject must predict the binary outcome of an event where each outcome occurs with a certain probability. The rational solution is to pick the outcome that is most likely to occur. Rats were found to predict the correct event significantly more accurately than humans. These findings support the application of game theory in the modelling of biological evolution.

Finally, in 1994, John Nash was awarded the Nobel prize in economics together with Hungarian-American economist John Harsanyi and German economist Reinhard Selten for their contributions to non-cooperative game theory. The importance of the field can be accredited to the eleven game theorists who have won the Nobel prize in economics, the latest being Jean Tirole in 2014 for his work on market power and regulation.

For a further, more detailed account of the history of game theory the reader is referred to Paul Walker's chronology of game theory [76] or William Poundstone's book titled *Prisoner's dilemma: John von Neumann, game theory and the puzzle of the bomb* [59].

3.2 Defining, classifying and analysing games

Game theory provides a basic mathematical framework according to which conflicting situations can be defined, classified and analysed. This section contains definitions and explanations of a number of basic game theoretic notions employed in the remainder of this thesis.

3.2.1 Basic concepts in game theory

A game is an abstract formulation of an interactive decision situation with possibly conflicting interests. In game theory, there are two different ways of representing a game: Either in extensive-form or in normal-form. In the former case, the game is represented as a rooted tree. Each vertex of the tree represents a possible state of the game and each edge represents an event. An event can either represent the enactment of a move by a player or the outcome of a stochastic event. This is particularly beneficial in the analysis of incomplete information or asynchronous games. Each extensive-form game can, however, also be represented as a normal-form game. The latter is the standard form in which games are presented.

John Nash [46] first formally defined the notion of a normal-form game in terms of a game's players, their feasible actions (also called *pure strategies*) and the utilities or pay-off values associated with each possible combination of actions that can be chosen by the players.

Definition 1. ***(Normal form of a game)***
The normal-form *of a finite, n-person game is a tuple* $(N, A, \boldsymbol{u})$*, where*

1. N *is a finite set of* n *players;*
2. $A = A_1 \times A_2 \times \cdots \times A_n$*, where* A_i *is a finite set of actions available to player* i*;*
3. $\boldsymbol{u} = (u_i, \ldots, u_n)$*, where* $u_i : A_i \mapsto \mathbb{R}$ *is a real-valued utility function for player* i*.*

In the case where there are only two players, $N = \{1, 2\}$, and the sets of available strategies $A_1 = \{s_{1,1}, \ldots, s_{1,m}\}$ and $A_2 = \{s_{2,1}, \ldots, s_{2,m}\}$ are discrete, it is customary to write the game in bi-matrix form $\boldsymbol{G} = (\boldsymbol{A}, \boldsymbol{B}^T)$ which is the shorthand form for the pay-off matrix

$$\boldsymbol{\Psi} = \begin{array}{c} \\ s_{1,1} \\ \vdots \\ s_{1,m} \end{array} \begin{array}{c} \begin{array}{ccc} s_{2,1} & \cdots & s_{2,m} \end{array} \\ \begin{bmatrix} (\boldsymbol{A}_{11}, \boldsymbol{B}_{11}^T) & \cdots & (\boldsymbol{A}_{1m}, \boldsymbol{B}_{1m}^T) \\ \vdots & \ddots & \vdots \\ (\boldsymbol{A}_{m1}, \boldsymbol{B}_{m1}^T) & \cdots & (\boldsymbol{A}_{mm}, \boldsymbol{B}_{mm}^T) \end{bmatrix} \end{array},$$

where $\boldsymbol{A}_{ij} = u_1(a_{1,i}, a_{2,j})$ and $\boldsymbol{B}_{ij}^T = u_2(a_{1,i}, a_{2,j})$.

The strategy of a player (*i.e.* a row or column label in the pay-off matrix), is a pure strategy. A pure strategy is one in which the player has a predetermined set of actions that are adopted by the player according to the possible actions that can be taken by the opponent. In many games, however, the players can play mixed strategies, which are probability distributions over pure strategies. A player therefore randomly chooses the pure strategy to be adopted.

Definition 2. ***(Mixed strategy)***
Let $A_i = \{a_1^i, a_2^i, \ldots, a_{m_i}^i\}$ be the set of actions available to player i in a finite, n-person game, for all $i = 1, \ldots, n$. Then a mixed strategy *for player i is a vector $(p_1^i, p_2^i, \ldots, p_{m_i}^i)$ where $p_j^i \in [0, 1]$ for all $j = 1, \ldots, m$ satisfying $p_1^i + p_2^i + \cdots + p_m^i = 1$. Such a strategy dictates that player i will choose action a_j^i with probability p_j^i, for all $i = 1, \ldots, n$ and all $j = 1, \ldots, m$. The set of all mixed strategies available to a player is called the player's* strategy set*.*

A *pure strategy* is therefore a mixed strategy in which p_j^i is a binary number for all $j = 1, \ldots, m$.

Definition 3. ***(Strategy profile)***
A collection of strategies $s_1, \ldots, s_n$ adopted by the players of an n-person game is called a strategy profile *of the game and is denoted by $\boldsymbol{s} = (s_1, s_2, \ldots, s_n)$.*

The timing of a game in normal form is that players independently, but simultaneously, choose one of their feasible actions without knowing the decisions of the other players. Players then receive pay-off values according to the strategy profile realised.

3.2.2 A classification of games

A game can be classified according to its players and their strategies. Referring to a game as an $N \times |S|$ game is an example of such a classification, where N represents the number of players and $|S|$ the number of pure strategies available to each player. For example, a 2×2 game represents a game containing two players who each has two pure strategies available.

Games are often also classified according to their pay-off structure or the type of rules employed. A *cooperative game* is a game in which all agreements, promises and threats are fully binding and enforceable. Players are also allowed to communicate in cooperative games. The opposite is true in *non-cooperative games* [22]. Only *non-cooperative* games are considered in this thesis.

A game can either be *symmetric* or *asymmetric*. In a symmetric game, all game players have identical strategy options and pay-off values. If $\boldsymbol{M}$ is the pay-off matrix for player 1 in a two-player symmetric game, then $\boldsymbol{M}^T$ is the pay-off matrix for player 2. It is therefore irrelevant whether a player is considered in the role of player 1 or that of player 2. Hence, a two-player symmetric game can be denoted by $\boldsymbol{G} = (\boldsymbol{A}, \boldsymbol{A}^T)$. The well-known PD, the Hawk-Dove and the coordination games are all examples of two-person symmetric games. Two-person asymmetric games, on the other hand, are denoted by $\boldsymbol{G} = (\boldsymbol{A}, \boldsymbol{B}^T)$, where $\boldsymbol{A} \neq \boldsymbol{B}$. In this case, it makes a difference whether a player is considered in the role of player 1 or player 2.

A two-person *zero-sum* game is a two-player game in which the pay-off value of one player is equal to that of the second player, but different in sign. In this case, the game may be denoted

by $\boldsymbol{G} = (\boldsymbol{A}, -\boldsymbol{A})$. The same game can also be referred to as a *constant-sum* game, as the pay-off values can alternatively add up to a constant other than zero. This is because the player utility functions are linear, allowing for the application of linear transformations to the pay-off vector without changing the outcome of the game.

Definition 4. ***(Zero-sum game)***
Let A_j denote the set of actions of player j in a finite two-person game and let $u_j : A \mapsto \mathbb{R}$ denote the utility function of player $j \in \{1, 2\}$. Then the game is called a zero-sum game if there exists some real constant c such that $u_1(a) + u_2(a) = c$ for all $a \in A_1 \times A_2$.

The players of a game can implement their strategies simultaneously or sequentially. A game can therefore be classified as either a *synchronous* game or an *asynchronous* game. In asynchronous games, players have some knowledge of the decisions made by other players during earlier moves of the game. As mentioned previously, the extensive form of a game is often used to represent asynchronous games. A game may also incorporate a combination of sequential and simultaneous events.

A game of *perfect information* is one in which all players know the exact state of the game as well as which decisions are made within each round of the game. An example of a game with perfect information is chess. Each player knows the rules of the game and observes all moves made by the other player. If this property does not hold for a game, it is known as a game of *imperfect information*. An example of such a game is bridge, in which the players have limited knowledge of the cards held by the opposite player. In a game of *complete information*, every player knows the strategies and pay-offs available to the other players, but not necessarily their actions.

3.2.3 Analysing games

In order to analyse a game and determine which strategies will be optimal for the various players, a solution concept is required. A *solution concept* is a formal rule for predicting how a game will be played. Depending on the complexity of the game, various solution concepts have been developed over the years.

Minimax and maximin strategies

In order to determine which action is best for each player within a zero-sum game, two solution concepts have been defined. According to the *minimax* concept, each player minimises its opponent's maximal pay-off values, whereas according to the *maximin* concept, each player maximises its own minimal pay-off values. According to a theorem by Von Neumann [75], the minimax and maximin solutions are identical in zero-sum games. For non-zero games, however, they are not generally equivalent.

Strategy dominance

When comparing various strategies within a game, the notion of strategy dominance is central. Strategy dominance occurs when one strategy is better than another strategy for one player regardless of the actions taken by the player's opponents. The formal definition of strategy dominance and its use as a solution concept of the game is as follows. A dominant strategy can either be weakly or strictly dominant.

Definition 5. ***(Weakly dominant strategy)***
Consider an n-player game in which the strategy set and the utility function of player i are denoted by S_i and u_i, respectively, for all $i = 1, \ldots, n$. A strategy $s_i \in S_i$ is a (weakly) dominant strategy for player i if $u_i(s_1, \ldots, s_{i-1}, s_i, s_{i+1}, \ldots, s_n) \geq u_i(s_1, \ldots, s_{i-1}, s'_i, s_{i+1}, \ldots, s_n)$ for all $s'_i \in S_i$ and all $s_j \in S_j$, $j \in \{1, \ldots, i-1, i+1, \ldots, n\}$.

In the case of a strictly dominant strategy (for player i), the inequality in Definition 5 changes to $u_i(s_1, \ldots, s_{i-1}, s_i, s_{i+1}, \ldots, s_n) > u_i(s_1, \ldots, s_{i-1}, s'_i, s_{i+1}, \ldots, s_n)$ for all $s'_i \in S_i$ with $s'_i \neq s_i$.

According to the standard minimal definition of rationality [2], rational players seek to optimise their pay-off values and therefore always play dominant strategies. Therefore, if the solution to a game may be predicted by simply eliminating all strictly non-dominant strategies, it is said to be *dominant solvable*. Eliminating non-dominant strategies may not always be sufficient to reach a single, unique solution, and so further requirements may often be necessary. A stronger solution concept, which is applicable to all games, is the concept of a Nash equilibrium.

A Nash equilibrium

The most influential concept developed in classical game theory is a *Nash Equilibrium*, developed by John Nash in his PhD dissertation entitled *Non-cooperative games* [46]. He proved that each game with a finite set of players and actions will have at least one Nash Equilibrium. The proof is based on Kakutani's fixed point theorem [32]. In order to define a Nash Equilibrium, the concept of a *best response* is required. If a player knows what strategy the other players are going to play, it can determine its *best response* following the approach of single-agent utility-maximisation.

Definition 6. ***(Best response)***
Consider an n-player game in which the strategy set and the utility function of player i are denoted by S_i and u_i, respectively, for all $i = 1, \ldots, n$. Given strategies $s_j \in S_j$ for all players other than player i, a best response for player i is a strategy $s_i \in S_i$ such that $u_i(s_1, \ldots, s_{i-1}, s_i, s_{i+1}, \ldots, s_n) \geq u_i(s_1, \ldots, s_{i-1}, s'_i, s_{i+1}, \ldots, s_n)$ for all $s'_i \in S_i$.

The best response can be unique in the case where it is a pure strategy. Otherwise, it is a mixed strategy and hence there may be infinitely many best responses.

Informally, a Nash equilibrium is a solution in which no player has the incentive to change its strategy to enhance its pay-off value, given that all other players keep to their original strategies.

Definition 7. ***(Nash equilibrium)***
Consider an n-player game in which the strategy of player i is denoted by s_i, for all $i = 1, \ldots, n$. A strategy profile $\boldsymbol{s} = (s_1, \ldots, s_n)$ is a Nash equilibrium if s_i is a best response for all $i = 1, \ldots, n$.

More than one Nash equilibrium may exist for a given game and identifying these equilibria can be difficult. *Pareto efficiency* is a refinement of the notion of a Nash equilibrium which provides a mechanism for equilibrium selection when the Nash equilibrium criterion alone would provide more than one solution. A *Pareto efficient solution* is an outcome of a game for which there is no other outcome that renders every player at least as well off (in terms of their pay-off values), with at least one player strictly better off.

One of the most intriguing aspects of a Nash equilibrium is that it is not necessarily Pareto efficient in terms of the aggregate social welfare. Two archetypical examples of this situation are the PD and the *Tragedy of the commons*. Such situations are called *social dilemmas* and their analysis, avoidance or possible resolution is one of the most fundamental issues in economics and the social sciences.

Risk dominance and *pay-off dominance* are two refinements of the Nash equilibrium established by John Harsanyi and Reihard Selten [24]. A Nash equilibrium is considered pay-off dominant if it is Pareto efficient with respect to all other Nash equilibria in the game, while a Nash equilibrium is considered risk dominant if it has the largest natural attraction (*i.e.* the more uncertain players are about the actions of their opponents, the more likely they will choose the strategy associated with the risk dominant Nash equilibrium).

The evolutionary stable strategy

In evolutionary game theory, the most important solution concept is the *evolutionary stable strategy* (ESS) which is closely related to that of a Nash equilibrium. Maynard Smith and Price [42] defined an ESS as "a strategy such that, if most of the members of a population adopt it, there is no 'mutant' strategy that would give a higher reproductive fitness." Players playing an ESS fare better than players playing only mutant strategies and therefore outperform and expel invaders.

Definition 8. ***(Evolutionary stable strategy)***
Given a two-player symmetric game and a player utility function u, a mixed strategy $\boldsymbol{s}$ is an ESS if there exists a positive real number $\epsilon \ll 1$ such that $u(\boldsymbol{s}, (1-\epsilon)\boldsymbol{s} + \epsilon\boldsymbol{s}') > u(\boldsymbol{s}', (1-\epsilon)\boldsymbol{s} + \epsilon\boldsymbol{s}')$ for all $\boldsymbol{s}' \neq \boldsymbol{s}$.

An ESS can also be defined in terms of two properties. More specifically, a strategy is an ESS if, for all $\boldsymbol{s'} \neq \boldsymbol{s}$, either

1. $u(\boldsymbol{s}, \boldsymbol{s}) > u(\boldsymbol{s}', \boldsymbol{s})$, or else
2. $u(\boldsymbol{s}, \boldsymbol{s}) = u(\boldsymbol{s}', \boldsymbol{s})$ and $u(\boldsymbol{s}, \boldsymbol{s}') \geq u(\boldsymbol{s}', \boldsymbol{s}')$

is satisfied. An ESS is therefore a refinement of the notion of a Nash equilibrium. All ESSs are Nash equilibria, but a Nash equilibrium is not necessarily an ESS.

3.3 Types of 2-person, 2-strategy games

Since symmetric 2-person, 2-strategy games with pure strategies are the focus of this thesis, this type of game is considered in more detail in this section. Suppose the strategies available to the players in this case are cooperation (denoted by C) and defection (denoted by D). Then the pay-off matrix takes the form

$$\boldsymbol{\Psi} = \begin{matrix} \\ C \\ D \end{matrix} \begin{matrix} \begin{matrix} C & D \end{matrix} \\ \begin{bmatrix} R & S \\ T & P \end{bmatrix} \end{matrix}, \tag{3.1}$$

where the pay-off values included in the matrix are those received by the row player, where R is called the *reward for mutual cooperation*, P is called the *punishment for mutual defection*, T is called the *temptation to defect* and S is called the *sucker's pay-off*. Various orderings of these pay-off values define different well-known games. The (S, T)-phase plane is shown in Figure 3.1, forming various well-known games when the pay-off matrix is normalised so that $R = 1$ and $P = 0$.

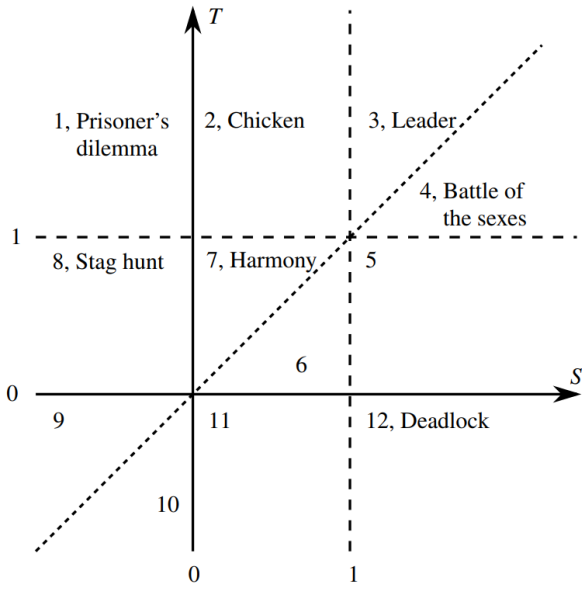

FIGURE 3.1: *Partitioning of the (S,T)-phase plane if $R = 1$ and $P = 0$ in (3.1). Each of the 12 regions refers to a specific type of 2×2 game. Those of particular interest are named in the diagram.*

3.3.1 The prisoner's dilemma

The best-known game in game theory is the PD. The game was proposed in 1950 by Albert Tucker who gave the game its name and interpretation based on numerical experimentation by Flood and Dresher at RAND Corporation, a military-subsidised think tank based in the United States [45]. The game was soon recognised as an important and fundamental analytical tool in the context of conflict situations [60]. Due to the threats of moral considerations emerging from technological development, it has been argued that the PD is "one of the premier philosophical and scientific issues of our time."

The dilemma is presented in the form of a parable in which two suspects are arrested by the police. Having insufficient evidence to convict them, the police offer both prisoners the same deal separately: Each prisoner can either *defect (D)* and hence testify against the other prisoner, or *cooperate (C)* by remaining silent. If both prisoners choose to cooperate, they are each sentenced to a short prison term, represented by a pay-off value R. If, however, one prisoner defects while the other cooperates, the former goes free and hence receives a pay-off value T while the latter receives the full sentence and hence a pay-off value S. If both prisoners defect, they share the sentence and each receives a pay-off value P. Under the PD model's standard restrictions, the parameter ordering condition $T > R > P > S$ holds for the pay-off values. The dilemma is therefore that each prisoner, unable to communicate with the other prisoner, should decide on a strategy which maximises his own reward or pay-off value by minimising his prison sentence.

Defection is known to be the best response for both players in a single PD, resulting in a Nash equilibrium. The optimal solution, allowing for maximum individual benefit, however, is for both players to cooperate [58]. If the PD is considered within an evolutionary context, it is modelled as repeated rounds and called the *iterated prisoner's dilemma* (IPD). A central underlying assumption of the IPD is that the number of rounds is unknown in advance to all the players. Within this context cooperation has been observed to emerge as an optimal strategy [58].

3.3.2 The hawk-dove game

Upon altering the parameter condition of the PD so that $S > P$, hence resulting in the alternative inequality chain $T > R > S > P$, the well-known *hawk-dove game* is obtained which is sometimes also referred to as the *game of chicken* or the *snowdrift game* [42].

The game was first introduced by Sugden [66] and derives the name hawk-dove from the situation where individuals compete for a shared resource. Players can either contest for the resource, known as *playing hawk*, or share the resource, known as *playing dove*. If both players play hawk and fight for the resource, they both incur a large cost whereas if both players play dove, they share the resource with no cost incurred. If, however, one player plays hawk and the other dove, then the hawk gains the entire resource and the dove nothing. A hawk will always contest for sole ownership of the resource while the dove is willing to share the resource.

3.3.3 The stag-hunt game

Constricting the parameters of the pay-off matrix by the inequality chain $R > T > P > S$ results in the so-called *stag-hare game*. The stag-hunt game may also be explained by means of a parable [63]: Two hunters going on a hunt are able to choose whether to hunt a deer (stag) or a hare. In order to succeed in hunting a deer, a hunter requires the cooperation of the other hunter. A hunter is, however, able to hunt a hare independently, but hunting a hare is worth less than hunting a deer.

The stag-hunt game has two Nash-equilibria: Where both players cooperate or where both players defect. The first is considered pay-off dominant, while the latter is considered risk dominant.

3.3.4 The public good game

The public good game is played by N players who are each able to cooperate or defect. Each cooperating player contributes a benefit b to the public good, while incurring a cost c to himself. On the other hand, each defecting player does not contribute anything to the public good and also does not incur any cost. The total current public wealth is distributed equally among all the players regardless of their strategy.

This game is also known as *the Tragedy of the commons* [21], which exemplifies the major related concerns of political philosophy and economic thinking, of which the tragedy is that without central planning and global control, private incentives lead to over-utilisation of public resources and insufficient contribution to public goods.

3.4 Evolutionary game theory

Evolutionary game theory is based on the assumption that players have limited knowledge of the game and only bounded rationality. The games in evolutionary game theory are repeated in rounds and players are given the opportunity to adapt and learn good strategies as the game repetition occurs. Evolutionary game theory emerged as a refinement of classical static games, but now deals with more dynamic games of adaptation [76].

3.4.1 Classical *vs* evolutionary game theory

Classical game theory is based on two key assumptions, namely that all players have perfect rationality and that this is common knowledge. *Perfect rationality* means that players have well-defined pay-off functions and that they are fully aware of their own and their opponents' strategy options and pay-off values. They have no cognitive limitations in deducing the best possible way of playing despite the complexity of the game. Hence, computation is costless and occurs instantaneously. *Common knowledge* implies that all players know that all other players are rational, and that all players know that all other players know that they are all rational [20, 21].

As described in §3.2, classical game theory is concerned with *games*, defined in terms of *players*, *strategies* and *utilities*. The objective is to find a *solution concept*, *i.e.* a set of solution strategies for each player [67].

Evolutionary game theory branched off from classical game theory due to three key deficiencies of the latter field. The first is that of equilibrium selection by rational agents in the case of multiple Nash equilibria. The second problem is hyper-rationality, which is required to assign cardinal utility functions to the agents. Studies have shown that human behaviour rather coincides with the assumptions of hyper-rationality. The third difficulty lies in the lack of dynamism within classical game theory. Classical game theory assumes static preferences and does not address the process of rational deliberation and learning.

Evolutionary game theory is the theory of dynamic adaptation and learning in infinitely repeated games played by bounded rational agents. The key assumptions are that players have limited knowledge of the game and only bounded rationality. Players are given the opportunity to adapt and learn as game repetition occurs. The focus in evolutionary game theory is therefore on strategies and how they persist through time.

In classical game theory, each player's rationality and self-interest serve as the agent of optimisation, whereas in evolutionary game theory, the selection process serves as the agent of optimisation. For a more detailed discussion on the differences between the two sub-fields of game theory, the reader is referred to Maynard Smith's seminal paper *Evolutionary game theory* [41].

3.4.2 Evolution and natural selection

Evolutionary game theory originated from observations in nature exhibiting evolution and natural selection. In biology, evolution is the generational change in the physical, genetic or behavioural characteristics of a population enabled through natural selection. *Genes* are the basic heritable unit which collectively form an organism's phenotype. When a heritable characteristic provides a reproductive advantage, it becomes more abundant in a population as time progresses. Wright [80] introduced the concept of a fitness landscape in which fitness is plotted against gene frequency. Fitness is a measure of an individual's ability to survive and reproduce.

Evolutionary game theory centres on the study of evolution when selection depends on the relative abundance of game strategies in a game strategy population, hence the study of the dynamics of a game strategy population's fitness landscape. The interactions between members that affect their fitness are conceptualised as a game, with pay-off values representative of reproductive success. Vincent and Brown [73] provided a detailed discussion on evolutionary game theory and its application to studying natural selection. They described a game in evolutionary game theory as consisting of two parts: The *inner game*, defining the available strategies and

pay-off values achieved by the players, and the *outer game*, describing the game dynamics where pay-off values are translated into changing strategy frequencies.

3.4.3 Strategies

As mentioned, the focus in evolutionary game theory is on the evolution of game strategies. Axelrod [3] proposed a set of criteria for a strategy to be evolutionary viable.

Robustness. A strategy must be able to survive in an environment containing a variety of strategies.

Stability. A strategy must be able to resist invasion by another, mutant strategy.

Invasiveness. A strategy must be able to invade an environment dominated by rival strategies.

Axelrod and Hamilton [4] were the first to investigate the evolutionary viability of various strategies in the context of the IPD. They conducted a computer tournament in which various strategies competed within a mixed population of strategies. Sixty two different strategies were formulated by professional game theorists and scientists globally. Each strategy competed against each other strategy in a round-robin fashion. The strategy that scored the highest average over all the rounds was declared the winner. It was found that the most successful strategies in the IPD are those in which the following three attributes prevail:

Niceness. Defection is never played first.

Forgiveness. Cooperation is restored after an accidental defection.

Retaliation. If the opponent starts playing the strategy of defection, react by also playing the strategy of defection.

The most successful strategy in Axelrod and Hamilton's tournament was the *tit-for-tat* strategy. The tit-for-tat strategy is one in which a player cooperates during the first round of the game, after which it merely mirrors the opponent's move during the previous round. If the opponent played the strategy of defection during the previous round, the player plays the strategy of defection during the current round. The tit-for-tat strategy was shown to be evolutionary viable. It therefore demonstrated that cooperation based on reciprocity can emerge in a population of egoists, with a small portion of reciprocates, and resist invasion by mutant strategies.

Nowak and Sigmund [53] also investigated and analysed the Pavlov strategy, which was found to be extremely effective in situations where the IPD is played in an evolutionary context among more than two players. The Pavlov strategy is based on the "law of effect" or "win-stay/lose-shift." Hence, the Pavlov strategy cooperates on the first move and thereafter repeats its previous move if the opponent cooperated, otherwise it switches.

In evolutionary game theory, players are given the opportunity to learn and adapt their strategies. This process is modelled by a dynamic updating rule which showcases the way in which evolution is incorporated.

3.4.4 Updating rules

In an evolutionary game theoretic model, each round is partitioned into two phases: The playing phase followed by the updating phase. During the playing phase the game is played by each player against a subset of its neighbours. Within the updating phase, each player is given the possibility of changing its strategy to either cooperation or defection during the next game round. The updating phase is determined by a dynamic updating rule. Various updating rules are available in the literature, such as the *replicator rule*, the *Moran rule* and the *unconditional imitation rule*.

The replicator rule

Player i randomly chooses one of its neighbours to play the game against. If the chosen neighbour player j achieves a larger pay-off value then player i, player i adopts the strategy of player j during the next round with a probability proportional to the difference of their pay-off values. Therefore, the replicator rule is a local updating rule as it does not look at the entire neighbourhood of player i.

Often the noise caused by the effect of irrational choice is also modelled. In this case, the aforementioned probability depending on the difference in pay-off values is taken as

$$H_{i \mapsto j} = \frac{1}{1 + \exp[(\pi_i - \pi_j)/\kappa]}, \tag{3.2}$$

where κ characterises the noise reflecting irrational choices. Hence, $\kappa = 0$ and $\kappa = \infty$ denote completely deterministic and completely random selection, respectively. The effect of the parameter κ on the cooperation frequency has been studied in detail in [37]. The reader is also referred to Mukherji *et al.* [50] for a detailed account of the role of stochasticity upon this updating rule.

The Moran rule

At the end of each playing phase, player i evaluates a set of probabilities, one for each neighbour proportional to that neighbour's pay-off value. Player i then randomly selects the neighbour's strategy for adoption during the next round according to the set of probabilities. Hence there is a chance that an agent can select a strategy that performed worse during previous rounds. As the rule involves the entire neighbourhood of player i, it is referred to as a global updating rule.

The unconditional imitation rule

This rule is a completely deterministic rule. It is based on the principle of imitating the best. Player i is chosen randomly for updating. It adopts the strategy of one of its neighbours or retains its own strategy based purely on which pay-off value is largest (*i.e.* the strategy of the player in player i's closed neighbourhood with the largest pay-off value). The unconditional imitation rule is also a global updating rule.

3.5 Evolutionary spatial games

Mathematical analyses of evolutionary games have shown that costly cooperation between members of a population cannot evolve unless there is some mechanism in the evolutionary process

that supports them. Spatial structure is one such mechanism. The main focus of this thesis is on evolutionary spatial games.

The emergence of cooperation can be enhanced when an evolutionary game is combined with spatial effects. Spatial structure within a population of players allows for localised interactions. According to this structure, individuals play a game against specified neighbours as opposed to against random opponents or all members of the population. The interaction between the players is typically modelled by an underlying graph. This kind of spatial structure promotes the survival of cooperators by allowing clusters of cooperators to form, enabling the benefit of mutual cooperation to outweigh losses incurred against defectors and allowing for cooperation to persist. This also facilitates the invasion of populations of defectors by clusters of cooperators.

3.5.1 The social structure of a game

Spatial effects were not considered in early evolutionary game theoretic studies. A well-mixed population was typically assumed instead, in which different individuals interact with each other, depending on their relative frequency within the population. The pay-off value of a strategy was then related to its change in frequency. The dynamics of these games were typically described by time-continuous differential equations of the form

$$\frac{\mathrm{d}x_i}{\mathrm{d}t} = x_i \left(\sum_{j=1}^{n} A_{ij} x_j - \sum_{i=1}^{n} x_i \sum_{j=1}^{n} A_{ij} x_j \right),$$

where x_i is the frequency of strategy $i \in \{1, \ldots, n\}$, A_{ij} is the pay-off matrix of the game and t denotes time. For an extensive mathematical analysis of the use of differential equations for modelling game dynamics the reader is referred to [28].

In order to model a game taking spatial structure into account, a graph may alternatively be used to define the underlying topology of the game. The vertices of the graph represent the players, and edges joining the vertices represent playing interactions between players. Each player plays a PD against each of its neighbours independently. The underlying topologies that are commonly considered include complete graphs, lattices, small-world networks and scale-free networks [67]. Mean-field games assume a complete graph as their underlying topology, as any player is equally likely to interact with every other player.

3.5.2 Numerical analysis of spatial games

Axelrod [3] was the first to suggest placing the players of an ESPD on a two-dimensional spatial array, where in each round each player plays a PD with each of its immediate neighbours independently. He focused his investigation on analysing the effectiveness of various strategies within this spatio-temporal game setting. More specifically, he carried out a mathematical analysis showing that cooperation based on reciprocity can emerge in a population of egoists with a small proportion of reciprocators, and resist invasion by mutant strategies. This strategy of reciprocity is the *tit-for-tat strategy*.

Based on Axelrod's work, Nowak and May [51, 52] performed the ground work for evolutionary games in spatial contexts, adopting a computer simulation approach. They showed that it is possible for cooperation and defection to co-exist on a two-dimensional spatial array, where each player plays a PD against each of its neighbours independently. The PD was adopted and strategic complexities and memories of past encounters by players were neglected. A discrete-time model was assumed together with a deterministic update rule. The outcome of the model

depended on both the initial configuration and the rescaled pay-off matrix described by a single parameter b, characterising the measure of temptation to defect. Nowak and May studied the ESPD on square lattices where players interact with their four or eight nearest neighbours. Hexagonal lattices were also considered as the underlying graph where players interact with six neighbours, including or excluding self-interaction. The analysis focused on parameter values within the range $b \in (1.8, 2)$. This region allows for the emergence of unstable clusters of cooperators, eventually exhibiting spatial chaos and dynamic fractals with chaotic fluctuations around long-term averages. The asymptotic proportion of sites occupied by cooperators fluctuate around 0.318. In the case of symmetric initial conditions and symmetric update rules, "evolutionary kaleidoscopes" were found, which are reminiscent of Persian carpets and Andalusian tiles. The final states of these evolutionary kaleidoscopes were shown to be unpredictable, thereby combining chaos and symmetry.

The typical shape and growth of clusters of cooperators or defectors in these models were also analysed. It was observed that for some parameter values, a square of cooperators expands at its corners, but shrinks along its sides. A lone defector, on the other hand, was shown to do well initially, but by prospering, defectors surround themselves with other defectors, thereby diminishing their own return. This process of cooperator and defector growth yielded highly intricate patterns. The model's outputs for the case where a single defector is placed in the centre of a 49×49 array of cooperators with fixed boundary conditions and $b = 1.85$ is shown in Figure 3.2.

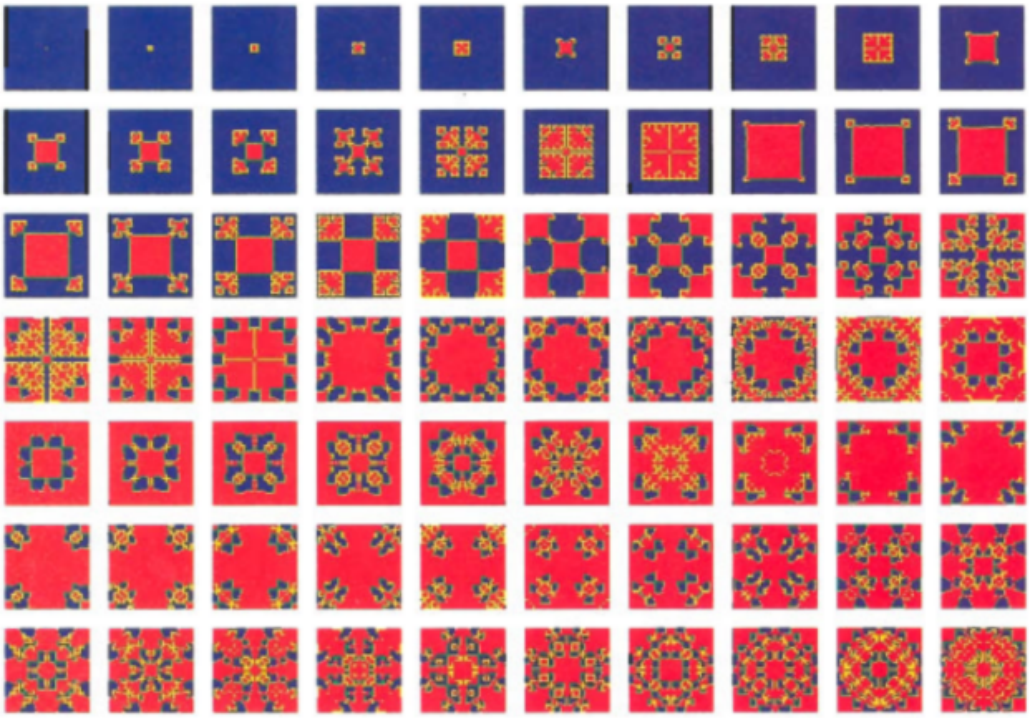

FIGURE 3.2: *Simulation results obtained by Nowak and May [51] for the case of placing a single defector in the centre of a* 49×49 *array of cooperators with fixed boundary conditions and* $b = 1.85$. *Each grid shows the spatial distribution after 200 generations. The colour coding is as follows: blue = cooperation, red = defection, green = cooperation changing its strategy to defection, and yellow = defection changing its strategy to cooperation [51].*

Nowak and May's deterministic model is equivalent to a two-state cellular automaton[9] with the property that the transition rule depends on the state of the nearest neighbours as well as on that of *their* nearest neighbours. Comprehensive studies have been performed in respect of cellular automata, most recently by Wolfram [79]. One of the most famous cellular automata is Conway's *Game of life* [7]. Nowak and May's model exhibited most of the gadgetry of Conway's Game of life (such as periodic blinkers and gliders of cooperators).

Hubermann and Glance [30] studied a similar model to that considered by Nowak and May, namely an ESPD on a two-dimensional lattice, but employed continuous-time simulations in their analysis, where players are chosen at random for strategy updating purposes. The model therefore allows for asynchronous updating. They considered the possibility of the co-existence of cooperators and defectors in both continuous and discrete time in the stochastic case.

Szabo and Toke [68] studied the ESPD with a square lattice as the underlying topology and employed systematic *Monte Carlo simulation* and generalised *mean-field techniques* in order to calculate the asymptotic density of cooperators as a function of the parameter b for different noise levels.

Killingback and Doebeli [34] conducted a similar study as that of Nowak and May, but considered the Hawk-Dove game instead of the PD. They showed that the long-term proportion of Hawks is smaller than the equilibrium proportion predicted by classical evolutionary game theory. They also observed a complex dynamic that is different from the spatio-temporal chaos observed in the ESPD studied by Nowak and May. For a substantial range of parameters, their system organises itself into a state in which its dynamic behaviour is governed by long-range spatial and temporal correlations, and by power laws. One such property is that the system exhibits extremely long transients initially from very complicated dynamics to very simple periodic orbits.

A systematic study of various 2×2 games on lattices and random graphs was conducted by Hauert [25]. He considered two-dimensional regular lattices and random networks as the underlying graph, each with degree 4, 6 and 8, separately. A simulation approach was adopted to study the ESPD with the parameters in the pay-off matrix set to $R = 1$, $P = 0$, $-1 < S < 1$ and $0 < T < 2$. The various quadrants in the (S, T)-phase plane were considered independently. An investigation was also carried out in respect of the *replicator rule*, the *multiple replicator rule*, the *Moran rule* and the *unconditional imitation rule* as update rules. They found that combinations of various graph structures and various parameter values either enhanced or prevented the emergence of cooperation. It was shown, in particular, that lattices, as well as random graphs, promote the evolution of cooperation. The adoption of random graphs and lattices of the same degree yielded very similar results. An increase of the graph regularity from 4 to 6 and further to 8 resulted in a larger degree of cooperation along a wide range of parameter values. The results also showcased the existence of phase transitions, with clear boundaries between different regions in the phase plane. It was further shown that the effect of spatial structure on the persistence of cooperation is strongly dependent on the updating rule adopted.

Roca *et al.* [61] took this work further by conducting an analysis of small world networks. They showed that the effect of spatial structure promoting cooperation is directly linked to clustering in the underlying graph. Hence, small-world networks with large clustering coefficients were studied and shown to promote the emergence of cooperation. The property of small characteristic path lengths of small-world networks create "shortcuts," thereby allowing cooperation to spread quicker. It was thus established that games with a small-world network as underlying topology reach equilibrium quicker than when employing regular lattices.

[9] A cellular automaton, first conceived by Von Neumann [75], is a collection of cells arranged in a grid of a specified shape that evolves through discrete time steps according to specified updating rules based on neighbouring cell states.

Further work has been done on scale-free weighted networks by Du and Zheng [15]. Weighted networks were examined to investigate the effect of contact frequency between players. The authors considered the effect of edge weight heterogeneity on the cooperation frequency within a network when an IPD game is played on a scale-free network. They used the Barabasi-Albert (BA) scale-free network model to generate the network as well as to assign the edges' weights according to the formula $w_{ij} = (k_i \times k_j)^{\beta}$, where k_i and k_j represent the degree of vertices i and j, respectively. The value of β controls the heterogeneity of the edge weights. The larger β, the higher the heterogeneity. Through the use of simulation, the authors found that cooperation frequency exhibits strong dependence on the value of β. The system's cooperation frequency is maximised when $\beta = 0$ or when $\beta < 0$ and $|\beta|$ is large.

3.5.3 Algebraic analyses of spatial games

A minimal amount of algebraic analysis (*i.e.* analysis without the use of computer simulation) has been carried out in the context of the ESPD. This is due to the enormous number of possible configurations that can arise. Burger *et al.* [10, 11], however, conducted an asymptotic analysis of the ESPD on paths and cycles. Both the steady states and the initial states that lead to the emergence of cooperation were characterised in the case of these underlying graph structures. The probability that a randomly generated initial state will result in persistent cooperation was also determined.

Van der Merwe [72] further studied the ESPD on very small grid structures, again adopting an analytical approach. The game dynamics for small grids were characterised. The phase plane of an ESPD on a grid with or without wrapping at the edges was analysed and the influence of the size of the grid on the isoclines present in the phase plane was determined. In order to analyse the ESPD on grids, the authors enumerated the ESPD state space for the ESPD in $n \times m$ grids with and without wrapping at the edges (excluding the case where $n = m$).

Bergroth [6] studied the ESPD analytically in respect of graphs with infinitely many players and an equal number of neighbours for each player. He determined the probability that cooperation survives in an evolutionary fashion on these graph structures. Formally, Bergroth [6] determined the probability $\pi_p^i(C) = \lim_{t\to\infty} P(s_t^i(p) = C)$, where $s_t^i(p)$ denotes the strategy adopted by player i at time t and where p denotes the probability that the player starts with the strategy of cooperation when $t = 0$. For a one-dimensional lattice, it was found that $\pi_p^i(C)$ is independent of the pay-off parameters values. For a one-dimensional and a two-dimensional lattice, the expectation of an i-cluster of cooperators was also determined. The author further determined the probability $\pi_p^i(C)$ for the ESPD on binary and $(n-1)$-nary trees, and also on d-dimensional lattices.

3.5.4 Other analysis approaches of spatial games

Various other approaches have also been adopted towards placing the PD in a spatial setting. Hutson and Vickers [31], as well as Ferriere and Michod [17], considered one-dimensional reaction-diffusion models which lead to travelling waves of players adopting a tit-for-tat strategy invading inveterate defectors. Hertz [27] took the approach of viewing the ESPD as an *Ising-type* model from the realm of statistical mechanics. In such models, the behaviour of games are studied in terms of their pay-off structure and the abstract fitness landscape that develops.

Doebeli and Knowlton [14] considered mutualistic interaction between different species playing an ESPD. In their model, the two species occupy two different superimposed lattices. Interspe-

cific interactions occur between individuals at corresponding locations in these lattices and the pay-off values of these interactions determine the competition within each lattice. The authors showed that spatial structure is even more essential for the evolution of mutualism in this setting than in one-lattice games.

Ohtsuki *et al.* [57] considered the evolution of cooperation in an ESPD involving a population whose structure is partitioned into an *interactive graph* H, defining against whom PD instances are played, and a *replacement graph* G, specifying evolutionary competition and updating of strategies. This model structure was assumed to accommodate the fact that decision-making is often based on additional information about interacting players obtained through networks that rarely overlap perfectly with the network of interactions. The authors found that whenever the symmetry between the graphs G and H is broken, the probability of the emergence of cooperation and its frequency reduces compared to the case where the two graphs coincide.

3.6 Chapter summary

Various basic definitions and concepts in classical and evolutionary game theory were reviewed in this chapter. The notions of classical game theory, together with a brief history of the important developments within the field, were reviewed in §3.1. In §3.2, the basic mathematical framework and required definitions for representing games were recounted. Various methods for classifying games and a review of a number of solution concepts (for analysing games) were also presented. A number of types of 2-person, 2-strategy games in the literature on evolutionary game theory were finally reviewed. In §3.4, the development of evolutionary game theory from classical game theory was recounted as were the core differences between the two sub-felds. The connection between evolutionary game theory and biology was also discussed in terms of evolution and natural selection. Various strategies from the literature adopted by players of evolutionary games were presented and this was followed by a review of a number of updating rules that may govern the dynamics of an evolutionary game. In the final section of the chapter, §3.5, the field of evolutionary spatial game theory was briefly reviewed. The literature was analysed according to the various methods adopted to analyse the evolution of cooperation, either adopting a numerical approach, an analytical approach or other less conventional approaches.

CHAPTER 4

The modelling of ESPD game dynamics

Contents

A framework for representing games on graphs is established in this chapter. The framework is similar to those developed by Nowak and May [51, 52] and by Burger *et al.* [10, 11] where each player plays a PD instance against each of its neighbours based on an underlying topology. The chapter opens with a mathematical representation of a game instance, followed by a description of the techniques used to model the game dynamics. The notion of a state graph is then considered as a visualisation tool of the ESPD game dynamics. The assumptions made in respect of the pay-off values in order to reduce the complexity of modelling the game are also outlined in this chapter. Finally, the chapter closes with a discussion on the construction of the parameter phase plane associated with an ESPD instance.

4.1 The mathematical representation of a game

An evolutionary game can be represented by a pair, $\Upsilon = (\Pi, G)$. The first element of this pair, $\Pi = \{T, R, S, P\}$, is the set of pay-off parameters contained within the two-player PD pay-off matrix

$$\begin{array}{c} \\ \text{C} \\ \text{D} \end{array} \begin{array}{c} \begin{array}{cc} \text{C} & \text{D} \end{array} \\ \begin{bmatrix} R & S \\ T & P \end{bmatrix} \end{array},$$

where C denotes the strategy of cooperation and D represents the strategy of defection. The second element of Υ is the *underlying graph* G which represents the structure according to which the PDs are played. It may occur, in general, that the game is governed by two underlying graphs, an *interaction graph* G_i and an *replacement graph* G_r. The graph G_i determines players' neighbourhoods according to which their pay-off values are calculated, while the graph G_r determines the update neighbourhoods of the players. In this thesis, however, $G_i = G_r$. Therefore, a single underlying graph G is sufficient to describe the structure of the game.

A state of the ESPD is captured by a 2-colouring of the vertices of the underlying graph, denoting the distribution of the strategies adopted by the various players during a particular round of the game. A state of the ESPD is therefore represented by a pair $S = (G, X)$, where G is the aforementioned underlying graph with vertex set $V(G)$ and edge set $E(G)$. Furthermore, X is a function $f : V(G) \mapsto \{C, D\}$ that assigns the two strategies of cooperation C or defection D to each vertex of G. In graphical representations of ESPD states, players adopting the strategy of cooperation are denoted by solid vertices (*i.e.* coloured black) and players adopting the strategy of defection are denoted by open vertices (*i.e.* coloured white). An example of such a graphical representation of an ESPD state is shown in Figure 4.1 where each vertex represents a player, the vertex colouring captures the strategies of the players during a particular round of the game, and each edge indicates an independent PD that is to be played by the players represented by the two vertices incident with the edge.

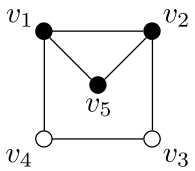

$G_{4.1}$

FIGURE 4.1: *The graphical representation of an ESPD state with the graph $G_{4.1}$ as underlying graph. Defecting players are denoted by solid vertices, while cooperating players are denoted by open vertices.*

The underlying graph of the ESPD is therefore interpreted as a labelled graph, as each vertex represents a specific player participating in the game. Due to the possible symmetries that may exist in the underlying graph, as well as the inherent symmetry of the update rule, certain distinct ESPD states may nevertheless be considered equivalent. The set of states may therefore be partitioned into equivalence classes. Recall, from §2.1.5, the notion of an *automorphism*. An automorphism ϕ between two ESPD states $s_1 = (G, X_1)$ and $s_2 = (G, X_2)$ is the one-to-one mapping of the set of vertex labels in $V(G)$ onto itself so that adjacency, as well as the particular colouring of the underlying graph, is preserved. In particular, $uv \in E(G)$ if and only if $\phi(u)\phi(v) \in E(G)$ and $X_1(v) = X_2(\phi(v))$ for all $v \in V(G)$. Two ESPD states are said to be *automorphic* if there exists an automorphism between them. Note that when two states are automorphic, the states obtained after playing one round of the ESPD, starting from these states, will again be automorphic. Automorphic ESPD states therefore exhibit equivalent game dynamics.

An *automorphism class* is a maximum set of automorphic game states. A class representative is associated with each automorphism class. Because each state of an automorphism class exhibits equivalent game dynamics, only the class representative has to be considered in an exhaustive game dynamic analysis. The state with the smallest *lexicographical order* in an automorphism class is chosen as the class representative.

Lexicographical order is the convention according to which words are ordered alphabetically in terms of their component letters. In order to determine the lexicographical order of a number of distinct game states, each state's vertices are first considered in the order in which they are labelled. These ordered vertices induce a string of characters from the set $\{C, D\}$ that can then be ordered lexicographically. A solid vertex, representing a player adopting the strategy of cooperation, is denoted by the character C in this string, while an open vertex, representing a player adopting the strategy of defection, is denoted by the character D. As $C < D$ alphabetically, a solid vertex precedes an open vertex. Therefore, the smaller of two states is the one with the smallest strategy (*i.e.* C) corresponding to the first vertex of the underlying graph for which the

two states differ in strategy. An example of the lexicographical order of pairs of ESPD states is shown in Figure 4.2. The number of solid vertices within a state is called the *weight* of the state. Note that a state with a larger weight than another state may precede the latter state in lexicographical order, as illustrated in Figure 4.2(c).

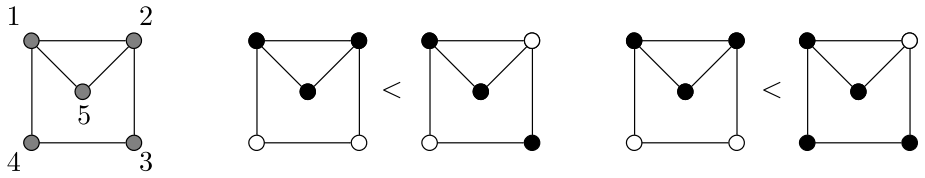

(a) vertex labelling (b) $G_{4.1} < G_{4.2}$ (c) $G_{4.1} < G_{4.3}$

FIGURE 4.2: *Examples of the lexicographical ordering of game states. (a) The labelling of the vertices of the underlying graph $G_{4.1}$. (b) and (c) Examples of the lexicographical order of pairs of game states. In (c), the graph $G_{4.3}$ precedes $G_{4.1}$ lexicographically but has a larger weight than $G_{4.1}$.*

To elucidate the partitioning of distinct game states into automorphism classes, consider the ESPD instance with $G_{4.1}$, as shown in Figure 4.1, as underlying graph. Note that the graph contains a vertical symmetry axis through vertex 5, therefore admitting a single reflectional symmetry. The $2^5 = 32$ distinct ESPD states are therefore partitioned into 20 automorphism classes as shown in Figure 4.3. Each class representative, which has the smallest lexicographical order within its class, is shown first in the figure.

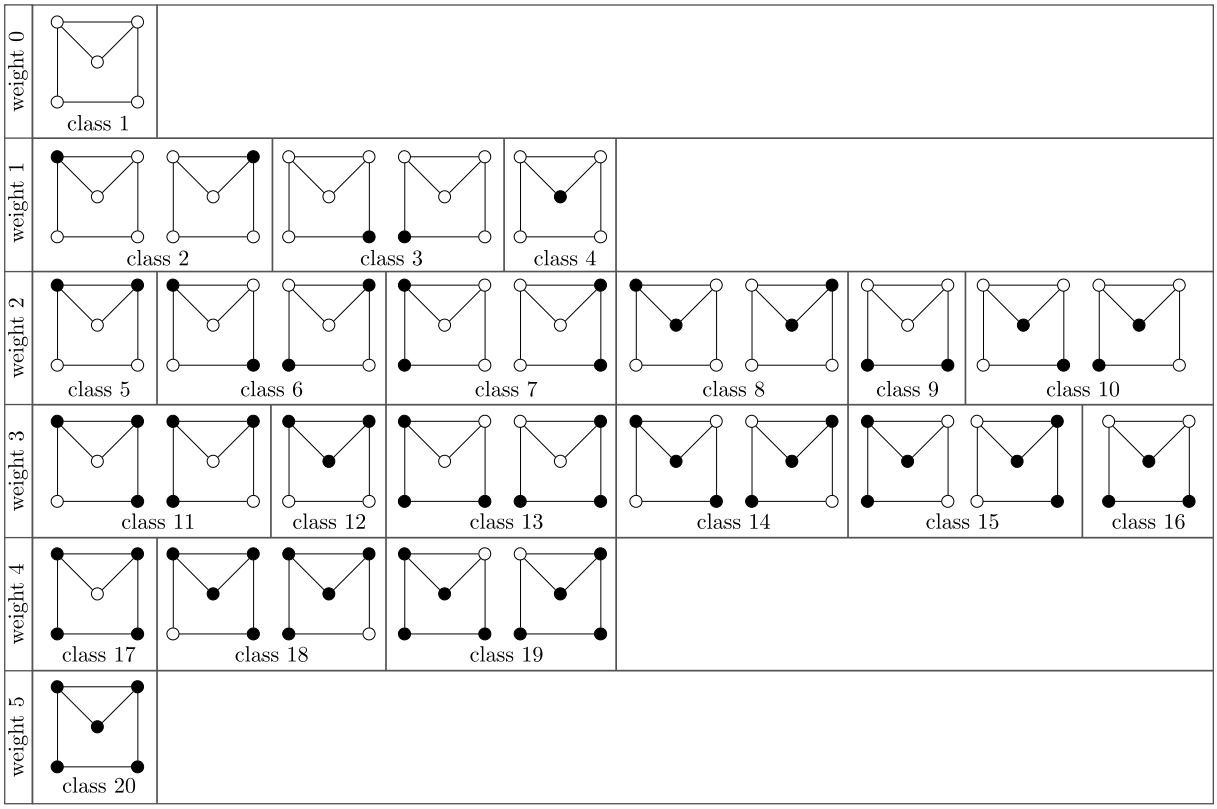

FIGURE 4.3: *The distinct states of the ESPD with $G_{4.1}$ as underlying graph, organised into automorphism classes. The first state displayed in each class is the class leader. The states have further been organised according to their weights as indicated by the various rows in the table.*

The shorthand notation $\langle C\rangle^i$ or $\langle D\rangle^i$ denotes i consecutive players adopting the strategy of cooperation or defection, respectively, in a string representation of an ESPD state when the players are considered in the order in which they are labelled. $\langle C\rangle^i$ is also referred to as a run of cooperators of length i within the remainder of this thesis, and similarly for $\langle D\rangle^i$.

4.2 Dynamic rules of a game

When modelling an instance of the ESPD, each player is first assigned a strategy in order to generate an initial game state, as described §4.1. The game is then played in *rounds*. Each round consists of two phases, the *playing phase* and the *updating phase*, respectively. During the playing phase, each player's score is determined, while during the updating phase each player updates its strategy. The game is terminated when either the system reaches a steady-state, a limit cycle or a pre-determined number of rounds have been played.

During the playing phase, each player plays an independent PD against each of its neighbours. The pay-off value of each player is calculated by determining the average pay-off value resulting from each of the PD games in which the player participates. Calculating the average pay-off values facilitates a comparison of the relative success of the various strategies when they are adopted by players that have different numbers of neighbours in the underlying graph. Consider, for example, a player v who has x neighbours adopting the strategy of cooperation and y neighbours adopting the strategy of defection. The pay-off value of player v in this case is

$$\pi_v = \begin{cases} \frac{1}{x+y}(xT + yP) & \text{if } v \text{ adopts the strategy of defection} \\ \frac{1}{x+y}(xR + yS) & \text{if } v \text{ adopts the strategy of cooperation.} \end{cases}$$

To elucidate the playing phase, consider the ESPD instance $\Upsilon = (\{5, 3, 0, 1\}, G_{4.1})$ illustrated in Figure 4.4. The labelling of vertices is shown in (a), where player i is represented by vertex v_i. In the initial game state shown in Figure 4.4(b), player 1 is represented by a solid vertex and therefore adopts the strategy of cooperation. The vertex v_1 is adjacent to two solid vertices v_2, v_5 and one open vertex v_4. Player 1 therefore has two cooperating neighbours and one defecting neighbour. The pay-off value of player 1 is consequently

$$\pi_1 = \frac{1}{2+1}(2(3) + 1(0)) = 2.$$

The pay-off value of each player is denoted next to its corresponding vertex in Figures 4.4(b)–(d).

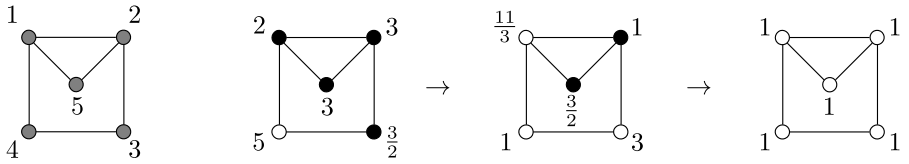

(a) vertex labelling (b) initial state (c) after one round (d) after two rounds

FIGURE 4.4: *An example of the game dynamics of the ESPD instance* $\Upsilon = (\{5, 3, 0, 1\}, G_{4.1})$. *(a) The labelling of the various players of the game. (b)–(d) Subsequent rounds of the game in which pay-off value of each player is denoted next to its corresponding vertex.*

During the updating phase of each round, the player updates his strategy according to a dynamic updating rule, as discussed in §3.4.4. The updating rule considered within this thesis is the local form of the unconditional imitation rule. A player updates his strategy by adopting the

strategy of the player with the largest pay-off value in its closed neighbourhood. If the player's own strategy achieves the largest pay-off value, it will retain its strategy. In the case of a tie between a player's own pay-off value and the largest pay-off value of a player in the player's open neighbourhood, it is assumed that the player will retain its own strategy. This assumption is based on a presumed reluctance of a player to change its strategy as there may be a small cost associated with this process.

As an example of an updating process, consider again the game $\Upsilon = (\{5, 3, 0, 1\}, G_{4.1})$ shown in Figure 4.4. Consider the initial game state shown in part (b) of the figure. Player 1 evaluates the maximum pay-off value in its closed neighbourhood $N_1 = \{3, 5, 3, 2\}$. The maximum pay-off value 5 is received by player 4, who adopts the strategy of defection. According to the updating rule, player 1 therefore imitates the strategy of player 4 by adopting the strategy of defection during the next round of the game. This is illustrated in the subsequent game state shown in part (c) of the figure in which player 1 is now represented by an open vertex. The same process is then repeated during subsequent rounds of the game. Consider next the game state resulting after a single round of the game, as shown in Figure 4.4(c). Player 1 again evaluates the pay-off values in its closed neighbourhood $N_1 = \{1, 1, \frac{3}{2}, \frac{11}{3}\}$. The largest pay-off value $\frac{11}{3}$ is obtained by player 1. Player 1 therefore retains its strategy of defection during the next round of the game. The resulting game state, after having applied the updating process to each player in the game, is shown in part (d) of the figure. Note that all players in Figure 4.4(d) adopt the strategy of defection. Hence, the all-defector steady state has been reached. As all subsequent rounds of the game will result in the same game state, the end of the game has been reached.

4.3 The state graph

The state graph of an ESPD instance is a vertex-weighted pseudo-digraph in which each vertex corresponds to the automorphism class of a game state, represented by its class representative. Within the state graph, a vertex u is adjacent to a vertex v if the associated game state u in Υ transitions within a single round to the associated game state v. The weight of the vertex is the weight of the associated game state. The state graph therefore captures the dynamics of the game in the form of transitions between its successive game states. An example of the state graph of the ESPD instance $\Upsilon = (\{5, 3, 0, 1\}, G_{4.1})$ is shown in Figure 4.5.

As can be seen in Figure 4.5, the roots of the various components of the state graph represent the steady states of the game. In the state graph, a *steady state* is therefore a state that is adjacent to itself. A limit cycle is represented by a directed cycle of length at least two. The state graph in Figure 4.5 does not contain a limit cycle. The state graph in the figure contains 20 vertices organised into three components. The game can end in any one of three steady states. Note that the vertices of this state graph correspond to the 20 automorphic classes shown in Figure 4.3.

4.4 The pay-off values

Both the topology of the underlying graph and the pay-off values $\Pi = \{T, R, S, P\}$ influence the outcome of an instance of the ESPD. The pay-off values can, however, be normalised to reduce the number of parameter regions in the ESPD phase space that have to be considered. A normalisation of the pay-off values is introduced in this section, and this is followed by an analysis of resulting parameter regions that have to be considered independently when modelling ESPD game dynamics.

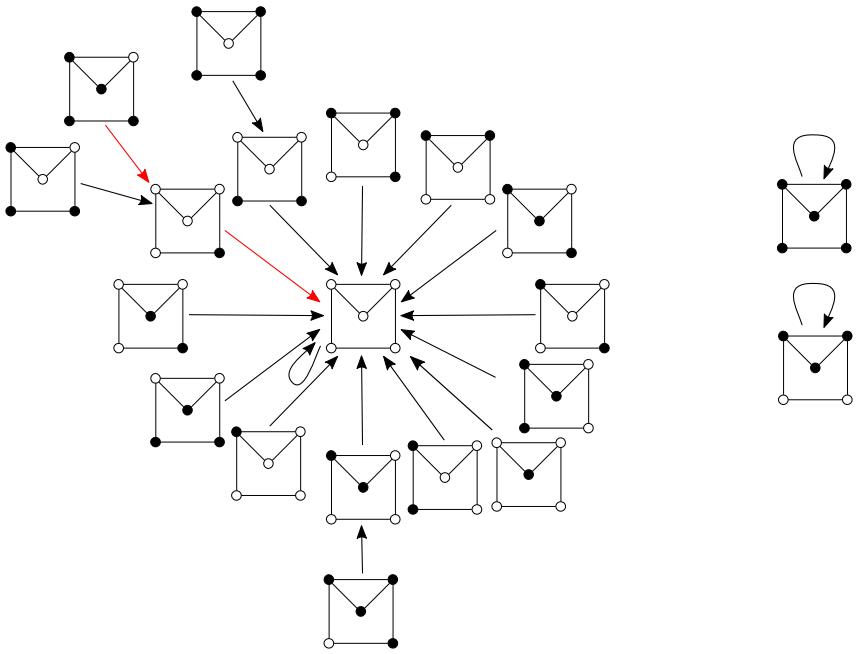

FIGURE 4.5: *The state graph of the ESPD instance* $\Upsilon = (\{5, 3, 0, 1\}, G_{4.1})$. *The red arrows in the graph represent the particular game dynamics illustrated in Figure 4.4.*

4.4.1 Normalisation of the pay-off values

Burger *et al.* [10, 11] showed that by normalising the parameter values of the ESPD it is possible to model the game dynamics in terms of two parameters only, instead of four. This reduces the complexity of the modelling process considerably as far fewer parameter combinations have to be considered. The game is modelled in the remainder of this thesis in terms of the normalised pay-off values $\Pi = \{T, 1, 0, P\}$. This normalisation does not influence the game dynamics [72]. The pay-off matrix is therefore replaced by the normalised pay-off matrix,

$$\begin{array}{c} \\ \text{C} \\ \text{D} \end{array} \begin{array}{c} \begin{array}{cc} \text{C} & \text{D} \end{array} \\ \begin{bmatrix} R & S \\ T & P \end{bmatrix} \end{array} \rightarrow \begin{array}{c} \\ \text{C} \\ \text{D} \end{array} \begin{array}{c} \begin{array}{cc} \text{C} & \text{D} \end{array} \\ \begin{bmatrix} 1 & 0 \\ T & P \end{bmatrix} \end{array},$$

where the parameter inequalities $T > 1$ and $0 < P < 1$ hold.

4.4.2 The phase plane

When a change in the parameter values influences the outcome of the updating process of one or more players during the game, the change is called a *phase transition*. A *phase plane* may be constructed by plotting the values of T and P for which such phase transitions occur. The lines in the phase plane associated with phase transitions are called *isoclines*. These isoclines partition the phase plane into disjoint parameter regions. Any pair of T and P values in the same region of the phase plane will result in equivalent game dynamics.

During the updating process, a player compares the pay-off values of the highest scoring cooperator and defector in its closed neighbourhood. Let the pay-off value of player v adopting the strategy of cooperation or defection, with i cooperators and j defectors in its open neighbourhood, be denoted by $c_{i,j}$ and $d_{i,j}$, respectively. Then the values of $c_{i,j}$ and $d_{i,j}$ are functions of the parameters T and P. It is customary to find the isoclines of the phase plane where $c_{i,j} = d_{k,\ell}$

for $i, j, k, \ell \in (0, d_v)$. This is because a change in the outcome of the game only occurs when the pay-off values of players adopting different strategies are compared.

Since a player's pay-off value is determined by the average of the pay-off values of the players in its open neighbourhood, an important quantity in the analysis of phase plane transitions is the proportion of cooperators or defectors in a player's open neighbourhood. As $c_{i,0} = c_{j,0}$, $d_{i,0} = d_{j,0}$, $c_{i,i} = c_{j,j}$ and $d_{i,i} = d_{j,j}$ for all $i, j \in \mathbb{N}_0$ only one of these pay-off values need to be considered when identifying the various isoclines. Furthermore, there are no isoclines associated with the value of $d_{0,i}$ for any $i \in \mathbb{Z}$. This is because the defector has no cooperators in his closed neighbourhood, and will hence continue to adopt the strategy of defection independently of the value of the parameters T and P. Therefore, the parameter values do not influence the updating process of a player with pay-off value $d_{0,i}$.

It is further noted that the isoclines of the phase plane are only concerned with $c_{i,j} = d_{k,\ell}$ if $\frac{k}{k+\ell} < \frac{i}{i+j}$. This is because a defector with a larger proportion of cooperators in its open neighbourhood will always achieve a larger pay-off value than a cooperator with an equivalent or smaller proportion of cooperators in its open neighbourhood. In order to understand this, note that if $\frac{k}{k+\ell} \geq \frac{i}{i+j}$, then $d_{k,\ell} > c_{i,j}$, as the parameter inequalities $T > 1$ and $P > 0$ result in the inequality chain

$$d_{k,\ell} = \frac{1}{k+\ell}(kT + \ell P) > \frac{k}{k+\ell}T > \frac{k}{k+\ell} \geq \frac{i}{i+j} = c_{i,j}.$$

As an example of the construction of a phase plane, consider again the ESPD $\Upsilon = (\{T, 1, 0, P\}, G_{4.1})$. The graph contains vertices of degree two and three. Therefore, the possible different pay-off values that a player can achieve are $c_{0,2}, c_{0,3}, c_{1,1}, c_{1,2}, c_{2,0}, c_{2,1}, c_{3,0}, d_{0,2}, d_{0,3}, d_{1,1}, d_{1,2}, d_{2,0}, d_{2,1}$ and $d_{3,0}$, which may be written in terms of the parameters T and P as $0, 0, \frac{1}{2}, \frac{1}{3}, 1, \frac{2}{3}, 1, P, P, \frac{1}{2}T + \frac{1}{2}P, \frac{1}{3}T + \frac{2}{3}P, T, \frac{2}{3}T + \frac{1}{3}P$, and T, respectively. Again it is true that $d_{k,\ell} > c_{i,j}$ if $\frac{k}{k+\ell} \geq \frac{i}{i+j}$, while $d_{0,2}$ and $d_{0,3}$ does not affect the outcome of the updating process of a player in the game. Therefore, the transitions in the phase plane are given by the six equations

$$\begin{aligned}
c_{3,0} = d_{2,1} &\Rightarrow 3 = 2T + P,\\
c_{3,0} = d_{1,1} &\Rightarrow 2 = T + P,\\
c_{3,0} = d_{1,2} &\Rightarrow 3 = T + 2P,\\
c_{2,1} = d_{1,1} &\Rightarrow 4 = 3(T + P),\\
c_{2,1} = d_{1,2} &\Rightarrow 2 = T + 2P, \text{ and}\\
c_{1,1} = d_{1,2} &\Rightarrow 3 = 2(T + 2P).
\end{aligned}$$

These isoclines result in a phase plane with nine parameter regions which potentially induce different game dynamics, as shown in Figure 4.6. When investigating the game dynamics, each of these parameter regions therefore has to be analysed separately.

All the underlying graphs considered within the remainder of this thesis are 4-regular. Therefore, if the number of cooperators i in a player's open neighbourhood is known, the number of defectors j can be calculated as $j = 4 - i$. Therefore, the shorthand notation $c_i = c_{i,j}$ and $d_i = d_{i,j}$ is adopted within the remainder of this thesis.

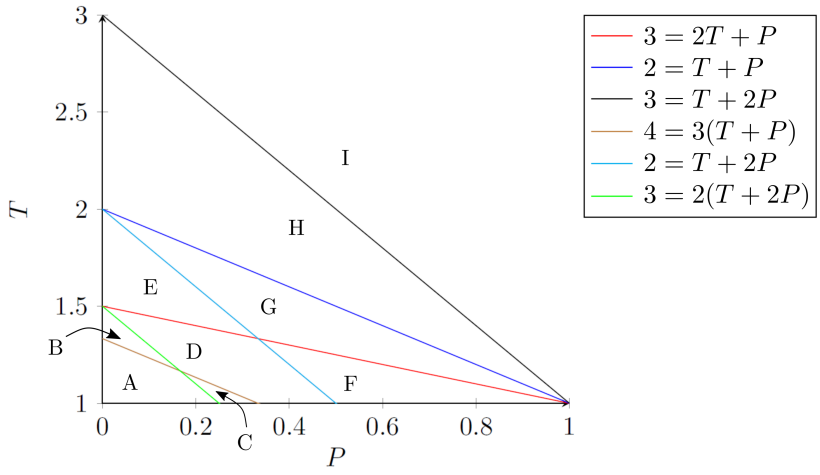

FIGURE 4.6: *The P-T phase plane for the ESPD* $\Upsilon = (\{T, 1, 0, P\}, G_{4.1})$. *There are nine disjoint parameter regions, labelled from A to I.*

4.5 Chapter summary

A mathematical representation of an ESPD instance, consisting of an ordered pair containing a set of pay-off parameters and an underlying graph, was proposed at the start of this chapter, and this was followed by a description of the framework adopted in this thesis to model a game state. The modelling of the entire game dynamics was also discussed, making use of the notion of a state graph as a visual representation tool. An important concept also introduced is that of an automorphism class of game states. In the final section of the chapter, a normalisation of the pay-off matrix was suggested to reduce the complexity of the game analysis without influencing the game dynamics. This was followed by a discussion on the construction of a (pay-off parameter) phase plane. The various parameter regions of this phase plane have to be considered separately when analysing the game dynamics of an ESPD instance.

CHAPTER 5

The ESPD on a circulant

Contents

In this chapter, an analytical approach void of computer-based support is adopted to investigate the game dynamics of the ESPD on the circulant $C_n\langle 1,2\rangle$ as underlying graph. The game dynamics on the cycle $C_n \simeq C_n\langle 1\rangle$ as underlying graph has previously been studied [11]. The main objective of the analysis in this chapter is to determine how an extension of each player's neighbourhood affects the likelihood of persistent cooperation when players are arranged in a cyclic topology.

The chapter opens with a brief background on the previous investigation of the game dynamics of the ESPD with a cycle as underlying graph. The focus of the chapter then shifts to the investigation of the game dynamics of the ESPD with $C_n\langle 1,2\rangle$ as underlying graph. First the various parameter regions of the phase plane which induce different game dynamics are identified. All equilibrium states are then characterised and enumerated for each parameter region. These enumerations are next employed to present various results that facilitate an investigation of the game dynamics to be investigated without explicitly having to play the ESPD for each distinct game state and underlying graph order. The probability of persistent cooperation is then calculated for a general underlying circulant graph order. The chapter finally closes with a comparison of the results emanating from the analysis of the game dynamics of the ESPD on a circulant underlying topology (contained within this chapter) and those emanating from the aforementioned previous analysis of the game dynamics of the ESPD on a cyclic underlying topology (found in the literature).

5.1 Background

Recall, from §3.5.3, that Burger *et al.* [11] studied the long-term behaviour of the ESPD with a cycle of order n as underlying graph. They characterised and enumerated all steady states

associated with this instance of the ESPD. They also computed the probability of randomly generating an initial state which leads to some form of persistent cooperation. Figure 5.1 contains an illustration of the resulting relationship between the order of the underlying cycle and the probability of cooperation persisting for the two different parameter regions of the phase plane.

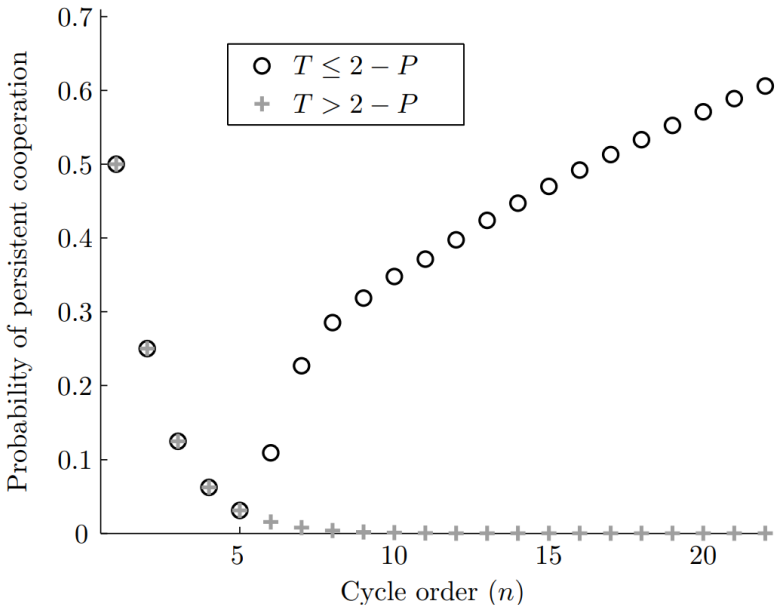

FIGURE 5.1: *The probability of a randomly generated initial state for the ESPD on a cycle of order n resulting in any form of persistent cooperation [11].*

The main objective in this chapter is to determine the effect of an extension of each player's cyclic neighbourhood from that in $C_n\langle 1\rangle$ to $C_n\langle 1, 2\rangle$ (*i.e.* so that each player plays a PD with each of its direct neighbours as well as with their neighbours) has on the characteristics of the equilibrium states and the probability of cooperation persisting. The cycle $C_8 = C_8\langle 1\rangle$, as well as the circulant $C_8\langle 1, 2\rangle$, is depicted in Figure 5.2. Note the change in each player's neighbourhood size as indicated in the figure by dotted lines for the player marked in red.

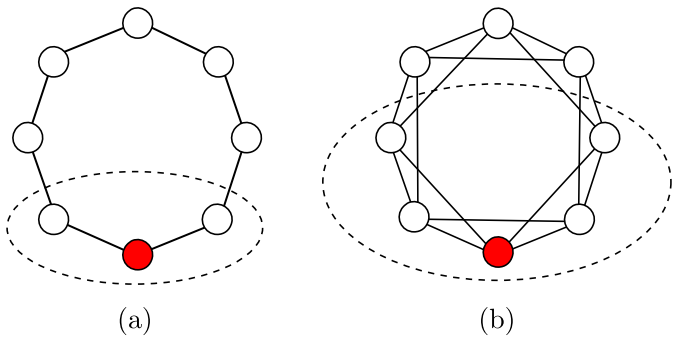

FIGURE 5.2: *The extension of each player's neighbourhood from two to four players, when changing the ESPD underlying graph from (a) C_8 to (b) $C_8\langle 1, 2\rangle$.*

The remainder of this chapter builds on the work of Burger *et al.* [11], in the sense that the evolutionary behaviour of the ESPD with the circulant $C_n\langle 1, 2\rangle$ as underlying graph is investigated and compared with the game dynamics of the ESPD with $C_n\langle 1\rangle$ as underlying graph.

5.2 Representation and enumeration of game states

In order to analyse the ESPD with the circulant $C_n\langle 1,2\rangle$ as underlying graph, the isometric representation of the underlying graph shown in Figure 5.3(c) is adopted in the remainder of this chapter. This form of visualisation is used to facilitate a classification and enumeration of the equilibrium states of the game. To elucidate this isometric representation, consider the circulant $C_8\langle 1,2\rangle$ represented in its well-known circular form in Figure 5.3(a). An isometric representation of the same graph is shown in Figure 5.3(b), exhibiting a triangular lattice structure. Adopting this structure, but omitting the three edges joining the left-most and right-most most vertices, indicated in red in Figure 5.3(b), the isometric representation in Figure 5.3(c) is obtained. Hence, only a subgraph of the underlying graph is, in fact, shown in part (c) of the figure, with the dotted lines on either side of the graph representing the remaining edges (and also vertices in the case of $C_n\langle 1,2\rangle$ for $n > 8$) omitted.

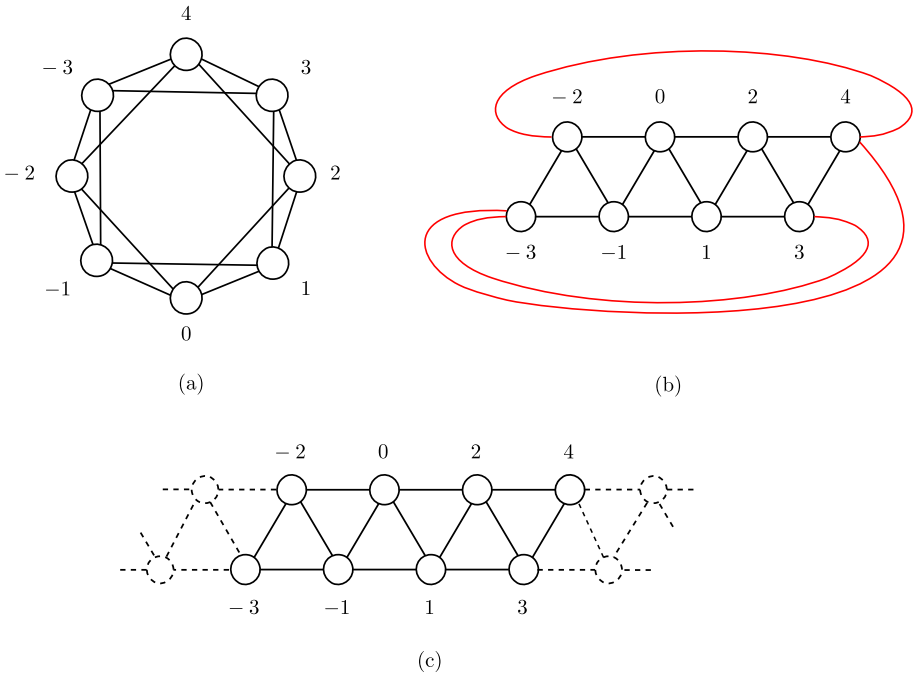

FIGURE 5.3: *(a) A standard representation of the circulant $C_8\langle 1,2\rangle$, (b) a triangular lattice representation of the same graph, and (c) an isometric representation of $C_n\langle 1,2\rangle$.*

In this chapter, it is assumed that the underlying graph of the ESPD is the circulant $C_n\langle 1,2\rangle$ whose vertices are labelled $-\lfloor\frac{n-1}{2}\rfloor,\ldots,-2,-1,0,1,2,\ldots,\lceil\frac{n-1}{2}\rceil$. Vertex $\lceil\frac{n-1}{2}\rceil$ is assumed to be adjacent to $-\lfloor\frac{n-1}{2}\rfloor$ and $-\lfloor\frac{n-1}{2}\rfloor+1$, while vertex $\lceil\frac{n-1}{2}\rceil-1$ is assumed to be adjacent to $-\lfloor\frac{n-1}{2}\rfloor$. The labelling of vertices -3 to 4 is illustrated in Figure 5.3(c).

There are 2^n different ways of assigning one of the two strategies, C or D, to each of the n vertices in the aforementioned labelled underlying graph. Many of these states are, however, equivalent as a result of rotational symmetry, reflectional symmetry and glide reflection symmetry in the underlying graph. Rotational symmetry occurs about an axis orthogonal to the page and through the centre of the ciruculant in its standard representation shown in Figure 5.3(a) by degree either $\frac{360i}{n}$ where $i\in\{1,\ldots,n-1\}$. Reflectional symmetry occurs about an axis in the plane of the page and running through the vertices i and $i+\frac{n}{2}$ if n is even, or otherwise through the vertex i and the centre of the edge joining vertices $i+\lfloor\frac{n}{2}\rfloor$ and $i+\lceil\frac{n}{2}\rceil$ if n is odd, where $i\in\{0,\ldots,\lfloor\frac{n}{2}\rfloor\}$. Glide reflection symmetry occurs as a result of the composition of any of the above two possible

symmetries. The equivalent states resulting from these symmetries can therefore be organised into automorphism classes, as described in §4.1. The number of these automorphism classes for $C_n\langle 1,2\rangle$ is equal to that for the cycle $C_n\langle 1\rangle$. This is because the additional edges of $C_n\langle 1,2\rangle$ over and above those of $C_n\langle 1\rangle$ do not change the symmetry properties of the underlying graph. The number of automorphism classes of game states for the ESPD with the circulant $C_n\langle 1,2\rangle$ underlying graph is given by

$$\Lambda(n) = \begin{cases} \sum_{d|n} \frac{\phi(d)2^{n/d}}{2n} + 2^{\frac{n-1}{2}} & \text{if } n \text{ is odd,} \\ \sum_{d|n} \frac{\phi(d)2^{n/d}}{2n} + 2^{\frac{n}{2}-1} + 2^{\frac{n}{2}-2} & \text{if } n \text{ is even,} \end{cases} \tag{5.1}$$

where $\phi(\cdot)$ is the well-known *Euler totient*[1] [18]. The sequence $\Lambda(n)$ is listed as Sloane's sequence A000029 [64]. Investigating the enumeration of game states is equivalent to a well-known counting problem documented in the literature in which the number of necklaces that can be created from a total of n beads of 2 possible colours are enumerated. The reader is reminded that because all states in an automorphism class lead to similar game dynamics, it is only necessary to investigate the ESPD game dynamics resulting from the various automorphism class representatives.

5.3 The phase plane of the ESPD on $C_n\langle 1,2\rangle$

When investigating the game dynamics of the ESPD, not only does the underlying graph topology, but also the values of the parameters T and P in the pay-off matrix, have to be considered as these parameter values may affect the dynamics of the game. In this section, the phase plane for the ESPD with $C_n\langle 1,2\rangle$ as underlying graph is constructed using the notation and technique described in §4.4. The various parameter regions in which game dynamics are to be investigated independently are then identified from the phase plane.

The circulant $C_n\langle 1,2\rangle$ is 4-regular (*i.e.* each player of the ESPD with $C_n\langle 1,2\rangle$ as underlying graph has four other players in its open neighbourhood). Therefore, if the number of cooperators i in a player's open neighbourhood is known, the number of defectors j can be calculated as $j = 4 - i$. The pay-off value of player v adopting the strategy of cooperation or defection, with i cooperators in its open neighbourhood, is denoted by c_i or d_i, respectively. Hence the possible different pay-off values that a player can achieve are $c_0, c_1, c_2, c_3, c_4, d_0, d_1, d_2, d_3$ and d_4, which may be written in terms of the parameters T and P as $0, \frac{1}{4}, \frac{1}{2}, \frac{3}{4}, 1, P, \frac{1}{4}T + \frac{3}{4}P, \frac{1}{2}T + \frac{1}{2}P, \frac{3}{4}T + \frac{1}{4}P$ and T, respectively.

Recall, from §4.4, that $d_i > c_j$ for all values of i and j satisfying $i \geq j$. The pay-off value d_0 also does not affect the outcome of the updating process of a player in the game. Therefore, the transitions in the phase plane are given by the six equations

$$\begin{aligned} c_4 = d_3 &\Rightarrow 4 = 3T + P, \\ c_4 = d_2 &\Rightarrow 4 = 2T + 2P, \\ c_4 = d_1 &\Rightarrow 4 = T + 3P, \\ c_3 = d_2 &\Rightarrow 3 = 2T + 2P, \\ c_3 = d_1 &\Rightarrow 3 = T + 3P, \text{ and} \\ c_2 = d_1 &\Rightarrow 2 = T + 3P. \end{aligned}$$

[1] The Euler totient of a positive integer $n > 1$ is the number of positive integers less than n that are relatively prime to (*i.e.* do not contain any factor larger than 1 in common with) n [38].

These isoclines result in a phase plane with eleven parameter regions which potentially induce different game dynamics, as shown in Figure 5.4.

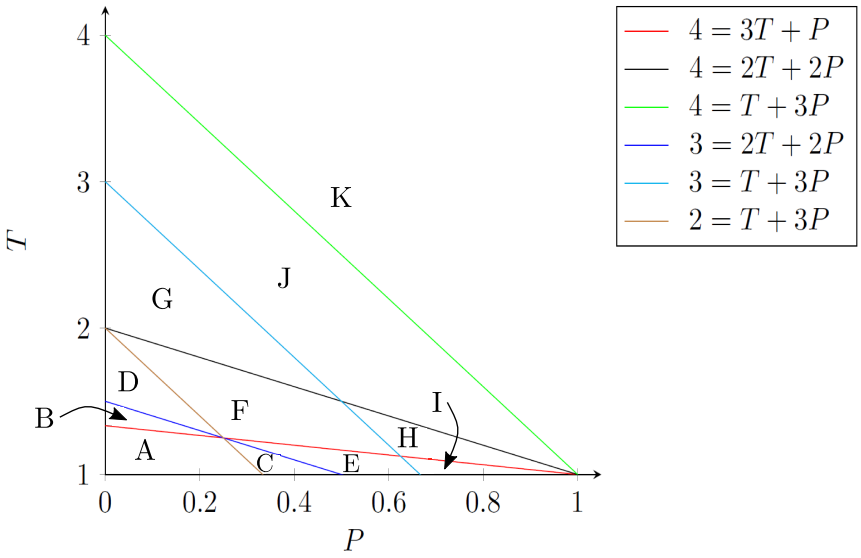

FIGURE 5.4: *The P-T phase plane for the ESPD with the circulant $C_n\langle 1,2\rangle$ as underlying graph, containing eleven disjoint parameter regions, labelled A to K.*

When considering the various cases for which the ESPD with the circulant $C_n\langle 1,2\rangle$ as underlying graph will result in each of the six isoclines mentioned, it can be seen that for certain isoclines, the outcome of the updating process depends on another isocline. Therefore, the isocline considered does not result in a phase transition and may hence be ignored in the subsequent phase plane analysis.

Consider, for example, the isocline $4 = T + 3P$. The case in which a player compares the pay-off values c_4 and d_1 is illustrated in Figure 5.5. The players achieving c_4 and d_1 are marked in red. As each player compares the pay-off values of the largest-valued cooperator and defector in its closed neighbourhood, all players between the two red marked players rather compare the pay-off values of c_4 and d_2. The updating process therefore depends on the isocline $4 = 2T + 2P$. Hence, the isocline $4 = T + 3P$ does not change the dynamics of the game, and therefore need not be considered. Applying similar analyses to each isocline in turn, a simplified phase plane may be constructed from which the isoclines $4 = T + 3P$, $3 = T + 3P$ and $2 = T + 3P$ are absent. The resulting phase plane with five distinct parameter regions is shown in Figure 5.6.

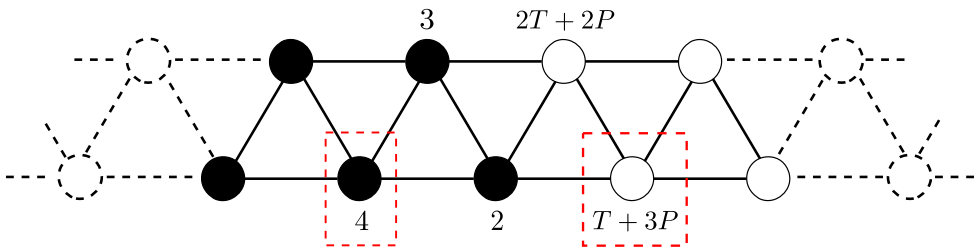

FIGURE 5.5: *The case of the isocline $4 = T + 3P$ for the ESPD with the circulant $C_n\langle 1,2\rangle$ as underlying graph. Black vertices represent players adopting the strategy of cooperation, while white vertices represent players adopting the strategy of defection. The pay-off values of the players are shown above the corresponding vertices. The two players with pay-off values of c_4 and d_1 are marked in red.*

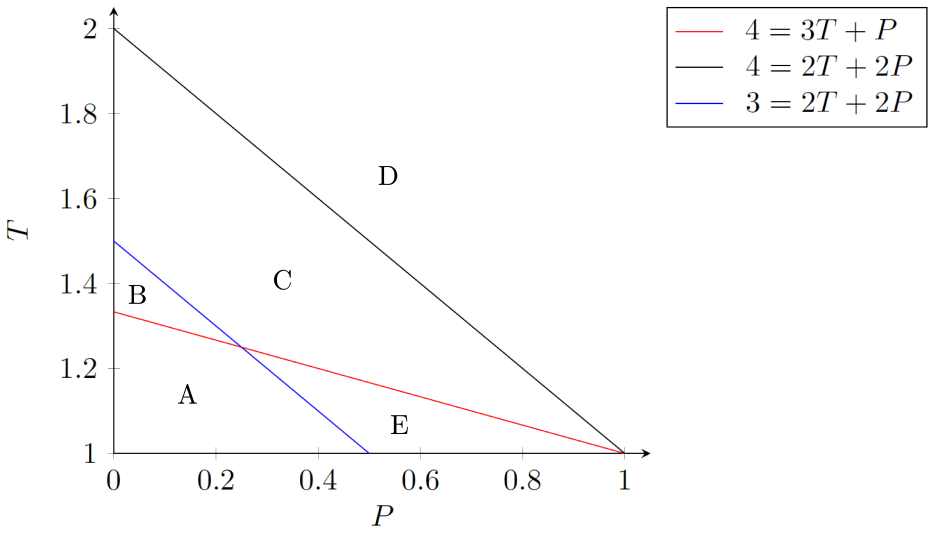

FIGURE 5.6: *The simplified P-T phase plane for the ESPD with the circulant $C_n\langle 1, 2\rangle$ as underlying graph, containing five disjoint parameter regions, labelled A to E.*

5.4 Equilibrium states analysis

In order to study the long-term behaviour of the ESPD with the circulant $C_n\langle 1, 2\rangle$ as underlying graph, each region of the phase plane shown in Figure 5.6 is studied independently due to the potentially different game dynamics induced by these parameter regions. In this section, it is first shown that parameter region D is incapable of inducing persistent cooperation, while parameter regions A, B, C and E all allow for the possibility of persistent cooperation. For the latter set of parameter regions, the equilibrium states are characterised in each case in order to facilitate the construction of corresponding state graphs for the ESPD with the circulant $C_n\langle 1, 2\rangle$ as underlying graph.

5.4.1 Characterisation of equilibrium states

Burger *et al.* [11] showed that for any connected graph G of order n with maximum degree Δ, the state graph of the ESPD with G as underlying graph has exactly two components if $T > \Delta(1 - P) + P$. Applying this theorem to the ESPD with $C_n\langle 1, 2\rangle$ as underlying graph, it follows that if $T > 4(1-P)+P$, or equivalently, if $T > 4-3P$ (*i.e.* the game parameters lie within region D of the phase plane in Figure 5.6), then the state graph has exactly two components. These two components contain the all-cooperator state $\langle C\rangle^n$ and the all-defector steady state $\langle D\rangle^n$, respectively. All states except $\langle C\rangle^n$ are attracted by the all-defector steady state $\langle D\rangle^n$ in this case. Hence persistent cooperation is not possible unless the strategy of cooperation is universally adopted by all players initially.

Each of the other four parameter regions is considered independently. Lemmas 1, 2, 3 and 4 elucidate the various strategy adoption structures required for cooperation to persist to the next round of the game for parameter regions A, B, C and E, respectively. Only the proof of Lemma 1 is provided in this section. The same proof technique may, however, be applied to establish the results of Lemmas 2, 3 and 4, as demonstrated in Appendix A.

Lemma 1. *If the underlying graph of the ESPD is the circulant $C_n\langle 1,2\rangle$ and the parameter inequalities $3T+P<4$ and $2T+2P<3$ hold (i.e. the game parameters lie within region A of the phase plane in Figure 5.6), then*

(a) no cooperation run of length one, two or three can persist intact to the next round of the game,

(b) a cooperation run of length four can persist intact to the next round of the game if and only if it is flanked by two defection runs, each of length at least three, and

(c) a cooperation run of length at least five can persist to the next round of the game if and only if it is flanked on both sides by either a run of defectors of length at least two or by a run of the form DCD.

Proof:

(a) A cooperation run of length one has the form DCD. Figure 5.7 illustrates this configuration for the ESPD with the circulant $C_n\langle 1,2\rangle$ as underlying graph. Black vertices represent players adopting the strategy of cooperation, while white vertices represent players adopting the strategy of defection. Grey vertices represent players with unknown strategies. This graphical representation format is used in all figures throughout this proof.

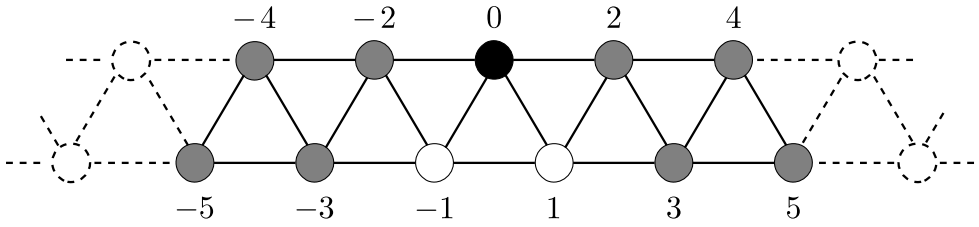

FIGURE 5.7: *Configuration of a cooperation run of length one for the ESPD with the circulant $C_n\langle 1,2\rangle$ as underlying graph.*

In the configuration shown in Figure 5.7, for the cooperating player 0 to persist to the next round of the game, it requires a pay-off value at least as large as the largest pay-off value of the two defecting players -1 and 1 in its open neighbourhood. As shown previously, $d_i > c_j$ if $i \geq j$ for all $i,j \in \mathbb{Z}$. Let

$$a_i = \begin{cases} 0, & \text{if player } i \text{ adopts the strategy of defection, or} \\ 1, & \text{if player } i \text{ adopts the strategy of cooperation.} \end{cases}$$

Therefore, the pay-off value of the cooperating player 0 is $c_{a_{-2}+a_2}$ and the pay-off values of the defecting players -1 and 1 are $d_{1+a_{-2}+a_{-3}}$ and $d_{1+a_2+a_3}$, respectively. It can now be seen that $a_{-2}+a_2 \leq 1+a_{-2}+a_{-3}$ and $a_{-2}+a_2 \leq 1+a_2+a_3$. Therefore, $d_{1+a_{-2}+a_{-3}} > c_{a_{-2}+a_2}$ and $d_{1+a_2+a_3} > c_{a_{-2}+a_2}$. The cooperating player 0 will consequently not be able to achieve a pay-off value at least as large as either of its two defecting neighbouring players -1 and 1, and will hence adopt the strategy of defection during the next round of the game. This shows that no cooperation run of length one can remain intact to the next round of the game.

Consider next a cooperation run of length two. Such a run has the form $DCCD$. This configuration is shown in Figure 5.8 for the ESPD with the circulant $C_n\langle 1,2\rangle$ as underlying graph.

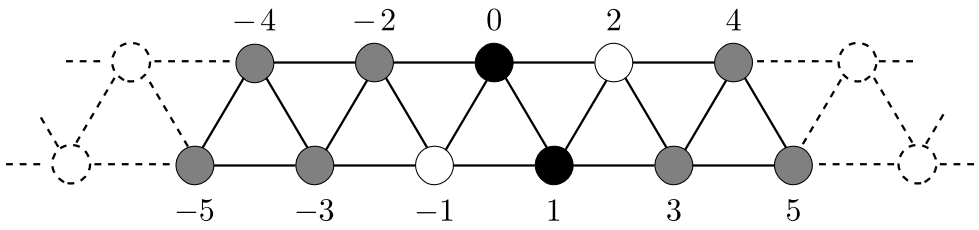

FIGURE 5.8: *Configuration of a cooperation run of length two for the ESPD with the circulant* $C_n\langle 1,2\rangle$ *as underlying graph.*

The pay-off values of the cooperating players 0 and 1 are $c_{1+a_{-2}}$ and c_{1+a_3}, respectively, while the pay-off values of the defecting players -1 and 2 are $d_{2+a_{-2}+a_{-3}}$ and $d_{2+a_3+a_4}$, respectively. Therefore, using a similar logic as for a cooperation run of length one above, it can be seen that the inequalities $c_{1+a_{-2}} < d_{2+a_{-2}+a_{-3}}$ and $c_{1+a_3} < d_{2+a_3+a_4}$ hold as a result of the fact that $1+a_{-2} < 2+a_{-2}+a_{-3}$ and $1+a_3 < 2+a_3+a_4$. The two cooperating players 0 and 1 are hence unable to achieve pay-off values at least as large as those of their two defecting neighbours -1 and 2, and will consequently adopt the strategy of defection during the next round of the game. This shows that no cooperation run of length two can remain intact to the next round of the game.

Finally, consider a cooperation run of length three. Such a run has the form $DCCCD$. This configuration is shown in Figure 5.9 for the ESPD with the circulant $C_n\langle 1,2\rangle$ as underlying graph.

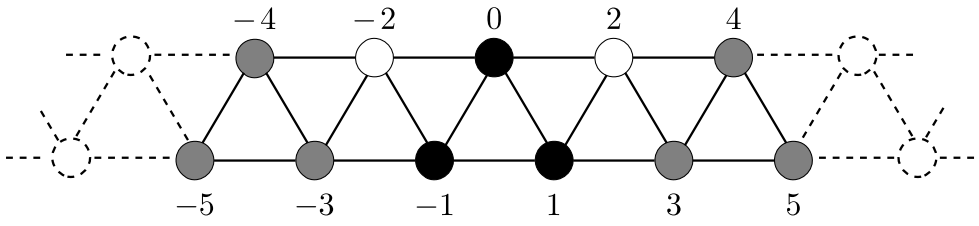

FIGURE 5.9: *Configuration of a cooperation run of length three for the ESPD with the circulant* $C_n\langle 1,2\rangle$ *as underlying graph.*

The pay-off values of cooperating players 0, 1 and -1 are c_2, $c_{2+a_{-3}}$ and c_{2+a_3}, respectively, while the pay-off values of the defecting players -2 and 2 are $d_{2+a_{-3}+a_{-4}}$ and $d_{2+a_3+a_4}$, respectively. Therefore, using a similar logic as for a cooperation run of length one, this results in the inequalities $d_{2+a_{-3}+a_{-4}} > c_{2+a_{-3}}$, $d_{2+a_{-3}+a_{-4}} > c_2$, $d_{2+a_3+a_4} > c_{2+a_3}$ and $d_{2+a_3+a_4} > c_2$ because of the relationships $2 + a_{-3} + a_{-4} \geq 2 + a_{-3}$, $2 + a_{-3} + a_{-4} \geq 2$, $2 + a_3 + a_4 \geq 2 + a_3$ and $2 + a_3 + a_4 \geq 2$. The three cooperating players 0, 1 and -1 are therefore unable to achieve pay-off values at least as large as those of their two defecting neighbours -2 and 2, and will hence adopt the strategy of defection during the next round of the game. This shows that no cooperation run of length three can remain intact to the next round of the game.

(b) A cooperation run of length four has the form $DCCCCD$. This configuration is illustrated in Figure 5.10 for the ESPD with the circulant $C_n\langle 1,2\rangle$ as underlying graph.

The pay-off values of players $-1, 0, 1, 2$, representing the run of cooperators of length four, are $c_{2+a_{-3}}, c_3, c_3$ and c_{2+a_4}, respectively. The largest cooperator pay-off value is therefore c_3. Since only the largest-valued cooperator is relevant in each player's closed neighbourhood during the

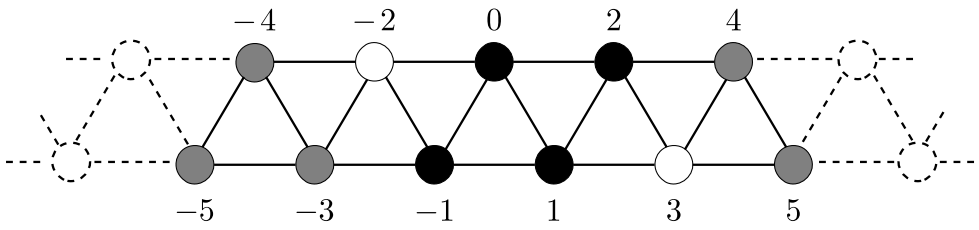

FIGURE 5.10: *Configuration of a cooperation run of length four for the ESPD with the circulant $C_n\langle 1,2\rangle$ as underlying graph.*

updating process, only c_3 is compared with the pay-off value of the players in the cooperation run of length four. The pay-off values achieved by the defecting players -2 and 3 are $d_{2+a_{-3}+a_{-4}}$ and $d_{2+a_4+a_5}$, respectively. In the parameter region A, however, $c_3 > d_2$. Therefore, in order for the inequalities $c_3 > d_{2+a_{-3}+a_{-4}}$ and $c_3 > d_{2+a_4+a_5}$ to hold, ensuring the largest-valued cooperator has a larger pay-off value then the largest-valued defector, it must hold that $a_{-3} + a_{-4} = 0$ and $a_4 + a_5 = 0$. In order for these equalities to be satisfied, it is required that $a_{-4} = a_{-3} = a_4 = a_5 = 0$. It can therefore be deduced that, in order for the run of cooperators of length four to persist intact to the next round of the game, it must be flanked by two defection runs, each of length at least three.

(c) A cooperation run of length five has the form $DCCCCCD$. This configuration is illustrated in Figure 5.11 for the ESPD with the circulant $C_n\langle 1,2\rangle$ as underlying graph.

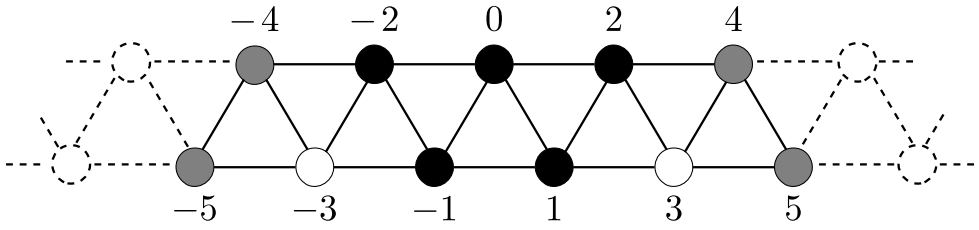

FIGURE 5.11: *Configuration of a cooperation run of length five for the ESPD with the circulant $C_n\langle 1,2\rangle$ as underlying graph.*

The run of cooperators of length five, consisting of players $-2, -1, 0, 1$ and 2, achieve the pay-off values $c_{2+a_{-4}}, c_3, c_4, c_3$ and c_{2+a_4}, respectively. The largest pay-off value achieved by a cooperator in this run is therefore c_4. Since each player compares the pay-off value achieved by the largest-valued cooperator and defector in its closed neighbourhood, only the largest pay-off value c_4 is relevant. The two neighbouring defectors, players -3 and 3, achieve the pay-off values $d_{2+a_{-4}+a_{-5}}$ and $d_{2+a_4+a_5}$, respectively. According to the parameter region inequalities, however, $d_3 < c_4$. Therefore, in order for the inequalities $d_{2+a_{-4}+a_{-5}} < c_4$ and $d_{2+a_4+a_5} < c_4$ to hold, it is required that $2 + a_{-4} + a_{-5} \leq 3$ and $2 + a_4 + a_5 \leq 3$. Hence, both $a_{-4} + a_{-5} \leq 1$ and $a_4 + a_5 \leq 1$ must hold. There are only three binary combinations of (a_{-4}, a_{-5}), namely $(0,0)$, $(1,0)$ or $(0,1)$, which satisfy the first inequality $a_{-4} + a_{-5} \leq 1$. These combinations represent the three possible configurations DD, CD or DC which are required to flank the negative side of $DCCCCCD$. In the combinations in which $a_{-4} = 0$ (*i.e.* player -4 adopts the strategy of defection), the strategy of player -5 is shown to be irrelevant to the outcome of the updating processes of the players within the cooperation run of length five. This is because a_{-5} either has the value of 0 or 1 for the above inequality to hold. There are also three binary combinations of (a_4, a_5), namely $(0,0)$,

$(1,0)$ or $(0,1)$, satisfying the second inequality, $a_4 + a_5 \leq 1$. This allows for the positive side of $DCCCCCD$ to be flanked only by either DD, DC or CD. In the combinations in which $a_4 = 0$ (*i.e.* player 4 adopts the strategy of defection), the strategy of player 5 is again irrelevant to the outcome of the updating processes of the players within the cooperation run of length five. It can therefore be deduced that, in order for the run of cooperators of length five to persist intact to the next round of the game, the run must be flanked on both sides by either a defection run of length two or by the configuration DCD.

A run of cooperators of length greater than five has the form $D\langle C\rangle^i D$ for $i > 5$. Within this configuration, the largest cooperator pay-off value is c_4. The two outer defectors, namely players $\lfloor -\frac{n-1}{2} \rfloor$ and $\lceil \frac{n-1}{2} \rceil$ obtain the pay-off values $d_{2+a_{-\lceil \frac{i}{2} \rceil - 1}+a_{-\lceil \frac{i}{2} \rceil - 2}}$ and $d_{2+a_{\lceil \frac{i}{2} \rceil + 1}+a_{\lceil \frac{i}{2} \rceil + 2}}$, respectively. These pay-off values are similar to those for a cooperation run of length five. Since each player compares the pay-off value achieved by the largest-valued cooperator and defector in its closed neighbourhood and these are equivalent to the situation for a cooperation run of length five, the same result as mentioned above is obtained. It can therefore be deduced that, in order for the run of cooperators of length $i \geq 5$ to persist intact to the next round of the game, the run must be flanked on both sides by either a run of defectors of length two or by the configuration DCD. □

Lemmas 2, 3 and 4 establish the various strategy adoption structures required for cooperation to persist to the next round of the game for parameter regions B, C and E, respectively, as indicated in Figure 5.6.

Lemma 2. *If the underlying graph of the ESPD is the circulant $C_n\langle 1,2\rangle$ and the parameter inequalities $3T + P > 4$ and $2T + 2P < 3$ hold (i.e. the parameters lie within region B of the phase plane in Figure 5.6), then*

(a) no cooperation run of length one, two or three can persist intact to the next round of the game, and

(b) a cooperation run of length at least four can persist to the next round of the game if and only if it is flanked on both sides by a run of defectors of length at least three.

The proof of Lemma 2 may be found in Appendix A.

Lemma 3. *If the underlying graph of the ESPD is the circulant $C_n\langle 1,2\rangle$ and the parameter inequalities $3T + P > 4$, $2T + 2P > 3$ and $2T + 2P < 4$ hold (i.e. the parameters lie within region C of the phase plane in Figure 5.6), then*

(a) no cooperation run of length one, two, three or four can persist intact to the next round of the game, and

(b) a cooperation run of length at least five can persist to the next round of the game if and only if it is flanked on both sides by a run of defectors of length at least three.

The proof of Lemma 3 may be found in Appendix A.

Lemma 4. *If the underlying graph of the ESPD is the circulant $C_n\langle 1,2\rangle$ and the parameter inequalities $3T + P < 4$ and $2T + 2P > 3$ hold (i.e. the parameters lie within region E of the phase plane in Figure 5.6), then*

(a) no cooperation run of length one, two, three or four can persist intact to the next round of the game, and

(b) a cooperation run of length at least five can persist to the next round of the game if and only if it is flanked on both sides by either a run of defectors of length at least two or by a run of the form DCD.

The proof of Lemma 4 may be found in Appendix A.

5.4.2 Enumeration of equilibrium states

Using the structures identified in Lemmas 1–4 that allow cooperation to persist to the next round of the game, all possible equilibrium states of the game can be enumerated. In order to enumerate the equilibrium states, a well-known fact characterising distribution problems in the realm of combinatorial analysis is first presented in Lemma 5. The equilibrium states for each of the parameter regions in the phase plane of Figure 5.6 are thereafter enumerated. Only the proof for parameter region B is presented in this chapter. The same proof technique may, however, be applied for parameter regions A, C and D, as demonstrated in Appendix B.

In combinatorial distribution problems, the following lemma, whose proof can be found in [39], may be adopted to enumerate all possible distributions of indistinguishable objects into distinguishable containers.

Lemma 5. *There are $\binom{m+n-1}{m}$ distinct ways of distributing m indistinguishable objects among n distinguishable containers in the case where empty containers are allowed.*

Consider an example of six distinguishable containers in which ten indistinguishable objects are arbitrarily distributed according to the representation $\bullet\,\bullet\,|\bullet\,\bullet\,|\bullet\,\bullet\,||\bullet\,\bullet\,\bullet\,|\bullet$, where an object is denoted by the symbol "$\bullet$" and a divider separating the objects into different containers is denoted by the symbol "|". Note that only five divider symbols are shown, but six containers are, in fact, represented. Therefore, the number of dividers is one fewer than the number of containers. The first and last container are not delimited by a divider at the beginning or end of the string of symbols, respectively. If the string starts or ends with the character "|", the first or last container is therefore considered to be empty. It can also be seen that the fourth container in the example above contains no "$\bullet$" and is therefore empty.

The quantity enumerated in Lemma 5 is therefore equivalent to the number of distinct strings which can be constructed by a linear arrangement of $n-1$ indistinguishable characters, denoted by "|", and m indistinguishable characters, denoted by "$\bullet$". There are $(m+n-1)!$ different ways of forming strings from $m+n-1$ distinguishable characters. Discounting the number of ways of arranging the m indistinguishable characters "$\bullet$" and the n distinguishable characters "|" results in the number of distinct strings being

$$\frac{(m+n-1)!}{m!(n-1)!} = \binom{m+n-1}{m}.$$

The result of Lemma 5 is used in the proof of the following result.

Theorem 4. *Suppose the underlying graph of the ESPD is the circulant $C_n\langle 1,2\rangle$.*

(a) If the parameter inequalities $3T+P<4$ and $2T+2P<3$ hold (i.e. the parameters lie within region A of the phase plane in Figure 5.6), then the number of equilibrium states

of the game is given by

$$
\begin{aligned}
&2+\sum_{i=1}^{\lfloor \frac{n}{7} \rfloor} \frac{1}{2i}\left[\binom{n-5i-1}{2i-1}+\sum_{j\in S_1}\binom{(n-5i)\gcd(i,j)/i-1}{2\gcd(i,j)-1}+i\sum_{k=0}^{\lfloor \frac{n-7i}{2} \rfloor}(n-7i-2k+1)\binom{k+i-2}{i-2}\right]\\
&+\sum_{i=1}^{\lfloor \frac{n}{7} \rfloor} \frac{1}{i}\left[\binom{n-6i-1}{i-1}+\sum_{j\in S_1}\binom{(n-6i)\gcd(i,j)/i-1}{\gcd(i,j)-1}+i\sum_{k=0}^{\lfloor \frac{n-7i}{2} \rfloor}(n-7i-2k+1)\binom{k+\lfloor \frac{i}{2} \rfloor-2}{\lfloor \frac{i}{2} \rfloor-2}\right]\\
&+\sum_{i_1=1}^{\lfloor \frac{n-8}{7} \rfloor}\sum_{i_2=1}^{\lfloor \frac{n-7i_1}{8} \rfloor}\frac{1}{2i_1+i_2}\left[\left(\frac{(i_1+i_2-2)!}{(i_1-1)!(i_2-1)!}\right)\binom{n-5i_1-7i_2-1}{2i_1+i_2-1}+\right.\\
&\left(\frac{(gcd(2i_1+i_2,j)-2)!}{(\frac{i_1}{(2i_1+i_2)/gcd(2i_1+i_2,j)}-1)!(\frac{i_2}{(2i_1+i_2)/gcd(2i_1+i_2,j)}-1)!}\right)\\
&\sum_{j\in S_2}\binom{(n-7i_1-8i_2)\gcd(2i_1+i_2,j)/(2i_1+i_2)+\gcd(2i_1+i_2,j)-1}{\gcd(2i_1+i_2,j)-1}\\
&\left.+(2i_1+i_2)\left(\frac{(\frac{i_1+i_2-2}{2})!}{(\frac{i_1-1}{2})!(\frac{i_2-1}{2})!}\right)\sum_{k=0}^{\lfloor \frac{n-7i_1-8i_2}{2} \rfloor}(n-7i_1-8i_2-2k+1)\binom{k+\lfloor \frac{2i_1+i_2}{2} \rfloor-2}{\lfloor \frac{2i_1+i_2}{2} \rfloor-2}\right],
\end{aligned}
\tag{5.2}
$$

where S is the set $\{x \in \mathbb{N} \mid (i_1+i_2)$ divides $n\gcd(i_1+i_2,x)$ and $x<(i_1+i_2)\}$.

(b) Else if the parameter inequalities $3T+P>4$ and $2T+2P<3$ hold (i.e. the parameters lie within region B of the phase plane in Figure 5.6), then the number of equilibrium states is given by

$$
2+\sum_{i=1}^{\lfloor \frac{n}{7} \rfloor} \frac{1}{2i}\left[\binom{n-5i-1}{2i-1}+\sum_{j\in \hat{S}}\binom{(n-5i)\gcd(i,j)/i-1}{2\gcd(i,j)-1}+i\sum_{k=0}^{\lfloor \frac{n-7i}{2} \rfloor}(n-7i-2k+1)\binom{k+i-2}{i-2}\right],
\tag{5.3}
$$

where $\hat{S}$ is the set $\{x \in \mathbb{N} \mid i$ divides $n\gcd(i,x)$ and $x<i\}$.

(c) Else if the parameter inequalities $3T+P>4$, $2T+2P>3$ and $2T+2P<4$ hold (i.e. the parameters lie within region C of the phase plane in Figure 5.6), then the number of equilibrium states is given by

$$
2+\sum_{i=1}^{\lfloor \frac{n}{8} \rfloor} \frac{1}{2i}\left[\binom{n-6i-1}{2i-1}+\sum_{j\in \bar{S}}\binom{(n-6i)\gcd(i,j)/i-1}{2\gcd(i,j)-1}+i\sum_{k=0}^{\lfloor \frac{n-8i}{2} \rfloor}(n-8i-2k+1)\binom{k+i-2}{i-2}\right],
\tag{5.4}
$$

where $\bar{S}$ is the set $\{x \in \mathbb{N} \mid i$ divides $n\gcd(i,x)$ and $x<i\}$.

(d) Else if the parameter inequalities $3T+P<4$ and $2T+2P>3$ hold (i.e. the parameters lie within region E of the phase plane in Figure 5.6), then the number of equilibrium states is given by

$$
2+\sum_{i=1}^{\lfloor \frac{n}{8} \rfloor} \frac{2^{i-1}}{i}\left[\binom{n-6i-1}{2i-1}+\sum_{j\in \tilde{S}}\binom{(n-6i)\gcd(i,j)/i-1}{2\gcd(i,j)-1}+i\sum_{k=0}^{\lfloor \frac{n-8i}{2} \rfloor}(n-8i-2k+1)\binom{k+i-2}{i-2}\right],
\tag{5.5}
$$

where $\tilde{S}$ is the set $\{x \in \mathbb{N} \mid i$ divides $n\gcd(i,x)$ and $x<i\}$.

Outline of Proof: The equilibrium state enumeration process is carried out for the case in which the parameters lie within region B of the phase plane in Figure 5.6. As the technique used to enumerate equilibrium game states when the parameters lie within the regions C and E is similar, only the enumeration formulae are shown. A slight adaptation of the proof technique is required to enumerate the equilibrium states when the parameters lie within region A. This adaptation is described at the end of the proof outline.

Recall, from Lemma 2, that for cooperation to persist to the next round of the game, a cooperation run of length at least four flanked on both sides by a run of defectors of length at least three is required. In order to enumerate the number of equilibrium states resulting from such a configuration, the number of states containing only the substates $\langle D\rangle^{n_1}\langle C\rangle^{n_2}\langle D\rangle^{n_3}$ has to be counted, where $n_1 \geq 3$, $n_2 \geq 4$ and $n_3 \geq 3$. These states have the form

$$\underbrace{CCCC\ldots}_{\text{run } 1}\underbrace{DDD\ldots}_{\text{run } 2}\underbrace{CCCC\ldots}_{\text{run } 3}\underbrace{DDD\ldots}_{\text{run } 4}\cdots\underbrace{CCCC\ldots}_{\text{run } 2i-1}\underbrace{DDD\ldots}_{\text{run } 2i}, \tag{5.6}$$

where each run has been populated above with the smallest number of cooperators and defectors, as appropriate. As the underlying graph is a circulant, it is vertex-transitive. The endpoints in the partial state (5.6) have therefore been chosen arbitrarily.

Note that the structure of (5.6) is similar to the string containing the characters "|" and " • " mentioned above. Each separating character "|" is now represented by either the run $CCCC$ or DDD, and each object character " • " by either the symbol C or D. As the ordering of the cooperation and defection runs has already been fixed in (5.6), the symbols C and D can be considered indistinguishable for enumeration purposes, serving merely as place holders from a combinatorial point of view. The partial state (5.6) contains $7i$ symbols, leaving $n - 7i$ indistinguishable symbols to be distributed amongst the $2i$ distinguishable runs.

All equilibrium states can be represented by (5.6), except for the all-cooperator and all-defector steady states. As deduced from Lemma 2, no run of cooperators of length smaller than four or run of defectors of length smaller than three prevails in any steady state. Therefore, let Q_i denote the number of states, up to automorphism, comprising i cooperation runs and i defection runs, starting in a run of cooperators and ending in a run of defectors as shown in (5.6). The total number of equilibrium classes is therefore given by

$$2 + \sum_{i=1}^{\lfloor \frac{n}{7} \rfloor} Q_i.$$

Let χ be the set of all states of the form (5.6). In order to determine Q_i, the game states within the set χ have to be partitioned into game state equivalence classes (in order to prevent the enumeration of equivalent states) and the number of classes enumerated. Let G be the group of permutations that partitions χ into its equivalence classes. Recall, from §2.2.2, that the Cauchy-Frobenius Lemma can be used to determine the number of these equivalence classes. The value of Q_i for $i \in \{1, 2, \ldots, \lfloor \frac{n}{7} \rfloor\}$ is therefore given by

$$Q_i = \frac{1}{|G|}\sum_{g\in G}|F_g|, \tag{5.7}$$

where $|F_g|$ is the number of states in χ that remain invariant under a permutation g.

In order to determine the symmetry group of the states of the form (5.6), let ι be the identity permutation on the sequence of runs of a state $s \in \chi$. Let ρ^j be the permutation which modular shifts each run in (5.6) j positions to the right. Let δ furthermore be the operation that reverses the order of the runs in (5.6) so that the first run remains in its original position followed by runs $i, i-1, \ldots$ The symmetry group $G = \{\iota, \rho^1, \rho^2, \ldots, \rho^{i-1}, \delta, \delta\rho^1, \delta\rho^2, \ldots, \delta\rho^{i-1}\}$ of order $2i$ is thus formed under the binary operation of permutation composition. In order to calculate Q_i, according to (5.7), all states that remain invariant under each permutation within G has to be considered.

First, consider the identity operator ι. This operator leaves all elements of χ invariant and therefore $|F_\iota| = |\chi|$. To calculate the number of states within χ, the number of ways of distributing $n - 7i$ indistinguishable symbols amongst $2i$ distinguishable runs has to be determined. Using Lemma 5, it follows that

$$|F_\iota| = \binom{n - 5i + 2i - 1}{2i - 1} = \binom{n - 5i - 1}{2i - 1}. \tag{5.8}$$

Next, consider the permutation ρ^j. For a state to remain invariant under the permutation ρ^j, the first j pairs of runs have to be equivalent to all subsequent runs. To elucidate this claim, consider applying ρ^1 to a state $s \in \chi$. When performing this operation, run i is mapped to run $i + 2$ which, in turn, is mapped to run $i + 4$, and so on. Hence, the numbers of symbols in runs 1 and 2 determine the numbers of symbols in runs 3 and 4 as well as the numbers of symbols in runs 5 and 6, and so on. Therefore, each pair of runs have to be equivalent. Hence, the number of possible states that remain invariant under ρ^1 can be determined by finding the number of distinct ways of distributing $\frac{2}{2i}(n - 7i)$ symbols among two containers, which is given by

$$|F_{\rho^1}| = \binom{\frac{n-7i}{i} + 2 - 1}{2 - 1} = \frac{n - 7i}{i} + 1.$$

Note that if j exactly divides i, then the first j pairs of runs determine the remaining $2(i - j)$ runs. Otherwise, the first $d = \gcd(i, j)$ pairs of runs determine the remaining $2(i - d)$ runs. The number of possible states that remain invariant under ρ^j can therefore be determined by finding the number of ways to distribute $\frac{2d}{2i}(n - 7i)$ symbols among the first $2d$ runs. The enumeration is given by

$$|F_{\rho^j}| = \binom{\frac{2d}{2i}(n - 7i) + 2d - 1}{2d - 1} = \binom{\frac{d}{i}(n - 5i) - 1}{2d - 1}.$$

If, however, $\frac{d}{i}n$ is not an integer, then there are not enough symbols to complete the pattern of runs in order to achieve an invariant state and so $|F_{\rho^j}| = 0$. Therefore,

$$|F_{\rho^j}| = \begin{cases} \binom{\frac{\gcd(i,j)}{i}(n-5i)-1}{2\gcd(i,j)-1}, & \text{if } \frac{\gcd(i,j)}{i}n \in \mathbb{Z} \text{ or} \\ 0, & \text{otherwise.} \end{cases} \tag{5.9}$$

Consider next the permutation δ, which reverses the order of the runs so that the first run remains in its original position, the second run is projected onto the last run, the third run is projected onto the second last run, and so on. Runs 1 and $i + 1$ are projected onto themselves, while runs 2 to i map onto runs $i+2$ to $2i$, respectively. Let k be the number of indistinguishable symbols that are distributed among the $i-1$ distinguishable runs not mapping onto themselves. The number of ways of distributing the k symbols among these $i-1$ runs is $\binom{k+i-2}{i-2}$, provided that the inequality $0 \leq k \leq n - 7i$ holds. The remaining $n - 7i - 2k$ symbols are distributed among the two runs that map onto themselves, which can be done in $\binom{n-7i-2k+2-1}{2-1} = n - 7i - 2k + 1$ distinct ways. In order to enumerate the number of distinct game states that remain invariant under the permutation δ, all possible values of k are to be considered. Therefore,

$$|F_\delta| = \sum_{k=0}^{\lfloor \frac{n-7i}{2} \rfloor} (n - 7i - 2k + 1)\binom{k + i - 2}{i - 2}. \tag{5.10}$$

Finally, consider the permutation composition $\delta\rho^j$ which shifts the runs j positions to the left and then reverses the order of the runs. Under this permutation, runs $j + 1$ and $i + j + 1$ map

onto themselves, while runs $j+2$ to $i+j$ map onto runs $j-1$ to $i+j+2$, respectively. Once again k indistinguishable symbols can be distributed among $i-1$ distinguishable runs that do not map onto themselves in $\binom{k+i-2}{i-2}$ different ways, provided that the inequality $0 \leq k \leq n-7i$ holds. Again, the remaining $n-7i-2k$ symbols can be distributed among the two runs that map onto themselves in $\binom{n-7i-2k+2-1}{2-1} = n-7i-2k+1$ distinct ways. Therefore, the number of distinct game states that remain invariant under the permutation $\delta\rho^j$ equals the number in (5.10).

Taking all the various permutations into account and therefore substituting (5.8),(5.9) and (5.10) into (5.7), the number of equilibrium states for the ESPD with $C_n\langle 1,2\rangle$ as underlying graph and for which the inequalities $3T+P>4$ and $2T+2P<3$ hold (*i.e.* the parameters lie within region B of the phase plane in Figure 5.6) is

$$Q_i = \frac{1}{2i}\left[\binom{n-5i-1}{2i-1} + \sum_{j\in S}\binom{(n-5i)\gcd(i,j)/i-1}{2\gcd(i,j)-1} + i\sum_{k=0}^{\lfloor\frac{n-7i}{2}\rfloor}(n-7i-2k+1)\binom{k+i-2}{i-2}\right],$$

where S is the set $\{x \in \mathbb{N} \mid i \text{ divides } n\ \gcd(i,x) \text{ and } x<i\}$. □

In the same way the enumeration of the equivalence classes for parameter regions C and E, given by (5.4) and (5.5), can be carried out. For the enumeration of the equivalence classes corresponding to parameter region A an adaptation of the proof is required. This is because an equilibrium state can take on more than one form in this case. Recall, from Lemma 1, that in order for cooperation to persist to the next round of the game, either a cooperation run of length four flanked on both sides by a defector run of length at least two or a cooperation run of length greater than four flanked on both sides by either a run of defectors of length at least two or by the configuration DCD is required. It can be shown in the latter case that the configuration DCD flanking the cooperator run will transform into the configuration DDD during the next round of the game. This claim is proved in the following lemma and then used to illustrate the adaptation of the enumeration of equivalence classes for parameter region B previously presented, in the case of parameter region A.

Lemma 6. *If the underlying graph of the ESPD is the circulant $C_n\langle 1,2\rangle$ and the parameter inequalities $3T+P<4$ and $2T+2P<3$ hold (i.e. the parameters lie within region A of the phase plane in Figure 5.6), then an equilibrium state must contain the following for cooperation to persist:*

(a) A cooperation run of length four flanked on both sides by a defection run of length at least three, or
(b) a cooperation run of length at least five flanked on both sides by a defection run of length at least two.

Outline of Proof: Consider a run of cooperators of length greater than four with one side flanked by DCD. A substate of this configuration consisting of a cooperation run of length five flanked on the right by DCD is illustrated in Figure 5.12.

Consider the playing and updating phases during a single round of the game for the player marked in red in the figure. During the playing phase, the pay-off value achieved by this player is at most $c_2 = 2$. Furthermore, during the updating phase, the defector and cooperator with the largest pay-off value in this player's closed neighbourhood are compared. The defector with the largest pay-off value achieves the pay-off value $d_3 = 3T+P$ and is marked in blue in the figure. In order to determine the cooperator with the largest pay-off value, the strategy of the grey player is required. The grey player can either adopt the strategy of cooperation or

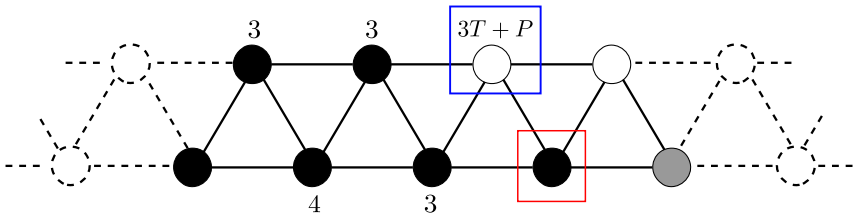

FIGURE 5.12: *Configuration of a cooperation run of length five flanked on the right side by DCD. The parameter values that are known for the various players within the configuration are denoted above or below the corresponding vertices. The player marked in red, will adopt the strategy of defection during the next round of the game, if the parameter values T and P lie within parameter region A.*

defection. In the case where the grey player adopts the strategy of cooperation, it is able to achieve the largest pay-off value $c_3 = 3$ of all the cooperating players in the red player's closed neighbourhood. Otherwise, in the case where the grey player adopts the strategy of defection, the red player achieves the largest pay-off value of all the cooperators. In the two cases, the inequalities $d_3 > c_3$ and $d_3 > c_2$ hold, respectively. The player indicated in red will therefore adopt the strategy of defection during the next round of the game. The resulting configuration after a single round of the game is subsequently $\langle C\rangle^5 DDD$. Hence, in order for cooperation to be present in an equilibrium state, a run of cooperators of length four flanked on both sides by a run of defectors of length at least three or a run of cooperators of length greater than four flanked on both sides by a run of defectors of length at least two is required. □

Employing Lemma 6, the adaptation of the enumeration of the number of equivalence classes for parameter region B so as to be applicable to parameter region A can now be demonstrated. First, the set of all possible game states S can be partitioned into two sets X and Y as illustrated in Figure 5.13. The set X consists of all states that contain the configuration $DDD\langle C\rangle^4 DDD$, while the set Y consists of all states that contain the configuration $DD\langle C\rangle^n DD$, for some $n \geq 5$. The set $X \cap Y$ contains all states that contain both the configuration $DDD\langle C\rangle^4 DDD$ and $DD\langle C\rangle^n DD$, for some $n \geq 5$. The number of equilibrium states $|\chi|$ is therefore $|X|+|Y|-|X\cap Y|$. In order to enumerate the overall number of equivalence classes, the number of equivalence classes in each set can be determined using the same technique as that used to enumerate the number of equivalence classes for parameter region B. The number of equilibrium states for the ESPD with $C_n\langle 1, 2\rangle$ as underlying graph is illustrated in Figure 5.14 for $1 \leq n \leq 20$ for each of the parameter regions in the phase plane of Figure 5.6.

5.4.3 Enumeration of the components in the state graph

The enumeration of the equilibrium states presented in Theorem 4 may be utilised to enumerate the components in the state graph. A fundamental prerequisite to the enumeration of the components in the state graph is, however, that the state graph is a rooted pseudo-forest. In order to establish this property it is necessary to investigate the existence of limit cycles within this graph. More specifically, the possibility of oscillation of game states in the state graph must be ruled out in order to establish that limit cycles do not exist. To that end, the following result, namely that defection is inherently more stable than cooperation, is useful. This result can be used to show that oscillation between game states is not possible and therefore that limit cycles do not exist. The result, however, only holds for the ESPD with $C_n\langle 1, 2\rangle$ as underlying graph and for the parameter regions C, D or E of the phase plane in Figure 5.6. The enumeration of the components in the state graph is therefore only carried out for these cases.

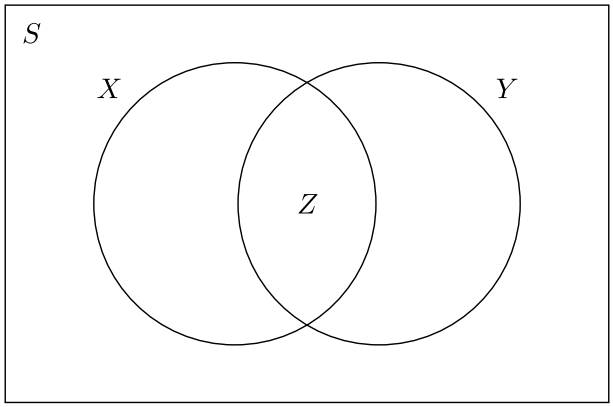

FIGURE 5.13: *A Venn diagram illustrating the partition of the set of all game states into subsets. The set X consists of all states that contain the configuration $DDD\langle C\rangle^4 DDD$, while the set Y consists of all states that contain the configuration $DD\langle C\rangle^n DD$, where $n \geq 5$.*

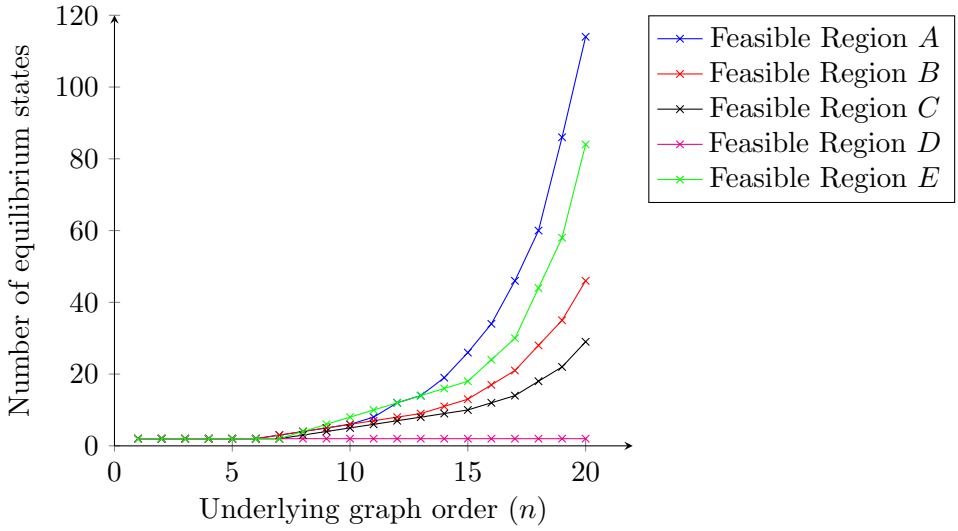

FIGURE 5.14: *The enumeration of the equilibrium states, up to automorphism, of the ESPD with $C_n\langle 1,2\rangle$ as underlying graph for the various parameter regions of the phase plane in Figure 5.6.*

Lemma 7. *If the underlying graph of the ESPD is the circulant $C_n\langle 1,2\rangle$ and the parameter inequality $2T + 2P > 3$ holds (i.e. the parameters lie within region C, D or E of the phase plane in Figure 5.6), then each component of the state graph is a rooted pseudo-tree.*

Proof: Consider a player adopting the strategy of defection. In order to investigate the ability of the player changing its strategy to cooperation, three cases in which the player has different open neighbourhood configurations have to be considered. In the first two cases, the defecting player is shown to retain its strategy, while in the third the defecting player retains its strategy only under certain parameter conditions.

First, consider the case where the defector has four defectors in its open neighbourhood. In this case, the defector will certainly defect again during the next round because there are only defectors in its closed neighbourhood. Consider next, a defector with one cooperator in its open neighbourhood. The configuration is illustrated in Figure 5.15, where player 0 is the defector and player 2 is the cooperator.

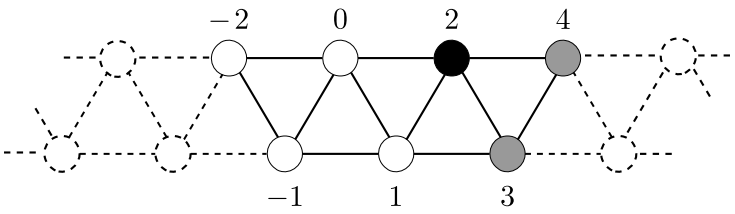

FIGURE 5.15: *Configuration of a defector with one cooperator in its open neighbourhood.*

Player 0, adopting the strategy of defection, achieves a pay-off value of $T + 3P$, while player 2, adopting the strategy of cooperation, achieves a pay-off value of either 0, 1 or 2, depending on the strategies of players 3 and 4. In the configuration shown, one of player 0's defecting neighbours will always be adjacent to the cooperating player 2 (*i.e.* player 1). Player 1 achieves the pay-off value of $3T + P$ or $2T + 2P$, depending on the strategy of player 3. Player 1's pay-off value is strictly larger than player 2's pay-off value for each possible strategy configuration assigned to players 3 and 4, as $T > 1$. Therefore, the player with the maximum pay-off value in the closed neighbourhood of player 0 is player 1. According to the local imitation rule, player 0 will therefore retain the strategy of defection during the next round of the game.

Finally, consider the case where the defector has at least two cooperators in its neighbourhood. The pay-off value of the defector is at least $2T + 2P$ and the pay-off value of the cooperator is at most 3. This configuration is illustrated in Figure 5.16, where the defector with pay-off value $2T + 2P$ is represented by player 0 and the cooperator with pay-off value 3 is represented by player 2.

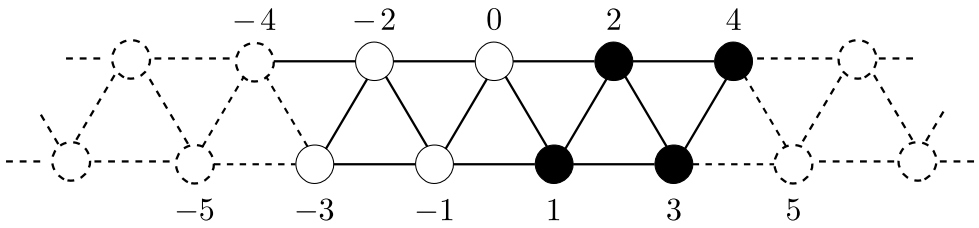

FIGURE 5.16: *Configuration of a defector with two cooperators in its open neighbourhood. The case in which the cooperator positioned at vertex 2 has the largest possible pay-off value of c_3 is shown.*

If the inequality, $2T + 2P > 3$ holds (*i.e.* the parameters lie within the parameter region C, D or E in the phase plane in Figure 5.6), player 0, adopting the strategy of defection, will always achieve a larger pay-off value than each of the cooperators in its open neighbourhood. Therefore, the defector will retain its strategy of defection during the next round of the game. On the other hand, if the inequality $2T + 2P < 3$ holds (*i.e.* the parameters lie within feasible region A or B in the phase plane of Figure 5.6), the cooperator will achieve the largest pay-off value. The defector will therefore adopt the strategy of cooperation during the next round of the game, and so defection is only inherently more stable than cooperation if the inequality $2T + 2P > 3$ holds.

As the ESPD is deterministic (every game state gives rise to a unique game state during the next round of the game), every vertex in the state graph has out-degree 1. As a defector will persist with its strategy under the condition $2T + 2P > 3$, it follows that a player is unable to change its strategy from defection to cooperation and then back to defection. Therefore, no oscillation of game states is possible. Hence, the state graph of the ESPD with $C_n\langle 1, 2\rangle$ as underlying graph does not contain any limit cycles and so the state graph is a rooted pseudo-forest, and each component of the state graph has a steady state as its root. □

It follows from Lemma 7 that the enumeration of the components of the state graph of the ESPD with $C_n\langle 1,2\rangle$ as underlying graph and parameters lying within region C, D or E of the phase plane in Figure 5.6 is equivalent to the enumeration of the equilibrium states as presented in Theorem 4.

5.5 The probability of persistent cooperation

In order to determine the probability that a random initial game state will lead to some form of persistent cooperation, all possible substates that allow for cooperation to persist are identified. This allows for the enumeration of all possible states that contain these substates, thereby facilitating computation of the probability of a state containing one of these substates.

The following theorem characterises the initial game states of the ESPD with the circulant $C_n\langle 1,2\rangle$ as underlying graph which lead to some form of persistent cooperation and therefore are not attracted by the all-defector state $\langle D\rangle^n$ for the various parameter regions of the phase plane in Figure 5.6.

Theorem 5. *Suppose the underlying graph of the ESPD is the circulant $C_n\langle 1,2\rangle$.*

(a) Suppose the parameter inequalities $3T+P<4$ and $2T+2P<3$ hold (i.e. the parameters lie within region A of the phase plane in Figure 5.6), then if and only if a state contains at least one of the substates $DDD\langle C\rangle^4DDD$, $DD\langle C\rangle^5DD$, $DCD\langle C\rangle^5DCD$, $DD\langle C\rangle^5DCD$, $\langle C\rangle^6DD$, $DCD\langle C\rangle^6DCD$ $\langle C\rangle^7DCD$, $\langle C\rangle^8$ (or any of their reverses) it is not in the component of the state graph which contains the all-defector steady state.

(b) Suppose the parameter inequalities $3T+P>4$ and $2T+2P<3$ hold (i.e. the parameters lie within region B of the phase plane in Figure 5.6), then if and only if a state contains at least one of the substates $DDD\langle C\rangle^4DDD$, $DDD\langle C\rangle^5DDD$, $\langle C\rangle^6DDD$, $\langle C\rangle^8$ (or any of their reverses) it is not in the component of the state graph which contains the all-defector steady state.

(c) Suppose the parameter inequalities $3T+P>4$, $2T+2P>3$ and $2T+2P<4$ hold (i.e. the parameters lie within region C of the phase plane in Figure 5.6), then if and only if a state contains at least one of the substates $DDD\langle C\rangle^5DDD$, $DDD\langle C\rangle^6DDD$, $\langle C\rangle^7DDD$, $\langle C\rangle^9$ (or any of their reverses) it is not in the component of the state graph which contains the all-defector steady state.

(d) Suppose the parameter inequalities $3T+P<4$ and $2T+2P>3$ hold (i.e. the parameters lie within region E of the phase plane in Figure 5.6), then if and only if a state contains at least one of the substates $DD\langle C\rangle^5DD$, $DCD\langle C\rangle^5DCD$, $DD\langle C\rangle^5DCD$, $DD\langle C\rangle^6DD$, $DCD\langle C\rangle^6DCD$, $DD\langle C\rangle^6DCD$, $\langle C\rangle^7DD$, $\langle C\rangle^7DCD$, $\langle C\rangle^9$ (or any of their reverses) it is not in the component of the state graph which contains the all-defector steady state.

Outline of Proof: All the substates that allow for cooperation to persist are determined according to Lemma 1 for each parameter region in Figure 5.6. This is established by considering successively all states consisting of cooperation runs of length $i\in\{4,5,6,7,8\}$. In this way, all states that lead to one of the characterised states mentioned in Lemma 1 after a single round of the game are considered. If any of the states contains a previously considered state as a substate it is not included as it has already been considered. This enables all the possible subsets to be characterised that will lead to cooperation persisting. □

The probability $P(n)$ that some form of cooperation will persist from a randomly generated initial state for the ESPD with $C_n\langle 1,2\rangle$ as underlying graph can now be expressed as

$$P(n) = 1 - \frac{b_n}{2^n},$$

where b_n denotes the total number of states that contain none of the substrings mentioned in the statement of the theorem, but contain at least one D. In order to determine the value of b_n, the *transfer matrix method* is adopted.[2]

In order to demonstrate the use of the transfer matrix method, consider the ESPD with $C_n\langle 1,2\rangle$ as underlying graph in the case where the inequalities $3T + P < 4$ and $2T + 2P < 3$ hold (*i.e.* the parameters lie within region A of the phase plane in Figure 5.6). In order to determine $P(n)$, the total number of binary strings b_n containing none of the substrings $DDD\langle C\rangle^4 DDD$, $DD\langle C\rangle^5 DD$, $DCD\langle C\rangle^5 DCD$, $DD\langle C\rangle^5 DCD$, $D\langle C\rangle^6 DDD$, $D\langle C\rangle^6 DCD$, $\langle C\rangle^7 DD$, $\langle C\rangle^7 DCD$ and $\langle C\rangle^8$ are to be enumerated. Classify a string containing the characters C and D as a *legal string* if it contains none of the above-mentioned forbidden substrings. Therefore, b_n denotes the number of possible legal strings.

In order to calculate b_n, a digraph D_{11} of order $2^{11} = 2\,048$ is constructed, because the largest forbidden substring has length 11 (*i.e.* $DCD\langle C\rangle^5 DCD$). Within the digraph each vertex represents a possible string containing the characters C and D. As there are 2 048 possible combinations, the graph contains 2 048 vertices. A vertex v_i representing the string $s_1s_2s_3s_4s_5s_6s_7s_8s_9s_{10}s_{11}$ is incident to vertex v_j representing the string $s_2s_3s_4s_5s_6s_7s_8s_9s_{10}s_{11}s_{12}$ in D_{11} if and only if $s_1s_2s_3s_4s_5s_6s_7s_8s_9s_{10}s_{11}s_{12}$ is a legal string. The digraph D_{11} is depicted in Figure 5.17, merely to illustrate its complexity. Each legal string of length n has an associated closed, directed walk of length n in D_{11}, for some $n \geq 12$. Therefore, in order to determine the value of b_n the number of closed directed walks of length n can be counted. This principle is illustrated in Figure 5.18, where the closed, directed walk associated with the legal string $DCDCDDDCDDCDD$ is shown. Note that the string consists of 13 characters and that the directed walk also has length 13.

Recall, from §2.1.3, that the number of closed walks $C_D(n)$ of length n in a digraph D with adjacency matrix $\boldsymbol{A}$, is

$$\sum_{n=1} C_D(n)x^n = \frac{-xQ'(x)}{Q(x)},$$

where $Q(x) = \det(\boldsymbol{I} - x\boldsymbol{A})$.

Let $\boldsymbol{A}$ be the adjacency matrix of the digraph D_{11} in Figure 5.17. The structure of $\boldsymbol{A}$ is illustrated graphically in Figure 5.19. In fact, $\det(\boldsymbol{I} - x\boldsymbol{A}) = 1 - x - x^2 - x^3 - x^4 - x^5 - x^6 - x^7 + 2x^8 + x^9$. As $b_n = C_D(n)$, it therefore follows that

$$\sum_{n=1}^{\infty} b_n x^n = \frac{-x(-1 - 2x - 3x^2 - 4x^3 - 5x^4 - 6x^5 - 7x^6 + 16x^7 + 9x^8)}{1 - x - x^2 - x^3 - x^4 - x^5 - x^6 - x^7 + 2x^8 + x^9}. \tag{5.11}$$

The Taylor expansion of the function in (5.11) is given by

$$F(x) = x + 3x^2 + 7x^3 + 15x^4 + 31x^5 + 63x^6 + 106x^7 + 215x^8 + 430x^9 + 843x^{10} + 1\,651x^{11} + \ldots \tag{5.12}$$

The coefficient of the term x^n in this expansion is the number of closed walks of length n. There are thus, three closed walks of length two, seven closed walks of length three, and so on.

[2] The transfer matrix method is a method for determining the number of directed walks of a specified length in a directed graph. The interested reader is referred to [65] for a detailed description of the method.

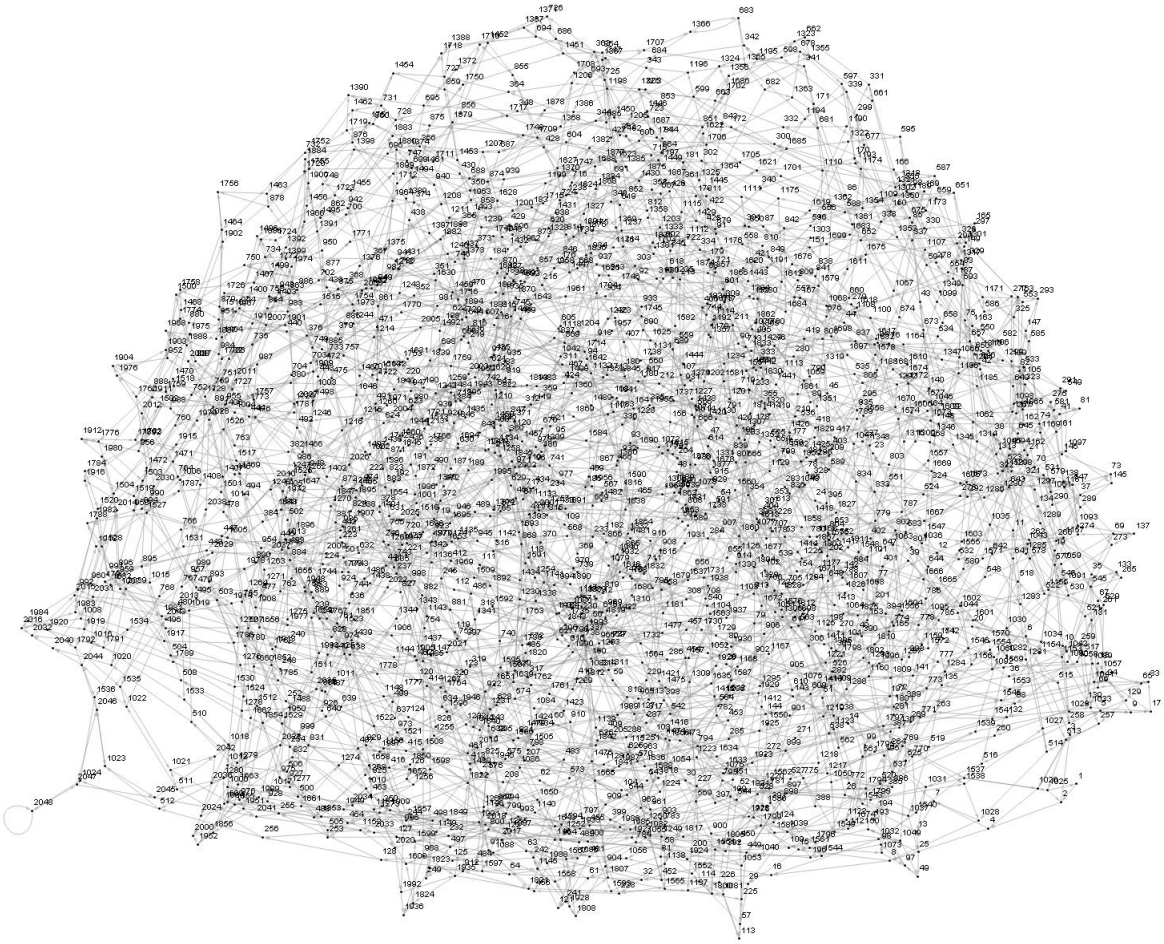

FIGURE 5.17: *The digraph D_{11} for parameter region A. The vertices are labelled by integer representations in the set $\{1, \ldots, 2048\}$.*

According to the transfer matrix method, the value of b_n may therefore be calculated recursively by solving the linear recurrence relation

$$b_n = b_{n-1} + b_{n-2} + b_{n-3} + b_{n-4} + b_{n-5} + b_{n-6} + b_{n-7} - 2b_{n-8} - b_{n-9}. \tag{5.13}$$

The seed values for (5.13) can be found from the coefficients of the Taylor expansion in (5.12). These seed values are listed in Table 5.1.

b_1^*	b_2^*	b_3^*	b_4^*	b_5^*	b_6^*	b_7^*	b_8^*	b_9^*	b_{10}^*	b_{11}^*
1	3	7	15	31	63	106	215	430	843	1 651

TABLE 5.1: *The seed values required to solve the recurrence equation (5.13).*

Adopting this approach for each parameter region, the probability that a randomly generated initial state will lead to some form of persistent cooperation can be calculated for the ESPD with $C_n\langle 1, 2\rangle$ as underlying graph, as demonstrated in the following theorem.

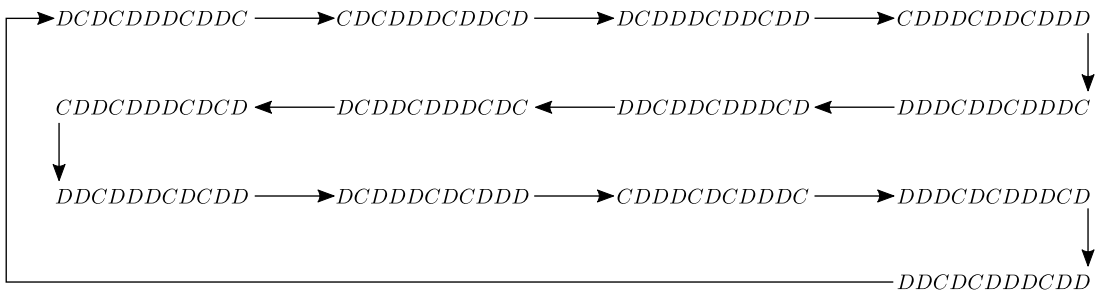

FIGURE 5.18: *A closed walk in D_{11} associated with the string $DCDCDDDCDDCDD$.*

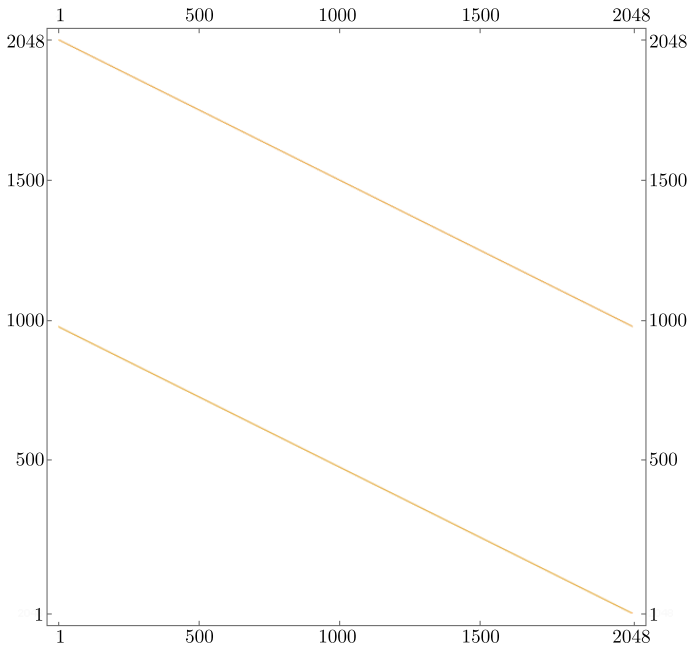

FIGURE 5.19: *Positions of the unit entries in the adjacency matrix of the digraph D_{11}.*

Theorem 6. *The probability that some form of cooperation persists from a randomly generated initial state of the ESPD with the circulant $C_n\langle 1,2\rangle$ as underlying graph is given by*

$$P(n) = 1 - \frac{b_n}{2^n}, \tag{5.14}$$

where b_n satisfies one of the following relationships with seed values as specified in Table 5.2 for the associated parameter regions of the game.

(a) If the parameter inequalities $3T + P < 4$ and $2T + 2P < 3$ hold (i.e. the parameters lie within region A of the phase plane in Figure 5.6), then the value of b_n satisfies

$$b_n = b_{n-1} + b_{n-2} + b_{n-3} + b_{n-4} + b_{n-5} + b_{n-6} + b_{n-7} - 2b_{n-8} - b_{n-9}. \tag{5.15}$$

(b) If the parameter inequalities $3T + P > 4$ and $2T + 2P < 3$ hold (i.e. the parameters lie within region B of the phase plane in Figure 5.6), then the value of b_n satisfies

$$b_n = b_{n-1} + b_{n-2} + b_{n-3} + b_{n-4} + +b_{n-5} - b_{n-6} - b_{n-7} + b_{n-8} + b_{n-9}. \tag{5.16}$$

(c) If the parameter inequalities $3T + P > 4$, $2T + 2P > 3$ *and* $2T + 2P < 4$ *hold (i.e. the parameters lie within region C of the phase plane in Figure 5.6), then the value of* b_n *satisfies*

$$b_n = b_{n-1} + b_{n-2} + b_{n-3} + b_{n-4} + b_{n-5} - b_{n-6} - 2b_{n-7} + b_{n-8} + b_{n-9}. \tag{5.17}$$

(d) If the parameter inequalities $3T + P < 4$ *and* $2T + 2P > 3$ *hold (i.e. the parameters lie within region E of the phase plane in Figure 5.6), then the value of* b_n *satisfies*

$$b_n = b_{n-1} + b_{n-2} + b_{n-3} + b_{n-4} + b_{n-5} + b_{n-6} + b_{n-7} - b_{n-8} - b_{n-9}. \tag{5.18}$$

	b_1^*	b_2^*	b_3^*	b_4^*	b_5^*	b_6^*	b_7^*	b_8^*	b_9^*	b_{10}^*	b_{11}^*
Region A	1	3	7	15	31	63	106	215	430	843	1 651
Region B	1	3	7	15	31	63	113	223	457	903	1 772
Region C	1	3	7	15	31	63	120	231	457	903	1 816
Region E	1	3	7	15	31	63	127	239	475	953	1 893

TABLE 5.2: *The seed values required to calculate* b_n *in the recurrence relations (5.15)–(5.18).*

The results of Theorem 6 are illustrated graphically in Figure 5.20 for an underlying circulant of order $n \in \{5, \ldots, 100\}$.

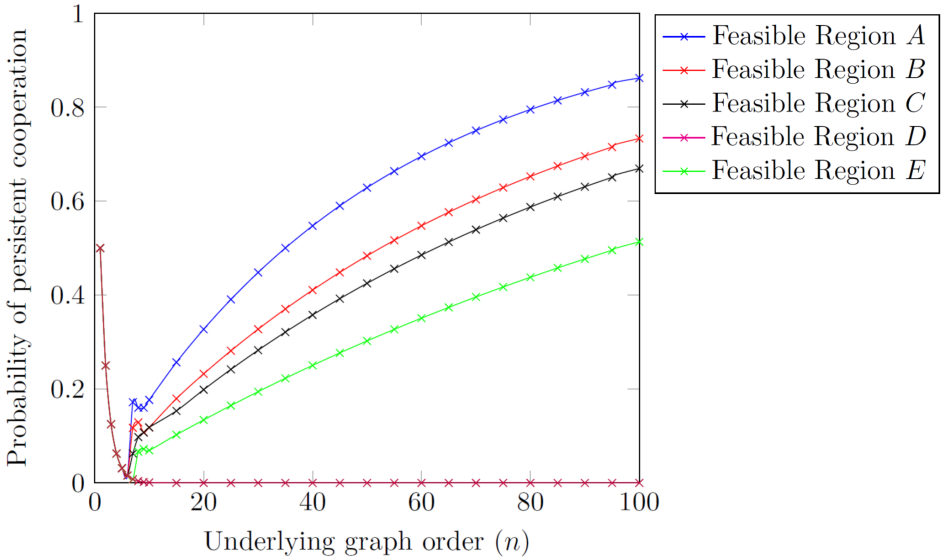

FIGURE 5.20: *The probability of a randomly generated initial state of the ESPD with* $C_n\langle 1, 2\rangle$ *as underlying graph leading to the persistence of some form of cooperation.*

In order to investigate the asymptotic behaviour of the probability $P(n)$ in (5.14), it is shown next that the sequence $b_1, b_2, b_3, \ldots$ is positive and strictly increasing for parameter regions A, B, C and E in Figure 5.6. This result is, however, only proven for the case where the parameters lie within the region A of the phase plan in Figure 5.6. The same technique may be used to prove the result for the remaining regions (in these cases, only the result is stated).

Lemma 8. *The terms in the sequence* $b_1, b_2, b_3, \ldots$ *are positive and strictly increasing for each set of recursive relationships and seed values presented in Theorem 6.*

Proof: The proof is given in the strong form of mathematical induction for case (a) in Theorem 6 only. Consider the sequence $b_1, b_2, b_3, \ldots$ satisfying the relationship $b_n = b_{n-1} + b_{n-2} + b_{n-3} + b_{n-4} + b_{n-5} + b_{n-6} + b_{n-7} - 2b_{n-8} - b_{n-9}$ as specified in Theorem 6(a) and the seed values in the first row of Table 5.1 for parameter region A of the phase plane in Figure 5.6.

Suppose the induction hypothesis $b_n > b_{n-1} > 0$ holds for all $n \leq k$. It can be seen from the seed values in Table 5.1 that the result of the lemma holds for $1 \leq n \leq 12$. This serves as the base case for the induction process. Substituting $n = k + 1$ for all instances of k in the above recurrence relation gives

$$b_{k+1} = b_k + b_{k-1} + b_{k-2} + b_{k-3} + b_{k-4} + b_{k-5} + b_{k-6} - 2b_{k-7} - b_{k-8}.$$

By the induction hypothesis, the inequality $b_{k-4} > b_{k-5} > b_{k-6} > b_{k-7} > b_{k-8}$ holds. By repeated use of the induction hypothesis the inequality $b_{k-4} + b_{k-5} + b_{k-6} > 2b_{k-7} + b_{k-8}$ therefore also holds. It is therefore known that $b_{k-4} + b_{k-5} + b_{k-6} - 2b_{k-7} - b_{k-8} > 0$. As all the other terms in the substituted recurrence relation are positive, it follows that $b_{k+1} > b_k > 0$. Therefore, the sequence $b_1, b_2, b_3, \ldots$ is positive and strictly increasing. □

The following asymptotic result may now be established.

Theorem 7. *If the underlying graph of the ESPD is the circulant $C_n\langle 1, 2\rangle$ and if the parameter inequality $T + P < 2$ holds (i.e. the parameters lie within region A, B, C or E of the phase plane in Figure 5.6), then*

$$\lim_{n\to\infty} P(n) = 1.$$

Proof: Consider the relationship $b_n = b_{n-1}+b_{n-2}+b_{n-3}+b_{n-4}+b_{n-5}+b_{n-6}+b_{n-7}-2b_{n-8}-b_{n-9}$ specified in Theorem 6 for parameter region A of the phase plane in Figure 5.6.

Let $T_n = b_{n-2} + b_{n-3} + b_{n-4} + b_{n-5} + b_{n-6} + b_{n-7} - 2b_{n-8} - b_{n-9}$. Then

$$b_n = b_{n-1} + T_n. \tag{5.19}$$

If the indices in the recurrence relation (5.15) are shifted one position to the left, the relationship yields

$$b_{n-1} = b_{n-2} + b_{n-3} + b_{n-4} + b_{n-5} + b_{n-6} + b_{n-7} + b_{n-8} - 2b_{n-9} - b_{n-10}. \tag{5.20}$$

Taking the difference between b_{n-1} and T_n, and substituting (5.20) and (5.19) into b_{n-1} and T_n, respectively, it follows that

$$b_{n-1} - T_n = 3b_{n-8} - b_{n-9} - b_{n-10}.$$

By Lemma 8, $b_{n+1} > b_n > 0$ and therefore by the repeated use of this inequality $3b_{n-8} - b_{n-9} - b_{n-10} > 0$. Consequently, $T_n < b_{n-1}$, and so it follows from (5.19) that $0 < b_n < 2b_{n-1}$. Dividing each term in this inequality by 2^n, it follows that

$$0 < \frac{b_n}{2^n} < \frac{b_{n-1}}{2^{n-1}}.$$

The value of $b_n/2^n$ is therefore decreasing by the above inequality and positive by Lemma 8, and so, for some non-negative real constant c,

$$\lim_{n\to\infty} \frac{b_n}{2^n} = c. \tag{5.21}$$

In order to determine the value of c, note that substituting (5.15) into (5.21), gives

$$\begin{aligned}\lim_{n\to\infty}\frac{b_n}{2^n} &= \lim_{n\to\infty}\frac{b_{n-1}+b_{n-2}+b_{n-3}+b_{n-4}+b_{n-5}+b_{n-6}+b_{n-7}-2b_{n-8}-b_{n-9}}{2^n}\\ &= \frac{1}{2}\lim_{n\to\infty}\frac{b_{n-1}}{2^{n-1}}+\frac{1}{2^2}\lim_{n\to\infty}\frac{b_{n-2}}{2^{n-2}}+\frac{1}{2^3}\lim_{n\to\infty}\frac{b_{n-3}}{2^{n-3}}+\frac{1}{2^4}\lim_{n\to\infty}\frac{b_{n-4}}{2^{n-4}}+\frac{1}{2^5}\lim_{n\to\infty}\frac{b_{n-5}}{2^{n-5}}\\ &\quad+\frac{1}{2^6}\lim_{n\to\infty}\frac{b_{n-6}}{2^{n-6}}+\frac{1}{2^7}\lim_{n\to\infty}\frac{b_{n-7}}{2^{n-7}}-\frac{2}{2^8}\lim_{n\to\infty}\frac{b_{n-8}}{2^{n-8}}-\frac{1}{2^9}\lim_{n\to\infty}\frac{b_{n-9}}{2^{n-9}} \qquad (5.22)\\ &= c\left(\frac{1}{2}+\frac{1}{2^2}+\frac{1}{2^3}+\frac{1}{2^4}+\frac{1}{2^5}+\frac{1}{2^6}+\frac{1}{2^7}-\frac{2}{2^8}-\frac{1}{2^9}\right)\\ &= c.\end{aligned}$$

In order to satisfy (5.22), it is therefore required that $c = 0$. Hence,

$$\lim_{n\to\infty}P(n) = \lim_{n\to\infty}\left(1-\frac{b_n}{2_n}\right) = 1$$

by (5.14). □

The same argument may be employed to determine the same asymptotic behaviour of the probability $P(n)$ for parameter regions B, C and E as demonstrated in Appendix C. These relationships are illustrated graphically in Figure 5.20.

5.6 The effect of extending each player's neighbourhood

The number of equilibrium states of the ESPD with the cycle $C_n\langle 1\rangle$, as well as with the circulant $C_n\langle 1,2\rangle$, as underlying graph is shown in Figure 5.21. As may be seen in the figure, the number of equilibrium states decreases as each player extends its neighbourhood. The relationship between the number of equilibrium states and the graph order is exponential for both underlying graph topologies. The number of components in the state graph is equivalent to the number of equilibrium states for the ESPD with the cycle as underlying graph, as well as for the ESPD with the circulant as underlying graph, but only if the inequality $2T + 2P > 3$ holds (*i.e.* the parameters lie within the region C, D or E in the phase plane of Figure 5.6.) Therefore, as each player extends its neighbourhood in these cases, the number of components in the state graph also decreases.

The change in the relationship between the probability of cooperation persisting and the graph order for the ESPD on a cycle and the ESPD on a circulant is illustrated in Figure 5.22. As may be seen in the figure, the probability of cooperation persisting decreases as each player extends its neighbourhood. As the size of the underlying graph increases, however, the probability of cooperation persisting nevertheless increases towards certainty for both graph topologies, unless the inequality $T > 2 - P$ holds. If this inequality holds (*i.e.* for the case where the underlying graph is a circulant and the parameters lie within region E of the phase plane in Figure 5.6), cooperation is unable to persist for both graph topologies, unless the strategy of cooperation is universally adopted by all players initially. Therefore, in the latter case, the likelihood of cooperation persisting tends towards impossibility as the order of the underlying graph increases, as also illustrated in Figure 5.22.

It may furthermore be concluded that the values of the parameters T and P have a more significant effect on the probability of cooperation persisting for the ESPD where the underlying graph is the circulant $C_n\langle 1,2\rangle$ than in the case of the cycle $C_n\langle 1\rangle$. For the cycle, there are only

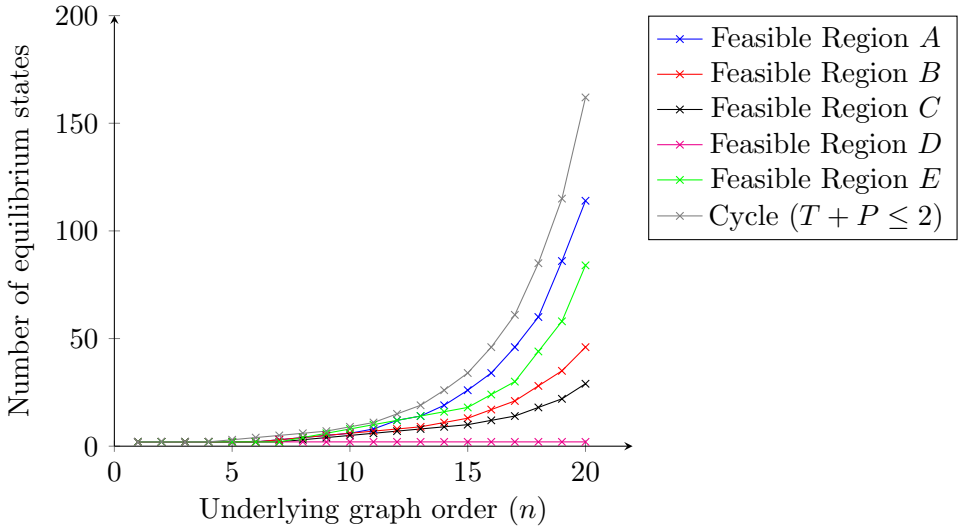

FIGURE 5.21: *The number of the equilibrium game states, up to automorphism, of the ESPD with either the circulant $C_n\langle 1, 2\rangle$ or the cycle $C_n\langle 1\rangle$ of order n as underlying graph.*

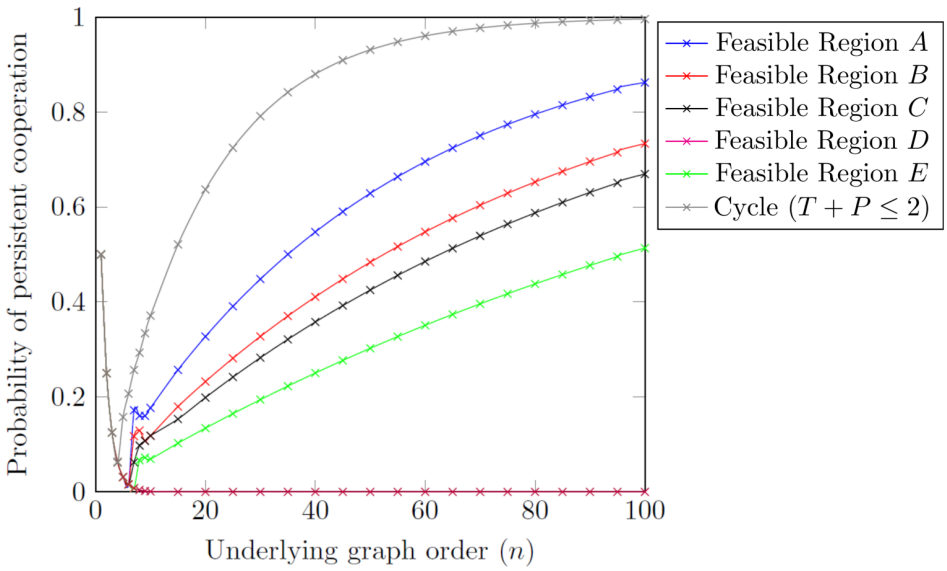

FIGURE 5.22: *The probability of cooperation persisting for a randomly generated initial state of the ESPD with the circulant $C_n\langle 1, 2\rangle$ or the cycle $C_n\langle 1\rangle$ as underlying graph as a function of graph order.*

two parameter regions within the phase plane leading to different game dynamics [11], while for the circulant, five parameter regions induce different game dynamics (as shown in Figure 5.6). It may also be seen in Figure 5.22 that for the ESPD with the circulant as underlying graph, the parameter P more sensitively affects the probability of cooperation persisting than does the parameter T, as a marginal increase in the parameter P results in a larger decrease in the probability of cooperation persisting than the same increase in the value of the parameter T. This supports the modelling choice of Nowak and May [51] of keeping the parameter T constant and only investigating the change in game dynamics for various values of parameter P in their work.

5.7 Chapter summary

Analytical means were employed in this chapter to analyse the long-term game dynamics of the ESPD with the circulant $C_n\langle 1,2\rangle$ as underlying graph. The aim was to determine how the extension of each player's (cyclic) neighbourhood affects the likelihood of persistent cooperation when players are arranged in a cyclic topology.

In §5.1, a brief overview of the analysis of the game dynamics of the ESPD with a cycle as underlying graph was reviewed from the literature. The focus of the chapter then shifted to an investigation of the game dynamics of the ESPD with the circulant $C_n\langle 1,2\rangle$ as underlying graph. An appropriate isometric representation of the ESPD with $C_n\langle 1,2\rangle$ as underlying graph was first established in §5.2, in order to facilitate an understanding of the work presented in the remainder of the chapter. The phase plane was then constructed in §5.3, in which five regions were identified to induce different game dynamics.

A characterisation and enumeration of the possible ESPD equilibrium states followed in §5.4 for each of the parameter regions identified in the previous section. The number of equilibrium states was shown to exhibit an exponential relationship with the order of the underlying graph. The property that the state graph is a rooted pseudo-forest was also shown to hold if the parameter inequality $2T + 2P > 3$ holds. This property facilitated enumeration of the components of the state graph to be equivalent to the number of equilibrium states previously enumerated.

Using the characterisation of the equilibrium states in §5.4, the probability of persistent cooperation resulting from a random initial state was calculated for each of the parameter regions in §5.5. This probability tended towards certainty as the order of the underlying graph increases for parameter regions A, B, C and E.

Finally, the chapter closes with an investigation of the effect of each player extending its cyclic neighbourhood from that of a cycle as underlying graph in §5.6. This entailed a comparison of the game dynamics of the ESPD with a cycle as underlying graph with that of the ESPD with the circulant $C_n\langle 1,2\rangle$ as underlying graph. It was found that as each player extends its neighbourhood, the number of equilibrium states, as well as the probability of cooperation persisting, decreases.

CHAPTER 6

The ESPD on a toroidal grid graph

Contents

This chapter contains an analysis of the game dynamics of the ESPD with a small toroidal grid as underlying graph. The objective is to investigate the ability of the toroidal grid graph to facilitate persistent cooperation in the ESPD. The complexity of this analysis is elucidated in §6.1 and §6.2, in terms of an inherent combinatorial explosion in the analysis and the various parameter regions in the phase plane in which the game has to be analysed (independently). Furthermore, a toroidal grid as underlying graph does not lead to the situation where each component of the ESPD state graph is a rooted psuedo-tree. This gives rise to the potential presence of cycles within the state graph, further increasing the complexity of the analysis. A new analysis visualisation tool, called the equilibrium state diagram, is therefore proposed in §6.3, which may replace the state graph for larger toroidal grid dimensions in analyses of the ESPD game dynamics. Section 6.4 contains explanations of a number of algorithms (and their implementations) for constructing the equilibrium state graph. The equilibrium state diagram of the ESPD is presented in §6.5 for the case of small toroidal grids as underlying graphs. The underlying toroidal grids $C_2 \times C_6$, $C_3 \times C_3$, $C_3 \times C_4$, $C_3 \times C_5$, $C_3 \times C_6$, $C_4 \times C_4$, $C_4 \times C_5$, $C_4 \times C_6$, $C_5 \times C_5$, $C_5 \times C_6$ and $C_6 \times C_6$ are considered. The chapter concludes with a collective analysis of the ability of small grids to allow for the persistence of cooperation.

6.1 A combinatorial explosion

As noted by Nowak [51], the mathematical analysis of evolutionary games on graphs is a complicated task due to the large number of different configurations that such games can exhibit if the underlying graphs are large. This chapter is therefore primarily concerned with an investigation of the game dynamics on *small* toroidal grids.

Consider the ESPD with a toroidal $n \times m$ grid as underlying graph. There are 2^{nm} ways of assigning the strategies C or D to the various players in such an ESPD instance. Table 6.1 shows the number of distinct initial states for $m, n \in \{1, \ldots, 6\}$. The exponential increase in the number of distinct initial states can clearly be seen in the table as the dimensions of the underlying graph increases. A combinatorial explosion is, in fact, prevalent even for very small toroidal grid graphs.

TABLE 6.1: *The number of distinct initial states for the ESPD with the toroidal grid graph $C_n \times C_m$ as underlying graph. The state graphs corresponding to the entries in boldface are known [72]. A study of the game dynamics of the ESPD for the underlying toroidal grid graphs corresponding to entries indicated in red is contributed in this chapter.*

n \ m	1	2	3	4	5	6
1	**2**	**4**	**8**	**16**	**32**	**64**
2		**16**	**64**	**256**	**1 024**	4 096
3			**512**	4 096	32 768	262 144
4				65 536	1 048 576	16 777 216
5					33 554 432	1 073 741 824
6						68 719 476 740

Because the underlying toroidal grid contains a high level of symmetry as a result of its rectangular or square shape, a number of the states in Table 6.1 may, however, be considered equivalent. Van der Merwe [72] enumerated the number of game state automorphism classes for the ESPD with the toroidal grid graph $C_n \times C_m$ as underlying graph. Table 6.2 contains the numbers of game state automorphism classes for $n, m \in \{1, \ldots, 6\}$. The reader is reminded that all initial states within an automorphism class result in equivalent game dynamics. Therefore, when investigating the ESPD game dynamics in this chapter, only the class representatives are considered. As the number of non-isomorphic states in Table 6.2 are significantly smaller (two or three orders of magnitude smaller than the corresponding entries in Table 6.1), this reduces the combinatorial complexity of the analysis. Figure 6.1 contains an organisation of the $2^9 = 512$ distinct game states for the ESPD with $C_3 \times C_3$ as underlying graph into 26 distinct game automorphism classes as a means of validation for the entry in row 3 and column 3 of Table 6.2.

TABLE 6.2: *The number of game state automorphism classes for the ESPD with the toroidal grid graph $C_n \times C_m$ as underlying graph [72]. The state graphs corresponding to the entries in boldface are known [72]. A study of the game dynamics of the ESPD for the underlying toroidal grid graphs corresponding to the entries indicated in red is contributed in this chapter.*

n \ m	1	2	3	4	5	6
1	**2**	**3**	**4**	**6**	**8**	**13**
2		**6**	**13**	**34**	**78**	237
3			**26**	158	708	4 236
4				805	14 676	184 854
5					172 112	8 999 762
6						239 114 084

The boldfaced entries in Tables 6.1 and 6.2 correspond to the various underlying toroidal grids for which ESPD game dynamics have already been investigated within the literature [72]. The red entries in the tables represent the underlying toroidal grids for which ESPD game dynamics are newly investigated in this chapter.

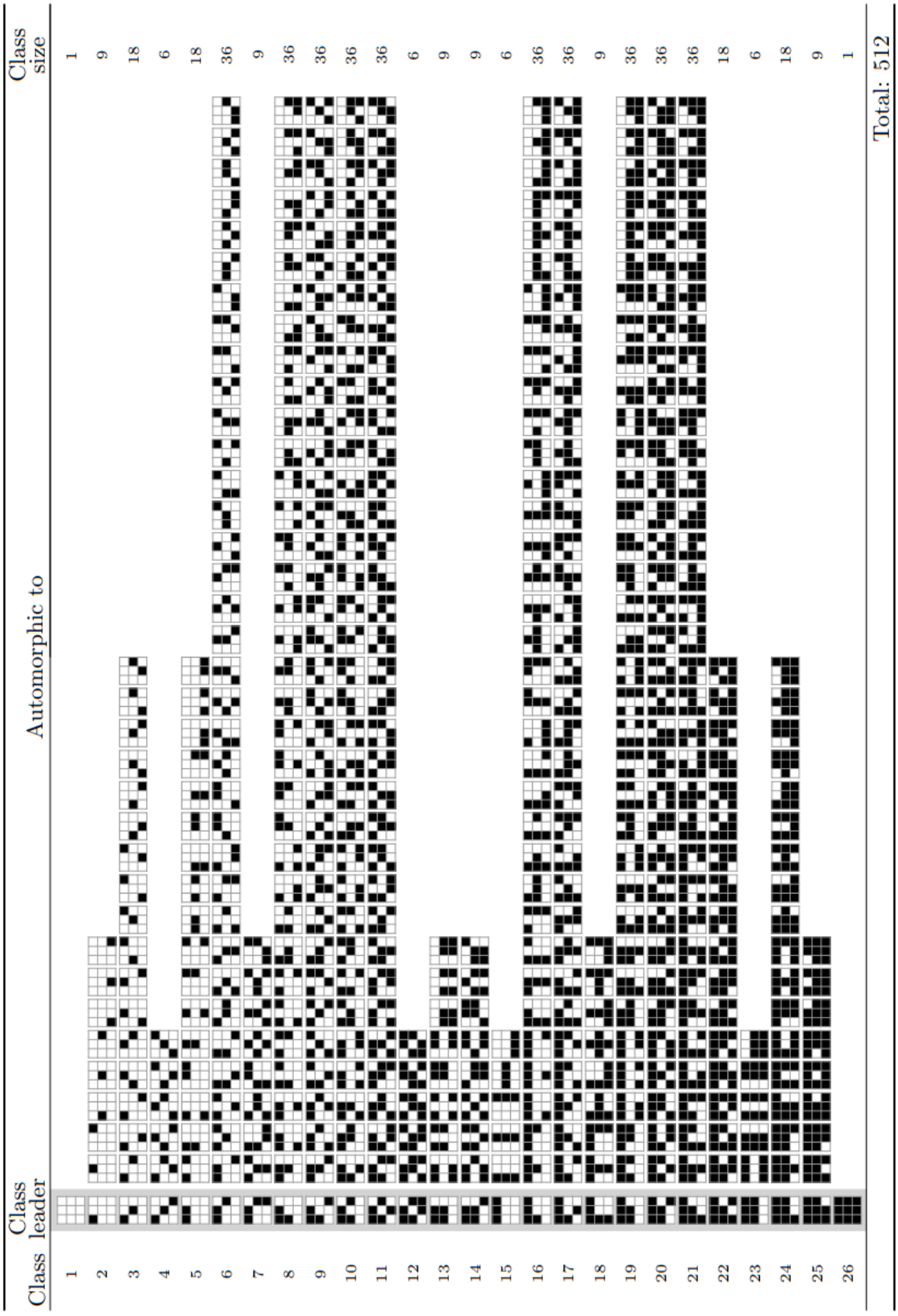

FIGURE 6.1: *The distinct states of the ESPD with the toroidal grid $C_3 \times C_3$ as underlying graph. The second column contains the class leaders of the various state automorphism classes that are indicated in the rows of the figure [72]. Black cells represent players adopting the strategy of cooperation, while white cells represent players adopting the strategy of defection.*

6.2 The phase plane

Recall, from §4.3, that the values of the parameters T and P in the normalised pay-off matrix of the ESPD influence the dynamics of the game significantly. When a change in these parameter values result in an outcome of the game that is different from that with the original choice of parameter values, the change is called a phase transition. As discussed in §5.3, the structure of the underlying graph fundamentally determines where phase transitions occur. When investigating the dynamics of the ESPD, these phase transitions should, of course, also be considered. Consider the ESPD with the Cartesian product $C_n \times C_m$ as the underlying graph. The local playing structure and neighbourhood of each player is shown in Figure 6.2.

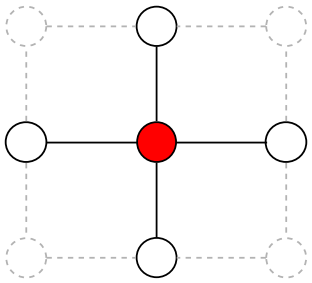

FIGURE 6.2: *The structure of the closed neighbourhood of a player indicated in red is shown for the ESPD with the toroidal grid graph $C_n \times C_m$ as underlying graph.*

The graph underlying the ESPD in this case is 4-regular (*i.e.* each player has four other players in its open neighbourhood). Therefore, adopting the same notation and methodology as in §5.3, the transitions in the phase plane are given by the six isoclines

$$\begin{aligned}
c_4 = d_3 &\Rightarrow 4 = 3T + P,\\
c_4 = d_2 &\Rightarrow 4 = 2T + 2P,\\
c_4 = d_1 &\Rightarrow 4 = T + 3P,\\
c_3 = d_2 &\Rightarrow 3 = 2T + 2P,\\
c_3 = d_1 &\Rightarrow 3 = T + 3P, \text{ and}\\
c_2 = d_1 &\Rightarrow 2 = T + 3P.
\end{aligned}$$

These isoclines result in a phase plane with eleven parameter regions which potentially induce different game dynamics, as shown in Figure 6.3.

Note that the phase plane in Figure 6.3 is not equivalent to that of the ESPD with the circulant $C_n\langle 1, 2\rangle$ as underlying graph, because isoclines were removable in the case of the circulant as underlying graph. The removal of the isoclines for the circulant $C_n\langle 1, 2\rangle$ was possible due to special cases in which no change in the game dynamics was caused by the specific underlying topology. Similar special cases for a toroidal grid as underlying graph only occur for grids of dimension $n \times m$, where either $n \leq 3$ or $m \leq 3$. Hence, for the underlying grids considered in this thesis, no isoclines can be removed and all eleven parameter regions are to be studied independently. As the game is to be analysed for each parameter region, this further increases the complexity of the analysis.

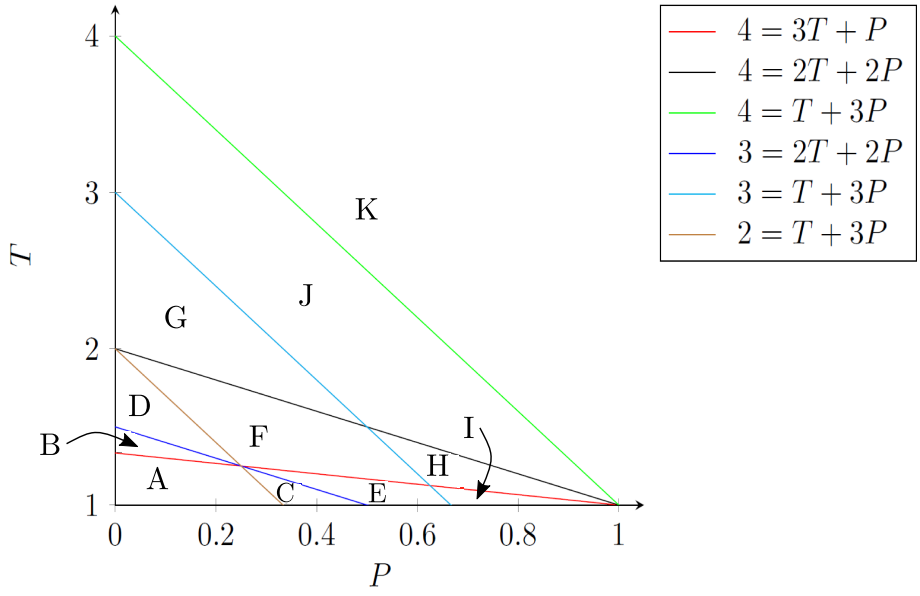

FIGURE 6.3: *The P-T phase plane for the ESPD with the toroidal grid $C_n \times C_m$ as underlying graph, containing eleven disjoint parameter regions, labelled A to K.*

6.3 The equilibrium state diagram

The exponential increase in the number of automorphism class representatives as the dimensions of the underlying toroidal grid graph increases, as well as the presence of cycles within the state graph facilitated by its topology, limits the effective use of a state graph as an analysis and visualisation tool. A new visualisation mechanism for investigating the game dynamics of an ESPD with larger toroidal grids as underlying graphs is therefore introduced in this section.

6.3.1 The need for a new visualisation mechanism

The game dynamics of the ESPD have been investigated exhaustively for the toroidal grids $C_2 \times C_2$, $C_2 \times C_3$, $C_2 \times C_4$, $C_2 \times C_5$ and $C_3 \times C_3$ as underlying graphs [72]. In order to investigate these game dynamics, state graphs were constructed, as discussed in §4.4. As only *very small* grid sizes were considered, these constructions were achievable by hand. Due to the combinatorial explosion discussed in §6.1 and illustrated in Table 6.2, however, it is no longer plausible to attempt an analysis by hand when considering toroidal grids of larger dimensions as underlying graphs for the ESPD.

Consider, for example, the case of the toroidal grid $C_4 \times C_4$ as underlying graph. Initially, 65 536 distinct game states have to be organised into 805 automorphism classes. Thereafter, a state graph containing 805 vertices has to be constructed. The state graph to be constructed in this case is sufficiently large that it becomes a tedious form of representation. A more compact visualisation tool is clearly required. The notion of an *equilibrium state diagram* is therefore proposed in this section as a simplified summary of the information contained in a state graph. This new visualisation mechanism is subsequently used throughout the chapter instead of the notion of a state graph.

Before the equilibrium state diagram is proposed, however, it is important to note that, unlike for the previous underlying graph structures considered both by Burger *et al.* [10, 11] and Van der

Merwe [72], each component of the state graph of the ESPD with a toroidal grid as underlying graph is no longer necessarily a rooted-pseudo tree. As there may potentially be no root, the game does not necessarily tend towards a steady state.

To elucidate the statement above, consider the neighbourhood topology of each player, as shown in Figure 6.2, for an ESPD with the toroidal grid $C_n \times C_m$ as underlying graph. There are cases of the ensuing game dynamics in which a defector adopts the strategy of cooperation at a later stage of the game. An example of such a case is illustrated in Figure 6.4. Player 3, adopting the strategy of cooperation, receives the payoff value c_3, while player 6, adopting the strategy of defection, receives the payoff value d_1. For all parameter regions of the phase plane, except F, G, J and K, it holds that $c_3 > d_1$. Therefore, the defecting player will adopt the strategy of cooperation during the next round of the game in the case of the remaining phase plane regions, demonstrating that a defector does not always persist with its strategy as the game progresses. Hence it is potentially possible that a defector adopts the strategy of cooperation and then later readopts the strategy of defection in a subsequent round of the game. When such a case of evolutionary oscillation occurs, there is a possibility that the long-term game dynamics may result in alternative long-term attracting state structure, such as a *transient steady state* or a *limit cycle*. Hence, the game dynamics do not necessarily tend towards a *static steady state*. The components of a state graph can, therefore, potentially contain cycles (which are prohibited in a rooted-pseudo forest state graph structure). Formal definitions of the aforementioned types of alternative "equilibrium" states are provided in the next section. Although the above phenomenon potentially holds for all toroidal grids, the state graphs of the ESPD with *very small* toroidal grids as underlying graphs (*i.e.* $C_1 \times C_n$ where $n = 1, \ldots, 6$, $C_2 \times C_2$, $C_2 \times C_3$, $C_2 \times C_4$, $C_2 \times C_5$ and $C_3 \times C_3$) which have already been considered in the literature, do not admit any limit cycles. An important problem considered in this chapter is therefore to find the smallest underlying toroidal grid dimensions for which the state graph of the ESPD exhibits a limit cycle.

The visualisation tool proposed in this thesis by which to summarise the dynamics of the ESPD for larger underlying toroidal grids should facilitate, to some extent, both the notion of combinatorial explosion and the various possible types of equilibrium states that may occur in the game dynamics.

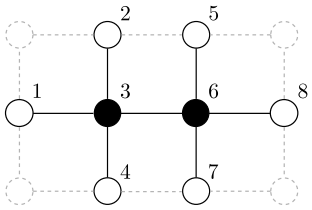

FIGURE 6.4: *A case in which it is possible that the strategy of cooperation is adopted later by a defecting player when the ESPD is played on a toroidal grid within parameter region A in the phase plane of Figure 6.3. Black nodes represent players adopting the strategy of cooperation, while white nodes represent players adopting the strategy of defection.*

6.3.2 The various equilibrium states defined

As mentioned in §3.2, an *equilibrium state* of the ESPD should be understood in the context of a Nash Equilibrium. The reader is reminded that this is the case when there is no mutant strategy that any member of the population can adopt that will result in a larger reproductive fitness value. In the context of a state graph component, an equilibrium state is therefore the

root of the corresponding pseudotree. An equilibrium state can either be a static steady state, a transient steady state or a limit cycle:

A static steady state is an evolutionary unvarying state in which all members of the population persist with their current strategy indefinitely (*i.e.* the game state remains constant for all subsequent rounds of the game).

A transient steady state is a set of evolutionary varying states between which the game varies in an cyclic fashion indefinitely. Furthermore, these states have the property that each game state in the cycle is automorphic to the previous game state. Therefore, each game state contained within the transient steady state forms part of the same automorphism class. The number of game states within a full period of oscillation is known as the *length* of the transient steady state.

A limit cycle is also a set of evolutionary varying states between which the state of the game varies in an cyclic fashion indefinitely, but in which at least two game states are not members of the same automorphism class. The number of game states in a full period of oscillation is again called the *length* of the limit cycle.

Both static and transient steady states are represented in the state graph as a vertex that is adjacent to itself. Because each vertex within the state graph represents an automorphism class, oscillation between members of a class cannot be accommodated in the state graph (that is, the state graph representation does not allow for a distinction between static and transient steady states). A limit cycle can, however, be represented in the state graph as a cycle of length at least two.

6.3.3 The equilibrium state diagram explained

The deficiency of the state graph representation in terms of being unable to distinguish between static and transient steady states of the ESPD mentioned above, as well as the exponential increase in game automorphism classes as the underlying grid dimensions increase, calls for a new visualisation mechanism for summarising the game dynamics of the game succinctly, which is effective even for relatively large instances of the underlying graph.

The notion of an *equilibrium state diagram* is proposed here for this purpose. This diagram represents each component in the state graph by its equilibrium state only. Each automorphism class is furthermore still represented by its class representative. The game state with the smallest lexicographical order within such a class is taken as the class representative. All three types of equilibrium states described in §6.3.2 are representable in the equilibrium state diagram, as illustrated in Figure 6.5. In order to convey the same information as can be found in the state graph, various labels are included in the diagram. These labels are also elucidated in the figure.

In the equilibrium state diagram, each state is labelled by a numerical value denoted by a in Figure 6.5. The conversion from a graphical game state representation to its numerical label equivalent is described later. The label denoted by b in the figure represents the weight of the game state (*i.e.* the number of cooperators present within the state). The label denoted by c in Figure 6.5 furthermore represents the number of distinct states within the automorphism class of the equilibrium state, while the number of distinct initial states that evolve to the particular equilibrium state is represented by a label denoted d. The length of a transient steady state or limit cycle is finally denoted by the parameter L and its value is given by e in Figure 6.5(b)–(c). The convention is adopted that the first state of a limit cycle given in the equilibrium state

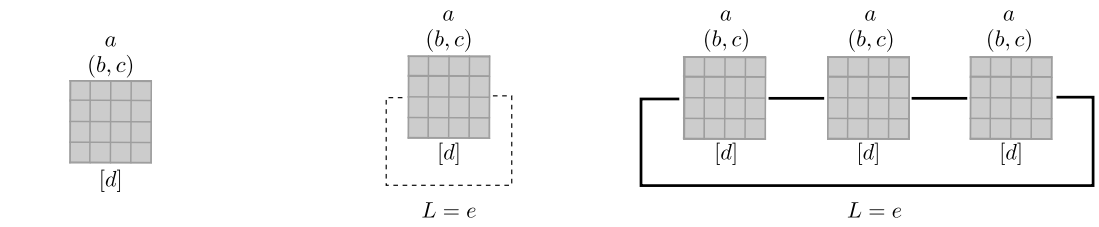

(a) static steady state (b) transient steady state (c) limit cycle

FIGURE 6.5: *Equilibrium state diagram representation of the various equilibrium game states. (a) A static steady state, (b) a transient steady state and (c) a limit cycle.*

diagram is the state of the cycle with the largest weight (the actual state displayed is once again the automorphism class representative). The remaining states of the cycle are given in the order in which they would appear if subsequent rounds of the game were to be played. Note that the latter states are therefore not necessarily the representatives of their various automorphism classes.

Figure 6.6(a) contains an illustration of how the all-defector steady state component of the ESPD with the toroidal grid $C_3 \times C_3$ as underlying graph would be represented in the state graph, while the same information is contained in the equilibrium state diagram representation in Figure 6.6(b), both for parameter region A of the phase plane in Figure 6.3.

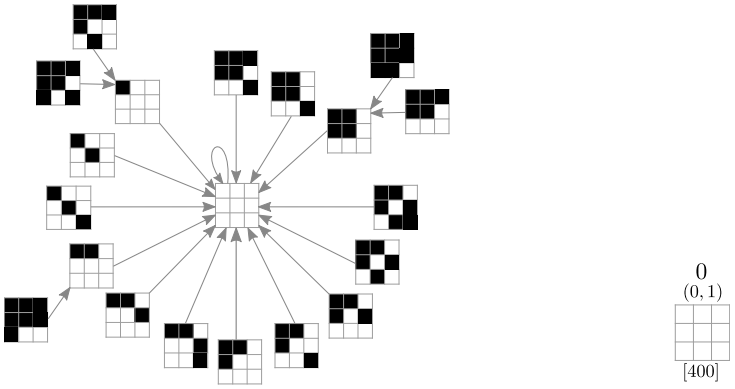

(a) (b)

FIGURE 6.6: *Representation of the state graph component containing the all-defector steady state for the ESPD with $C_3 \times C_3$ as underlying graph in parameter region A of the phase plane in Figure 6.3. Black cells represent players adopting the strategy of cooperation, while white cells represent players adopting the strategy of defection. (a) State graph representation and (b) Equilibrium state diagram representation.*

6.4 Computer-aided equilibrium state diagram generation

It is evident that computer aid is required in order to analyse the game dynamics of the ESPD, even for relatively small underlying toroidal grid graphs. The methods required for analysing ESPD game dynamics with toroidal grid graphs as underlying graphs is elaborated upon in this section. The analysis is divided into two main steps. First, the various distinct game states have to be organised into automorphism classes and their class representatives have to be found. The computer implementation of this step involves two algorithms, an explicit generation algorithm

and an improved implicit algorithm which reduces the computational expense of this analysis step. The second step entails identifying the various equilibrium states among the automorphism class representatives, when considered as initial game states. An algorithm is also proposed for this purpose in order to reduce the computational expense of this step. Finally, the results of the previous two steps are used to construct equilibrium state diagrams. All of the above algorithms are provided in pseudocode form and described in this section, which also contains a performance review of the various algorithmic implementations.

6.4.1 Encoding an ESPD game instance

In order to perform calculations that allow for the identification of equivalence classes and their associated class representatives, a means of representing or encoding game states is required. The following method for encoding a game state is adopted throughout this chapter.

Each player is able to adopt the strategy of either defection or cooperation. These two strategies may be represented by means of binary values. The binary values 0 and 1 are assigned to the strategies of defection and cooperation, respectively. As the game is played on an $n \times m$ toroidal grid, a given state can be represented as an $n \times m$ binary array, as demonstrated in Figure 6.7(a)–(c). This state encoding convention facilitates the required calculations in the analysis of the ESPD game dynamics. It also permits natural visualisation of a state due to the similar dimensions of the array representation in Figure 6.7(c) and its corresponding state in Figure 6.7(a), coupled with the simple mapping between the two strategies and their equivalent binary values.

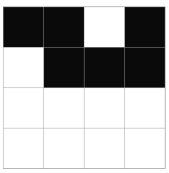

(a)

1	1	0	1
0	1	1	1
0	0	0	0
0	0	0	0

(b)

$$\begin{pmatrix} 1 & 1 & 0 & 1 \\ 0 & 1 & 1 & 1 \\ 0 & 0 & 0 & 0 \\ 0 & 0 & 0 & 0 \end{pmatrix}$$

(c)

$$(1\,1\,0\,1\,0\,1\,1\,1\,0\,0\,0\,0\,0\,0\,0\,0)_2 = (55\,040)_{10}$$

(d)

FIGURE 6.7: *The steps used to represent a graphical state as an array or integer value. (a) A graphical game state, (b)–(c) its representative binary array, and (d) the concatenated bit string with its equivalent integer value.*

In order to minimise computer memory requirements and facilitate timeous identification of game class representatives, a more efficient encoding method is, however, required for storing and comparing states within an equivalence class. For these purposes, each state is further represented by a binary value. This is achieved by concatenating the binary array into a bit string. The length of this bit string depends on the dimensions of the underlying grid graph. For instance, a 4×4 toroidal grid graph requires a bit string of $4 \times 4 = 16$ bits to represent a state. The bit string is then converted to a decimal value using the well-known binary to decimal conversion method. The resulting binary value, together with its decimal equivalent, is shown in Figure 6.7(d). This further state encoding step allows for each state to be associated with a unique numerical value which is used to label the state within the equilibrium state diagram.

6.4.2 The identification of automorphism class representatives

In order to identify all automorphism class representatives, the automorphism class associated with each game state has to be generated and its class representative identified. The generation of all the states in an automorphism class of a particular game state involves applying permutations of the symmetry group of the underlying toroidal grid graph to the game state in question. Consider the symmetry group $G = \{\iota, \rho_1, \rho_2, \rho_3, \mu_1, \mu_2, \delta_1, \delta_2\}$ of a square. Recall, from §2.2.2, that this symmetry group is a dihedral group. It therefore has the property that the various combinations of any two permutations within the group yields all the elements of the group. This property can be combined with the transformation of a toroidal grid along the x- and y-axis of a Cartesian grid representation by a unit value $z \in \{1, \ldots, n\}$ in order to generate all the states in the automorphism class of a given game state. This principle is employed in Algorithm 6.1 to generate the automorphism class of each state of the ESPD with the toroidal grid $C_n \times C_n$ as underlying graph.

The algorithm starts by constructing the automorphism class of each game state represented by a binary value in the integer range $\{2^{n^2-1}, \ldots, 2^{n^2}-1\}$. In the case of a 4×4 toroidal grid, for example, these game state values are the sequence $\{1000\,0000\,0000\,0000, \ldots, 1111\,1111\,1111\,1111\}$ (in binary form). As only the states represented by binary numbers starting with a 1 are considered, the search space is halved. As the class representatives are those with the smallest lexicographical order and therefore have the largest decimal values within their automorphism classes, all automorphism class leaders are represented within this reduced search space. The only exception is the all-defector state, which is therefore added to the list of class representatives at the end of the algorithm. Once each automorphism class has been generated by the algorithm, all values in such a class other than the class representative are removed from the list of states. This process prevents duplicate generation of automorphism classes, because the algorithm considers states in increasing lexicographical order. The output of the algorithm is a list of all the automorphism class representatives. As the search space is reduced and no unnecessary automorphism class generation takes place, the computational time of the algorithm is reduced significantly. All states are also stored in decimal representation form in order to minimise memory requirements.

Algorithm 6.1 is sufficient for the ESPD game dynamics analysis on an $n \times m$ toroidal grid where $n \leq 3$. Thereafter, the number of states becomes so large that the algorithm is no longer a practical means for automorphism class representative generation. An implicit search algorithm is therefore proposed for toroidal grids of larger dimensions. This search algorithm employs a tree structure to generate automorphism class representatives. More specifically, the search algorithm generates a tree in which each vertex represents an automorphism class representative. Each level of the tree represents the subset of automorphism class representatives of weight equal to the level in the tree. The algorithm is therefore able to utilise the previously determined automorphism class representatives (of a lower weight) in order to generate the automorphism class representatives of a particular weight. The algorithm is given in pseudocode form as Algorithm 6.2.

The search process starts in Step 1 of Algorithm 6.2, in which an all-defector game state is constructed and initialised as the root of the search tree. Each subset of automorphism class representatives of a certain weight (and hence within the same level in the search tree generated) is stored in a separate archive. Thus, the root node in level 0 of the tree is stored in archive 0. In Step 3, the algorithm then moves to the next level in the tree. Each leaf present in the previous level of the tree is then considered individually, as specified in Step 4. Steps 5 and 6 ensure that no terminated branch is visited. A branch is terminated if the last element in its array

Algorithm 6.1: Explicit generation of class representatives

Input : Dimensions of the underlying toroidal grid graph n.
Output: The set of automorphism class representatives.

```
1  Automorphism class representatives set ← [2^{n^2} − 1, 2^{n^2} − 2, ..., 2^{n^2−1} − 1, 2^{n^2−1}];
2  domain ← {1, 2, ..., n − 1, n};
3  i ← 1;
4  if i ≤ the length of Automorphism class representatives set then
5      original state ← i^{th} element of Automorphism class representatives set;
6      Convert original state into array form;
7      j ← 0;
8      k ← 0;
9      for j ← all elements in domain do
10         new state ← Translate original state to the left by j units;
11         for k ← all elements in domain do
12             new state ← Translate new state upwards by j units;
13             Add new state to Equivalence classes;
14             count ← 0;
15             repeat
16                 new state ← Rotate new state by 90;
17                 if new state is not an element in Equivalence class set then
18                     Add new state to Equivalence class;
19                 new state ← Reflect new state about y = 0;
20                 if new state is not an element in Equivalence class set then
21                     Add new state to Equivalence class;
22                 count← count+1;
23             until count=4 ;
24     Convert all elements in Equivalence class to decimal form;
25     for all elements in Equivalence class < original state do
26         Delete element from Automorphism class representatives set;
27     i ← i + 1;
28 Add 0 to Automorphism class representatives set;
```

representation corresponds to the strategy of cooperation. This ensures that all possible weights of the branch have already been considered. Steps 7–18 allow for the successive adoption of the strategy of cooperation for each player present within the ESPD following the last player within the current array who adopts the strategy of cooperation. In each case, an additional player of the game is assigned the strategy of cooperation. All states successively generated therefore correspond to a relative weight increase of 1. For each successive state thus generated, a test is performed to determine whether the state is automorphic to any other state already present in the current level of the tree. This is achieved by first following the process in Steps 9–23 of Algorithm 6.1 in order to generate a state's equivalence class. If the numerical representation of any state within its equivalence class is larger than the state being considered, it is not a class representative and the next state is considered. If, however, a state achieves the largest numerical representation, it is compared with the other states in the same level of the tree to ensure that the state has not been considered before. If it is found that the state has indeed been considered before, the next state is considered. Otherwise, the state is included in the archive of

Algorithm 6.2: Implicit generation of class representatives

Input : Dimensions of the underlying toroidal grid graph n.
Output: The set of automorphism class representatives.

```
1  Construct a n-square zero matrix and add to archive 0;
2  x ← 1;
3  for each level x < n²/2 do
4      for each array in archive x − 1 do
5          if n^{2th} element in array = 1 then
6              break;
7          else
8              current position ← the position of the last element in array with value 1;
9              i = current position +1;
10             for i ≤ n² do
11                 new array ← array;
12                 i^th element in new array ← 1;
13                 Check if new array is automorphic to any state within archive x;
14                 if new array is automorphic then
15                     break;
16                 else
17                     Add new array to archive x;
18                 i ← i + 1;
19     x ← x + 1;
```

states for the particular level of the search tree. When each leaf in the previous level of the tree has thus been considered, the next level of the tree is considered and the process is repeated. If level $\lfloor \frac{n^2}{2} \rfloor$ is reached, the algorithm terminates, because of the inverse property of the ESPD with a toroidal grid as underlying graph where the automorphism class representatives of weight x are equivalent to the inverses of the automorphism class representatives of weight $n^2 - x$. A large portion of the search space therefore does not have to be considered.

The class representative tree for the ESPD with the toroidal grid $C_3 \times C_3$ as underlying graph is shown as an example in Figure 6.8. As may be seen in the figure, each level of the tree partitions the automorphism class representative set into the various subsets according to the state weights, as indicated by the values of w. The tree contains 13 nodes, which is indeed half the number of equivalence classes previously enumerated by Van der Merwe [72]. The reduction in search space may be noted as only 42 state automorphism classes are compared in Algorithm 6.2, whereas 255 states are considered in Algorithm 6.1. This translates to a significant reduction in the required computation time associated with automorphism class representative generation.

6.4.3 The identification of ESPD equilibrium states

Once all the automorphism class representatives have been found, as discussed in §6.4.2, the game dynamics associated with each class representative has to be investigated and the various equilibrium states thus reached, identified. The results of this investigation can then be used to construct the equilibrium state diagram of the game. In order to identify the various equilibrium states in a computationally inexpensive manner, the search space is further reduced so as to avoid

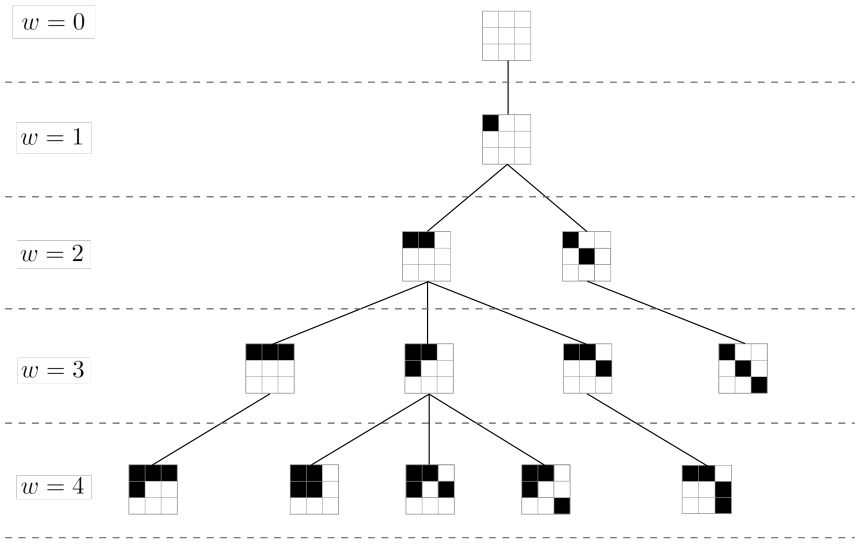

FIGURE 6.8: *Automorphism class representative tree for the ESPD with a $C_3 \times C_3$ as underlying graph, constructed by Algorithm 6.2.*

consideration of unnecessary automorphism class representatives. The portion of the search space thus removed is presented in pseudocode form in Algorithm 6.3 and is described in this section.

If a game state has weight 1, then the state consists of one cooperator and all other players adopt the strategy of defection. Regardless of the spatial position of the cooperator in the underlying toroidal grid graph, it will always contain four defectors in its neighbourhood. Therefore, as $c_0 < d_i$ for all $i \in \{0, 1, 2, 3, 4\}$, the cooperator will always adopt the strategy of defection during the next round of the game, while each defector in the cooperator's neighbourhood will persist with their strategy of defection. Since all initial states with weight 1 will lead to the all-defector steady state, such states do not have to be considered as possible initial states in game dynamics analysis investigation of Algorithm 6.3.

Consider next the case where the initial state of a game has weight two. If the cooperators are positioned on the underlying toroidal grid so that they are not adjacent, then (using the same argument as for an initial state of weight 1) it follows that the state will lead to the all-defector steady state. If, on the other hand, the two cooperators are adjacent in the underlying graph, as illustrated in Figure 6.9, each cooperator receives the pay-off value c_1 and each defector within the combined open neighbourhood of the two cooperators receives the pay-off value d_1. Since $d_1 > c_1$, all players in the cooperators' closed neighbourhoods will therefore adopt the strategy of defection during the next round of the game. Hence, regardless of the dimensions of the underlying toroidal grid graph, no automorphism classes of weight 1 or 2 have to be considered in Algorithm 6.3.

The remaining equivalence classes all have to be investigated in order to determine the various equilibrium states. It is computationally expensive to simulate the outcome of a number of rounds of the game until an equilibrium state is reached for any specified initial state and record the unique equilibrium states found. Algorithm 6.3 is consequently used to reduce the number of states that require a full game dynamic investigation. The algorithm identifies all static steady states and generates an archive of potential transient steady states or limit cycles that require a full game dynamic investigation.

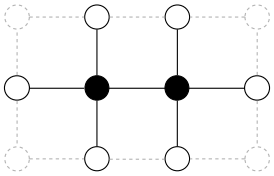

FIGURE 6.9: *The closed neighbourhood of two neighbouring cooperators of an ESPD state of weight 2 with a toroidal grid as underlying graph. The black nodes represent cooperating players, while the white nodes represent defecting players.*

Algorithm 6.3: Initial identification of equilibrium states

Input : Dimensions of the underlying toroidal grid graph n, the feasible region in which the game is to investigated and the pruned automorphism class representatives set, Class representatives.

Output: A set of all static steady states, static steady states and an archive of potential transient steady states or limit cycles, archive.

```
1 for each state within the Class representatives set do
2     new state ← one round of the ESPD is played on the current state;
3     if new state = current state then
4         Add new state to static steady states set;
5         weight 1 ← current state's weight;
6         weight 2 ← new state's weight;
7         if weight 2 ≥ weight 1 then
8             Add new state to archive;
```

The first steps in Algorithm 6.3 simulate a single round of the ESPD for each of the automorphism class representatives (with a weight greater than 2) as initial state. A single game round consists of both the playing phase and the updating phase according to the game dynamics described in §4.2. The newly generated game state is compared with the initial state in Steps 3–8. If the states are equivalent, the initial state is a static steady state and is therefore added to the set of static steady states. In order to identify the other types of equilibrium states, it should be noted that the weight of a transient steady state remains constant over the various game rounds, while for a limit cycle the weight of the game state can change as the game progresses. These properties of transient steady states and limit cycles can be used to facilitate a further reduction of the search space to be investigated. For this reason, the algorithm also compares the weights of the initial and newly generated states in the case of non-equivalent state pairs. If the weight of the state remains constant over a round of the game, the state can potentially be a transient steady state or a limit cycle. Such states are stored in an archive for further investigation. If the weight of the state increases, the state can potentially be a limit cycle. Hence, such states are also added to the algorithm's archive. The cases in which the weight of the game state decreases do not have to be considered because in these cases the game state will evolve to one of the game states that have already been considered.

The archive of states produced by Algorithm 6.3 therefore has to be investigated for all rounds of the game until an equilibrium state is reached. Since a reduced number of states have to be investigated for all rounds of the game, however, a significant reduction in the computational expense of identifying the equilibrium states is achieved. In the full game dynamic investigation, on the other hand, if a static steady state is reached it need not be recorded as all static steady

states have already been found. In this case, only transient steady states and limit cycles are recorded and classified. The aforementioned analyses are, of course, carried out for each parameter region of the phase plane separately. The set of static steady states, transient steady states and limit cycles thus found can then be used in constructing the equilibrium state diagrams corresponding to the various parameter regions.

6.4.4 Relative performance of algorithms

The algorithms described in the previous two sections were all implemented in Wolfram's Mathematica 11.0 [78] in order to construct equilibrium state diagrams for the ESPD with small toroidal grids as underlying graphs. The time and memory requirements associated with the identification of automorphism class representatives, as well as equilibrium states, are provided in Table 6.3. The computation times were measured on an Intel i7-4770 CPU running at 3.4GHz with 8GB RAM within a 64-bit Windows 7 operating system.

TABLE 6.3: *The time and memory requirements associated with the implementation of Algorithms 6.1–6.3.*

	Algorithm 6.1		Algorithm 6.2		Algorithm 6.3	
	CPU time (hh:mm:ss)	Memory (GB)	CPU time (hh:mm:ss)	Memory (GB)	CPU time (hh:mm:ss)	Memory (GB)
$C_2 \times C_6$	00:01:07	0.131	00:00:49	0.125	00:00:49	0.126
$C_3 \times C_3$	00:00:02	0.120	00:00:02	0.119	00:00:01	0.120
$C_3 \times C_4$	00:00:34	0.121	00:00:26	0.120	00:00:15	0.121
$C_3 \times C_5$	00:01:06	0.123	00:00:47	0.121	00:00:36	0.122
$C_3 \times C_6$	00:08:43	0.142	00:02:24	0.128	00:01:58	0.128
$C_4 \times C_4$			00:00:58	0.146	00:00:42	0.143
$C_4 \times C_5$			00:20:26	0.230	00:05:38	0.168
$C_4 \times C_6$			05:33:04	0.841	00:22:50	0.424
$C_5 \times C_5$			22:54:05	2.037	02:47:57	1.188
$C_5 \times C_6$			58:16:24	6.145	06:22:12	2.356
$C_6 \times C_6$			346:24:35	16.532	18:06:19	5.425

As shown in Table 6.3, Algorithm 6.2 reduces both the computation time and memory requirements compared to Algorithm 6.1. As the size of the underlying graph increases, a more significant improvement is observed. Algorithm 6.1 was only run for grids of dimensions at most $C_3 \times C_6$.

Note that the computer memory requirements of Algorithm 6.2 for the case associated with the $C_6 \times C_6$ grid as underlying graph is larger than the available computer's RAM. Therefore, a parallel computing approach was adopted for this case. More specifically, this entailed partitioning the state space into subsets and running Algorithm 6.2 for each subset on various computers and then rerunning the algorithm with a combination of the reduced subsets as the starting state space. The memory and computational times were calculated merely as a sum of these processes. As a slightly different implementation approach was taken, the times and memory requirements for this underlying grid, as shown in Table 6.3, should not be evaluated in comparison with the other underlying toroidal grid graphs' time and memory requirements contained in the table.

The algorithmic approach adopted was sufficient for the dimensions of the underlying toroidal grids considered within the scope of this thesis. However, if the ESPD with larger toroidal grids

as underlying graphs are to be investigated, the computational power and memory requirements would become so large that this approach becomes infeasible (even if a low-level programming language, such as C++, were to be used instead of Mathematica). In such a case, either a massively parallel approach should be undertaken or else further pruning rules are required in order to render this analytical approach tractable.

6.5 Analysis of the ESPD dynamics

The results of the long-time game dynamics of the ESPD are presented in this section for the following eleven toroidal grids as underlying graphs: $C_2 \times C_6$, $C_3 \times C_3$, $C_3 \times C_4$, $C_3 \times C_5$, $C_3 \times C_6$, $C_4 \times C_4$, $C_4 \times C_5$, $C_4 \times C_6$, $C_5 \times C_5$, $C_5 \times C_6$ and $C_6 \times C_6$. The equilibrium state diagrams in each case are first presented and the number of components in the corresponding state graph enumerated for every region of the phase plane. This is followed by an analysis of the probability of reaching a persistent pocket of cooperation from a prescribed initial state for the various cases.

6.5.1 Equlibrium state analysis

Equilibrium state diagrams for the ESPD with $C_3 \times C_3$ as underlying graph are shown in Figure 6.10. Van der Merwe [72] has already constructed the state graph for a grid of dimension 3×3. His results were used to validate the results returned by the algorithms of §6.4.2 and §6.4.3 employed to construct the equilibrium state diagrams in Figure 6.10. All the equilibrium states identified within the equilibrium state diagrams of Figure 6.10 are static steady states.

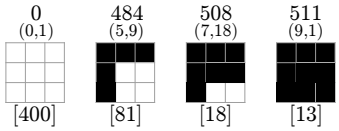

(a) Parameter region A

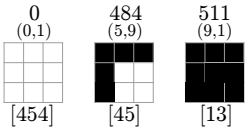

(b) Parameter region B

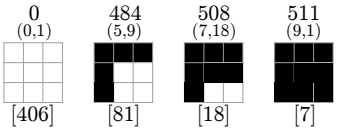

(c) Parameter region C

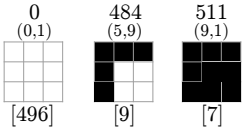

(d) Parameter region D

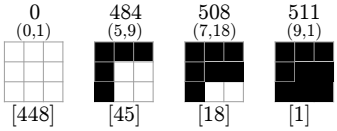

(e) Parameter region E/I

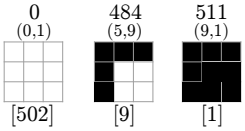

(f) Parameter region F/H

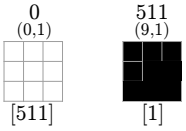

(g) Parameter region G/J/K

FIGURE 6.10: *Equilibrium state diagrams for the ESPD with $C_3 \times C_3$ as underlying graph. The relevant parameter regions A–K of the phase plane are elucidated in Figure 6.3.*

The full equilibrium state diagrams for the ESPD with $C_2 \times C_6$, $C_3 \times C_4$, $C_3 \times C_5$, $C_3 \times C_6$, $C_4 \times C_4$, $C_4 \times C_5$, $C_4 \times C_6$, $C_5 \times C_5$, $C_5 \times C_6$ and $C_6 \times C_6$ are listed in Appendix D. The label d denoting the number of distinct initial states that evolve to the particular equilibrium state is omitted in the case of the equilibrium state diagrams for the ESPD with $C_3 \times C_6$, $C_4 \times C_5$, $C_4 \times C_6$, $C_5 \times C_5$, $C_5 \times C_6$ and $C_6 \times C_6$ as underlying graphs. This is due to the excess computation and memory required. In these cases the label d is only included for the all-defector steady state, in order to facilitate computation of the probability of cooperation persisting.

It was found that the smallest toroidal grid graph exhibiting a transient steady state within its equilibrium state diagram is the graph $C_3 \times C_4$, while the smallest toroidal grid exhibiting a limit cycle within its equilibrium state diagram is the graph $C_5 \times C_5$. The longest limit cycle found during the course of the analysis was of length six and is contained in the equilibrium state diagram of the ESPD with $C_6 \times C_6$ as underlying graph. All these equilibrium states are shown in Figure 6.11.

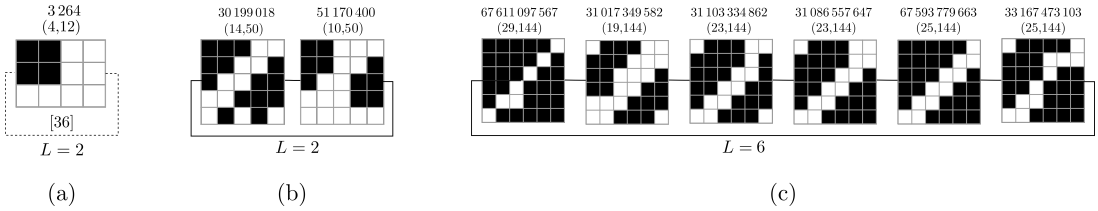

FIGURE 6.11: *(a) A transient steady state for the smallest underlying toroidal grid ($C_3 \times C_4$), (b) a limit cycle for the smallest underlying toroidal grid ($C_5 \times C_5$) and (c) the longest limit cycle in the ESPD with $C_6 \times C_6$ as underlying graph.*

Enumerations of the equilibrium states in each of the equilibrium state diagrams are shown in Table 6.4. The relationships between the number of equilibrium states and the dimensions of the underlying graph are also illustrated in Figures 6.12 and 6.13 for each of the parameter regions in the phase plane of Figure 6.3. A weakly defined exponential relationship between the number of equilibrium states and the dimensions of the underlying graph is observed for parameter regions A, B, C, E, F, H and I in the phase plane.

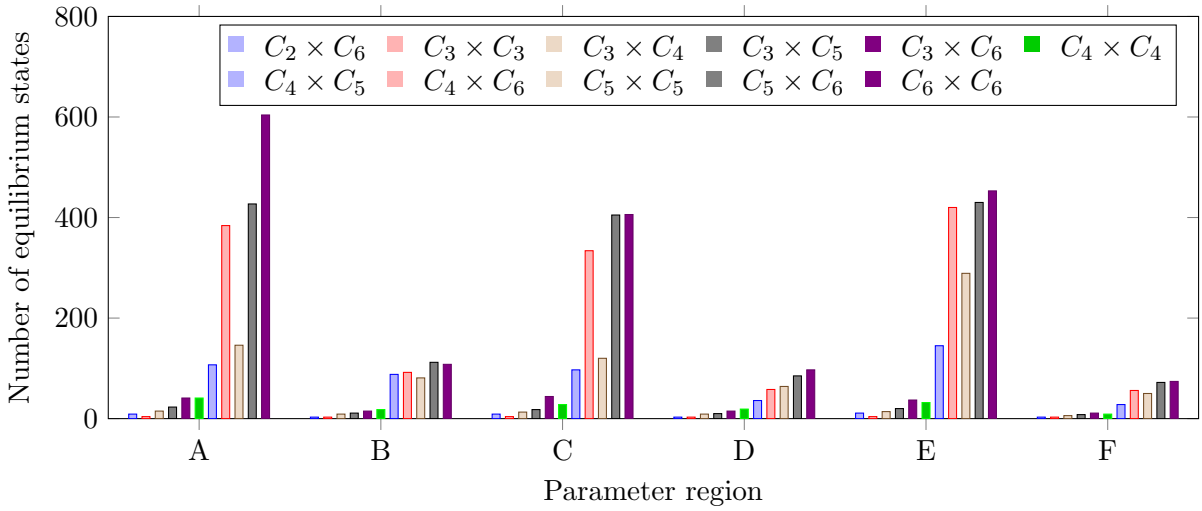

FIGURE 6.12: *The number of equilibrium states in the equilibrium state diagrams for the ESPD with the various small toroidal grids as underlying graphs for the parameter regions A–F in the phase plane of Figure 6.3.*

TABLE 6.4: *The number of equilibrium states in the equilibrium state diagram for the ESPD with various small toroidal grids as underlying graph.*

Region	Number of equilibrium states										
	$C_2 \times C_6$	$C_3 \times C_3$	$C_3 \times C_4$	$C_3 \times C_5$	$C_3 \times C_6$	$C_4 \times C_4$	$C_4 \times C_5$	$C_4 \times C_6$	$C_5 \times C_5$	$C_5 \times C_6$	$C_6 \times C_6$
A	9	4	15	23	41	41	107	384	146	427	604
B	3	3	9	11	15	18	88	92	81	112	108
C	9	4	13	18	44	28	97	334	120	405	406
D	3	3	9	10	15	19	36	58	64	85	97
E	11	4	13	20	37	32	145	420	289	430	453
F	3	3	6	8	11	9	29	57	51	72	74
G	2	2	2	2	3	2	4	4	5	6	6
H	5	3	5	9	14	7	20	52	33	79	76
I	14	4	11	20	40	21	95	280	203	336	401
J	2	2	2	3	4	2	3	4	3	4	4
K	2	2	2	2	2	2	2	2	2	2	2

TABLE 6.5: *Probability of cooperation persisting for the ESPD with various small toroidal grids as underlying graph derived from the equilibrium state diagrams (rounded to five decimal places).*

Region	Probability of persistent cooperation										
	$C_2 \times C_6$	$C_3 \times C_3$	$C_3 \times C_4$	$C_3 \times C_5$	$C_3 \times C_6$	$C_4 \times C_4$	$C_4 \times C_5$	$C_4 \times C_6$	$C_5 \times C_5$	$C_5 \times C_6$	$C_6 \times C_6$
A	0.36792	0.21900	0.26099	0.24832	0.31411	0.43568	0.46519	0.50753	0.56163	0.58991	0.61236
B	0.18408	0.11300	0.03613	0.01645	0.02554	0.10854	0.09601	0.10758	0.13981	0.13283	0.18055
C	0.26758	0.20700	0.21240	0.23557	0.27216	0.28444	0.34892	0.36522	0.39878	0.42134	0.46288
D	0.18408	0.03100	0.03613	0.01645	0.02554	0.10854	0.09601	0.09878	0.12558	0.12896	0.16433
E	0.22876	0.12500	0.13257	0.15338	0.18479	0.17995	0.21501	0.24845	0.25322	0.27540	0.28321
F	0.06616	0.02000	0.01978	0.00964	0.01002	0.03713	0.03289	0.03326	0.03515	0.03873	0.04832
G	0.03833	0.00200	0.00122	0.00216	0.00261	0.00014	0.00015	0.00002	7.24×10^{-5}	4.53×10^{-7}	7.36×10^{-9}
H	0.00903	0.02000	0.01880	0.00766	0.00720	0.03822	0.03322	0.03418	0.03501	0.03623	0.04622
I	0.20679	0.12500	0.13159	0.15277	0.18362	0.17714	0.21386	0.23066	0.25084	0.26651	0.28529
J	0.00464	0.00200	0.00024	0.00018	0.00007	0.00026	0.00001	$4,05 \times 10^{-6}$	6.26×10^{-7}	1.77×10^{-8}	3.78×10^{-10}
K	0.00024	0.00200	0.00024	0.00003	3.81×10^{-6}	0.00002	9.54×10^{-7}	5.96×10^{-8}	2.98×10^{-8}	9.31×10^{-10}	1.46×10^{-11}

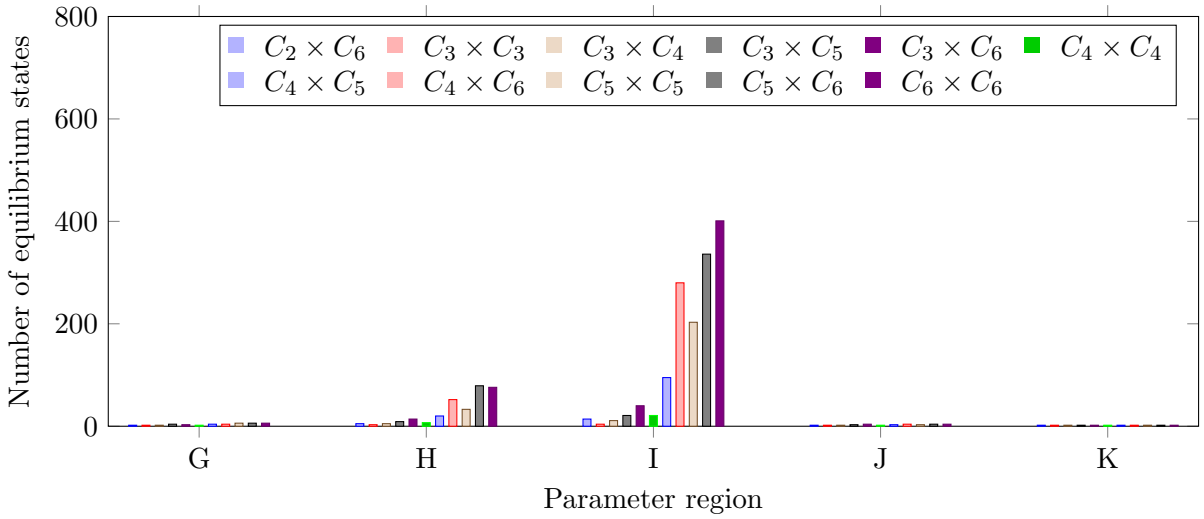

FIGURE 6.13: *The number of equilibrium states in the equilibrium state diagrams for the ESPD with the various small toroidal grids as underlying graphs for parameter regions G–K in the phase plane of Figure 6.3.*

6.5.2 The probability of persistent cooperation

Using the constructed equilibrium state diagrams, the probability that some form of cooperation will persist from a randomly generated initial state of the ESPD with $C_2 \times C_6$, $C_3 \times C_3$, $C_3 \times C_4$, $C_3 \times C_5$, $C_3 \times C_6$, $C_4 \times C_4$, $C_4 \times C_5$, $C_4 \times C_6$, $C_5 \times C_5$, $C_5 \times C_6$ and $C_6 \times C_6$ as underlying graphs was determined. These probabilities are shown in Table 6.5 for each parameter region in the phase plane of Figure 6.3. The relationships between the probability of cooperation persisting and the dimensions of the underlying toroidal grid graph are illustrated in Figures 6.14 and 6.15. It can be seen in this figure that as the dimensions of the underlying toroidal grid graph increase, so does the probability of cooperation persisting, except for parameter regions G, J and K in which it decreases and is approximately zero.

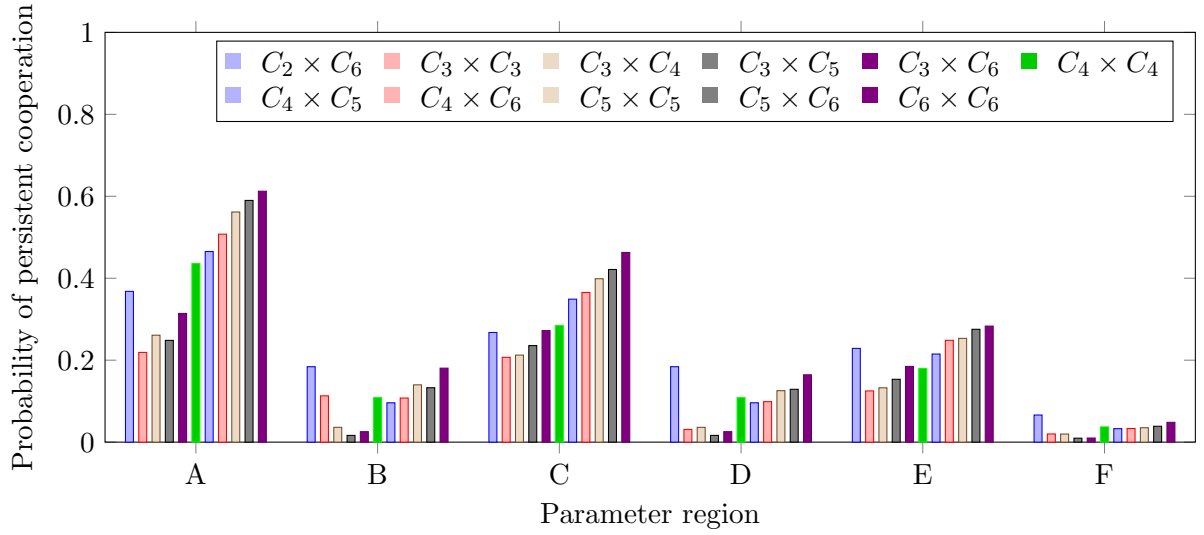

FIGURE 6.14: *The probability that some form of cooperation will persist for the ESPD with the various small toroidal grids as underlying graphs for parameter regions A–F in the phase plane.*

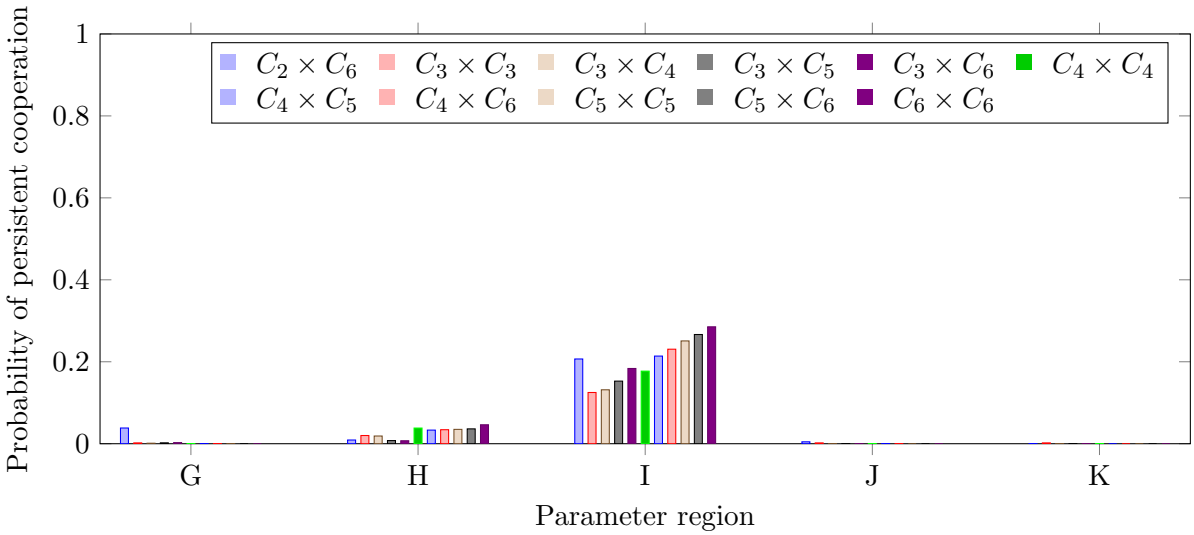

FIGURE 6.15: *The probability that some form of cooperation will persist for the ESPD with the various small toroidal grids as underlying graphs for parameter regions G–K in the phase plane.*

In order to further analyse the ability of the small toroidal grid graphs to facilitate the persistence of cooperation, the conditional probabilities that initial game states of specified weights will lead to some form of persistent cooperation in the long run are investigated for each of the underlying toroidal grid graphs.

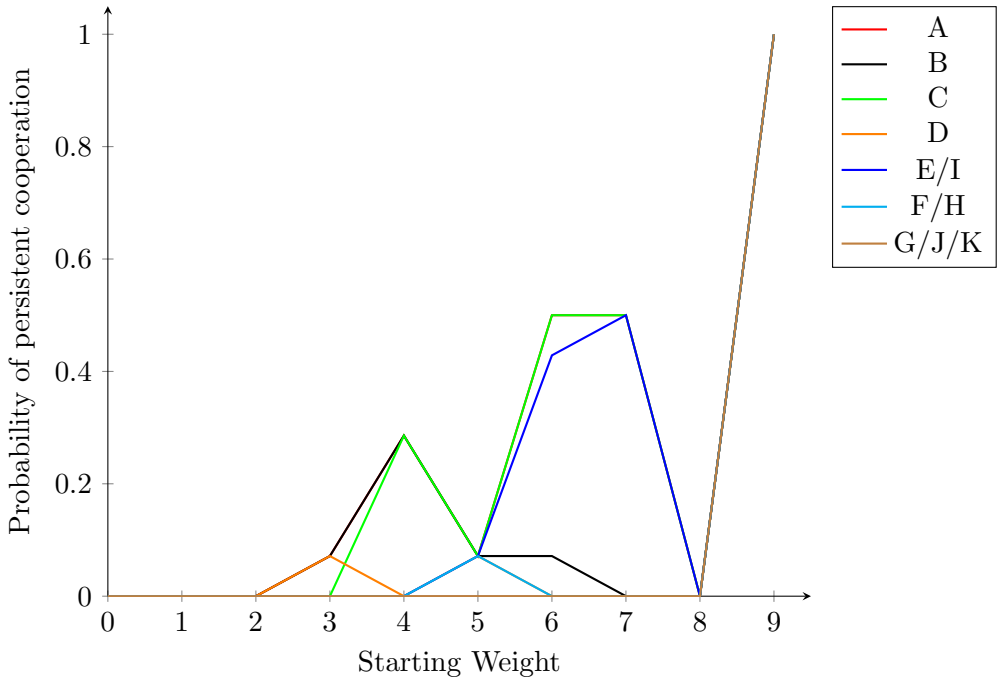

FIGURE 6.16: *The conditional probability that, given an initial state with a certain weight, some form of cooperation will persist for the ESPD with $C_3 \times C_3$ as underlying graph for the various parameter regions in the phase plane in Figure 6.3.*

First, consider the ESPD with $C_3 \times C_3$ as underlying graph. The conditional probabilities that initial game states of specified weights will lead to some form of persistent cooperation in the long run are shown in Figure 6.16 for each parameter region of the phase plane of Figure 6.3.

It is interesting to note the nonlinear relationship between the weight of the initial game state (*i.e.* the number of cooperators initially present) and the probability of cooperation persisting in the long run. If a maximum probability of cooperation is desired and the starting weight is associated with a cost function, the varying graph gradients in the figure should be considered carefully. For example, the decreasing gradient sections of the graphs (*i.e.* for a starting weight of 8 in all regions of the phase plane or a starting weight of 5 for regions A, B and C) will reduce the probability of cooperation with an increased cost. It may also be seen that for a starting weight of 8 (*i.e.* the toroidal grid containing exactly one defector) no form of persistent cooperation is possible for any region of the phase plane.

The conditional probabilities that initial game states of specified weights will lead to some form of persistent cooperation in the long run are shown for each of the remaining underlying toroidal grids in Figures 6.17 for the various parameter regions of the phase plane in Figure 6.3.

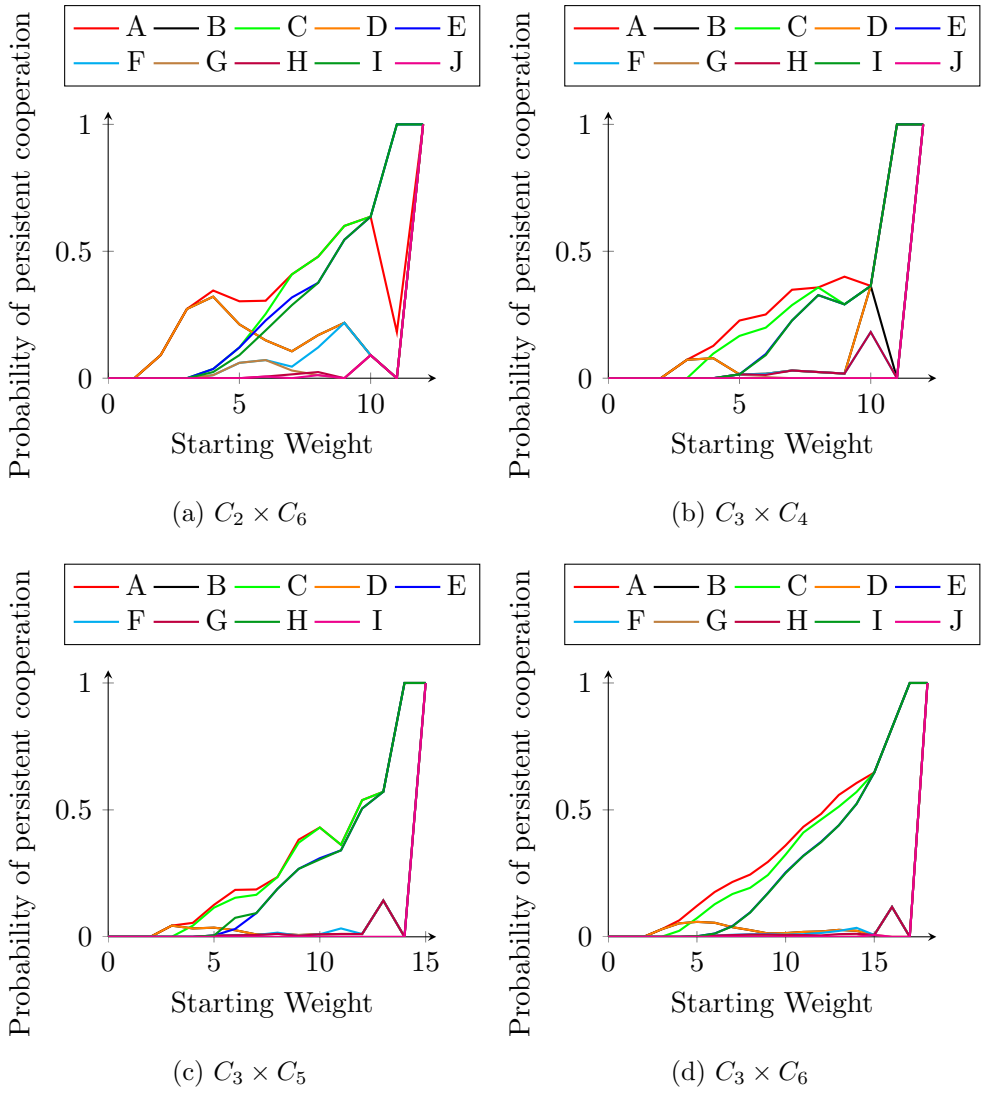

(a) $C_2 \times C_6$ (b) $C_3 \times C_4$

(c) $C_3 \times C_5$ (d) $C_3 \times C_6$

FIGURE 6.17: *The conditional probability that, given an initial state with a certain weight, some form of cooperation will persist for the ESPD with* $C_2 \times C_6$, $C_3 \times C_4$, $C_3 \times C_5$, $C_3 \times C_6$, $C_4 \times C_4$ *and* $C_4 \times C_5$ *as underlying graphs. The legends correspond to the various parameter regions in the phase plane of Figure 6.3.*

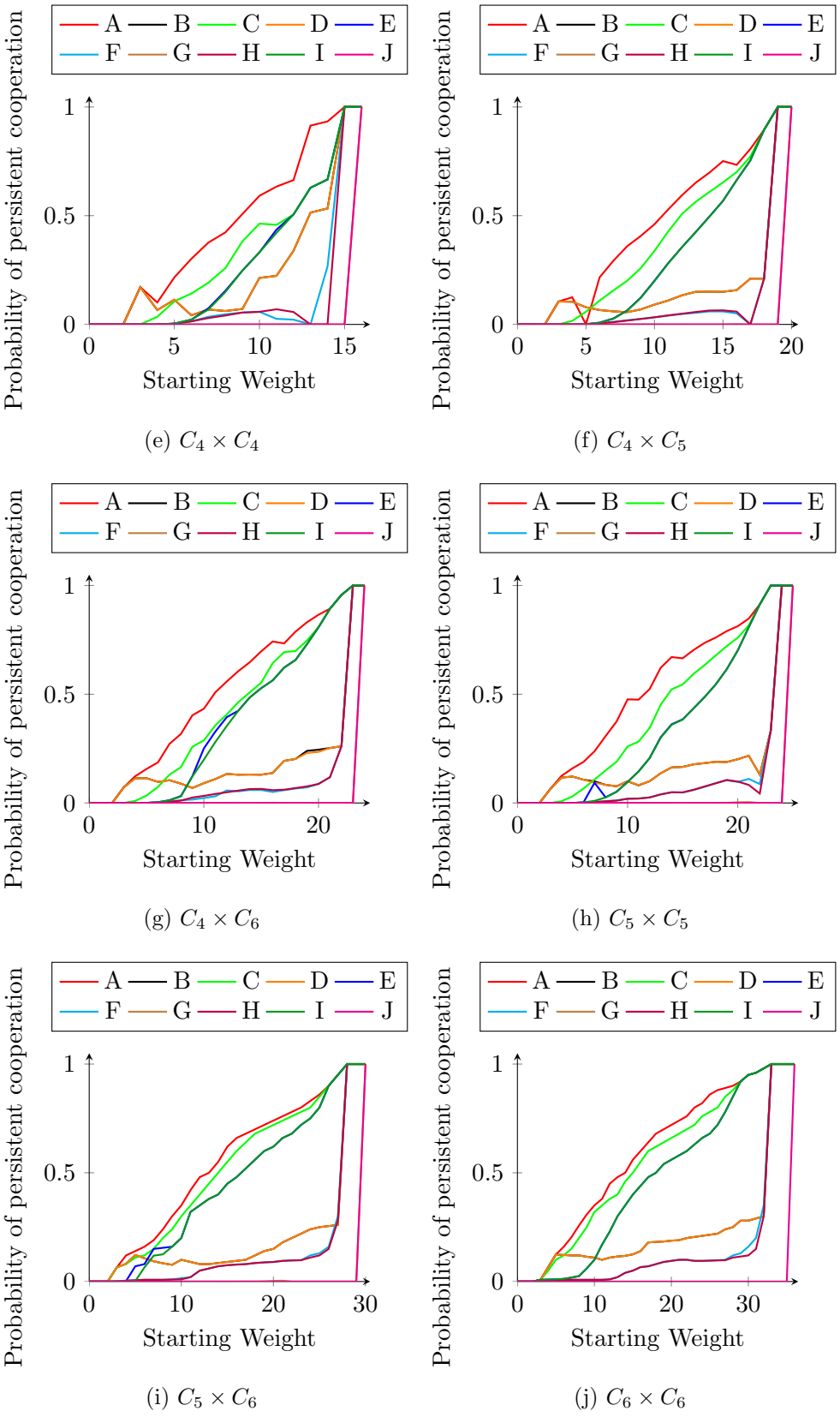

(e) $C_4 \times C_4$ (f) $C_4 \times C_5$

(g) $C_4 \times C_6$ (h) $C_5 \times C_5$

(i) $C_5 \times C_6$ (j) $C_6 \times C_6$

FIGURE 6.17 (continued): *The conditional probability that, given an initial state with a certain weight, some form of cooperation will persist for the ESPD with $C_4 \times C_6$, $C_5 \times C_5$, $C_5 \times C_6$ and $C_6 \times C_6$ as underlying graphs. The legends correspond to the various parameter regions in the phase plane of Figure 6.3.*

It can be seen in these figures that for parameter regions A, C, E and I as the dimensions of the underlying toroidal grid increases, the probability that cooperation persists according to a fixed weight of the initial state tends towards a linear relationship. For the remaining parameter regions B, D, F, G, H and J, on the other hand, the probability that cooperation persists is small if the grid starts with less than approximately 80% cooperators; thereafter the probability rapidly increases towards certainty. This relationship also becomes more pronounced as the dimensions of the underlying toroidal grid increases. It is perhaps surprising to note that the relationship between the probability of cooperation persisting and the weight of the initial state, for the most part, coincides for the pairs of parameter regions (B,D), (I,E), (F,H) and (G,J).

6.6 The persistence of cooperation in small toroidal grids

The collective ability of small toroidal grids (*i.e.* grids of dimensions $C_n \times C_m$ where $n, m \in \{1, \ldots, 6\}$ to allow for the emergence of persistent cooperation is shown in Figure 6.18 for each of the parameter regions in the phase plane of Figure 6.3. The probabilities of cooperation persisting for the toroidal grids $C_1 \times C_m$ where $m \in \{1, \ldots, 6\}$ were obtained from the work of Burger *et al.* [10] in which the probability of cooperation persisting for the ESPD with a cyclic underlying topology ($C_n \backsimeq C_1 \times C_n$) was considered. Furthermore, the probability of cooperation persisting for the ESPD with underlying graphs $C_2 \times C_2$, $C_2 \times C_3$, $C_2 \times C_4$ and $C_2 \times C_5$ were calculated from the state graphs constructed by Van der Merwe [72]. The probabilities for the remaining underlying toroidal grids were presented in Table 6.5 in §6.5. In Figure 6.18, only the upper triangular half of each grid graph is shown. This is because the $C_n \times C_m$ toroidal grid is isomorphic to the $C_m \times C_n$ toroidal grid, and so the bottom triangular half of each graph shown in Figure 6.18 is symmetric to its upper triangular half.

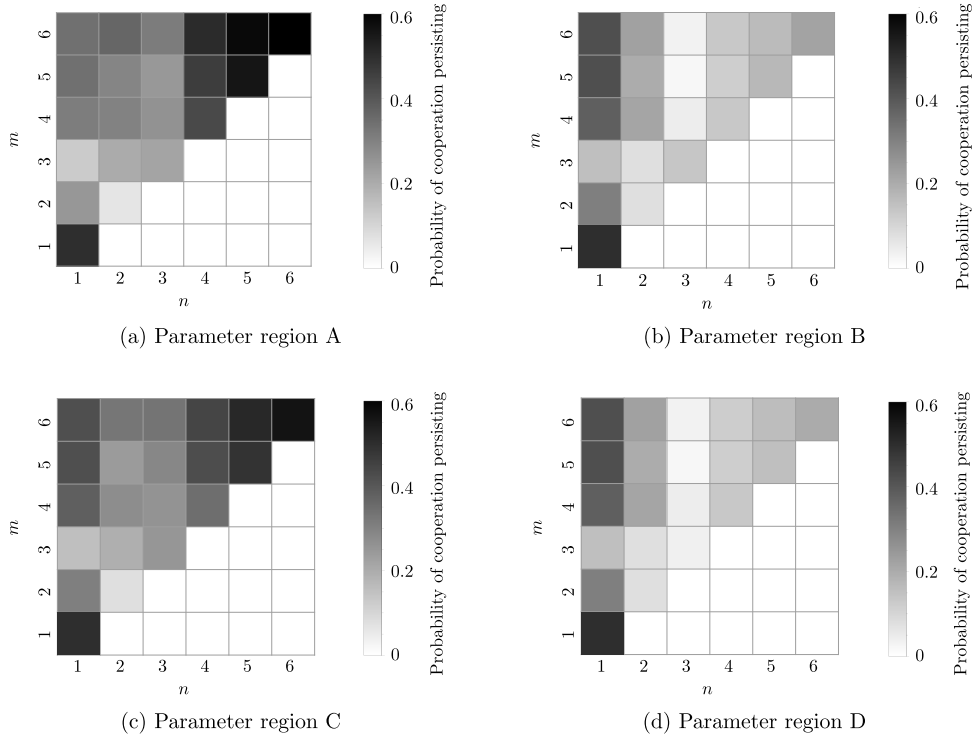

(a) Parameter region A

(b) Parameter region B

(c) Parameter region C

(d) Parameter region D

FIGURE 6.18: *The probability that some form of cooperation will persist for the ESPD with the toroidal grid $C_n \times C_m$ (where $n \in \{1, \ldots, 6\}$ and $m \in \{1, \ldots, 6\}$) as underlying graph for parameter regions A–D in the phase plane of Figure 6.3.*

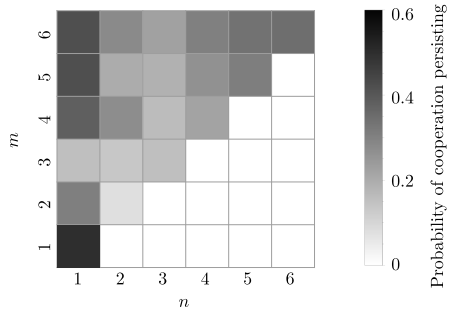

(e) Parameter region E

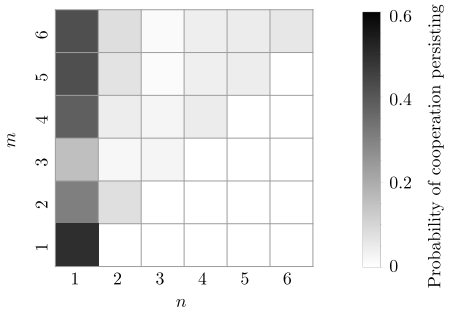

(f) Parameter region F

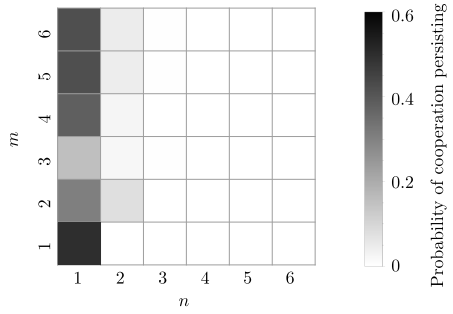

(g) Parameter region G

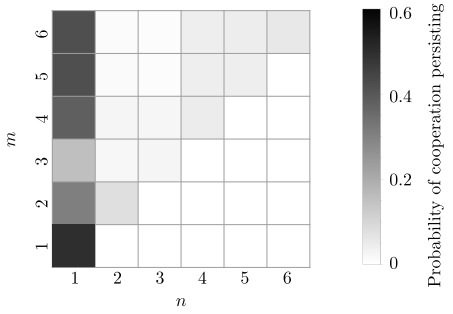

(h) Parameter region H

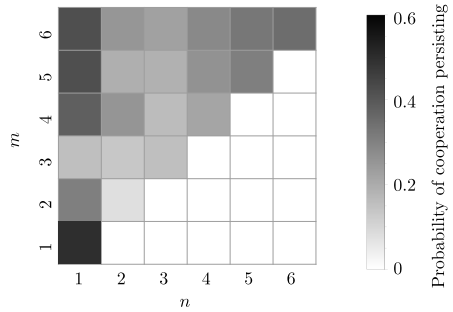

(i) Parameter region I

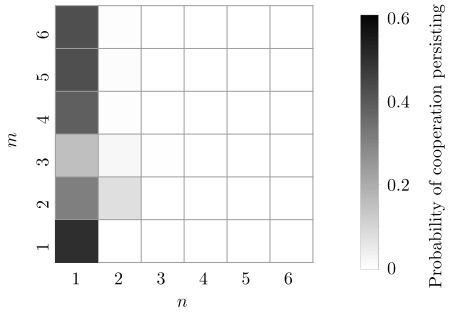

(j) Parameter region J

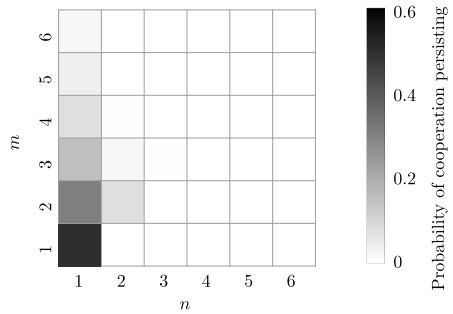

(k) Parameter region K

FIGURE 6.18 (continued): *The probability that some form of cooperation will persist for the ESPD with the toroidal grid $C_n \times C_m$ (where $n \in \{1, \ldots, 6\}$ and $m \in \{1, \ldots, 6\}$) as underlying graph for parameter regions A–D in the phase plane of Figure 6.3.*

6.7 Chapter summary

Analytical means together with computer aid were employed in this chapter to investigate the dynamics of the ESPD with small toroidal grids as underlying graphs.

In §6.1, the need of computer aid in the analysis was motivated due to the inherent combinatorial explosion. The phase plane was then constructed in §6.2, in which eleven regions were identified to induce different game dynamics. Because of the combinatorial complexity of the ensuing analysis, a new analysis visualisation tool, called the equilibrium state diagram, was proposed in §6.3 to replace the state graph for larger toroidal grid dimensions during analyses of the ESPD game dynamics.

Various algorithms for the computation of the equilibrium state diagrams were proposed in §6.4. An explicit algorithm and an implicit algorithm for the identification of automorphism class leaders were proposed and their implementations discussed. The implicit algorithm achieved a significant improvement in terms of both computational time and computer memory requirements over the explicit algorithm. A third algorithm for the identification of static steady states and a reduction of the state space that requires full game investigation was also presented with its associated computing time and memory performance evaluated.

The game dynamics for the ESPD with the underlying grid graphs $C_2 \times C_6$, $C_3 \times C_3$, $C_3 \times C_4$, $C_3 \times C_5$, $C_3 \times C_6$, $C_4 \times C_4$, $C_4 \times C_5$, $C_4 \times C_6$, $C_5 \times C_5$, $C_5 \times C_6$ and $C_6 \times C_6$ were then investigated in §6.3. First, the equilibrium state diagrams were computed for each of the underlying toroidal grids and for all the parameter regions in the phase plane, employing the proposed algorithms. The algorithms were validated against the $C_3 \times C_3$ equilibrium state diagram previously analysed by Van der Merwe [72]. The enumeration of all the components of the equilibrium state diagrams then followed for each parameter region. A weakly defined exponential increase in the number of components in the equilibrium state diagram were identified as the dimensions of the underlying graph increases. The likelihood of persistent cooperation emerging was also determined for each toroidal grid. As the dimensions of the underlying graph increases, it was found that the probability of persistent cooperation emerging also increased for all parameter regions of the phase plane, except for G, J and K. The conditional probabilities that initial game states of specified weights will lead to the emergence of persistent cooperation were also computed for each of the underlying toroidal grid graphs. The chapter finally closed with a collective analysis of the ability of small toroidal grid to facilitate the emergence of persistent cooperation in the ESPD.

CHAPTER 7

Conclusion and future work

Contents

This chapter comprises three sections. In the first section, a brief summary of the work contained in the thesis is presented while in the second, an appraisal is offered of the contributions of the thesis. The chapter then closes with a final section devoted to the documentation of possibilities for related future work.

7.1 Thesis summary

The thesis opened in Chapter 1 with a brief background on the paradoxical nature of the emergence of cooperation amongst egoistic individuals and the relevant theories that attempt to explain its occurrence. It was explained that the general area of focus of the research conducted in this thesis is the mathematical spatio-temporal analysis of cooperation in the context of games on graphs according to the theory of network reciprocity. The general lack of a fundamental understanding of the effect of the underlying spatial topology on the emergence of cooperation was highlighted within this realm of research and this led to the problem statement of this thesis. The thesis scope was delimited thereafter, with a focus on various assumptions made and the choice of graph classes to be considered in the thesis as a result of the complexity of analysing games on graphs in general. The chapter finally closed with the statement on the objectives pursued in the thesis as well as a description of the organisation of material in the remainder of the thesis.

Basic mathematical concepts underlying the work in this thesis were introduced in Chapter 2. In §2.1, fundamental notions from graph theory were reviewed. This review included the concepts of connectedness and graph isomorphism. Various types of graphs employed in the modelling of games on graphs, were then reviewed with an emphasis on circulant and grid graphs — the two graph structures considered in this thesis. The chapter closed in §2.2 with a brief review of basic notions from group theory, focusing specifically on the Cauchy-Frobenius Lemma as an enumerative combinatoric tool.

A survey of the literature on topics related to game theory was conducted in Chapter 3. In §3.1, basic concepts from classical game theory were reviewed based on the assumption that players are perfectly rational and that this assumption is common knowledge to all players. This was followed by a brief overview of the main historical developments within this field. A basic mathematical framework and various accompanying definitions required for modelling games were then recounted in §3.2. Various methods for classifying games, as well as their associated solution concepts, were also presented. In §3.3, various well-known 2-person 2-strategy games were reviewed from the literature on evolutionary game theory, focusing on the PD. The focus of the chapter shifted in §3.4 from classical game theory to evolutionary game theory, a field originating from the relaxation of various assumptions in classical game theory. The main assumptions of evolutionary game theory are that players have bounded rationality, limited knowledge of the game played, and are able to adapt and learn good strategies as a game progresses. The chapter closed with a discussion on the literature related to evolutionary spatial games with an emphasis on the various analysis techniques adopted (either analytical, numerical or other less common approaches). Chapter 3 stands in fulfilment of Thesis Objective I.

A mathematical framework for representing the ESPD on relatively simple, small graphs was presented in Chapter 4, in fulfilment of Thesis Objective II. In §4.1, an evolutionary spatial game was represented as an ordered pair containing a set of pay-off parameters and an underlying graph. The deterministic updating rule adopted for modelling the ESPD in this thesis was also described in §4.2. The notion of an automorphism strategy class was introduced in which all game states exhibit equivalent subsequent game dynamics. The utility of this notion was explained as that it reduces the number of initial game states that have to be invested in a full ESPD game dynamic analysis. Furthermore, the notion of a state graph was presented as a visualisation tool for a full game dynamic analysis. In §4.4, a normalisation of the pay-off values was proposed with the purpose of reducing the complexity of modelling the game without changing the overall game dynamics. The construction of a parameter phase plane was finally described in order to identify the various parameter value combinations that require independent game analyses.

In Chapter 5, analytical means (void computer aid) were employed to determine how the extension of each player's (cyclic) neighbourhood affects the likelihood of persistent cooperation when players are arranged in a cyclic topology. The chapter opened with a brief background on the analysis of the ESPD with a cycle as underlying graph, as found in the literature. The focus of the chapter then shifted to an investigation of the game dynamics of the ESPD with the circulant $C_n\langle 1,2\rangle$ as underlying graph. In order to facilitate this analysis, the phase plane of the ESPD with the circulant $C_n\langle 1,2\rangle$ as underlying graph was first constructed in §5.3. Five parameter regions were thus identified for which independent game dynamic analyses were required.

In §5.4, initial states that allow for the persistence of cooperation were then characterised for each parameter region of the phase plane. This characterisation was utilised in combination with the Cauchy-Frobenius Lemma to enumerate the equilibrium states of the game. It was found that the number of equilibrium states increases exponentially as the order of the underlying graph increases. The state graph of the ESPD with the circulant $C_n\langle 1,2\rangle$ as underlying graph was found to be a rooted pseudo-forest for three of the phase plane parameter regions. For each of these parameter regions the number of components in the state graph was shown to be equivalent to the number of equilibrium states. The characterisation and enumeration of the equilibrium states were then employed to compute the probability of cooperation persisting. It was found, in fulfilment of Thesis Objective III, that the likelihood of cooperation persisting tends towards certainty as the order of the underlying graph increases. The game dynamics of the ESPD with a cycle as underlying graph was finally compared with that of an ESPD with

the circulant $C_n\langle 1, 2\rangle$ as underlying graph, in fulfilment of Thesis Objective IV. It was found that as each player extends its neighbourhood, the number of equilibrium states, as well as the probability of the emergence of persistent cooperation, decreases.

The dynamics of instances of the ESPD with small toroidal grids as underlying graphs was investigated by analytical means (together with computer aid) in Chapter 6. The chapter opened with a motivation for the requirement of computer aid in the analysis: The inherent combinatorial explosion in the analysis as a result of an exponential increases in the initial game state space as the dimensions of the underlying graph increase rendered the previous analytical approach (void computer aid), adopted in Chapter 5, infeasible. In §6.2, the phase plane for the ESPD on a toroidal grid was constructed and eleven parameter regions were identified for which game dynamics had to be investigated independently. Because of the increased size of the state space (and hence an increased number of automorphism class representatives) the state graph was shown no longer to be a practical game dynamic analysis visualisation tool for all but the tiniest toroidal grids. The notion of an equilibrium state diagram was therefore proposed for the analysis of the ESPD with larger toroidal grids as underlying graphs in §6.3. The state graph of a grid cannot be classified as a rooted pseudo-forest for all the possible phase plane regions of the ESPD with a toroidal grid as underlying graph, it was demonstrated that three types of equilibrium states can emerge instead, namely a static steady state, a transient steady state and a limit cycle.

In §6.4, three algorithmic approaches towards constructing the equilibrium state diagram were put forward. In order to identify the automorphism class representatives, both an explicit and an implicit algorithm were proposed, together with appropriate pruning rules for reducing the initial game state space. The implicit algorithm demonstrated an ability to reduce both the computation and memory requirements significantly when compared to the explicit algorithm. A final algorithm was proposed for identifying all the static steady states by creating an archive of game instances that required further full game dynamic investigation.

In §6.5, the aforementioned algorithms were used to compute equilibrium state diagrams for the ESPD with the eleven toroidal grids $C_2 \times C_6$, $C_3 \times C_4$, $C_3 \times C_5$, $C_3 \times C_6$, $C_4 \times C_4$, $C_4 \times C_5$, $C_4 \times C_6$, $C_5 \times C_5$, $C_5 \times C_6$ and $C_6 \times C_6$ as underlying graphs. The equilibrium state diagrams were then used to enumerate the components in the corresponding state graphs. It was found that as the dimensions of the underlying grid increases, the number of components in the state graph also increases according to a weakly-defined exponential relationship. The grid $C_3 \times C_4$ was identified as the smallest toroidal grid capable of bringing forth an ESPD transient steady state in its equilibrium state diagrams, while the grid $C_5 \times C_5$ is the smallest toroidal grid capable of producing a limit cycle within its ESPD equilibrium state diagrams.

The probability of cooperation persisting in each of the underlying toroidal grids was also computed, in fulfilment of Thesis Objective V. It was found that as the dimensions of the underlying grid increases, the probability of cooperation persisting also increases. For each underlying spatial topology, the relationship between the weight of the initial state and the probability of cooperation persisting was also investigated. It was found that in four parameter regions of the phase plane the relationship between the weight of the initial state and the probability of cooperation persisting tends towards a linear relationship as the dimensions of the underlying toroidal grid increases. For the remaining six parameter regions, on the other hand, the probability that cooperation persists was found to be small if the game instance started with fewer than approximately 80% cooperators; thereafter the probability rapidly increased towards certainty. The chapter finally closed in §6.6 with an appraisal of the collective ability of toroidal grids of dimensions at most 6×6 facilitating the emergence of persistent cooperation in the ESPD.

7.2 Appraisal of thesis contributions

This section contains a brief appraisal of the five contributions of this thesis to the field of evolutionary spatial game theory.

Contribution 1 *An asymptotic analysis of the ESPD with $C_n\langle 1,2\rangle$ as underlying graph*

The phase plane was constructed for the ESPD with $C_n\langle 1,2\rangle$ as underlying graph. Five parameter regions were identified which required independent game dynamic analyses. The structures of the initial states that lead to equilibrium states which contain some form of persistent cooperation were characterised. An analytic approach (void computer aid) was adopted in order to enumerate the automorphism classes of these equilibrium states and to determine the likelihood that a random initial state will result in an equilibrium state accommodating some form of persistent cooperation.

Contribution 2 *Introduction of the notion of an equilibrium state diagram as a new visualisation tool for the analysis of ESPD game dynamics*

A new game dynamic analysis visualisation tool, called an equilibrium state diagram, was proposed to replace the earlier notion in the literature of a state graph during analyses of ESPD game dynamics with larger underlying graphs. As the dimensions of the underlying graph of the ESPD increases, so too does the number of automorphism class leaders (at an exponential rate, in fact). Therefore, the state graph becomes so large, even for moderately sized underlying graphs of the ESPD, that it is no longer a feasible form of steady state representation. The equilibrium state diagram conveys the same information required for game dynamic investigations as the state graph, but in a much more compact form. Furthermore, the equilibrium state diagram allows for the classification of static steady states, transient steady states and limit cycles, which is not possible when adopting the state graph as an analysis tool.

Contribution 3 *An asymptotic analysis of the ESPD with a small toroidal grid as underlying graph*

The complete set of equilibrium state diagrams for the ESPD with the toroidal grids $C_2 \times C_6$, $C_3 \times C_4$, $C_3 \times C_5$, $C_3 \times C_6$, $C_4 \times C_4$, $C_4 \times C_5$, $C_4 \times C_6$, $C_5 \times C_5$, $C_5 \times C_6$ and $C_6 \times C_6$ as underlying graphs was constructed. The algorithms designed for the construction of these equilibrium state diagrams are, however, limited to analyses of the ESPD with small toroidal grids as underlying graphs. As the dimensions of the underlying grid increases, so too do the computational time and memory requirements — so much so that the approach becomes intractable for toroidal grids of dimensions larger than 6×6. For this reason, a documentation of the number of states that lead to each specific equilibrium state within the equilibrium state diagram was also omitted for toroidal grids of dimensions larger than 4×4.

Contribution 4 *An investigation into the relationship between the amount of cooperation in an initial game state and the probability of cooperation persisting in the ESPD with a toroidal grid as underlying graph*

The probability that an initial game state with a specified weight will lead to an equilibrium state that accommodates some form of cooperation was computed for the ESPD with the toroidal

grids $C_2 \times C_6$, $C_3 \times C_3$, $C_3 \times C_4$, $C_3 \times C_5$, $C_3 \times C_6$, $C_4 \times C_4$, $C_4 \times C_5$, $C_4 \times C_6$, $C_5 \times C_5$, $C_5 \times C_6$ and $C_6 \times C_6$ as underlying graphs.

Contribution 5 *Identification of the smallest underlying toroidal grid that gives rise to a transient steady state or a limit cycle*

The graph $C_3 \times C_4$ was identified as the smallest underlying toroidal grid of the ESPD that exhibits a transient steady state in its equilibrium state diagrams. In a similar vein, the graph $C_5 \times C_5$ was identified as the smallest underlying toroidal grid of the ESPD that exhibits a limited cycle in its equilibrium state diagrams.

7.3 Ideas for future work

In this final section, five suggestions are made for possible avenues of future research, building on the work presented in this thesis, in fulfilment of Thesis Objective VI.

Analysis of the ESPD with $C_2 \times C_n$ as underlying graph

A similar analytic approach (without computer aid) as adopted in the game dynamic analysis of the ESPD with a circulant as underlying graph may be adopted to determine the probability of persistent cooperation emerging on the underlying toroidal grid $C_2 \times C_n$. The phase plane for this underlying spatial topology is equivalent to the phase plane constructed for toroidal grids in this thesis. Each of the eleven parameter regions therefore requires an independent game dynamic analysis. First, the characteristics of the steady states are to be ascertained by determining which structures allow for pockets of cooperation to persist to the next round of the game. These characterisations can then be used to enumerate the states that contain such structures. In this way, the probability of persistent cooperation emerging on the toroidal grid $C_2 \times C_n$ can be computed. The results of such an analysis may be compared with those obtained during the neighbourhood underlying spatial topology extension analysis from the cycle C_n to the circulant $C_n\langle 1, 2\rangle$ conducted in Chapter 5. In this manner, the effect of each player extending its neighbourhood from size two to three or four, when arranged in a cyclic topology, can be compared and the relationship between the sizes of the neighbourhoods further investigated.

The ESPD with larger grids and small-world networks as underlying graphs

It would be interesting to extend the analysis of Chapter 6 to include larger toroidal grids in order to determine whether the observed relationship between the emergence of persistent cooperation and the size of the underlying grid continues to manifest itself. It would also be interesting to continue the analysis of the relationship between the level of cooperation present in the initial game state and the probability of cooperation eventually persisting for the various parameter regions of the phase plane in the case of larger toroidal grid. Such research would shed light on whether or not the linear relationship observed for small grids between the weight of the initial game state and the probability of persistent cooperation emerging in the cases of parameter regions A, C, E and I of the phase plane continues or is an artefact of only considering small toroidal grids. In order to carry out such an analysis, however, it is anticipated that a computer simulation approach will be required, because the state space of the initial game states will quickly grow very large.

A natural extension of the work in Chapter 5 would be to continue increasing the neighbourhood sizes of the various players arranged in a cyclic topology. This would involve analysing the game dynamics of the ESPD on circulants with various connection sets of increasing sizes. As the size of the connection set increases, however, the size of the initial state space increases exponentially. Furthermore, as the connection set of the circulant increases in size, the analysis is complicated considerably by the emergence of additional symmetries. Hence, an analytical approach is no longer expected to be feasible (*i.e.* a simulation approach is advised for such an extended analysis). As a circulant structure can be used to generate a small-world network, the relationship between the average player neighbourhood size and the emergence of persistent cooperation in the context of a small-world network may also be investigated.

Fraction of cooperation present in the equilibrium state

A further area of interest is not only to investigate the probability of *any* form of cooperation persisting, but also to quantify the amount of cooperation present in the equilibrium states. In this thesis, only the level of cooperation present in an initial game state and how this affected the emergence of any form of persistent cooperation were considered. This scope of investigation may be extended to include variation in the level of cooperation present in game states as the game progresses and, finally, the level of cooperation present in the resulting equilibrium state. In this way, the growth and decline of the degree of cooperation within an ESPD game state can be investigated over time. Patterns of cluster growth similar to those investigated in Conway's game of life [7] (such as periodic blinkers and gliders) were observed in the game dynamics of instances of the ESPD with a toroidal grid as underlying graph, and this may be of interest when studying the possible dynamics of clusters of cooperators. Potential patterns and cluster shapes can be identified in initial game states in order to predict the level of cooperation that will be present in the corresponding equilibrium states.

The global shipping network and the spread of invasive species

The ESPD model may be applied in a real-world case study. An example of such an application area may be found in the problem of biofouling within the global shipping network. Kaluza *et al.* [33] investigated the relationship between economic growth, cargo trade and invasive species in this context and showed that the spread of invasive species incurred large economic costs to the countries where they established themselves. They demonstrated that the spread of invasive species is largely enhanced by cargo trade. In order to understand the relationship between these three factors, the authors investigated the structure of the international shipping network and the movement of vessels within this network, as well as their facilitation of bio-invasion. The global shipping network considered within their work is shown in Figure 7.1.

In order to prevent the spread of invasive species, the hulls of cargo ships are required to be scraped so as to prevent biofouling. This processes has to occur at the port of origin in order to prevent bio-invasion at the port of destination. Therefore, the cost of screening and cleaning the vessels fall to the exporter, while the direct benefit of this process is enjoyed by the importer. This situation is reminiscent of the type of player interaction in the PD within the context of the ESPD. Each port can be seen as a player in this context, with the global shipping network, illustrated in Figure 7.1, as underlying graph. The cost-benefit relationship of screening and cleaning export vessels can be translated into the ESPD pay-off matrix. Modelling this problem as an ESPD instance gives rise to the interesting research question: Can a sustainable invasive biological control programme emerge among some cluster of countries in the form of persistent

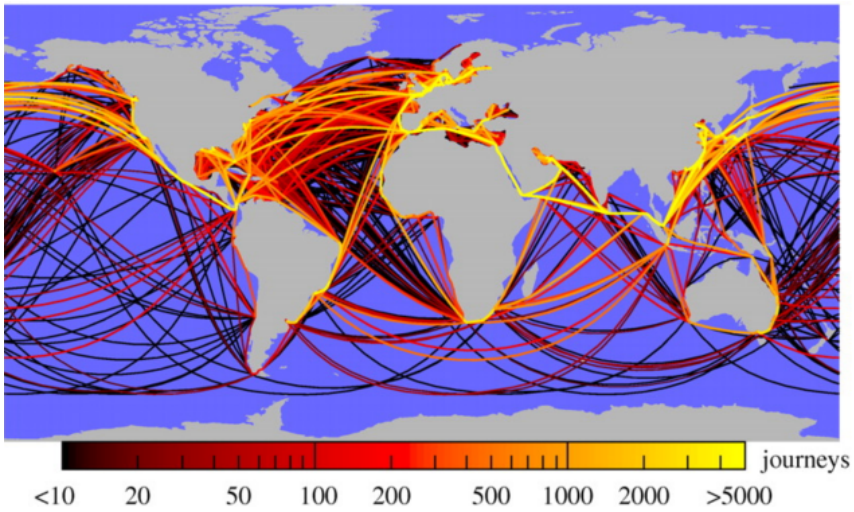

FIGURE 7.1: *The global shipping network showing the routes travelled by large cargo ships (larger than 10 000 GT) between the largest 300 ports globally. The colour scale indicates the number of ships travelling along each route, which is directly proportional to the associated bio-invasion probability [33].*

cooperation? The major obstacle of this research endeavour may be the accessibility of the required data. Currently, the data related to Figure 7.1 have to be purchased according to Kaluza *et al.* [33].

Variations on the ESPD

As described in §3.3, there are many versions of 2-player 2-strategy evolutionary spatial games in the literature. Similar analyses to those documented in this thesis may be applied to other variations on the ESPD, based on alternatives to the PD, such as the Hawk-Dove game. A particular advantage of the Hawk-Dove game model is that its pay-off matrix can be normalised to contain only a single pay-off parameter. This reduces the number of phase plane parameter regions that have to be considered. It was also assumed in this thesis that the interaction graph and the replacement graph of the evolutionary process in the ESPD are isomorphic. Situations may, however, be considered in which these graphs are not equivalent. Furthermore, the interaction between players, as well as with the underlying graph, was assumed to be static in this thesis. Similar investigations to those documented in Chapters 5 and 6 may also be carried out on the same relatively simple graph structures, but with co-evolution of strategies where networks are allowed to change over time.

References

[1] Ashworth T, 2000, *Trench warfare, 1914–1918: The live and let live system*, Pan Macmillan, London.

[2] Aumann R, 1992, *Irrationality in game theory*, pp. 214–227 in Dasgupta P, Gale D, Hart O & Maskin E (Eds), *Economic analysis of markets and games, essays in honor of Frank Hahn*, MIT Press, Cambridge (MA).

[3] Axelrod R, 1984, *The evolution of cooperation*, Basic Books, New York (NY).

[4] Axelrod R & Hamilton WD, 1981, *The evolution of cooperation*, Science, **211**, pp. 1390–1396.

[5] Barabási AL & Pósfai M, 2016, *Network science*, Cambridge University Press, Cambridge.

[6] Bergroth E, 2013, *Topics on game theory*, PhD Thesis, Chalmers University of Technology and Univeristy of Gothenburg, Göteborg.

[7] Berlekamo ER, Conway J & Guy RK, 2003, *Winning ways for your mathematical plays*, 2nd Edition, A K Peters, Natick (MA).

[8] Boccalett S, Latora V, Moreno Y, Chavez M & Hwang DU, 2006, *Complex networks: Structure and dynamics*, Physics Reports, **424**, pp. 175–308.

[9] Brafford B, 2003, *The problem of courage*, Statesmanship Thesis, Ashland University, Ashland (OH).

[10] Burger AP, van der Merwe M & van Vuuren JH, 2012, *An asymptotic analysis of the evolutionary prisoner's dilemma on a path*, Discrete Applied Mathematics, **160**, pp. 2075–2088.

[11] Burger AP, van der Merwe M & van Vuuren JH, 2013, *The evolutionary spatial prisoner's dilemma on a cycle*, ORiON, **29**, pp. 1–16.

[12] Darwin C, 1882, *The descent of man, and selection in relation to sex*, 2nd Edition, John Murray, London.

[13] Deo N, 2016, *Graph theory with applications to engineering and computer science*, Dover Publications, Mineola (NY).

[14] Doebeli M & Knowlton N, 1998, *The evolution of interspecific mutualisms*, Proceedings of the National Academy of Sciences, **95**, pp. 8676–8680.

[15] Du W, Zheng H & Hu M, 2008, *Evolutionary prisoner's dilemma game on weighted scale-free networks*, Physica A: Statistical Mechanics and its Applications, **387**, pp. 3796–3800.

[16] Durlauf SN & Blume LE (Eds), 2008, *The new Palgrave: A dictionary of economics*, 2nd Edition, Palgrave Macmillan, New York (NY).

[17] Ferrière R & Michod RE, 1996, *The evolution of cooperation in spatially heterogeneous populations*, The American Naturalist, **147**, pp. 692–717.

[18] Fine NJ, 1958, *Classes of periodic sequences*, Illinois Journal of Mathematics, **2**, pp. 285–302.

[19] Friedman D, 1998, *On economic applications of evolutionary game theory*, Journal of Evolutionary Economics, **8**, pp. 15–43.

[20] Fudenberg D & Tirole J, 1991, *Game theory*, MIT Press, Cambridge (MA).

[21] Gibbons R, 1992, *Game theory for applied economists*, Princeton University Press, Princeton (NJ).

[22] Graham C, 2008, *The economics of happiness*, pp. 41–55 in Durlauf SN & Blume LE (Eds), *The new Palgrave dictionary of economics*, Palgrave Macmillan, New York (NY).

[23] Hamilton WD, 1964, *The genetical evolution of social behaviour*, Journal of Theoretical Biology, **7**, pp. 1–16.

[24] Harsanyi JC & Selten R, 1988, *A general theory of equilibrium selection in games*, MIT Press, Cambridge (MA).

[25] Hauert CH, 2001, *Effects of space in* 2×2 *games*, International Journal of Bifurcation and Chaos, **12**, pp. 1531–1548.

[26] Henning MA & van Vuuren JH, *Graph and network theory*, In process.

[27] Herz AVM, 1994, *Collective phenomena in spatially extended evolutionary games*, Journal of Theoretical Biology, **169**, pp. 65–87.

[28] Hofbauer J & Sigmund K, 1998, *Evolutionary games and population dynamics*, Cambridge University Press, Cambridge.

[29] Holler MJ & Wickström BA, 1998, *The scandal matrix: The use of scandals in the progress of society*, CESifo Working Paper Series, **(159)**.

[30] Huberman BA & Glance NS, 1993, *Evolutionary games and computer simulations*, Proceedings of the National Academy of Sciences, **90**, pp. 7716–7718.

[31] Hutson VCL & Vickers GT, 1995, *The spatial struggle of tit-for-tat and defect*, Philosophical Transactions: Biological Sciences, **348**, pp. 393–404.

[32] Kakutani S, 1941, *A generalization of Brouwer's fixed point theorem*, Duke Mathematical Journal, **8**, pp. 457–459.

[33] Kaluza P, Kölzsch A, Gastner MT & Blasius B, 2010, *The complex network of global cargo ship movements*, Journal of the Royal Society Interface, **7**, pp. 1093–1103.

[34] Killingback T & Doebeli M, 1996, *Spatial evolutionary game theory: Hawks and doves revisited*, Proceedings of the Royal Society B: Biological Sciences, **263**, pp. 1135–1144.

[35] Kuhn H, 1953, *Extensive games and the problem of information*, pp. 193–216 in Kuhn HW & Tucker AW (Eds), *Contributions to the theory of games*, Princeton University Press, Princeton (NJ).

[36] Lévy P, 1954, *Théorie de l'addition des variables aléatoires*, 2nd Edition, Gauthier-Villars, Paris.

[37] Liu RR, Jia CX & Rong Z, 2015, *Diverse strategy-learning styles promote cooperation in evolutionary spatial prisoner's dilemma game*, Europhysics Letters, **112**, pp. 48005-1 to 48005-6.

[38] Long CT, 1995, *Elementary introduction to number theory*, 3rd Edition, Waveland Press, Chicago (IL).

[39] Martin GE, 2001, *Counting: The art of enumerative combinatorics*, Springer-Verlag, New York (NY).

[40] Maynard Smith J, 1982, *Evolution and the theory of games*, Cambridge University Press, Cambridge.

[41] Maynard Smith J, 1986, *Evolutionary game theory*, Physica D: Nonlinear Phenomena, **22**, pp. 43–49.

[42] Maynard Smith J & Price GR, 1973, *The logic of animal conflict*, Nature, **246**, pp. 15–18.

[43] Morrow JD, 1994, *Game theory for political scientists*, Princeton University Press, Princeton (NJ).

[44] Myerson RB, 1997, *Game theory: Analysis of conflict*, Harvard University Press, Cambridge (MA).

[45] Nasar S, 1995, *Albert W. Tucker, 89, pioneering mathematician*, The New York Times, January.

[46] Nash J, 1951, *Non-cooperative games*, Annals of Mathematics, **54**, pp. 286–295.

[47] Nash JF, 1950, *Equilibrium points in n-person games*, Proceedings of the National Academy of Sciences, **36**, pp. 48–49.

[48] Nisan N, Roughgarden T, Tardos E & Vazirani VV, 2007, *Algorithmic game theory*, Cambridge University Press, Cambridge.

[49] Nowak MA, 2006, *Five rules for the evolution of cooperation*, Science, **314**, pp. 1560–1563.

[50] Nowak MA, Bonhoeffer S & May RM, 1995, *Robustness of cooperation*, Nature, **379**, pp. 125–126.

[51] Nowak MA & May RM, 1992, *Evolutionary games and spatial chaos*, Nature, **359**, pp. 826–829.

[52] Nowak MA & May RM, 1993, *The spatial dilemmas of evolution*, International Journal of Bifurcation and Chaos, **3**, pp. 35–78.

[53] Nowak MA & Sigmund K, 1993, *A strategy of win-stay, lose-shift that outperforms tit-for-tat in the prisoner's dilemma game*, Nature, **364**, pp. 56–58.

[54] Nowak MA & Sigmund K, 1998, *Evolution of indirect reciprocity by image scoring*, Nature, **393**, pp. 573–577.

[55] Nowak MA & Sigmund K, 2004, *Evolutionary dynamics of biological games*, Science, **303**, pp. 793–799.

[56] O'Neill B, 1994, *Game theory models of peace and war*, pp. 995–1053 in Aumann RJ & Hart S (Eds), *Handbook of game theory with economic applications*, Elsevier-North Holland, Amsterdam.

[57] Ohtsuki H, Hauert C, Liberman E & Nowak MA, 2006, *A simple rule for the evolution of cooperation on graphs and social networks*, Nature, **441**, pp. 502–505.

[58] Petrosyan LA & Zenkevich NA, 2016, *Game theory*, 2nd Edition, World Scientific, Singapore.

[59] Poundstone W, 1993, *Prisoner's dilemma, John von Neumann, game theory and the puzzle of the bomb*, Anchor Books, New York (NY).

[60] Poundstone W, 2011, *Labyrinths of reason: Paradox, puzzles, and the frailty of knowledge*, Anchor Books, New York (NY).

[61] Roca CP, Cuesta JA & Sánchez A, 2009, *Effect of spatial structure on the evolution of cooperation*, Physical Review E, **80**, pp. 046106-1 to 046106-16.

[62] Shapley LS & Shubik M, 1988, *A method for evaluating the distribution of power in a committee system*, pp. 41–48 in Roth AE (Ed), *The Shapley value: Essays in honor of Lloyd S. Shapley*, Cambridge University Press, Cambridge.

[63] Skyrms B, 2001, *The stag hunt*, Proceedings and Addresses of the American Philosophical Association, **75**, pp. 31–41.

[64] Sloane NJA, 2018, *The on-line encyclopedia of integer sequences*, [Online], [Cited February 2018], Available from `https://oeis.org/`.

[65] Standley RP, 2012, *Enumerative combinatorics*, 2nd Edition, Cambridge University Press, Cambridge.

[66] Sugden R, 1989, *Spontaneous order*, Journal of Economic Perspectives, **3**, pp. 85–97.

[67] Sugden R, 2001, *The evolutionary turn in game theory*, Journal of Economic Methodology, **8**, pp. 113–130.

[68] Szabó G & Töke C, 1998, *Evolutionary prisoner's dilemma game on a square lattice*, Physical Review E, **58**, pp. 69–73.

[69] Traulsen A & Nowak MA, 2006, *Evolution of cooperation by multilevel selection*, Proceedings of the National Academy of Sciences, **103**, pp. 10952–10955.

[70] Trivers RL, 1971, *The evolution of reciprocal altruism*, The Quarterly Review of Biology, **46**, pp. 35–57.

[71] Turocy TL & von Stengel B, 2002, *Game theory*, pp. 403–420 in Bidgoli H (Ed), *Encyclopedia of information systems*, Elsevier, Amsterdam.

[72] van der Merwe M, 2013, *Non-cooperative games on networks*, MSc Thesis, Stellenbosch University, Stellenbosch.

[73] Vincent TL & Brown JS, 2005, *Evolutionary game theory, natural selection, and Darwinian dynamics*, Cambridge University Press, Cambridge.

[74] von Neumann J, 1928, *Zur Theorie der Gesellschaftsspiele*, Mathematische Annalen, **100**, pp. 295–320.

[75] von Neumann J & Morgenstern O, 1944, *Theory of games and economic behavior*, Princeton University Press, Princeton (NJ).

[76] Walker PW, 1995, *An outline of the history of game theory*, [Online], [Cited January 2018], Available from `http://euler.fd.cvut.cz/predmety/teorie_her/histf.html`.

[77] Watts DJ & Strogatz SH, 1998, *Collective dynamics of small-world networks*, Nature, **393**, pp. 440–442.

[78] Wolfram Research, 2018, *Mathematica, Version 11.0*, [Online], [Cited March 2018], Available from `http://www.wolfram.com/?source=nav`.

[79] Wolfram S, 1986, *Theory and applications of cellular automata*, World Scientific, Singapore.

[80] Wright S, 1932, *The roles of mutation, inbreeding, crossbreeding, and selection in evolution*, Proceedings of the 6th International Congress of Genetics, Ithaca (NY), pp. 356–366.

[81] Zermelo E, 1912, *Über eine Anwendung der Mengenlehre auf die Theorie des Schachspiels*, Proceedings of the 5th International Congress of Mathematicians, Cambridge, pp. 501–504.

APPENDIX A

Characterisation of equilibrium states

The proofs for Lemmas 2–4 of §5.4 are given in this appendix . The various lemmas elucidate the strategy adoption structures required for cooperation to persist to the next round of the ESPD with the circulant $C_n\langle 1,2\rangle$ as underlying graph for parameter regions B, C and E of the phase plane in Figure 5.6. In each case, the lemma is restated after which its proof is presented.

Lemma 2. *If the underlying graph of the ESPD is the circulant $C_n\langle 1,2\rangle$ and the parameter inequalities $3T + P > 4$ and $2T + 2P < 3$ hold (i.e. the parameters lie within region B of the phase plane in Figure 5.6), then*

(a) no cooperation run of length one, two or three can persist intact to the next round of the game, and

(b) a cooperation run of length at least four can persist to the next round of the game if and only if it is flanked on both sides by a run of defectors of length at least three.

Proof:

(a) A cooperation run of length one has the form DCD. Figure A.1 contains an illustration of this configuration for the ESPD with the circulant $C_n\langle 1,2\rangle$ as underlying graph. Black vertices represent players adopting the strategy of cooperation, while white vertices represent players adopting the strategy of defection. Grey vertices represent players with unknown strategies. This graphical representation format is used in all figures throughout this proof.

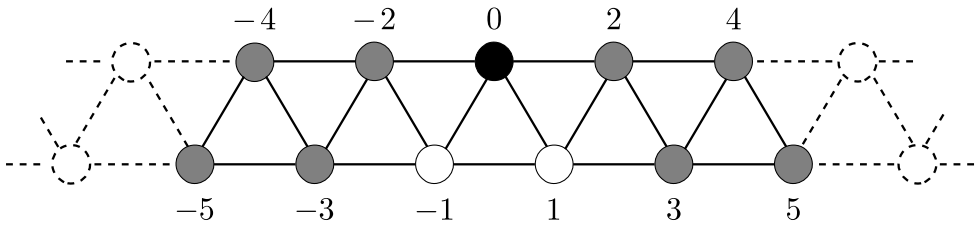

FIGURE A.1: *Configuration of a cooperation run of length one for the ESPD with the circulant $C_n\langle 1,2\rangle$ as underlying graph.*

In the configuration shown in Figure A.1, cooperating player 0 requires a pay-off value at least as large as the largest pay-off value of the two defecting players -1 and 1 in its open neighbourhood

in order to persist to the next round of the game. As shown previously, $d_i > c_j$ if $i \geq j$ for all $i, j \in \mathbb{N}_0$. Let

$$a_i = \begin{cases} 0, & \text{if player } i \text{ adopts the strategy of defection, or} \\ 1, & \text{if player } i \text{ adopts the strategy of cooperation.} \end{cases}$$

Therefore, the pay-off value of the cooperating player 0 is $c_{a_{-2}+a_2}$ and the pay-off values of the defecting players -1 and 1 are $d_{1+a_{-2}+a_{-3}}$ and $d_{1+a_2+a_3}$, respectively. It can now be seen that $a_{-2} + a_2 \leq 1 + a_{-2} + a_{-3}$ and $a_{-2} + a_2 \leq 1 + a_2 + a_3$. Therefore, $d_{1+a_{-2}+a_{-3}} > c_{a_{-2}+a_2}$ and $d_{1+a_2+a_3} > c_{a_{-2}+a_2}$. The cooperating player 0 will consequently not be able to achieve a pay-off value at least as large as either of its two defecting neighbouring players -1 and 1, and will hence adopt the strategy of defection during the next round of the game. This shows that no cooperation run of length one can remain intact to the next round of the game.

Consider next a cooperation run of length two. Such a run has the form $DCCD$. This configuration is shown in Figure A.2 for the ESPD with the circulant $C_n\langle 1, 2\rangle$ as underlying graph.

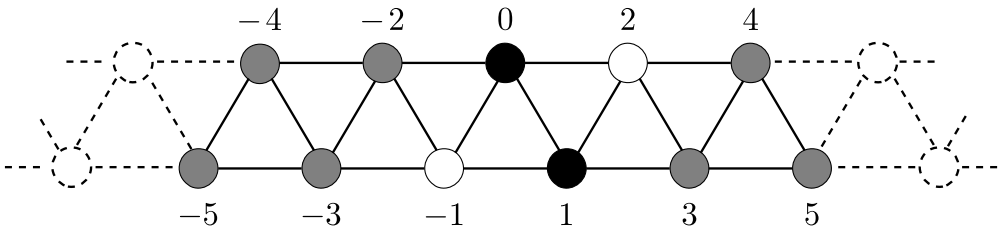

FIGURE A.2: *Configuration of a cooperation run of length two for the ESPD with the circulant* $C_n\langle 1, 2\rangle$ *as underlying graph.*

The pay-off values of the cooperating players 0 and 1 are $c_{1+a_{-2}}$ and c_{1+a_3}, respectively, while the pay-off values of the defecting players -1 and 2 are $d_{2+a_{-2}+a_{-3}}$ and $d_{2+a_3+a_4}$, respectively. Therefore, using a similar logic as for a cooperation run of length one above, it can be seen that the inequalities $c_{1+a_{-2}} < d_{2+a_{-2}+a_{-3}}$ and $c_{1+a_3} < d_{2+a_3+a_4}$ hold as a result of the fact that $1 + a_{-2} < 2 + a_{-2} + a_{-3}$ and $1 + a_3 < 2 + a_3 + a_4$. The two cooperating players 0 and 1 are hence unable to achieve pay-off values at least as large as those of their two defecting neighbours -1 and 2, and will consequently adopt the strategy of defection during the next round of the game. This shows that no cooperation run of length two can remain intact to the next round of the game.

Finally, consider a cooperation run of length three. Such a run has the form $DCCCD$. This configuration is shown in Figure A.3 for the ESPD with the circulant $C_n\langle 1, 2\rangle$ as underlying graph.

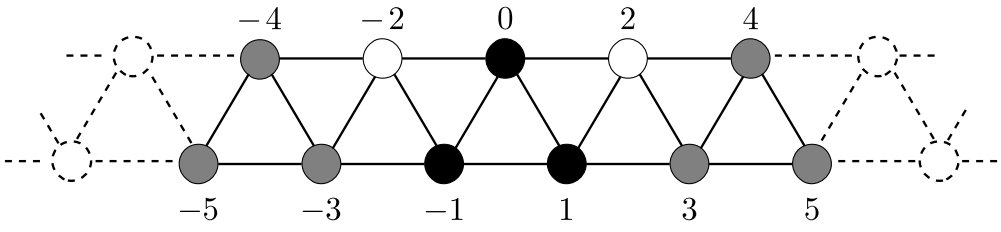

FIGURE A.3: *Configuration of a cooperation run of length three for the ESPD with on the circulant* $C_n\langle 1, 2\rangle$ *as underlying graph.*

The pay-off values of cooperating players 0, 1 and -1 are c_2, $c_{2+a_{-3}}$ and c_{2+a_3}, respectively, while the pay-off values of the defecting players -2 and 2 are $d_{2+a_{-3}+a_{-4}}$ and $d_{2+a_3+a_4}$, respectively. Therefore, using a similar logic as for a cooperation run of length one, this results in the inequalities $d_{2+a_{-3}+a_{-4}} > c_{2+a_{-3}}$, $d_{2+a_{-3}+a_{-4}} > c_2$, $d_{2+a_3+a_4} > c_{2+a_3}$ and $d_{2+a_3+a_4} > c_2$ because of the relationships $2 + a_{-3} + a_{-4} \geq 2 + a_{-3}$, $2 + a_{-3} + a_{-4} \geq 2$, $2 + a_3 + a_4 \geq 2 + a_3$ and $2 + a_3 + a_4 \geq 2$. The three cooperating players 0, 1 and -1 are therefore unable to achieve pay-off values at least as large as those of their two defecting neighbours -2 and 2, and will hence adopt the strategy of defection during the next round of the game. This shows that no cooperation run of length three can remain intact to the next round of the game.

(b) A cooperation run of length four has the form $DCCCCD$. This configuration is illustrated in Figure A.4 for the ESPD with the circulant $C_n\langle 1, 2\rangle$ as underlying graph.

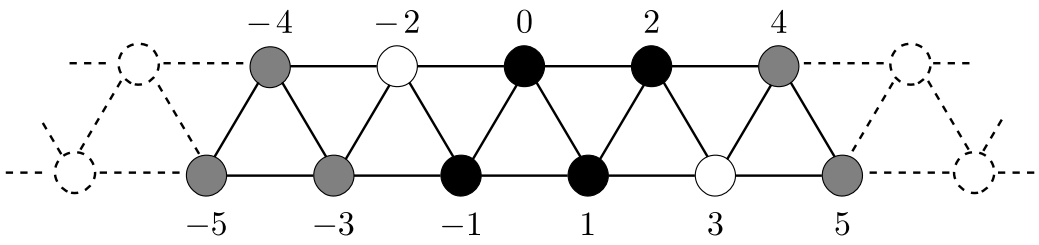

FIGURE A.4: *Configuration of a cooperation run of length four for the ESPD with the circulant $C_n\langle 1, 2\rangle$ as underlying graph.*

The pay-off values of players $-1, 0, 1, 2$, representing the run of cooperators of length four, are $c_{2+a_{-3}}, c_3, c_3$ and c_{2+a_4}, respectively. The largest cooperator pay-off value is therefore c_3. Since only the largest-valued cooperator is relevant in each player's closed neighbourhood during the updating process, only c_3 is compared with the pay-off value of the players in the cooperation run of length four. The pay-off values achieved by the defecting players -2 and 3 are $d_{2+a_{-3}+a_{-4}}$ and $d_{2+a_4+a_5}$, respectively. In the parameter region B, however, $c_3 > d_2$. Therefore, in order for the inequalities $c_3 > d_{2+a_{-3}+a_{-4}}$ and $c_3 > d_{2+a_4+a_5}$ to hold, ensuring the largest-valued cooperator has a larger pay-off value then the largest-valued defector, it must hold that $a_{-3} + a_{-4} = 0$ and $a_4 + a_5 = 0$. In order for these equalities to be satisfied, it is required that $a_{-4} = a_{-3} = a_4 = a_5 = 0$. It can therefore be deduced that, in order for the run of cooperators of length four to persist intact to the next round of the game, it must be flanked by two defection runs, each of length at least three.

A run of cooperators of length greater than four has the form $D\langle C\rangle^i D$ for $i > 4$. Within this configuration, the largest cooperator pay-off value is c_4. The two outer defectors, namely players $\lfloor -\frac{n-1}{2} \rfloor$ and $\lceil \frac{n-1}{2} \rceil$ obtain the pay-off values $d_{2+a_{-\lceil \frac{i}{2} \rceil - 1}+a_{-\lceil \frac{i}{2} \rceil - 2}}$ and $d_{2+a_{\lceil \frac{i}{2} \rceil + 1}+a_{\lceil \frac{i}{2} \rceil + 2}}$, respectively. According to the parameter region inequalities, $d_3 > c_4$ and $d_2 < c_3$. Therefore, in order for the inequalities $d_{2+a_{-\lceil \frac{i}{2} \rceil - 1}+a_{-\lceil \frac{i}{2} \rceil - 2}} < c_4$ and $d_{2+a_{\lceil \frac{i}{2} \rceil + 1}+a_{\lceil \frac{i}{2} \rceil + 2}} < c_4$ to hold, it is required that $2+a_{\lceil \frac{i}{2} \rceil + 1}+a_{\lceil \frac{i}{2} \rceil + 2} < 3$ and $2+a_{\lceil \frac{i}{2} \rceil + 1}+a_{\lceil \frac{i}{2} \rceil + 2} < 3$. Hence, both $a_{\lceil \frac{i}{2} \rceil + 1}+a_{\lceil \frac{i}{2} \rceil + 2} = 0$ and $a_{\lceil \frac{i}{2} \rceil + 1} + a_{\lceil \frac{i}{2} \rceil + 2} = 0$ must hold. In order for these inequalities to be satisfied, it is required that $a_{\lceil \frac{i}{2} \rceil + 1} = a_{\lceil \frac{i}{2} \rceil + 2} = a_{\lceil \frac{i}{2} \rceil + 1} = a_{\lceil \frac{i}{2} \rceil + 2} = 0$. It can therefore be deduced that, in order for the run of cooperators of length $i \geq 4$ to persist intact to the next round of the game, it must be flanked by two defection runs, each of length at least three. □

The following lemma is similar to Lemma 2, but holds for parameter region C of the phase plane in Figure 5.6. A similar method of proof is adopted.

Lemma 3. *If the underlying graph of the ESPD is the circulant $C_n\langle 1,2\rangle$ and the parameter inequalities $3T+P>4$, $2T+2P>3$ and $2T+2P<4$ hold (i.e. the parameters lie within region C of the phase plane in Figure 5.6), then*

(a) no cooperation run of length one, two, three or four can persist intact to the next round of the game, and

(b) a cooperation run of length at least five can persist to the next round of the game if and only if it is flanked on both sides by a run of defectors of length at least three.

Proof: (a) Note, that the proof of Theorem 2(a) is only restricted to the parameter region inequality $2T+2P<4$. Hence, the proof applies to all parameter regions except parameter region D in the phase plane of Figure 5.6. Therefore, no cooperation run of length one, two or three can remain intact to the next round of the game within parameter region C.

Consider a cooperation run of length four which has the form $DCCCCD$. This configuration is illustrated in Figure A.4 for the ESPD with the circulant $C_n\langle 1,2\rangle$ as underlying graph. The pay-off values of players $-1,0,1,2$, representing the run of cooperators of length four, are $c_{2+a_{-3}}, c_3, c_3$ and c_{2+a_4}, respectively. The largest cooperator pay-off value is therefore c_3. Since only the largest-valued cooperator is relevant in each player's closed neighbourhood during the updating process, only c_3 is compared with the pay-off value of the players in the cooperation run of length four. The pay-off values achieved by the defecting players -2 and 3 are $d_{2+a_{-3}+a_{-4}}$ and $d_{2+a_4+a_5}$, respectively. In the parameter region C, however, $d_2>3$. Therefore, $c_3<d_{2+a_{-3}+a_{-4}}$ and $c_3<d_{2+a_4+a_5}$ holds. The four cooperating players are therefore unable to achieve pay-off values at least as large as those of their two defecting neighbours, and will hence adopt the strategy of defection during the next round of the game. This shows that no cooperation run of length four can remain intact to the next round of the game.

(b) A cooperation run of length five has the form $DCCCCCD$. This configuration is illustrated in Figure A.5 for the ESPD with the circulant $C_n\langle 1,2\rangle$ as underlying graph.

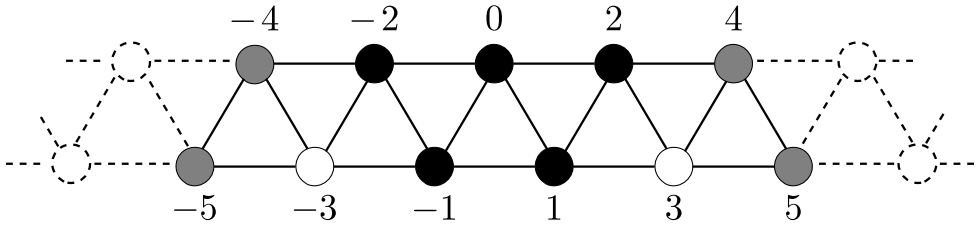

FIGURE A.5: *Configuration of a cooperation run of length five for the ESPD with the circulant $C_n\langle 1,2\rangle$ as underlying graph.*

The run of cooperators of length five, consisting of players $-2,-1,0,1$ and 2, achieve the pay-off values $c_{2+a_{-4}}, c_3, c_4, c_3$ and c_{2+a_4}, respectively. The largest pay-off value achieved by a cooperator in this run is therefore c_4. Since each player compares the pay-off value achieved by the largest-valued cooperator and defector in its closed neighbourhood, only the largest pay-off value c_4 is relevant. The two neighbouring defectors, players -3 and 3, achieve the pay-off values $d_{2+a_{-4}+a_{-5}}$ and $d_{2+a_4+a_5}$, respectively. According to the parameter region inequalities, however, $d_3>c_4$ and $3<d_2<4$. Therefore, in order for the inequalities $d_{2+a_{-4}+a_{-5}}<c_4$ and $d_{2+a_4+a_5}<c_4$ to hold, it must hold that $a_{-4}+a_{-5}=0$ and $a_4+a_5=0$. In order for these equalities to be satisfied, it is required that $a_{-5}=a_{-4}=a_4=a_5=0$. It can therefore

be deduced that, in order for the run of cooperators of length five to persist intact to the next round of the game, it must be flanked by two defection runs, each of length at least three.

A run of cooperators of length greater than five has the form $D\langle C\rangle^i D$ for $i > 5$. Within this configuration, the largest cooperator pay-off value is c_4. The two outer defectors, namely players $\lfloor -\frac{i+1}{2} \rfloor$ and $\lceil \frac{i+1}{2} \rceil$ obtain the pay-off values $d_{2+a_{-\lfloor \frac{i+1}{2} \rfloor -1}+a_{-\lfloor \frac{i+1}{2} \rfloor -2}}$ and $d_{2+a_{\lceil \frac{i+1}{2} \rceil +1}+a_{\lceil \frac{i+1}{2} \rceil +2}}$, respectively. These pay-off values are similar to those for a cooperation run of length five. Since each player compares the pay-off value achieved by the largest-valued cooperator and defector in its closed neighbourhood and these are equivalent to the situation for a cooperation run of length five, the same result as mentioned above is obtained. It can therefore be deduced that, in order for the run of cooperators of length $i \geq 5$ to persist intact to the next round of the game, the run must be flanked by two defection runs, each of length at least three. □

The last lemma in this appendix is similar to Lemmas 2 and 3, but holds instead for parameter region E in Figure 5.6. A similar proof technique is again employed.

Lemma 4. *If the underlying graph of the ESPD is the circulant $C_n\langle 1, 2\rangle$ and the parameter inequalities $3T + P < 4$ and $2T + 2P > 3$ hold (i.e. the parameters lie within region E of the phase plane in Figure 5.6), then*

(a) no cooperation run of length one, two, three or four can persist intact to the next round of the game, and

(b) a cooperation run of length at least five can persist to the next round of the game if and only if it is flanked on both sides by either a run of defectors of length at least two or by a run of the form DCD.

Proof:

(a) As the proof of Theorem 2(a) is only restricted by the parameter region inequality $2T+2P < 4$, its proof applies to all parameter regions in the phase plane of Figure 5.6, except for parameter region D. Therefore no cooperation run of length one, two or three can remain intact to the next round of the game within parameter region E.

A cooperation run of length four has the form $DCCCCD$. This configuration is illustrated in Figure A.4 for the ESPD with the circulant $C_n\langle 1, 2\rangle$ as underlying graph. The pay-off values of players $-1, 0, 1, 2$, representing the run of cooperators of length four, are $c_{2+a_{-3}}, c_3, c_3$ and c_{2+a_4}, respectively. The largest cooperator pay-off value is therefore c_3. Since only the largest-valued cooperator is relevant in each player's closed neighbourhood during the updating process, only c_3 is compared with the pay-off value of the players in the cooperation run of length four. The pay-off values achieved by the defecting players -2 and 3 are $d_{2+a_{-3}+a_{-4}}$ and $d_{2+a_4+a_5}$, respectively. In the parameter region E, however, $d_2 > 3$. Therefore, $c_3 < d_{2+a_{-3}+a_{-4}}$ and $c_3 < d_{2+a_4+a_5}$ hold. The four cooperating players are therefore unable to achieve pay-off values at least as large as those of their two defecting neighbours, and will hence adopt the strategy of defection during the next round of the game. This shows that no cooperation run of length four can remain intact to the next round of the game.

(b) A cooperation run of length five has the form $DCCCCCD$ and the configuration is illustrated in Figure A.5 for the ESPD with the circulant $C_n\langle 1, 2\rangle$ as underlying graph. The run of cooperators of length five, consisting of players $-2, -1, 0, 1$ and 2, achieve the pay-off values $c_{2+a_{-4}}, c_3, c_4, c_3$ and c_{2+a_4}, respectively. The largest pay-off value achieved by a cooperator in this run is therefore c_4. Since each player compares the pay-off value achieved by the largest-valued cooperator and defector in its closed neighbourhood, only the largest pay-off

value c_4 is relevant. The two neighbouring defectors, players -3 and 3, achieve the pay-off values $d_{2+a_{-4}+a_{-5}}$ and $d_{2+a_4+a_5}$, respectively. According to the parameter region inequalities, however, $d_3 < c_4$. Therefore, in order for the inequalities $d_{2+a_{-4}+a_{-5}} < c_4$ and $d_{2+a_4+a_5} < c_4$ to hold, it is required that $2+a_{-4}+a_{-5} \leq 3$ and $2+a_4+a_5 \leq 3$. Hence, both $a_{-4}+a_{-5} \leq 1$ and $a_4+a_5 \leq 1$ must hold. There are only three binary combinations of (a_{-4}, a_{-5}), namely $(0,0)$, $(1,0)$ or $(0,1)$, which satisfy the first inequality $a_{-4}+a_{-5} \leq 1$. These combinations represent the three possible configurations DD, CD or DC, respectively, which are required to flank the negative side of $DCCCCCD$. In the combinations in which $a_{-4} = 0$ (*i.e.* player -4 adopts the strategy of defection), the strategy of player -5 is irrelevant to the outcome of the updating processes of the players within the cooperation run of length five. This is because a_{-5} either has the value of 0 or 1 for the above inequality to hold. There are also three binary combinations of (a_4, a_5), namely $(0,0)$, $(1,0)$ or $(0,1)$, satisfying the second inequality, $a_4 + a_5 \leq 1$. This allows for the positive side of $DCCCCCD$ to be flanked only by either DD, DC or CD. In the combinations in which $a_4 = 0$ (*i.e.* player 4 adopts the strategy of defection), the strategy of player 5 is again irrelevant to the outcome of the updating processes of the players within the cooperation run of length five. It can thereby be deduced that, in order for the run of cooperators of length five to persist intact to the next round of the game, the run must be flanked on both sides by either a defection run of length at least two or by the configuration DCD.

A run of cooperators of length greater than five has the form $D\langle C\rangle^i D$ for $i > 5$. Within this configuration, the largest cooperator pay-off value is c_4. The two outer defectors, namely players $\lfloor -\frac{i+1}{2} \rfloor$ and $\lceil \frac{i+1}{2} \rceil$ obtain the pay-off values $d_{2+a_{-\lceil \frac{i+1}{2} \rceil - 1}+a_{-\lceil \frac{i+1}{2} \rceil - 2}}$ and $d_{2+a_{\lceil \frac{i+1}{2} \rceil + 1}+a_{\lceil \frac{i+1}{2} \rceil + 2}}$, respectively. These pay-off values are similar to those for a cooperation run of length five. Since each player compares the pay-off value achieved by the largest-valued cooperator and defector in its closed neighbourhood and these are equivalent to the situation for a cooperation run of length five, the same result as mentioned above is obtained. It can therefore be deduced that, in order for the run of cooperators of length $i \geq 5$ to persist intact to the next round of the game, the run must be flanked on both sides by either a run of defectors of length two or by the configuration DCD. □

APPENDIX B

Enumeration of equilibrium states

The proof of Theorem 4 in §5.4.2 for parameter regions A, C and E in the phase plane of Figure 5.6 is presented in this appendix. First the part of the theorem associated with the parameter region considered is given, after which its proof is presented in each case.

Theorem 4. *(a) Suppose the underlying graph of the ESPD is the circulant $C_n\langle 1,2\rangle$. If the parameter inequalities $3T+P<4$ and $2T+2P<3$ hold (i.e. the parameters lie within region A of the phase plane in Figure 5.6), then the number of equilibrium states of the game is given by*

$$
\begin{aligned}
&2+\sum_{i=1}^{\lfloor \frac{n}{7} \rfloor}\frac{1}{2i}\left[\binom{n-5i-1}{2i-1}+\sum_{j\in S_1}\binom{(n-5i)\gcd(i,j)/i-1}{2\gcd(i,j)-1}+i\sum_{k=0}^{\lfloor \frac{n-7i}{2} \rfloor}(n-7i-2k+1)\binom{k+i-2}{i-2}\right]\\
&+\sum_{i=1}^{\lfloor \frac{n}{7} \rfloor}\frac{1}{i}\left[\binom{n-6i-1}{i-1}+\sum_{j\in S_1}\binom{(n-6i)\gcd(i,j)/i-1}{\gcd(i,j)-1}+i\sum_{k=0}^{\lfloor \frac{n-7i}{2} \rfloor}(n-7i-2k+1)\binom{k+\lfloor \frac{i}{2} \rfloor-2}{\lfloor \frac{i}{2} \rfloor-2}\right]\\
&+\sum_{i_1=1}^{\lfloor \frac{n-8}{7} \rfloor}\sum_{i_2=1}^{\lfloor \frac{n-7i_1}{8} \rfloor}\frac{1}{2i_1+i_2}\left[\left(\frac{(i_1+i_2-2)!}{(i_1-1)!(i_2-1)!}\right)\binom{n-5i_1-7i_2-1}{2i_1+i_2-1}+\right.\\
&\left(\frac{(gcd(2i_1+i_2,j)-2)!}{(\frac{i_1}{(2i_1+i_2)/gcd(2i_1+i_2,j)}-1)!(\frac{i_2}{(2i_1+i_2)/gcd(2i_1+i_2,j)}-1)!}\right)\\
&\sum_{j\in S_2}\binom{(n-7i_1-8i_2)\gcd(2i_1+i_2,j)/(2i_1+i_2)+\gcd(2i_1+i_2,j)-1}{\gcd(2i_1+i_2,j)-1}\\
&\left.+(2i_1+i_2)\left(\frac{(\frac{i_1+i_2-2}{2})!}{(\frac{i_1-1}{2})!(\frac{i_2-1}{2})!}\right)\sum_{k=0}^{\lfloor \frac{n-7i_1-8i_2}{2} \rfloor}(n-7i_1-8i_2-2k+1)\binom{k+\lfloor \frac{2i_1+i_2}{2} \rfloor-2}{\lfloor \frac{2i_1+i_2}{2} \rfloor-2}\right],
\end{aligned}
\tag{B.1}
$$

where $S_1=\{x\in\mathbb{N}\mid i \text{ divides } n \text{ } gcd(i,x) \text{ and } x<i\}$ and $S_2=\{x\in\mathbb{N}\mid (2i_1+i_2)$ divides $n\gcd(2i_1+i_2,x)$ and $x<(2i_1+i_2)\}$.

Proof: Recall, from Lemma 6, that for cooperation to persist to the next round of the game, either a cooperation run of length four flanked on both sides by a defection run of length at least three or a cooperation run of length at least five flanked on both sides by a defection run of length at least two is required.

As demonstrated in Figure 5.13 of §5.4.2, the set of all possible game states S can be partitioned into two sets X and Y. The set X consists of all states that contain the configuration $DDD\langle C\rangle^4DDD$, while the set Y consists of all states that contain the configuration

$DD\langle C\rangle^n DD$, for some $n \geq 5$. The set $X \cap Y$ contains all states that contain both the configurations $DDD\langle C\rangle^4 DDD$ and $DD\langle C\rangle^n DD$, for some $n \geq 5$. In order to enumerate the number of equilibrium states of the game, each subset is enumerated and added to the enumeration of the all-defector and all-cooperator equilibrium states.

First consider the subset $X \setminus (X \cap Y)$ of S, consisting of all game states that contain the configuration $DDD\langle C\rangle^4 DDD$ but not the configuration $DD\langle C\rangle^n DD$, for any $n \geq 5$.

In order to enumerate the states in $X \setminus (X \cap Y)$, the number of states containing $\langle D\rangle^{n_1}\langle C\rangle^4\langle D\rangle^{n_2}$ as substate has to be determined, where $n_1 \geq 3$ and $n_2 \geq 3$. These states have the form

$$\underbrace{CCCCDDD\ldots}_{\text{run } 1}\underbrace{CCCCDDD\ldots}_{\text{run } 2} \cdots \underbrace{CCCCDDD\ldots}_{\text{run } i-1}\underbrace{CCCCDDD\ldots}_{\text{run } i}, \tag{B.2}$$

where each run has been populated above with the smallest number of defectors. As the underlying graph is a circulant, it is vertex-transitive. The endpoints in the partial state (B.2) have therefore been chosen arbitrarily.

Note that as the ordering of the cooperation and defection runs has already been fixed in (B.2), the symbols C and D can be considered indistinguishable for enumeration purposes, serving merely as place holders from a combinatorial point of view. The partial state (B.2) contains $7i$ symbols, leaving $n-7i$ indistinguishable symbols to be distributed amongst the i distinguishable runs.

Let Q_i denote the number of states, up to automorphism, comprising i cooperation runs and i defection runs, starting in a run of cooperators and ending in a run of defectors as shown in (B.2). The total number of equilibrium states in $X \setminus (X \cap Y)$ is therefore given by

$$\sum_{i=1}^{\lfloor \frac{n}{7} \rfloor} Q_i.$$

Let χ be the set of all states of the form (B.2). In order to determine Q_i, the game states within the set χ have to be partitioned into game state equivalence classes (in order to prevent the enumeration of equivalent states) and the number of classes enumerated. Let G be the group of permutations that partitions χ into its equivalence classes. Recall, from §2.2.2, that the Cauchy-Frobenius Lemma can be used to determine the number of these equivalence classes. The value of Q_i for $i \in \{1, 2, \ldots, \lfloor \frac{n}{7} \rfloor\}$ is given by

$$Q_i = \frac{1}{|G|} \sum_{g \in G} |F_g|, \tag{B.3}$$

where $|F_g|$ is the number of states in χ that remain invariant under the permutation $g \in G$.

In order to determine the symmetry group G of the states of the form (B.2), let ι be the identity permutation on the sequence of runs of a state $s \in \chi$. Let ρ^j be the permutation which modular shifts each run in (B.2) j positions to the right. Let δ furthermore be the operation that reverses the order of the runs in (B.2) so that the first run remains in its original position, followed by runs $\lfloor \frac{i}{2} \rfloor, \lfloor \frac{i}{2} \rfloor - 1, \ldots$ The symmetry group $G = \{\iota, \rho^1, \rho^2, \ldots, \rho^{\lfloor \frac{i}{2} \rfloor - 1}, \delta, \delta\rho^1, \delta\rho^2, \ldots, \delta\rho^{\lfloor \frac{i}{2} \rfloor - 1}\}$ of order i is thus formed under the binary operation of permutation composition. In order to calculate Q_i according to (B.3), the number of states that remain invariant under each permutation in G has to be determined.

First, consider the identity operator ι. This operator leaves all elements of χ invariant and therefore $|F_\iota| = |\chi|$. To calculate the number of states in χ, the number of ways of distributing

$n-7i$ indistinguishable symbols amongst i distinguishable runs has to be determined. Using Lemma 5, it follows that

$$|F_\iota| = \binom{n-7i+i-1}{i-1} = \binom{n-6i-1}{i-1}. \tag{B.4}$$

Next, consider the permutation ρ^j. For a state to remain invariant under the permutation ρ^j, the first j pairs of runs have to be equivalent to all subsequent runs. Note that if j exactly divides i, then the first j runs determine the remaining $(i-j)$ runs. Otherwise, the first $d = \gcd(i,j)$ runs determine the remaining $(i-d)$ runs. The number of possible states that remain invariant under ρ^j can therefore be determined by finding the number of ways to distribute $\frac{d}{i}(n-7i)$ symbols among the first d runs. The enumeration is given by

$$|F_{\rho^j}| = \binom{\frac{d}{i}(n-7i)+d-1}{d-1} = \binom{\frac{d}{i}(n-6i)-1}{d-1}.$$

If, however, $\frac{d}{i}n$ is not an integer, then there are not enough symbols to complete the pattern of runs in order to achieve an invariant state and so $|F_{\rho^j}| = 0$. Therefore,

$$|F_{\rho^j}| = \begin{cases} \binom{\frac{\gcd(i,j)}{i}(n-6i)-1}{\gcd(i,j)-1}, & \text{if } \frac{\gcd(i,j)}{i}n \in \mathbb{Z} \text{ or} \\ 0, & \text{otherwise.} \end{cases} \tag{B.5}$$

Consider next the permutation δ, which reverses the order of the runs so that the first run remains in its original position, the second run is projected onto the last run, the third run is projected onto the second last run, and so on. Runs 1 and $i+1$ are projected onto themselves, while runs 2 to i map onto runs $i+2$ to $2i$, respectively. Let k be the number of indistinguishable symbols that are distributed among the $i-1$ distinguishable runs not mapping onto themselves. The number of ways of distributing the k symbols among these $i-1$ runs is $\binom{k+i-2}{i-2}$, provided that the inequality $0 \leq k \leq n-7i$ holds. The remaining $n-7i-2k$ symbols are distributed among the two runs that map onto themselves, which can be done in $\binom{n-7i-2k+2-1}{2-1} = n-7i-2k+1$ distinct ways. In order to enumerate the distinct game states that remain invariant under the permutation δ, all possible values of k are to be considered. Therefore,

$$|F_\delta| = \sum_{k=0}^{\lfloor \frac{n-7i}{2} \rfloor} (n-7i-2k+1)\binom{k+i-2}{i-2}. \tag{B.6}$$

Finally, consider the permutation composition $\delta\rho^j$ which shifts the runs j positions to the left and then reverses the order of the runs. Under this permutation, runs $j+1$ and $\lfloor \frac{i}{2} \rfloor + j + 1$ map onto themselves, while runs $j+2$ to $\lfloor \frac{i}{2} \rfloor + j$ map onto runs $j-1$ to $\lfloor \frac{i}{2} \rfloor + j + 2$, respectively. Once again, k indistinguishable symbols can be distributed among $\lfloor \frac{i}{2} \rfloor - 1$ distinguishable runs that do not map onto themselves in $\binom{k+\lfloor \frac{i}{2} \rfloor - 2}{\lfloor \frac{i}{2} \rfloor - 2}$ different ways, provided that the inequality $0 \leq k \leq n-7i$ holds. Again, the remaining $n-7i-2k$ symbols can be distributed among the two runs that map onto themselves in $\binom{n-7i-2k+2-1}{2-1} = n-7i-2k+1$ distinct ways. Therefore, the number of distinct game states that remain invariant under the permutation $\delta\rho^j$ is the number in (B.6).

Taking all the various permutations into account and therefore substituting (B.4), (B.5) and (B.6) into (B.3), the number of equilibrium states for the ESPD with $C_n\langle 1,2\rangle$ as underlying

graph and for which the inequalities $3T + P < 4$ and $2T + 2P < 3$ hold (*i.e.* the parameters lie within region A of the phase plane in Figure 5.6) is

$$Q_i = \frac{1}{i}\left[\binom{n-6i-1}{i-1} + \sum_{j\in S}\binom{(n-6i)\gcd(i,j)/i - 1}{\gcd(i,j)-1} + i\sum_{k=0}^{\lfloor\frac{n-7i}{2}\rfloor}(n-7i-2k+1)\binom{k+\lfloor\frac{i}{2}\rfloor-2}{\lfloor\frac{i}{2}\rfloor-2}\right],$$

where S is the set $\{x \in \mathbb{N} \mid i \text{ divides } n\ \gcd(i,x) \text{ and } x < i\}$.

Next consider the subset $Y \setminus (X \cap Y)$ of the set S as illustrated graphically in Figure 5.13. This includes all game states that contain the configuration $DD\langle C\rangle^n DD$ as substate, for some $n \geq 5$ but not the configuration $DDD\langle C\rangle^4 DDD$. In order to enumerate the states in $Y \setminus (X \cap Y)$, the number of states containing substates of the form $\langle D\rangle^{n_1}\langle C\rangle^{n_2}\langle D\rangle^{n_3}$ has to be determined, where $n_1 \geq 2$, $n_2 \geq 5$ and $n_2 \geq 3$. These states have the form

$$\underbrace{CCCCC\ldots}_{\text{run 1}}\underbrace{DD\ldots}_{\text{run 2}}\underbrace{CCCCC\ldots}_{\text{run 3}}\underbrace{DD\ldots}_{\text{run 4}}\cdots\underbrace{CCCCC\ldots}_{\text{run } 2i-1}\underbrace{DD\ldots}_{\text{run } 2i}, \tag{B.7}$$

where each run has been populated above with the smallest number of cooperators and defectors, as appropriate. As the underlying graph is a circulant, it is vertex-transitive. The endpoints in the partial state (B.7) have therefore again been chosen arbitrarily.

As the ordering of the cooperation and defection runs has already been fixed in (B.7), the symbols C and D can be considered indistinguishable for enumeration purposes, serving merely as place holders from a combinatorial point of view. The partial state (B.7) contains $7i$ symbols, leaving $n - 7i$ indistinguishable symbols to be distributed amongst the $2i$ distinguishable runs.

Let Q_i denote the number of states, up to automorphism, comprising i cooperation runs and i defection runs, starting in a run of cooperators and ending in a run of defectors as shown in (B.7). The total number of equilibrium classes is therefore given by

$$\sum_{i=1}^{\lfloor\frac{n}{7}\rfloor} Q_i.$$

Let χ be the set of all states of the form (B.7). In order to determine Q_i, the game states in the set χ have to be partitioned into game state equivalence classes (in order to prevent the enumeration of equivalent states) and the number of classes enumerated. Let G be the group of permutations that partitions χ into its equivalence classes. Recall, from §2.2.2, that the Cauchy-Frobenius Lemma can be used to determine the number of these equivalence classes. The value of Q_i for $i \in \{1, 2, \ldots, \lfloor\frac{n}{7}\rfloor\}$ is therefore given by

$$Q_i = \frac{1}{|G|}\sum_{g\in G}|F_g|, \tag{B.8}$$

where $|F_g|$ is the number of states in χ that remain invariant under the permutation $g \in G$.

In order to determine the symmetry group G of the states of the form (B.7), let ι be the identity permutation on the sequence of runs of a state $s \in \chi$. Let ρ^j be the permutation which modular shifts each run in (B.7) j positions to the right. Let δ furthermore be the operation that reverses the order of the runs in (B.7) so that the first run remains in its original position, followed by runs $i, i-1, \ldots$ The symmetry group $G = \{\iota, \rho^1, \rho^2, \ldots, \rho^{i-1}, \delta, \delta\rho^1, \delta\rho^2, \ldots, \delta\rho^{i-1}\}$ of order $2i$ is thus formed under the binary operation of permutation composition. In order to calculate Q_i according to (B.8), the number of states that remain invariant under each permutation in G has to be determined.

First, consider the identity operator ι. This operator leaves all elements of χ invariant and therefore $|F_\iota| = |\chi|$. To calculate the number of states in χ, the number of ways of distributing $n - 7i$ indistinguishable symbols amongst $2i$ distinguishable runs has to be determined. Using Lemma 5, it follows that

$$|F_\iota| = \binom{n - 5i + 2i - 1}{2i - 1} = \binom{n - 5i - 1}{2i - 1}. \tag{B.9}$$

Next, consider the permutation ρ^j. For a state to remain invariant under the permutation ρ^j, the first j pairs of runs have to be equivalent to all subsequent runs. Note that if j exactly divides i, then the first j pairs of runs determine the remaining $2(i - j)$ runs. Otherwise, the first $d = \gcd(i, j)$ pairs of runs determine the remaining $2(i - d)$ runs. The number of states that remain invariant under ρ^j can therefore be determined by finding the number of ways to distribute $\frac{2d}{2i}(n - 7i)$ symbols among the first $2d$ runs. The enumeration is given by

$$|F_{\rho^j}| = \binom{\frac{2d}{2i}(n - 7i) + 2d - 1}{2d - 1} = \binom{\frac{d}{i}(n - 5i) - 1}{2d - 1}.$$

If, however, $\frac{d}{i}n$ is not an integer, then there are not enough symbols to complete the pattern of runs in order to achieve an invariant state and so $|F_{\rho^j}| = 0$. Therefore,

$$|F_{\rho^j}| = \begin{cases} \binom{\frac{\gcd(i,j)}{i}(n-5i)-1}{2\gcd(i,j)-1}, & \text{if } \frac{\gcd(i,j)}{i}n \in \mathbb{Z} \text{ or} \\ 0, & \text{otherwise.} \end{cases} \tag{B.10}$$

Consider next the permutation δ, which reverses the order of the runs so that the first run remains in its original position, the second run is projected onto the last run, the third run is projected onto the second last run, and so on. Runs 1 and $i + 1$ are projected onto themselves, while runs 2 to i map onto runs $i+2$ to $2i$, respectively. Let k be the number of indistinguishable symbols that are distributed among the $i-1$ distinguishable runs not mapping onto themselves. The number of ways of distributing the k symbols among these $i-1$ runs is $\binom{k+i-2}{i-2}$, provided that the inequality $0 \leq k \leq n - 7i$ holds. The remaining $n - 7i - 2k$ symbols are distributed among the two runs that map onto themselves, which can be done in $\binom{n-7i-2k+2-1}{2-1} = n - 7i - 2k + 1$ distinct ways. In order to enumerate the distinct game states that remain invariant under the permutation δ, all possible values of k are to be considered. Therefore,

$$|F_\delta| = \sum_{k=0}^{\lfloor \frac{n-7i}{2} \rfloor} (n - 7i - 2k + 1)\binom{k + i - 2}{i - 2}. \tag{B.11}$$

Finally, consider the permutation composition $\delta\rho^j$ which shifts the runs j positions to the left and then reverses the order of the runs. Under this permutation, runs $j + 1$ and $i + j + 1$ map onto themselves, while runs $j + 2$ to $i + j$ map onto runs $j - 1$ to $i + j + 2$, respectively. Once again k indistinguishable symbols can be distributed among $i - 1$ distinguishable runs that do not map onto themselves in $\binom{k+i-2}{i-2}$ different ways, provided that the inequality $0 \leq k \leq n - 7i$ holds. Again, the remaining $n - 7i - 2k$ symbols can be distributed among the two runs that map onto themselves in $\binom{n-7i-2k+2-1}{2-1} = n-7i-2k+1$ distinct ways. Therefore, the number of distinct game states that remain invariant under the permutation $\delta\rho^j$ is the number in (B.11).

Taking all the various permutations into account and therefore substituting (B.9), (B.10) and (B.11) into (B.8), the number of equilibrium states of the ESPD with $C_n\langle 1, 2\rangle$ as underlying

graph and for which the inequalities $3T + P < 4$ and $2T + 2P < 3$ hold (*i.e.* the parameters lie within region A of the phase plane in Figure 5.6) is

$$Q_i = \frac{1}{2i}\left[\binom{n-5i-1}{2i-1} + \sum_{j\in S}\binom{(n-5i)\gcd(i,j)/i-1}{2\gcd(i,j)-1} + i\sum_{k=0}^{\lfloor\frac{n-7i}{2}\rfloor}(n-7i-2k+1)\binom{k+i-2}{i-2}\right],$$

where S is the set $\{x \in \mathbb{N} \mid i \text{ divides } n \gcd(i,x) \text{ and } x < i\}$.

Finally, consider the subset $(X \cap Y)$ of S, consisting of game states that contain at least one configuration of the form $DDD\langle C\rangle^4 DDD$ and at least one configuration of the form $DD\langle C\rangle^n DD$ as substates, for some $n \geq 5$. These states have the form

$$\underbrace{DCCCCDDD\ldots}_{\text{run } 1} \cdots \underbrace{CCCCC\ldots}_{\text{run } 2i_1+i_2-1}\ \underbrace{DD\ldots}_{\text{run } 2i_1+i_2}, \tag{B.12}$$

where each run has been populated above with the smallest number of cooperators and defectors, as appropriate. Within this configuration there can be i_1 pairs of runs of the form $CCCCC\ldots$ and $DD\ldots$, and i_2 runs of the form $DCCCCDDD\ldots$ The state always starts with the configuration $DCCCCDDD\ldots$ and ends with the pair of configurations $CCCCC\ldots$ and $DD\ldots$

Let $Q_{(i_1,i_2)}$ denote the number of states, up to automorphism, comprising of i_1 pairs of runs of cooperators of length at least five and defectors of length at least two and i_2 runs of the form $DCCCCDDD\ldots$ as shown in (B.12). The total number of equilibrium classes of this form is therefore given by

$$\sum_{i_1=1}^{\lfloor\frac{n-8}{7}\rfloor}\sum_{i_2=1}^{\lfloor\frac{n-7i_1}{8}\rfloor} Q_{(i_1,i_2)}.$$

Let χ be the set of all states of the form (B.12). In order to determine $Q_{(i_1,i_2)}$, the game states in the set χ have to be partitioned into game state equivalence classes (in order to prevent the enumeration of equivalent states) and the number of classes enumerated. Let G be the group of permutations that partitions χ into its equivalence classes. Recall, from §2.2.2, that the Cauchy-Frobenius Lemma can be used to determine the number of these equivalence classes. The value of $Q_{(i_1,i_2)}$ for $i_1 \in \{1,2,\ldots,\lfloor\frac{n-8}{7}\rfloor\}$ and $i_2 \in \{1,2,\ldots,\lfloor\frac{n-7i_1}{8}\rfloor\}$ is therefore given by

$$Q_{(i_1,i_2)} = \frac{1}{|G|}\sum_{g\in G}|F_g|, \tag{B.13}$$

where $|F_g|$ is the number of states in χ that remain invariant under the permutation $g \in G$.

In order to determine the symmetry group G of the states of the form (B.12), let ι be the identity permutation on the sequence of runs of a state $s \in \chi$. Let ρ^j be the permutation which modular shifts each run in (B.12) j positions to the right. Let δ furthermore be the operation that reverses the order of the runs in (B.12) so that the first run remains in its original position followed by runs $\lceil\frac{2i_1+i_2}{2}\rceil, \lceil\frac{2i_1+i_2}{2}\rceil - 1, \ldots$ The symmetry group $G = \{\iota, \rho^1, \rho^2, \ldots, \rho^{\lceil\frac{2i_1+i_2}{2}\rceil-1}, \delta, \delta\rho^1, \delta\rho^2, \ldots, \delta\rho^{\lceil\frac{2i_1+i_2}{2}\rceil-1}\}$ of order $2i_1 + i_2$ is thus formed under the binary operation of permutation composition. In order to calculate $Q_{(i_1,i_2)}$ according to (B.13), the number of states that remain invariant under each permutation in G has to be determined.

First, consider the identity operator ι. This operator leaves all elements of χ invariant and therefore $|F_\iota| = |\chi|$. To calculate the number of states in χ, the number of ways of distributing $n-7i_1-8i_2$ indistinguishable symbols amongst i_1+2i_2 distinguishable runs has to be determined.

As the order of the different runs has not been fixed, except for the first and last run, the number of orderings of these runs also have to be considered. Using Lemma 5, it follows that

$$\begin{aligned}|F_\iota| =& \frac{(i_1+i_2-2)!}{(i_1-1)!(i_2-1)!}\binom{n-7i_1-8i_2+2i_1+i_2-1}{2i_1+i_2-1} \\ =& \frac{(i_1+i_2-2)!}{(i_1-1)!(i_2-1)!}\binom{n-5i_1-7i_2-1}{2i_1+i_2-1}.\end{aligned} \tag{B.14}$$

Next, consider the permutation ρ^j. For a state to remain invariant under the permutation ρ^j, the first j pairs of runs have to be equivalent to all subsequent runs. Note that if j exactly divides $2i_1+i_2$, then the first j runs determine the remaining $(2i_1+i_2-j)$ runs. Otherwise, the first $d=\gcd(2i_1+i_2,j)$ runs determine the remaining $(2i_1+i_2-d)$ runs. The number of possible states that remain invariant under ρ^j can therefore be determined by finding the number of ways to distribute $\frac{d}{2i_1+i_2}(n-7i_1-8i_2)$ symbols among the first d runs. As the ordering of the various different runs within the first d runs is only fixed for the first and the last run, the various run orders also have to be taken into account. The enumeration is therefore given by

$$|F_{\rho^j}| = \frac{(d-2)!}{(\frac{i_1}{(2i_1+i_2)/d}-1)!(\frac{i_2}{(2i_1+i_2)/d}-1)!}\binom{\frac{d}{2i_1+i_2}(n-7i_1-8i_2)+d-1}{d-1} \text{ if } \frac{d}{2i_1+i_2}n \in \mathbb{N}. \tag{B.15}$$

If, however, $\frac{d}{2i_1+i_2}n$ is not an integer, then there are not enough symbols to complete the pattern of runs in order to achieve an invariant state, and so $|F_{\rho^j}|=0$.

Consider next the permutation δ, which reverses the order of the runs so that the first run remains in its original position, the second run is projected onto the last run, the third run is projected onto the second last run, and so on. Runs 1 and $\lfloor\frac{2i_1+i_2}{2}\rfloor+1$ are projected onto themselves, while runs 2 to $\lfloor\frac{2i_1+i_2}{2}\rfloor$ map onto runs $\lfloor\frac{2i_1+i_2}{2}\rfloor+2$ to $2i_1+i_2$, respectively. Let k be the number of indistinguishable symbols that are distributed among the $\lfloor\frac{2i_1+i_2}{2}\rfloor-1$ distinguishable runs not mapping onto themselves. The number of ways of distributing the k symbols among these $\lfloor\frac{2i_1+i_2}{2}\rfloor-1$ runs is $\binom{k+\lfloor\frac{2i_1+i_2}{2}\rfloor-2}{\lfloor\frac{2i_1+i_2}{2}\rfloor-2}$, provided that the inequality $0\leq k\leq n-7i_1-8i_2$ holds. The remaining $n-7i_1-8i_2-2k$ symbols are distributed among the two runs that map onto themselves, which can be done in $\binom{n-7i_1-8i_2-2k+2-1}{2-1}=n-7i_1-8i_2-2k+1$ distinct ways. As the order of the various runs are not fixed, except for the first and last runs, the number of different run orders also has to be taken into account. In order to enumerate the distinct game states that remain invariant under the permutation δ, all possible values of k are to be considered. Therefore,

$$|F_\delta| = \frac{(\frac{i_1+i_2-2}{2})!}{(\frac{i_1-1}{2})!(\frac{i_2-1}{2})!}\sum_{k=0}^{\lfloor\frac{n-7i_1-8i_2}{2}\rfloor}(n-7i_1-8i_2-2k+1)\binom{k+\lfloor\frac{2i_1+i_2}{2}\rfloor-2}{\lfloor\frac{2i_1+i_2}{2}\rfloor-2}. \tag{B.16}$$

Finally, consider the permutation composition $\delta\rho^j$ which shifts the runs j positions to the left and then reverses the order of the runs. Under this permutation, runs $j+1$ and $\lfloor\frac{2i_1+i_2}{2}\rfloor+j+1$ map onto themselves, while runs $j+2$ to $\lfloor\frac{2i_1+i_2}{2}\rfloor+j$ map onto runs $j-1$ to $\lfloor\frac{2i_1+i_2}{2}\rfloor+j+2$, respectively. Once again, k indistinguishable symbols can be distributed among $\lfloor\frac{2i_1+i_2}{2}\rfloor-1$ distinguishable runs that do not map onto themselves in $\binom{k+\lfloor\frac{2i_1+i_2}{2}\rfloor-2}{\lfloor\frac{2i_1+i_2}{2}\rfloor-2}$ different ways, provided that the inequality $0\leq k\leq n-7i_1-8i_2$ holds. Again, the remaining $n-7i_1-8i_2-2k$ symbols can be distributed among the two runs that map onto themselves in $\binom{n-7i_1-8i_2-2k+2-1}{2-1}=n-7i_1-8i_2-2k+1$ distinct ways. Therefore, the number of distinct game states that remain invariant under the permutation $\delta\rho^j$ is the number in (B.16).

Taking all the various permutations into account and therefore substituting (B.14), (B.15) and (B.16) into (B.13), the number of equilibrium states of the ESPD with $C_n\langle 1,2\rangle$ as underlying graph and for which the inequalities $3T+P<4$ and $2T+2P<3$ hold (*i.e.* the parameters lie within region A of the phase plane in Figure 5.6) is

$$\begin{aligned}Q_{(i_1,i_2)} =& \frac{1}{2i_1+i_2}\Bigg[\left(\frac{(i_1+i_2-2)!}{(i_1-1)!(i_2-1)!}\right)\binom{n-5i_1-7i_2-1}{2i_1+i_2-1}\\ &+\left(\frac{(\gcd(2i_1+i_2,j)-2)!}{(\frac{i_1}{(2i_1+i_2)/\gcd(2i_1+i_2,j)}-1)!((2i_1+i_2)/\frac{i_2}{\gcd(2i_1+i_2,j)}-1)!}\right)\\ &\sum_{j\in S_2}\binom{(n-7i_1-8i_2)\gcd(2i_1+i_2,j)/(2i_1+i_2)+\gcd(2i_1+i_2,j)-1}{\gcd(2i_1+i_2,j)-1}\\ &+(2i_1+i_2)\left(\frac{(\frac{i_1+i_2-2}{2})!}{(\frac{i_1-1}{2})!(\frac{i_2-1}{2})!}\right)\sum_{k=0}^{\lfloor\frac{n-7i_1-8i_2}{2}\rfloor}(n-7i_1-8i_2-2k+1)\binom{k+\lfloor\frac{2i_1+i_2}{2}\rfloor-2}{\lfloor\frac{2i_1+i_2}{2}\rfloor-2}\Bigg],\end{aligned}$$

where S_2 is the set $\{x\in\mathbb{N}\mid (2i_1+i_2)$ divides $n\gcd(2i_1+i_2,x)$ and $x<(2i_1+i_2)\}$. □

The following result is similar to that of Theorem 4(b), but holds for parameter region C of the phase plane in Figure 5.6. A similar method of proof is adopted.

Theorem 4. *(c) Suppose the underlying graph of the ESPD is the circulant $C_n\langle 1,2\rangle$. If the parameter inequalities $3T+P>4$, $2T+2P>3$ and $2T+2P<4$ hold (i.e. the parameters lie within region C of the phase plane in Figure 5.6), then the number of equilibrium states is given by*

$$2+\sum_{i=1}^{\lfloor\frac{n}{8}\rfloor}\frac{1}{2i}\left[\binom{n-6i-1}{2i-1}+\sum_{j\in\bar{S}}\binom{(n-6i)\gcd(i,j)/i-1}{2\gcd(i,j)-1}+i\sum_{k=0}^{\lfloor\frac{n-8i}{2}\rfloor}(n-8i-2k+1)\binom{k+i-2}{i-2}\right], \tag{B.17}$$

where $\bar{S}$ is the set $\{x\in\mathbb{N}\mid i$ divides $n\gcd(i,x)$ and $x<i\}$.

Proof: Recall, from Lemma 3, that for cooperation to persist to the next round of the game, a cooperation run of length at least five flanked on each side by a run of defectors of length at least three is required. In order to enumerate the states resulting from such a configuration, the states containing substates of the form $\langle D\rangle^{n_1}\langle C\rangle^{n_2}\langle D\rangle^{n_3}$ have to be counted, where $n_1\geq 3$, $n_2\geq 5$ and $n_3\geq 3$. These states have the form

$$\underbrace{CCCCC\ldots}_{\text{run 1}}\underbrace{DDD\ldots}_{\text{run 2}}\underbrace{CCCCC\ldots}_{\text{run 3}}\underbrace{DDD\ldots}_{\text{run 4}}\cdots\underbrace{CCCCC\ldots}_{\text{run }2i-1}\underbrace{DDD\ldots}_{\text{run }2i}, \tag{B.18}$$

where each run has been populated above with the smallest number of cooperators and defectors, as appropriate. As the underlying graph is a circulant, it is vertex-transitive. The endpoints in the partial state (B.18) have therefore been chosen arbitrarily.

As the ordering of the cooperation and defection runs has already been fixed in (B.18), the symbols C and D can be considered indistinguishable for enumeration purposes, serving merely as place holders from a combinatorial point of view. The partial state (B.18) contains $8i$ symbols, leaving $n-8i$ indistinguishable symbols to be distributed amongst the $2i$ distinguishable runs.

All equilibrium states can be represented by (B.18), except for the all-cooperator and all-defector steady states. As deduced from Lemma 3, no run of cooperators of length smaller than five or run of defectors of length smaller than three prevails in any steady state. Therefore, let Q_i denote

the number of states, up to automorphism, comprising i cooperation runs and i defection runs, starting in a run of cooperators and ending in a run of defectors as shown in (B.18). The total number of equilibrium classes is therefore given by

$$2 + \sum_{i=1}^{\lfloor \frac{n}{8} \rfloor} Q_i.$$

Let χ be the set of all states of the form (B.18). In order to determine Q_i, the game states in the set χ have to be partitioned into game state equivalence classes (in order to prevent the enumeration of equivalent states) and the number of classes enumerated. Let G be the group of permutations that partitions χ into its equivalence classes. Recall, from §2.2.2, that the Cauchy-Frobenius Lemma can be used to determine the number of these equivalence classes. The value of Q_i for $i \in \{1, 2, \ldots, \lfloor \frac{n}{8} \rfloor\}$ is therefore given by

$$Q_i = \frac{1}{|G|} \sum_{g \in G} |F_g|, \tag{B.19}$$

where $|F_g|$ is the number of states in χ that remain invariant under the permutation $g \in G$.

In order to determine the symmetry group of the states of the form (B.18), let ι be the identity permutation on the sequence of runs of a state $s \in \chi$. Let ρ^j be the permutation which modular shifts each run in (B.18) j positions to the right. Let δ furthermore be the operation that reverses the order of the runs in (B.18) so that the first run remains in its original position, followed by runs $i, i-1, \ldots$ The symmetry group $G = \{\iota, \rho^1, \rho^2, \ldots, \rho^{i-1}, \delta, \delta\rho^1, \delta\rho^2, \ldots, \delta\rho^{i-1}\}$ of order $2i$ is thus formed under the binary operation of permutation composition. In order to calculate Q_i according to (B.19), the number of states that remain invariant under each permutation within G has to be determined.

First, consider the identity operator ι. This operator leaves all elements of χ invariant and therefore $|F_\iota| = |\chi|$. To enumerate the number of states in χ, the number of ways of distributing $n - 7i$ indistinguishable symbols amongst $2i$ distinguishable runs has to be determined. Using Lemma 5, it follows that

$$|F_\iota| = \binom{n - 6i + 2i - 1}{2i - 1} = \binom{n - 6i - 1}{2i - 1}. \tag{B.20}$$

Next, consider the permutation ρ^j. For a state to remain invariant under the permutation ρ^j, the first j pairs of runs have to be equivalent to all subsequent runs. To elucidate this claim, consider applying ρ^1 to a state $s \in \chi$. When performing this operation, run i is mapped to run $i + 2$ which, in turn, is mapped to run $i + 4$, and so on. Hence, the numbers of symbols in runs 1 and 2 determine the numbers of symbols in runs 3 and 4 as well as the numbers of symbols in runs 5 and 6, and so on. Therefore, each pair of runs have to be equivalent. Hence, the number of possible states that remain invariant under ρ^1 can be determined by finding the number of distinct ways of distributing $\frac{2}{2i}(n - 8i)$ symbols among two containers, which is given by

$$|F_{\rho^1}| = \binom{\frac{n-8i}{i} + 2 - 1}{2 - 1} = \frac{n - 8i}{i} + 1.$$

Note that if j exactly divides i, then the first j pairs of runs determine the remaining $2(i - j)$ runs. Otherwise, the first $d = \gcd(i, j)$ pairs of runs determine the remaining $2(i - d)$ runs. The number of possible states that remain invariant under ρ^j can therefore be determined by finding

the number of ways to distribute $\frac{2d}{2i}(n-8i)$ symbols among the first $2d$ runs. The enumeration is given by

$$|F_{\rho^j}| = \binom{\frac{2d}{2i}(n-8i)+2d-1}{2d-1} = \binom{\frac{d}{i}(n-6i)-1}{2d-1}.$$

If, however, $\frac{d}{i}n$ is not an integer, then there are not enough symbols to complete the pattern of runs in order to achieve an invariant state and so $|F_{\rho^j}| = 0$. Therefore,

$$|F_{\rho^j}| = \begin{cases} \binom{\frac{\gcd(i,j)}{i}(n-6i)-1}{2\gcd(i,j)-1}, & \text{if } \frac{\gcd(i,j)}{i}n \in \mathbb{Z} \text{ or} \\ 0, & \text{otherwise.} \end{cases} \tag{B.21}$$

Consider next the permutation δ, which reverses the order of the runs so that the first run remains in its original position, the second run is projected onto the last run, the third run is projected onto the second last run, and so on. Runs 1 and $i+1$ are projected onto themselves, while runs 2 to i map onto runs $i+2$ to $2i$, respectively. Let k be the number of indistinguishable symbols that are distributed among the $i-1$ distinguishable runs not mapping onto themselves. The number of ways of distributing the k symbols among these $i-1$ runs is $\binom{k+i-2}{i-2}$, provided that the inequality $0 \leq k \leq n-8i$ holds. The remaining $n-8i-2k$ symbols are distributed among the two runs that map onto themselves, which can be done in $\binom{n-8i-2k+2-1}{2-1} = n-8i-2k+1$ distinct ways. In order to enumerate the distinct game states that remain invariant under the permutation δ, all possible values of k are to be considered. Therefore,

$$|F_\delta| = \sum_{k=0}^{\lfloor \frac{n-8i}{2} \rfloor} (n-8i-2k+1)\binom{k+i-2}{i-2}. \tag{B.22}$$

Finally, consider the permutation composition $\delta\rho^j$ which shifts the runs j positions to the left and then reverses the order of the runs. Under this permutation, runs $j+1$ and $i+j+1$ map onto themselves, while runs $j+2$ to $i+j$ map onto runs $j-1$ to $i+j+2$, respectively. Once again, k indistinguishable symbols can be distributed among $i-1$ distinguishable runs that do not map onto themselves in $\binom{k+i-2}{i-2}$ different ways, provided that the inequality $0 \leq k \leq n-8i$ holds. Again, the remaining $n-8i-2k$ symbols can be distributed among the two runs that map onto themselves in $\binom{n-8i-2k+2-1}{2-1} = n-8i-2k+1$ distinct ways. Therefore, the number of distinct game states that remain invariant under the permutation $\delta\rho^j$ is the number in (B.22).

Taking all the various permutations into account and therefore substituting (B.20), (B.21) and (B.22) into (B.19), the number of equilibrium states of the ESPD with $C_n\langle 1,2\rangle$ as underlying graph and for which the inequalities $3T+P>4$, $2T+2P>3$ and $2T+2P<4$ hold (*i.e.* the parameters lie within region C of the phase plane in Figure 5.6) is

$$Q_i = \frac{1}{2i}\left[\binom{n-6i-1}{2i-1} + \sum_{j\in\bar{S}}\binom{(n-6i)\gcd(i,j)/i-1}{2\gcd(i,j)-1} + i\sum_{k=0}^{\lfloor \frac{n-8i}{2} \rfloor}(n-8i-2k+1)\binom{k+i-2}{i-2}\right],$$

where $\bar{S}$ is the set $\{x \in \mathbb{N} \mid i \text{ divides } n\ \gcd(i,x) \text{ and } x < i\}$. □

The following theorem is again similar to Theorem 4(b), but holds for parameter region E of the phase plane in Figure 5.6. A lemma is first established, however, demonstrating a simplification of the two possible configurations that allow for cooperation to persist to the next round of the game into a single configuration. Hereby, a similar method of proof as that of Theorem 4(b) can be adopted for the enumeration of the equivalence classes corresponding to parameter region E.

Recall, from Lemma 4, that in order for cooperation to persist to the next round of the game, a cooperation run of length at least five, flanked on each side by either a run of defectors of length at least two or by the configuration DCD is required. It can be shown in the latter case that a configuration DCD flanking the cooperator run will transform into the configuration DDD during the next round of the game. This claim is proved in the following lemma.

Lemma 5. *If the underlying graph of the ESPD is the circulant $C_n\langle 1,2\rangle$ and the parameter inequalities $3T+P<4$ and $2T+2P>3$ hold (i.e. the parameters lie within region E of the phase plane in Figure 5.6), then an equilibrium state must contain a cooperation run of length at least five flanked on each side by a defection run of length at least two for cooperation to persist.*

Proof: Consider a run of cooperators of length at least five with one side flanked by DCD. A substate of this configuration consisting of a cooperation run of length five flanked on the right by DCD is illustrated in Figure B.1.

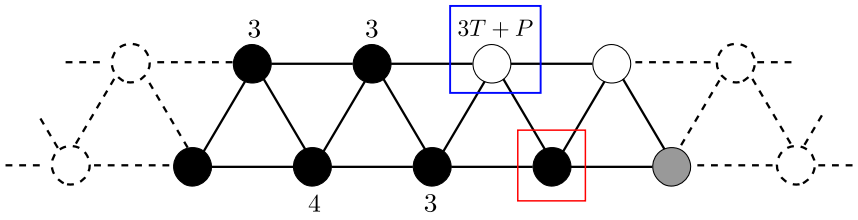

FIGURE B.1: *Configuration of a cooperation run of length five flanked on the right side by DCD. The pay-off values that are known for the various players within the configuration are denoted above or below the corresponding vertices. The player marked in red, will adopt the strategy of defection during the next round of the game, if the parameter values T and P lie within parameter region A.*

Consider the playing and updating phases during a single round of the game for the player marked in red in the figure. During the playing phase, the pay-off value achieved by this player is at most $c_2 = 2$. Furthermore, during the updating phase, the defector and cooperator with the largest pay-off value in this player's closed neighbourhood are compared. The defector with the largest pay-off value achieves the pay-off value $d_3 = 3T + P$ and is marked in blue in the figure. In order to determine the cooperator with the largest pay-off value, the strategy of the grey player is required. The grey player can either adopt the strategy of cooperation or defection. In the case where the grey player adopts the strategy of cooperation, it is able to achieve the largest pay-off value $c_3 = 3$ of all the cooperating players in the red player's closed neighbourhood. Otherwise, in the case where the grey player adopts the strategy of defection, the red player achieves the largest pay-off value of all the cooperators. In the two cases, the inequalities $d_3 > c_3$ and $d_3 > c_2$ hold, respectively. The player indicated in red will therefore adopt the strategy of defection during the next round of the game. The resulting configuration after a single round of the game is subsequently $\langle C\rangle^5 DDD$. Hence, in order for cooperation to be present in an equilibrium state, a run of cooperators of length at least five flanked on each side by a run of defectors of length at least two is required. □

The following result is similar to that of Theorem 4(b), but holds for parameter region E of the phase plane in Figure 5.6. A similar method of proof is again adopted.

Theorem 4. *(d) Suppose the underlying graph of the ESPD is the circulant $C_n\langle 1,2\rangle$. If the parameter inequalities $3T+P<4$ and $2T+2P>3$ hold (i.e. the parameters lie within region*

E of the phase plane in Figure 5.6), then the number of equilibrium states is given by

$$2+\sum_{i=1}^{\lfloor \frac{n}{7} \rfloor} \frac{1}{2i}\left[\binom{n-5i-1}{2i-1}+\sum_{j\in\tilde{S}}\binom{(n-5i)\gcd(i,j)/i-1}{2\gcd(i,j)-1}+i\sum_{k=0}^{\lfloor \frac{n-7i}{2} \rfloor}(n-7i-2k+1)\binom{k+i-2}{i-2}\right], \tag{B.23}$$

where $\tilde{S}$ *is the set* $\{x \in \mathbb{N} \mid i \text{ divides } n\gcd(i,x) \text{ and } x < i\}$.

Proof: Recall, from Lemma 5, that for cooperation to persist to the next round of the game, a cooperation run of length at least five flanked on each side by a run of defectors of length at least two is required. In order to enumerate the equilibrium states resulting from such a configuration, the number of states containing a substate of the form $\langle D\rangle^{n_1}\langle C\rangle^{n_2}\langle D\rangle^{n_3}$ has to be determined, where $n_1 \geq 2$, $n_2 \geq 5$ and $n_2 \geq 2$. These states have the form

$$\underbrace{CCCCC\ldots}_{\text{run 1}}\underbrace{DD\ldots}_{\text{run 2}}\underbrace{CCCCC\ldots}_{\text{run 3}}\underbrace{DD\ldots}_{\text{run 4}}\cdots\underbrace{CCCCC\ldots}_{\text{run } 2i-1}\underbrace{DD\ldots}_{\text{run } 2i}, \tag{B.24}$$

where each run has been populated above with the smallest number of cooperators and defectors, as appropriate. As the underlying graph is a circulant, it is vertex-transitive. The endpoints in the partial state (B.24) have therefore been chosen arbitrarily.

As the ordering of the cooperation and defection runs has already been fixed in (B.24), the symbols C and D can be considered indistinguishable for enumeration purposes, serving merely as place holders from a combinatorial point of view. The partial state (B.24) contains $7i$ symbols, leaving $n-7i$ indistinguishable symbols to be distributed amongst the $2i$ distinguishable runs.

All equilibrium states can be represented in the form (B.24), except for the all-cooperator and all-defector steady states. As deduced from Lemma 4, no run of cooperators of length smaller than five or run of defectors of length smaller than two prevails in any equilibrium state. Therefore, let Q_i denote the number of states, up to automorphism, comprising i cooperation runs and i defection runs, starting in a run of cooperators and ending in a run of defectors as shown in (B.24). The total number of equilibrium classes is therefore given by

$$2+\sum_{i=1}^{\lfloor \frac{n}{7} \rfloor} Q_i.$$

Let χ be the set of all states of the form (B.18). In order to determine Q_i, the game states in the set χ have to be partitioned into game state equivalence classes (in order to prevent the enumeration of equivalent states) and the number of classes enumerated. Let G be the group of permutations that partitions χ into its equivalence classes. Recall, from §2.2.2, that the Cauchy-Frobenius Lemma can be used to determine the number of these equivalence classes. The value of Q_i for $i \in \{1,2,\ldots,\lfloor \frac{n}{7} \rfloor\}$ is therefore given by

$$Q_i = \frac{1}{|G|}\sum_{g\in G}|F_g|, \tag{B.25}$$

where $|F_g|$ is the number of states in χ that remain invariant under the permutation $g \in G$.

In order to determine the symmetry group G of the states of the form (B.24), let ι be the identity permutation on the sequence of runs of a state $s \in \chi$. Let ρ^j be the permutation which modular shifts each run in (B.24) j positions to the right. Let δ furthermore be the operation that reverses the order of the runs in (B.24) so that the first run remains in its original position,

followed by runs $i, i-1, \ldots$ The symmetry group $G = \{\iota, \rho^1, \rho^2, \ldots, \rho^{i-1}, \delta, \delta\rho^1, \delta\rho^2, \ldots, \delta\rho^{i-1}\}$ of order $2i$ is thus formed under the binary operation of permutation composition. In order to calculate Q_i, according to (B.25), all states that remain invariant under each permutation within G has to be considered.

First, consider the identity operator ι. This operator leaves all elements of χ invariant and therefore $|F_\iota| = |\chi|$. To enumerate the states in χ, the number of ways of distributing $n - 7i$ indistinguishable symbols amongst $2i$ distinguishable runs has to be determined. Using Lemma 5, it follows that

$$|F_\iota| = \binom{n - 5i + 2i - 1}{2i - 1} = \binom{n - 5i - 1}{2i - 1}. \tag{B.26}$$

Next, consider the permutation ρ^j. For a state to remain invariant under the permutation ρ^j, the first j pairs of runs have to be equivalent to all subsequent runs. To elucidate this claim, consider applying ρ^1 to a state $s \in \chi$. When performing this operation, run i is mapped to run $i+2$ which, in turn, is mapped to run $i+4$, and so on. Hence, the numbers of symbols in runs 1 and 2 determine the numbers of symbols in runs 3 and 4 as well as the numbers of symbols in runs 5 and 6, and so on. Therefore, each pair of runs have to be equivalent. Hence, the number of possible states that remain invariant under ρ^1 can be determined by finding the number of distinct ways of distributing $\frac{2}{2i}(n - 7i)$ symbols among two containers, which is given by

$$|F_{\rho^1}| = \binom{\frac{n-7i}{i} + 2 - 1}{2 - 1} = \frac{n - 7i}{i} + 1.$$

Note that if j exactly divides i, then the first j pairs of runs determine the remaining $2(i - j)$ runs. Otherwise, the first $d = \gcd(i, j)$ pairs of runs determine the remaining $2(i - d)$ runs. The number of possible states that remain invariant under ρ^j can therefore be determined by finding the number of ways to distribute $\frac{2d}{2i}(n - 7i)$ symbols among the first $2d$ runs. The enumeration is given by

$$|F_{\rho^j}| = \binom{\frac{2d}{2i}(n - 7i) + 2d - 1}{2d - 1} = \binom{\frac{d}{i}(n - 5i) - 1}{2d - 1}.$$

If, however, $\frac{d}{i}n$ is not an integer, then there are not enough symbols to complete the pattern of runs in order to achieve an invariant state and so $|F_{\rho^j}| = 0$. Therefore,

$$|F_{\rho^j}| = \begin{cases} \binom{\frac{\gcd(i,j)}{i}(n-5i)-1}{2\gcd(i,j)-1}, & \text{if } \frac{\gcd(i,j)}{i}n \in \mathbb{Z} \text{ or} \\ 0, & \text{otherwise.} \end{cases} \tag{B.27}$$

Consider next the permutation δ, which reverses the order of the runs so that the first run remains in its original position, the second run is projected onto the last run, the third run is projected onto the second last run, and so on. Runs 1 and $i+1$ are projected onto themselves, while runs 2 to i map onto runs $i+2$ to $2i$, respectively. Let k be the number of indistinguishable symbols that are distributed among the $i-1$ distinguishable runs not mapping onto themselves. The number of ways of distributing the k symbols among these $i-1$ runs is $\binom{k+i-2}{i-2}$, provided that the inequality $0 \leq k \leq n - 7i$ holds. The remaining $n - 7i - 2k$ symbols are distributed among the two runs that map onto themselves, which can be done in $\binom{n-7i-2k+2-1}{2-1} = n - 7i - 2k + 1$ distinct ways. In order to enumerate the number of distinct game states that remain invariant under the permutation δ, all possible values of k are to be considered. Therefore,

$$|F_\delta| = \sum_{k=0}^{\lfloor \frac{n-7i}{2} \rfloor} (n - 7i - 2k + 1)\binom{k + i - 2}{i - 2}. \tag{B.28}$$

Finally, consider the permutation composition $\delta\rho^j$ which shifts the runs j positions to the left and then reverses the order of the runs. Under this permutation, runs $j+1$ and $i+j+1$ map onto themselves, while runs $j+2$ to $i+j$ map onto runs $j-1$ to $i+j+2$, respectively. Once again, k indistinguishable symbols can be distributed among $i-1$ distinguishable runs that do not map onto themselves in $\binom{k+i-2}{i-2}$ different ways, provided that the inequality $0 \leq k \leq n-7i$ holds. Again, the remaining $n-7i-2k$ symbols can be distributed among the two runs that map onto themselves in $\binom{n-7i-2k+2-1}{2-1} = n-7i-2k+1$ distinct ways. Therefore, the number of distinct game states that remain invariant under the permutation $\delta\rho^j$ equals the number in (B.28).

Taking all the various permutations into account and therefore substituting (B.26),(B.27) and (B.28) into (B.25), the number of equilibrium states for the ESPD with $C_n\langle 1,2\rangle$ as underlying graph and for which the inequalities $3T+P<4$ and $2T+2P>3$ hold (*i.e.* the parameters lie within region E of the phase plane in Figure 5.6) is

$$Q_i = \frac{1}{2i}\left[\binom{n-5i-1}{2i-1} + \sum_{j\in\tilde{S}}\binom{(n-5i)\gcd(i,j)/i-1}{2\gcd(i,j)-1} + i\sum_{k=0}^{\lfloor\frac{n-7i}{2}\rfloor}(n-7i-2k+1)\binom{k+i-2}{i-2}\right],$$

where $\tilde{S}$ is the set $\{x\in\mathbb{N} \mid i \text{ divides } n\ \gcd(i,x) \text{ and } x<i\}$. □

APPENDIX C

Asymptotic analysis of the likelihood of persistent cooperation

The proof of Theorem 7 in §5.5 is presented for parameter regions B, C and E in this appendix. The theorem is first restated and the proof for each parameter region given thereafter.

Theorem 7. *If the underlying graph of the ESPD is the circulant $C_n\langle 1,2\rangle$ and if the parameter inequality $T+P<2$ holds (i.e. the parameters lie within region A, B, C or E of the phase plane in Figure 5.6), then*

$$\lim_{n\to\infty} P(n) = 1.$$

Proof: (for parameter region B)
Consider the relationship $b_n = b_{n-1} + b_{n-2} + b_{n-3} + b_{n-4} + b_{n-5} - b_{n-6} - b_{n-7} + b_{n-8} + b_{n-9}$ specified in Theorem 6 for parameter region B of the phase plane in Figure 5.6, and let $T_n = b_{n-2} + b_{n-3} + b_{n-4} + b_{n-5} - b_{n-6} - b_{n-7} + b_{n-8} + b_{n-9}$. Then

$$b_n = b_{n-1} + T_n. \tag{C.1}$$

If the indices in the recurrence relation (5.16) are shifted one position to the left, the relationship becomes

$$b_{n-1} = b_{n-2} + b_{n-3} + b_{n-4} + b_{n-5} + b_{n-6} - b_{n-7} - b_{n-8} + b_{n-9} + b_{n-10}. \tag{C.2}$$

Taking the difference between b_{n-1} and T_n, and substituting (C.2) and (C.1) into b_{n-1} and T_n, respectively, it follows that

$$b_{n-1} - T_n = 2b_{n-6} - 2b_{n-8} + b_{n-10}.$$

By Lemma 8, $b_{n+1} > b_n > 0$ and therefore by the repeated use of this inequality it follows that $2b_{n-6} - 2b_{n-8} + b_{n-10} > 0$. Consequently, $T_n < b_{n-1}$, and so it follows from (5.19) that $0 < b_n < 2b_{n-1}$. Dividing each term in this inequality by 2^n, it follows that

$$0 < \frac{b_n}{2^n} < \frac{b_{n-1}}{2^{n-1}}.$$

The value of $b_n/2^n$ is therefore decreasing and positive by the above inequality, and so

$$\lim_{n\to\infty} \frac{b_n}{2^n} = c \tag{C.3}$$

for some non-negative real constant c.

In order to determine the value of c, note that substituting (5.16) into (C.3), gives

$$\begin{aligned}\lim_{n\to\infty}\frac{b_n}{2^n} &= \lim_{n\to\infty}\frac{b_{n-1}+b_{n-2}+b_{n-3}+b_{n-4}+b_{n-5}-b_{n-6}-b_{n-7}+b_{n-8}+b_{n-9}}{2^n}\\ &= \frac{1}{2}\lim_{n\to\infty}\frac{b_{n-1}}{2^{n-1}}+\frac{1}{2^2}\lim_{n\to\infty}\frac{b_{n-2}}{2^{n-2}}+\frac{1}{2^3}\lim_{n\to\infty}\frac{b_{n-3}}{2^{n-3}}+\frac{1}{2^4}\lim_{n\to\infty}\frac{b_{n-4}}{2^{n-4}}+\frac{1}{2^5}\lim_{n\to\infty}\frac{b_{n-5}}{2^{n-5}}\\ &\quad-\frac{1}{2^6}\lim_{n\to\infty}\frac{b_{n-6}}{2^{n-6}}-\frac{1}{2^7}\lim_{n\to\infty}\frac{b_{n-7}}{2^{n-7}}+\frac{1}{2^8}\lim_{n\to\infty}\frac{b_{n-8}}{2^{n-8}}+\frac{1}{2^9}\lim_{n\to\infty}\frac{b_{n-9}}{2^{n-9}}\\ &= c\left(\frac{1}{2}+\frac{1}{2^2}+\frac{1}{2^3}+\frac{1}{2^4}+\frac{1}{2^5}-\frac{1}{2^6}-\frac{1}{2^7}+\frac{2}{2^8}+\frac{1}{2^9}\right)\\ &= c. \end{aligned} \tag{C.4}$$

In order to satisfy (C.4), it is therefore required that $c = 0$. Hence,

$$\lim_{n\to\infty} P(n) = \lim_{n\to\infty}\left(1-\frac{b_n}{2_n}\right) = 1$$

by (5.14). □

Proof: (for parameter region C)
Consider the relationship $b_n = b_{n-1}+b_{n-2}+b_{n-3}+b_{n-4}+b_{n-5}-b_{n-6}-2b_{n-7}+b_{n-8}+b_{n-9}$ specified in Theorem 6 for parameter region C of the phase plane in Figure 5.6, and let $T_n = b_{n-2}+b_{n-3}+b_{n-4}+b_{n-5}-b_{n-6}-2b_{n-7}+b_{n-8}+b_{n-9}$. Then

$$b_n = b_{n-1}+T_n. \tag{C.5}$$

If the indices in the recurrence relation (5.17) are shifted one position to the left, the relationship becomes

$$b_{n-1} = b_{n-2}+b_{n-3}+b_{n-4}+b_{n-5}+b_{n-6}-b_{n-7}-2b_{n-8}+b_{n-9}+b_{n-10}. \tag{C.6}$$

Taking the difference between b_{n-1} and T_n, and substituting (C.6) and (C.5) into b_{n-1} and T_n, respectively, it follows that

$$b_{n-1}-T_n = 2b_{n-6}+b_{n-7}-3b_{n-8}+b_{n-10}.$$

By Lemma 8, $b_{n+1} > b_n > 0$ and therefore by the repeated use of this inequality, $2b_{n-6}+b_{n-7}-3b_{n-8}+b_{n-10} > 0$. Consequently, $T_n < b_{n-1}$ and so it follows from (C.5) that $0 < b_n < 2b_{n-1}$. Dividing each term in this inequality by 2^n, it follows that

$$0 < \frac{b_n}{2^n} < \frac{b_{n-1}}{2^{n-1}}.$$

The value of $b_n/2^n$ is therefore decreasing and positive by the above inequality, and so

$$\lim_{n\to\infty}\frac{b_n}{2^n} = c \tag{C.7}$$

for some non-negative real constant c.

In order to determine the value of c, note that substituting (5.17) into (C.7), gives

$$\begin{aligned}\lim_{n\to\infty}\frac{b_n}{2^n} &= \lim_{n\to\infty}\frac{b_{n-1}+b_{n-2}+b_{n-3}+b_{n-4}+b_{n-5}-b_{n-6}-2b_{n-7}+b_{n-8}+b_{n-9}}{2^n}\\ &= \frac{1}{2}\lim_{n\to\infty}\frac{b_{n-1}}{2^{n-1}}+\frac{1}{2^2}\lim_{n\to\infty}\frac{b_{n-2}}{2^{n-2}}+\frac{1}{2^3}\lim_{n\to\infty}\frac{b_{n-3}}{2^{n-3}}+\frac{1}{2^4}\lim_{n\to\infty}\frac{b_{n-4}}{2^{n-4}}+\frac{1}{2^5}\lim_{n\to\infty}\frac{b_{n-5}}{2^{n-5}}\\ &\quad-\frac{1}{2^6}\lim_{n\to\infty}\frac{b_{n-6}}{2^{n-6}}-\frac{2}{2^7}\lim_{n\to\infty}\frac{b_{n-7}}{2^{n-7}}+\frac{1}{2^8}\lim_{n\to\infty}\frac{b_{n-8}}{2^{n-8}}+\frac{1}{2^9}\lim_{n\to\infty}\frac{b_{n-9}}{2^{n-9}}\\ &= c\left(\frac{1}{2}+\frac{1}{2^2}+\frac{1}{2^3}+\frac{1}{2^4}+\frac{1}{2^5}-\frac{1}{2^6}-\frac{2}{2^7}+\frac{1}{2^8}+\frac{1}{2^9}\right)\\ &= c. \end{aligned} \tag{C.8}$$

In order to satisfy (C.8), it is therefore required that $c = 0$. Hence,

$$\lim_{n\to\infty} P(n) = \lim_{n\to\infty}\left(1-\frac{b_n}{2_n}\right) = 1$$

by (5.14). □

Proof: (for parameter region E)
Consider the relationship $b_n = b_{n-1}+b_{n-2}+b_{n-3}+b_{n-4}+b_{n-5}+b_{n-6}+b_{n-7}-b_{n-8}-b_{n-9}$ specified in Theorem 6 for parameter region E of the phase plane in Figure 5.6, and let $T_n = b_{n-2}+b_{n-3}+b_{n-4}+b_{n-5}+b_{n-6}+b_{n-7}-b_{n-8}-b_{n-9}$. Then

$$b_n = b_{n-1}+T_n. \tag{C.9}$$

If the indices in the recurrence relation (5.18) are shifted one position to the left, the relationship yields

$$b_{n-1} = b_{n-2}+b_{n-3}+b_{n-4}+b_{n-5}+b_{n-6}+b_{n-7}+b_{n-8}-b_{n-9}-b_{n-10}. \tag{C.10}$$

Taking the difference between b_{n-1} and T_n, and substituting (C.10) and (C.9) into b_{n-1} and T_n, respectively, it follows that

$$b_{n-1}-T_n = 2b_{n-8}-b_{n-10}.$$

By Lemma 8, $b_{n+1} > b_n > 0$ and therefore $2b_{n-8}-b_{n-10} > 0$. Consequently, $T_n < b_{n-1}$ and so it follows from (C.9) that $0 < b_n < 2b_{n-1}$. Dividing each term in this inequality by 2^n, it follows that

$$0 < \frac{b_n}{2^n} < \frac{b_{n-1}}{2^{n-1}}.$$

The value of $b_n/2^n$ is therefore decreasing and positive by the above inequality, and so

$$\lim_{n\to\infty}\frac{b_n}{2^n} = c \tag{C.11}$$

for some non-negative real constant c.

In order to determine the value of c, note that substituting (5.18) into (C.11), gives

$$\begin{aligned}
\lim_{n\to\infty}\frac{b_n}{2^n} &= \lim_{n\to\infty}\frac{b_{n-1}+b_{n-2}+b_{n-3}+b_{n-4}+b_{n-5}+b_{n-6}+b_{n-7}-b_{n-8}-b_{n-9}}{2^n}\\
&= \frac{1}{2}\lim_{n\to\infty}\frac{b_{n-1}}{2^{n-1}}+\frac{1}{2^2}\lim_{n\to\infty}\frac{b_{n-2}}{2^{n-2}}+\frac{1}{2^3}\lim_{n\to\infty}\frac{b_{n-3}}{2^{n-3}}+\frac{1}{2^4}\lim_{n\to\infty}\frac{b_{n-4}}{2^{n-4}}+\frac{1}{2^5}\lim_{n\to\infty}\frac{b_{n-5}}{2^{n-5}}\\
&\quad+\frac{1}{2^6}\lim_{n\to\infty}\frac{b_{n-6}}{2^{n-6}}+\frac{1}{2^7}\lim_{n\to\infty}\frac{b_{n-7}}{2^{n-7}}-\frac{1}{2^8}\lim_{n\to\infty}\frac{b_{n-8}}{2^{n-8}}-\frac{1}{2^9}\lim_{n\to\infty}\frac{b_{n-9}}{2^{n-9}}\\
&= c\left(\frac{1}{2}+\frac{1}{2^2}+\frac{1}{2^3}+\frac{1}{2^4}+\frac{1}{2^5}+\frac{1}{2^6}+\frac{1}{2^7}-\frac{1}{2^8}-\frac{1}{2^9}\right)\\
&= c. \qquad \text{(C.12)}
\end{aligned}$$

In order to satisfy (C.12), it is therefore required that $c = 0$. Hence,

$$\lim_{n\to\infty} P(n) = \lim_{n\to\infty}\left(1-\frac{b_n}{2_n}\right) = 1$$

by (5.14). □

APPENDIX D

Equilibrium state diagrams

This appendix contains the equilibrium state diagrams for the ESPD with $C_2 \times C_6$, $C_3 \times C_4$, $C_3 \times C_5$, $C_3 \times C_6$, $C_4 \times C_4$, $C_4 \times C_5$, $C_4 \times C_6$, $C_5 \times C_5$, $C_5 \times C_6$ and $C_6 \times C_6$ as underlying graphs, given in Figures D.1–D.10, respectively.

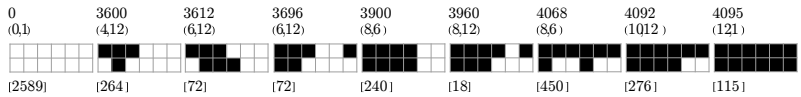

(a) Parameter region A

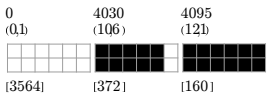

(b) Parameter region B

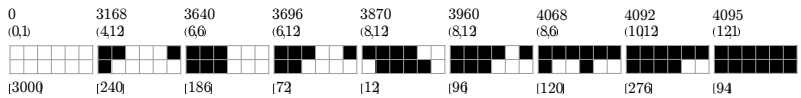

(c) Parameter region C

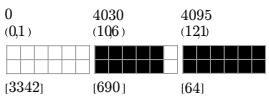

(d) Parameter region D

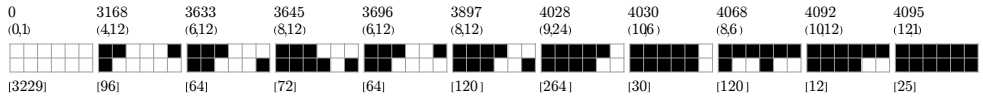

(e) Parameter region E

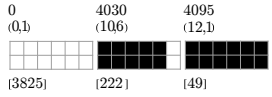

(f) Parameter region F

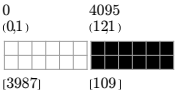

(g) Parameter region G

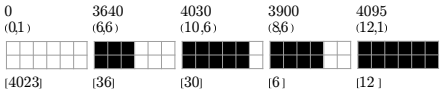

(h) Parameter region H

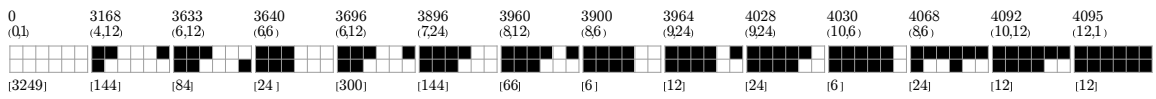

(i) Parameter region I

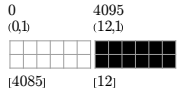

(j) Parameter region J/K

FIGURE D.1: *Equilibrium state diagrams for the ESPD with $C_2 \times C_6$ as underlying graph. The relevant parameter regions A–K of the phase plane are elucidated in Figure 6.3.*

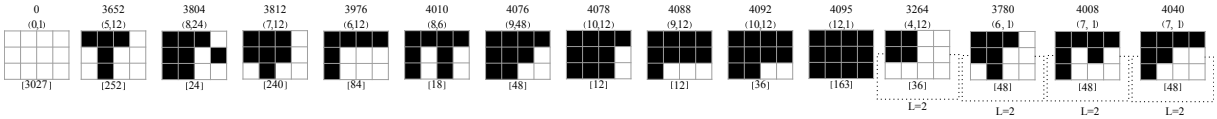

(a) Parameter region A

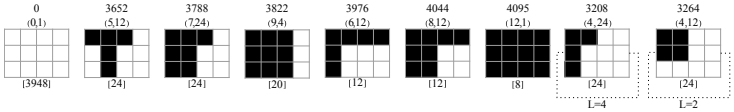

(b) Parameter region B

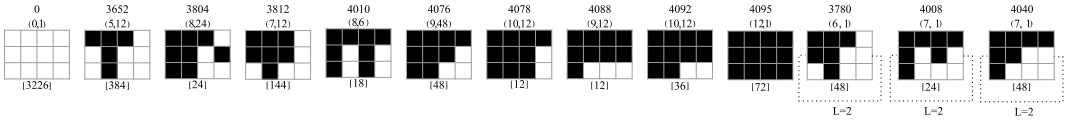

(c) Parameter region C

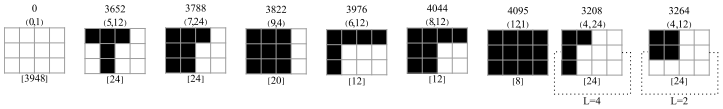

(d) Parameter region D

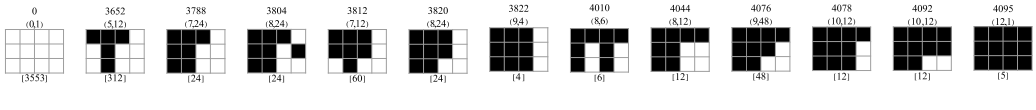

(e) Parameter region E

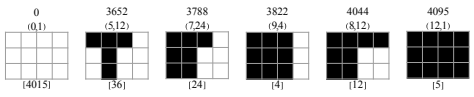

(f) Parameter region F

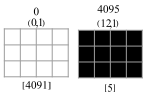

(g) Parameter region G

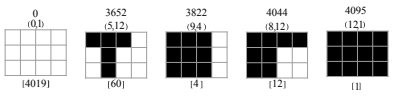

(h) Parameter region H

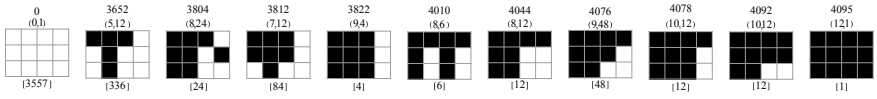

(i) Parameter region I

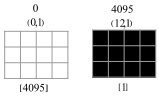

(j) Parameter region J/K

FIGURE D.2: *Equilibrium state diagrams for the ESPD with $C_3 \times C_4$ as underlying graph. The relevant parameter regions A–K of the phase plane are elucidated in Figure 6.3.*

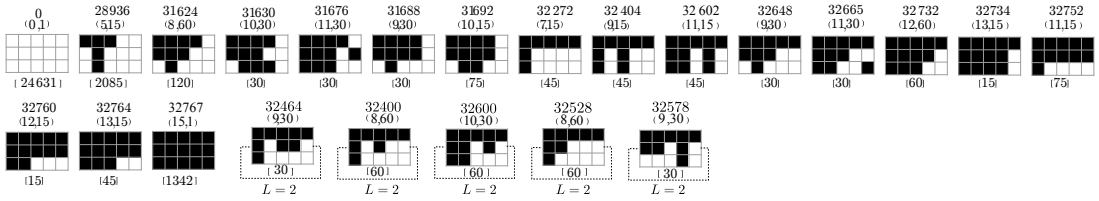

(a) Parameter region A

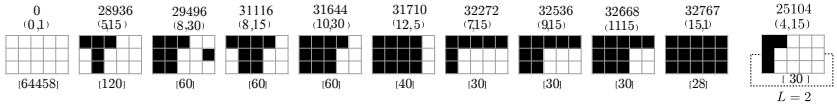

(b) Parameter region B

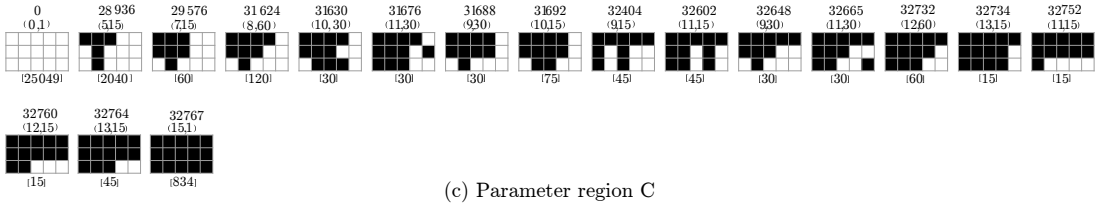

(c) Parameter region C

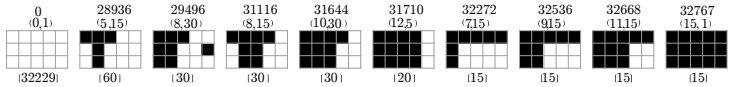

(d) Parameter region D

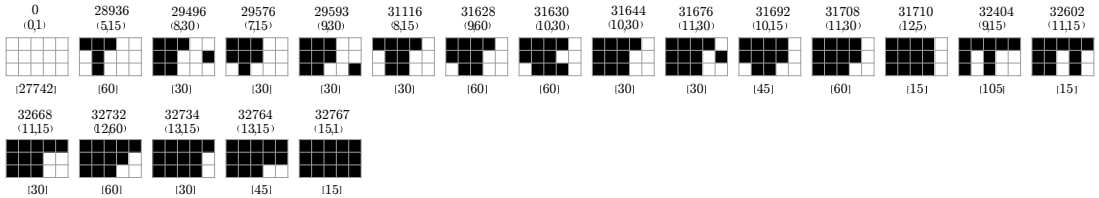

(e) Parameter region E

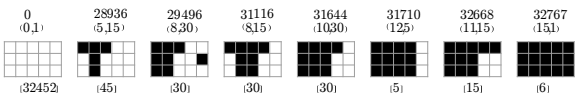

(f) Parameter region F

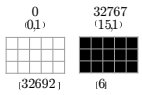

(g) Parameter region G

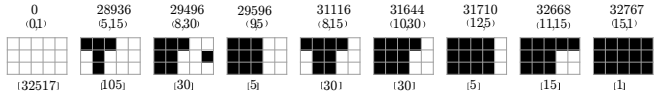

(h) Parameter region H

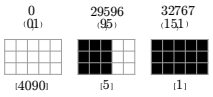

(i) Parameter region J

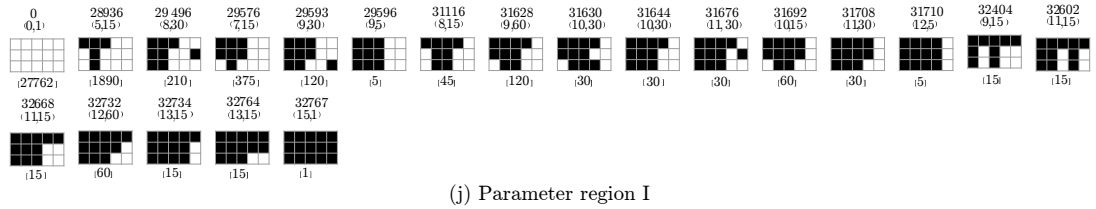

(j) Parameter region I

FIGURE D.3: *Equilibrium state diagrams for the ESPD with $C_3 \times C_5$ as underlying graph. The relevant parameter regions A–K of the phase plane are elucidated in Figure 6.3.*

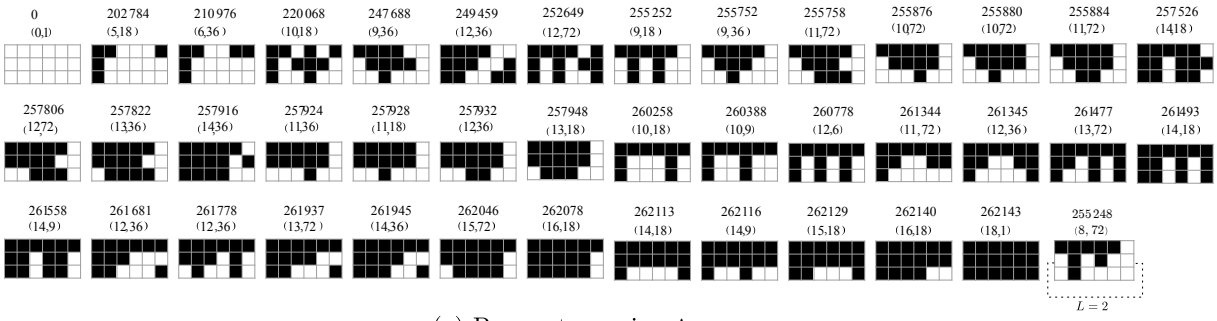

(a) Parameter region A

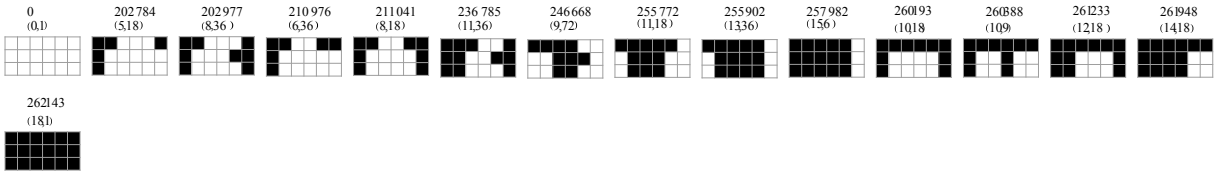

(b) Parameter region B

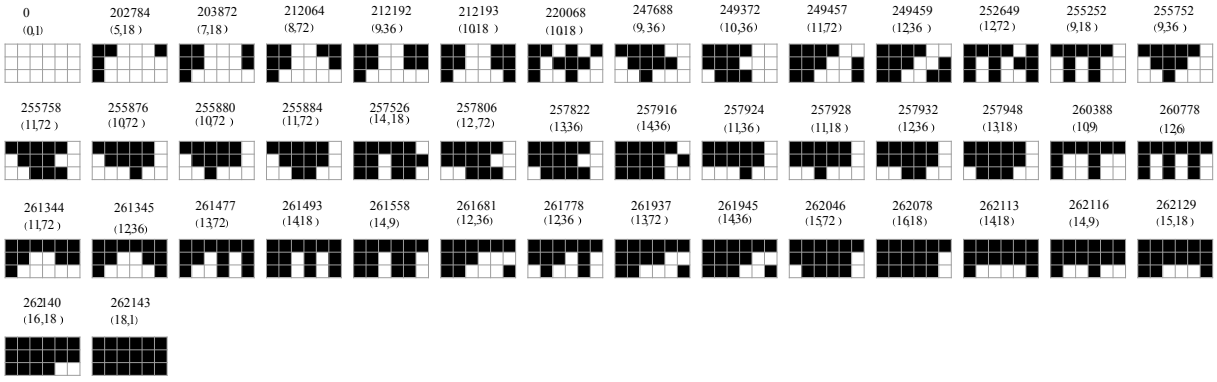

(c) Parameter region C

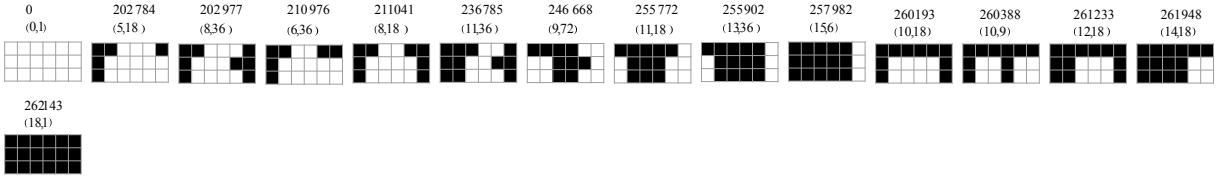

(d) Parameter region D

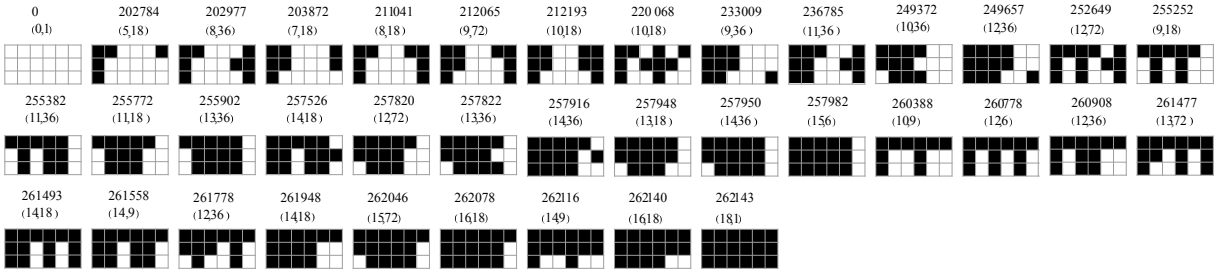

(e) Parameter region E

FIGURE D.4: *Equilibrium state diagrams for the ESPD with $C_3 \times C_6$ as underlying graph. The relevant parameter regions A–K of the phase plane are elucidated in Figure 6.3.*

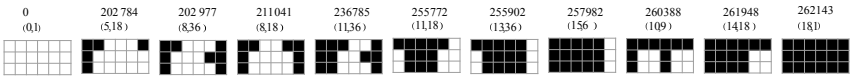

(f) Parameter region F

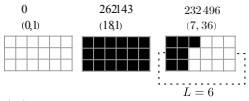

(g) Parameter region G

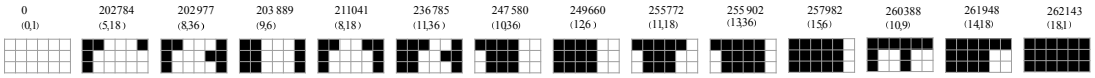

(h) Parameter region H

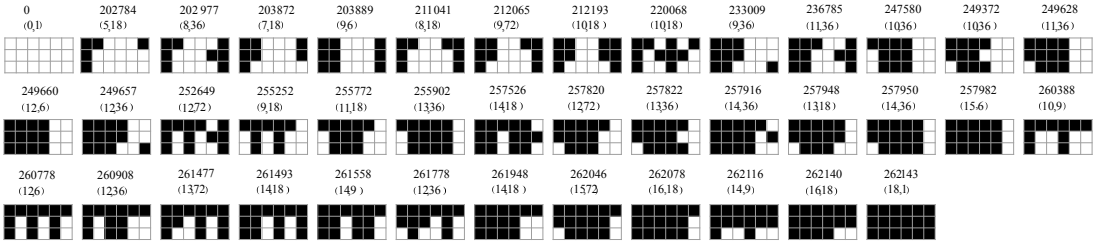

(i) Parameter region I

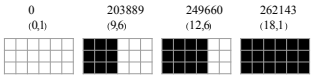

(j) Parameter region J

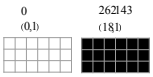

(k) Parameter region K

FIGURE D.4 (continued): *Equilibrium state diagrams for the ESPD with $C_3 \times C_6$ as underlying graph. The relevant parameter regions A–K of the phase plane are elucidated in Figure 6.3.*

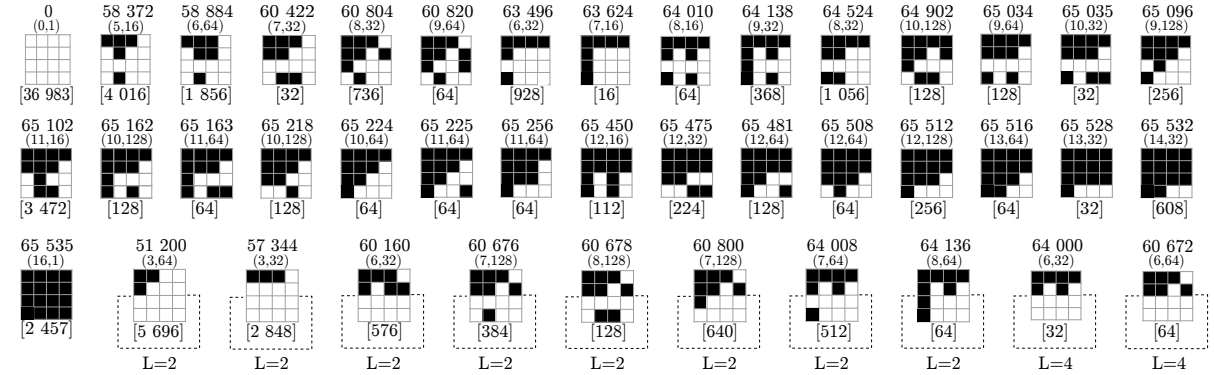

(a) Parameter region A

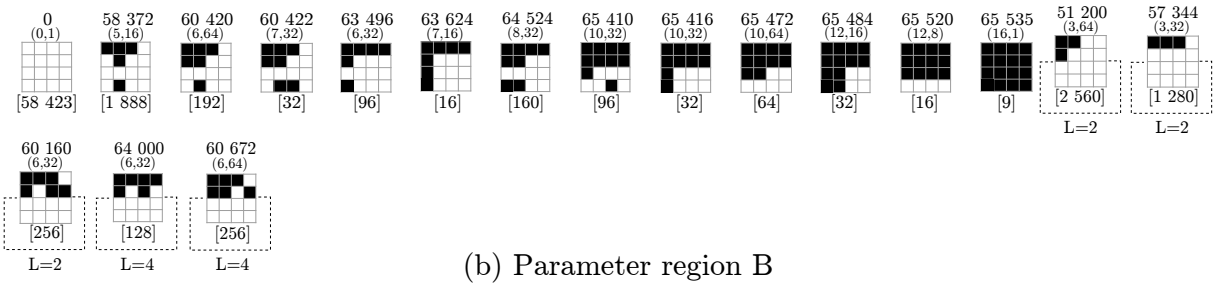

(b) Parameter region B

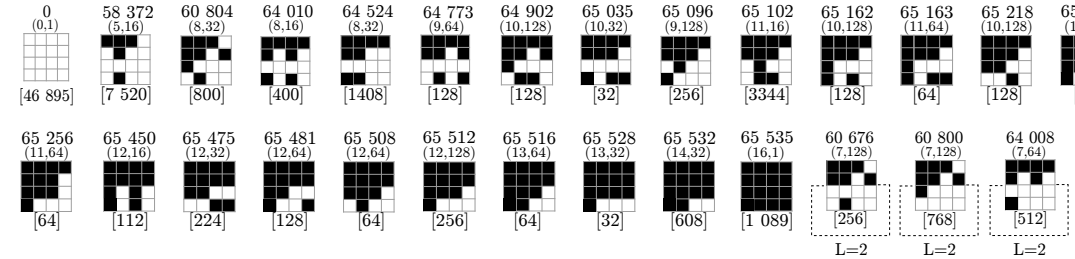

(c) Parameter region C

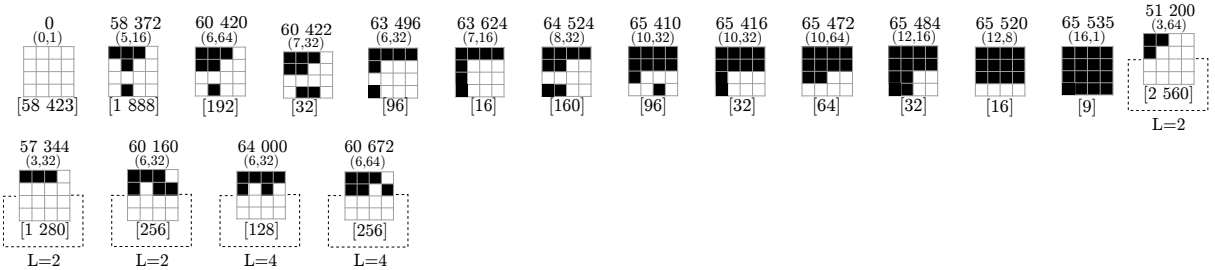

(d) Parameter region D

FIGURE D.5: *Equilibrium state diagrams for the ESPD with $C_4 \times C_4$ as underlying graph. The relevant parameter regions A–K of the phase plane are elucidated in Figure 6.3.*

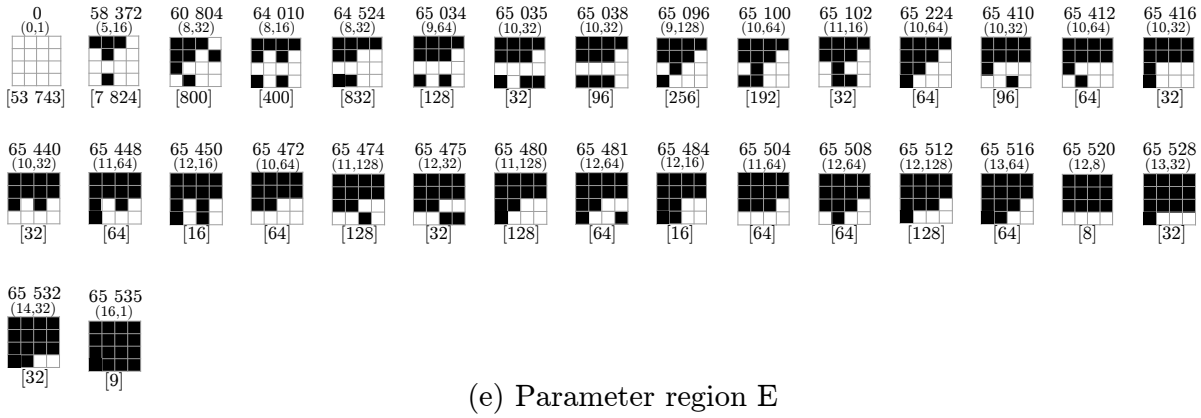

(e) Parameter region E

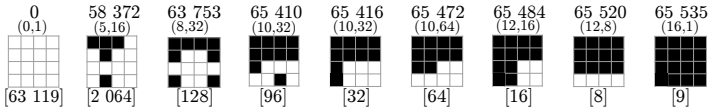

(f) Parameter region F

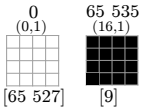

(g) Parameter region G

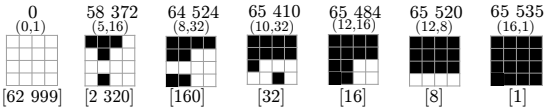

(h) Parameter region H

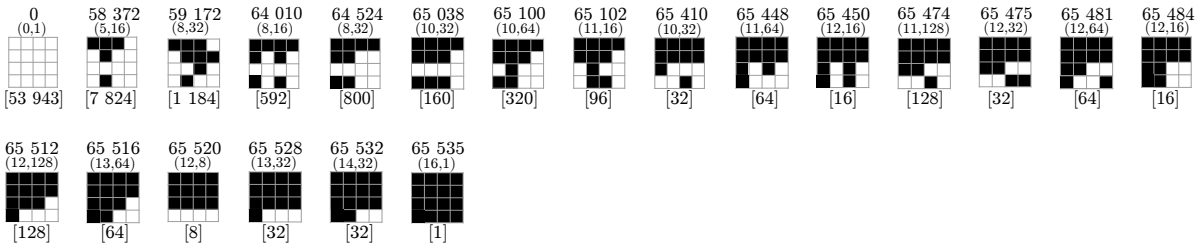

(i) Parameter region I

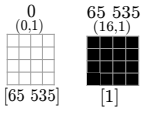

(j) Parameter region J, K

FIGURE D.5 (continued): *Equilibrium state diagrams for the ESPD with $C_4 \times C_4$ as underlying graph. The relevant parameter regions A–K of the phase plane are elucidated in Figure 6.3.*

(a) Parameter region A

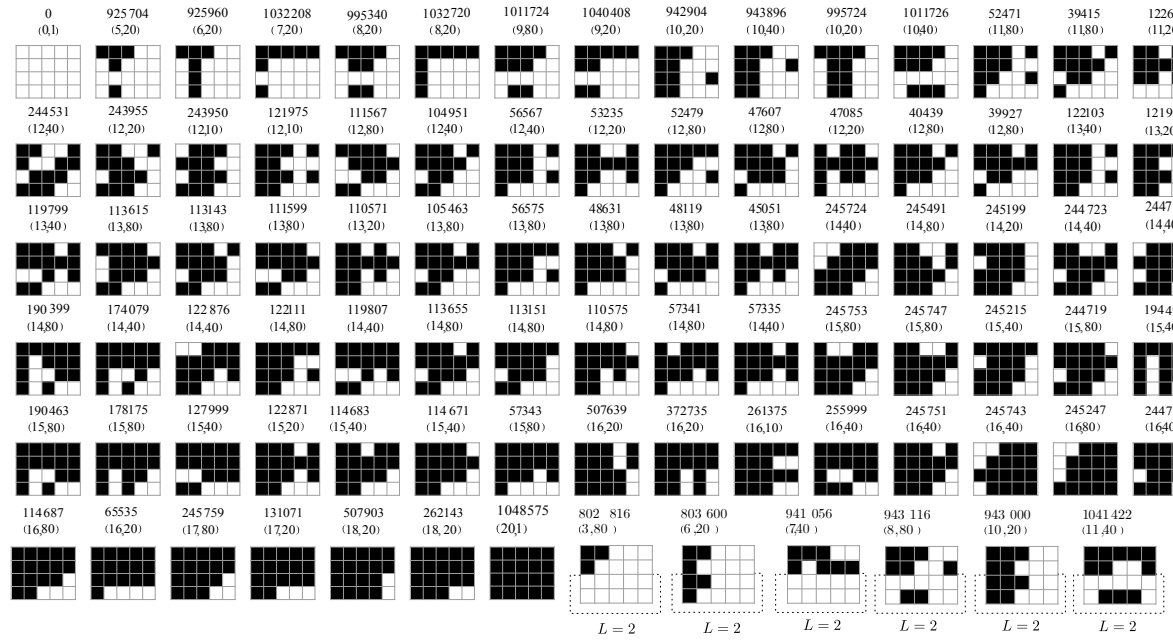

(b) Parameter region B

FIGURE D.6: *Equilibrium state diagrams for the ESPD with $C_4 \times C_5$ as underlying graph. The relevant parameter regions A–K of the phase plane are elucidated in Figure 6.3.*

(c) Parameter region C

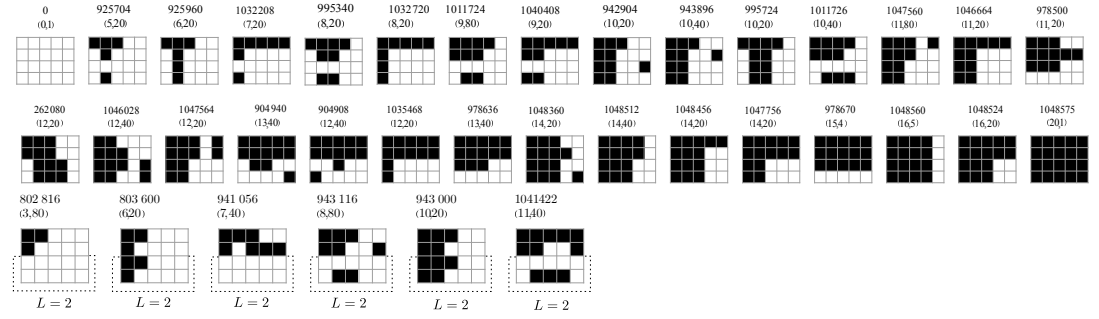

(d) Parameter region D

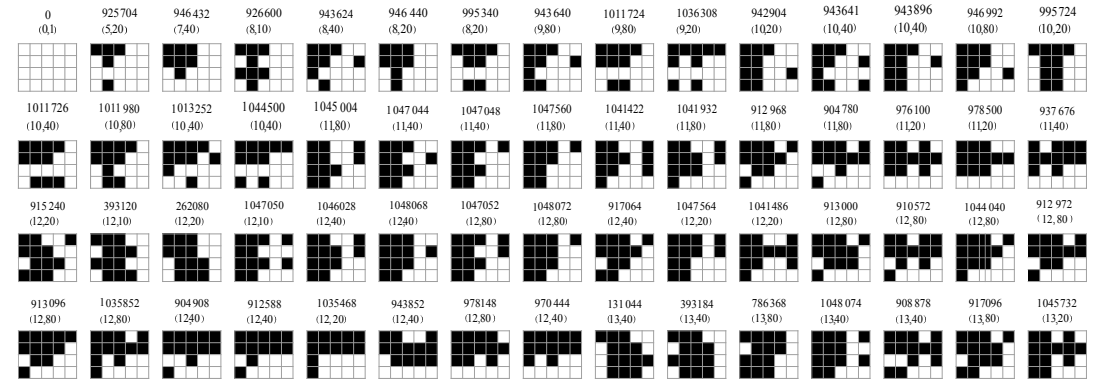

(e) Parameter region E

FIGURE D.6 (continued): *Equilibrium state diagrams for the ESPD with $C_4 \times C_5$ as underlying graph. The relevant parameter regions A–K of the phase plane are elucidated in Figure 6.3.*

(e) Parameter region E (cont.)

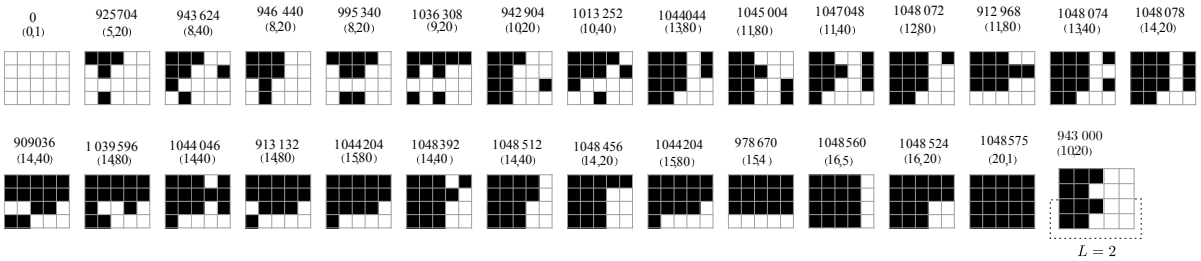

(f) Parameter region F

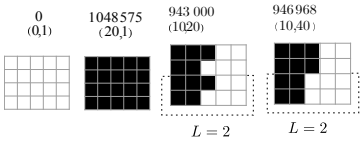

(g) Parameter region G

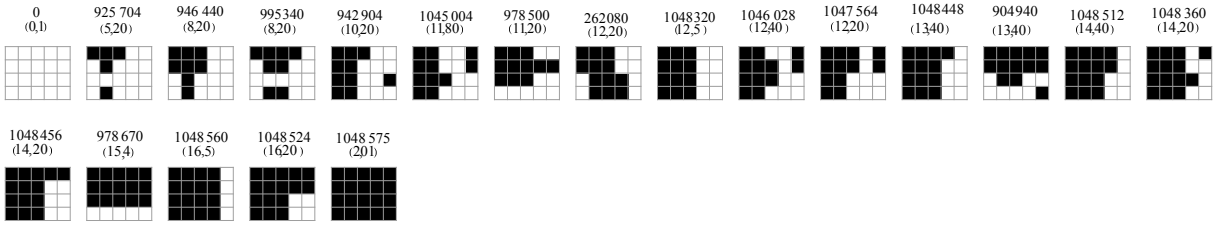

(h) Parameter region H

FIGURE D.6 (continued): *Equilibrium state diagrams for the ESPD with $C_4 \times C_5$ as underlying graph. The relevant parameter regions A–K of the phase plane are elucidated in Figure 6.3.*

(i) Parameter region I

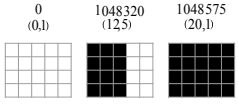

(j) Parameter region J

FIGURE D.6 (continued): *Equilibrium state diagrams for the ESPD with $C_4 \times C_5$ as underlying graph. The relevant parameter regions A–K of the phase plane are elucidated in Figure 6.3.*

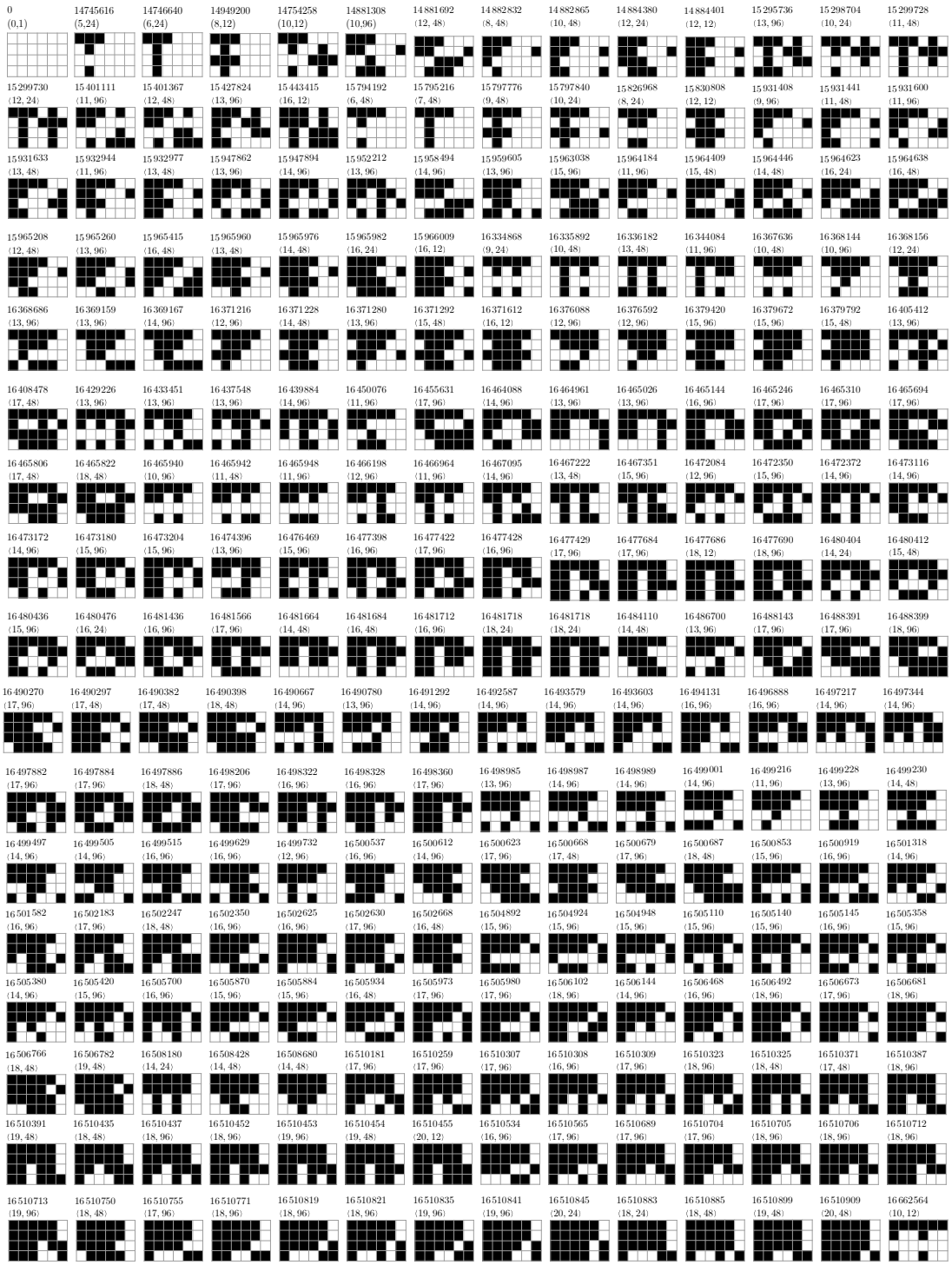

(a) Parameter region A

FIGURE D.7: *Equilibrium state diagrams for the ESPD with $C_4 \times C_6$ as underlying graph. The relevant parameter regions A–K of the phase plane are elucidated in Figure 6.3.*

(a) Parameter region A (cont.)

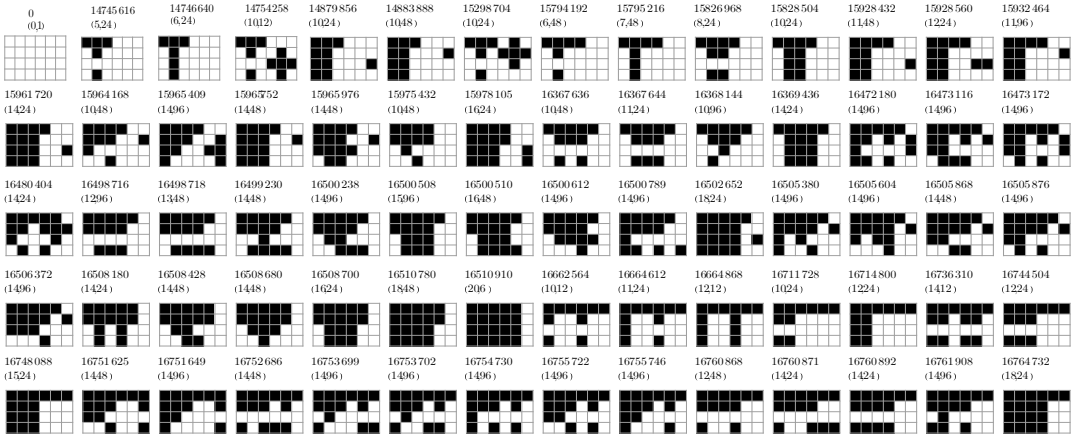

(b) Parameter region B

FIGURE D.7 (continued): *Equilibrium state diagrams for the ESPD with $C_4 \times C_6$ as underlying graph. The relevant parameter regions A–K of the phase plane are elucidated in Figure 6.3.*

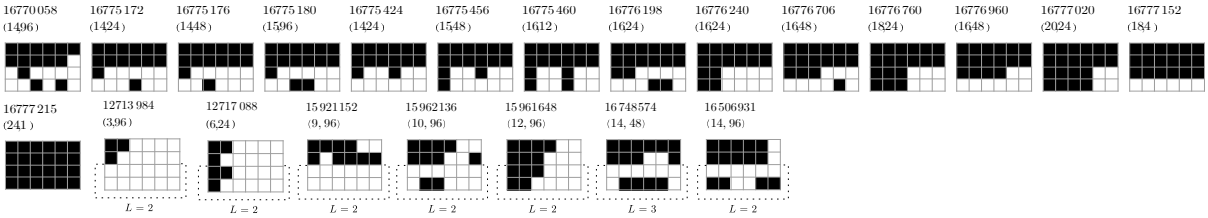

(b) Parameter region B (cont)

(c) Parameter region C

FIGURE D.7 (continued): *Equilibrium state diagrams for the ESPD with $C_4 \times C_6$ as underlying graph. The relevant parameter regions A–K of the phase plane are elucidated in Figure 6.3.*

(c) Parameter region C (cont.)

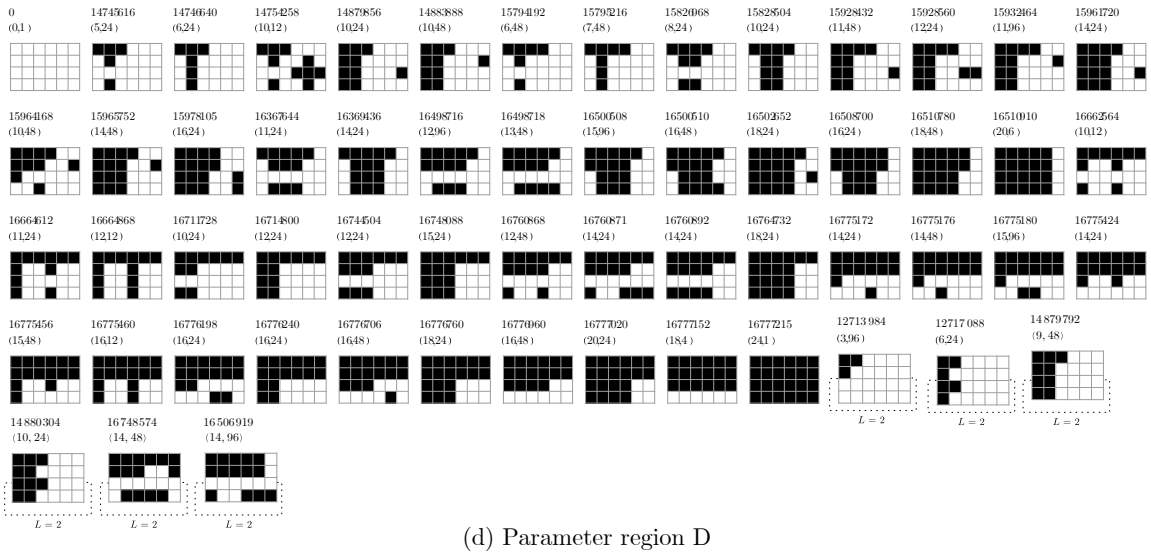

(d) Parameter region D

FIGURE D.7 (continued): *Equilibrium state diagrams for the ESPD with $C_4 \times C_6$ as underlying graph. The relevant parameter regions A–K of the phase plane are elucidated in Figure 6.3.*

(e) Parameter region E

FIGURE D.7 (continued): *Equilibrium state diagrams for the ESPD with $C_4 \times C_6$ as underlying graph. The relevant parameter regions A–K of the phase plane are elucidated in Figure 6.3.*

(e) Parameter region E (cont.)

FIGURE D.7 (continued): *Equilibrium state diagrams for the ESPD with $C_4 \times C_6$ as underlying graph. The relevant parameter regions A–K of the phase plane are elucidated in Figure 6.3.*

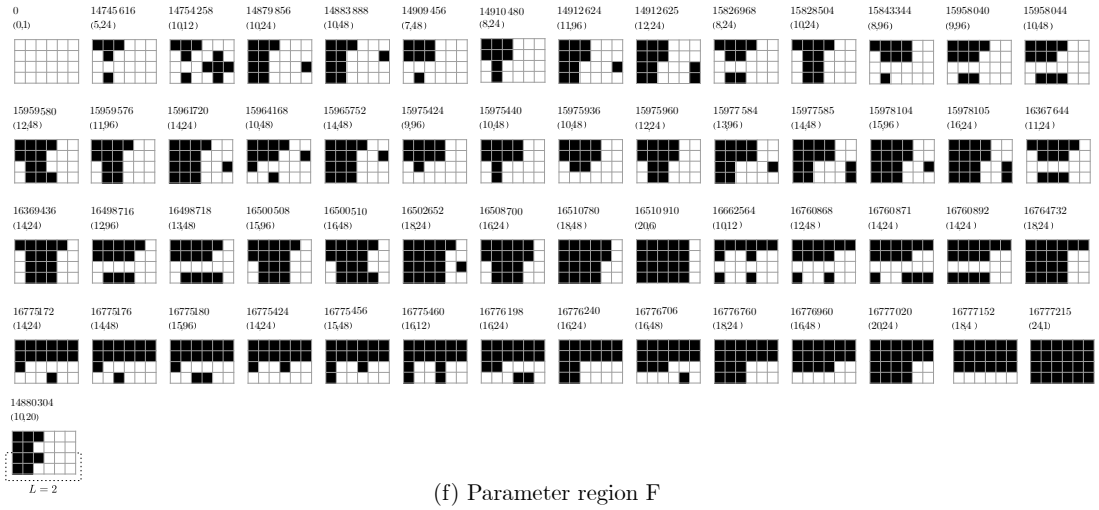

(f) Parameter region F

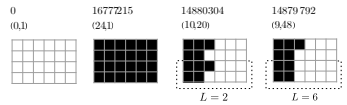

(g) Parameter region G

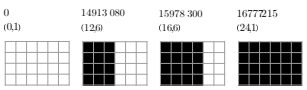

(h) Parameter region J

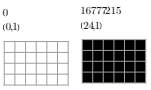

(i) Parameter region K

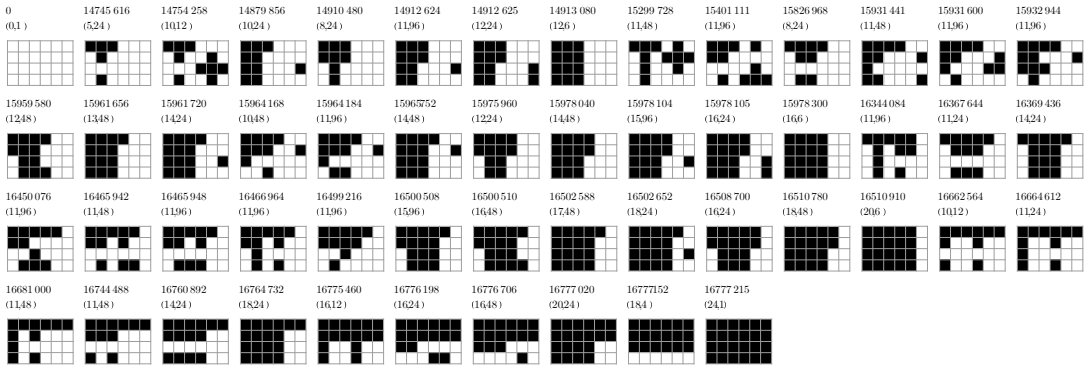

(j) Parameter region H

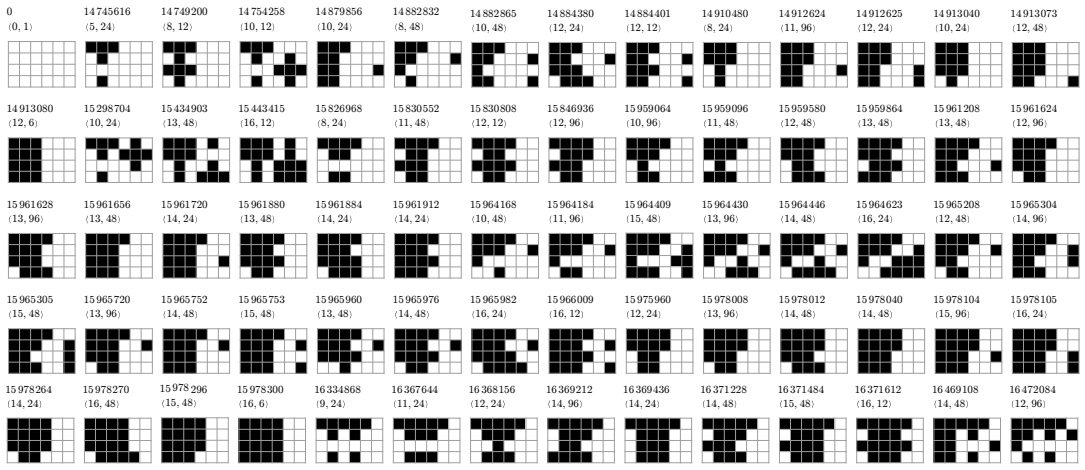

(k) Parameter region I

FIGURE D.7 (continued): *Equilibrium state diagrams for the ESPD with $C_4 \times C_6$ as underlying graph. The relevant parameter regions A–K of the phase plane are elucidated in Figure 6.3.*

(k) Parameter region I (cont.)

FIGURE D.7 (continued): *Equilibrium state diagrams for the ESPD with $C_4 \times C_6$ as underlying graph. The relevant parameter regions A–K of the phase plane are elucidated in Figure 6.3.*

(a) Parameter region A

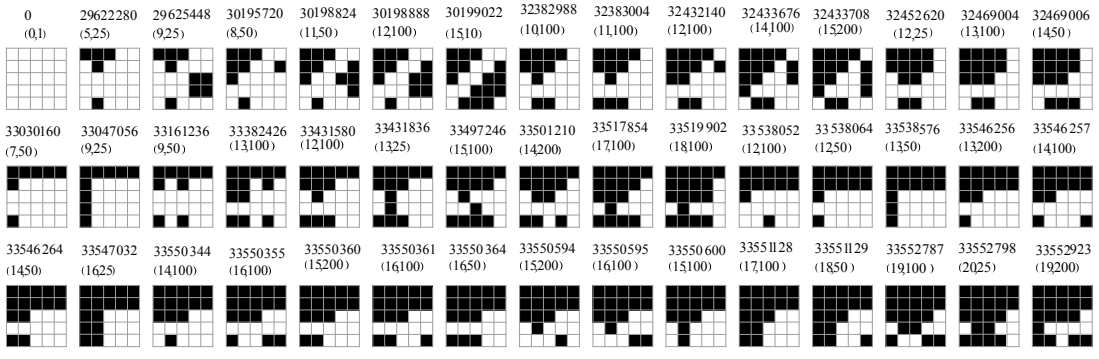

(b) Parameter region B

FIGURE D.8: *Equilibrium state diagrams for the ESPD with $C_5 \times C_5$ as underlying graph. The relevant parameter regions A–K of the phase plane are elucidated in Figure 6.3.*

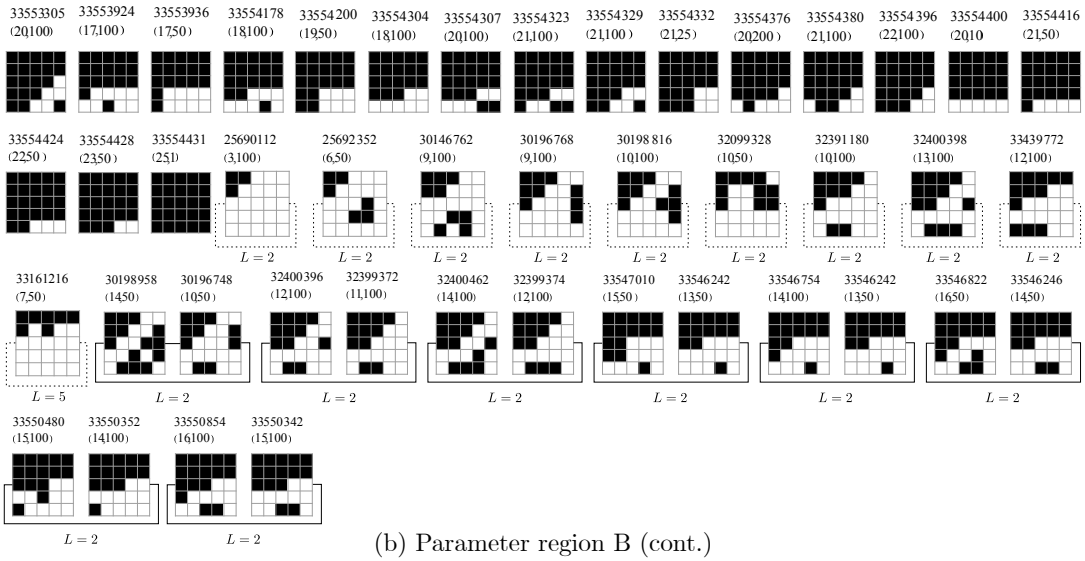

(b) Parameter region B (cont.)

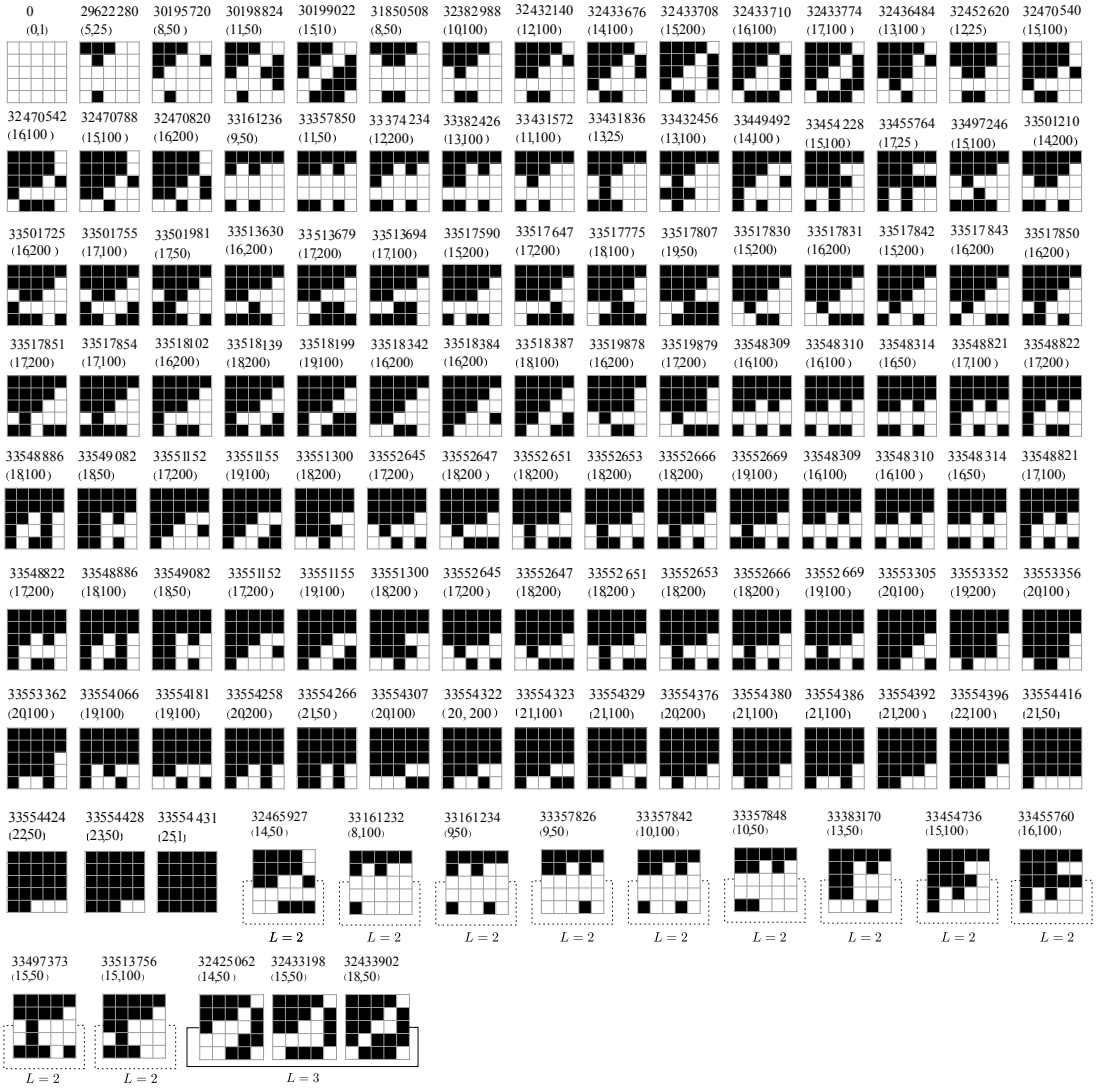

(c) Parameter region C

FIGURE D.8 (continued): *Equilibrium state diagrams for the ESPD with $C_5 \times C_5$ as underlying graph. The relevant parameter regions A–K of the phase plane are elucidated in Figure 6.3.*

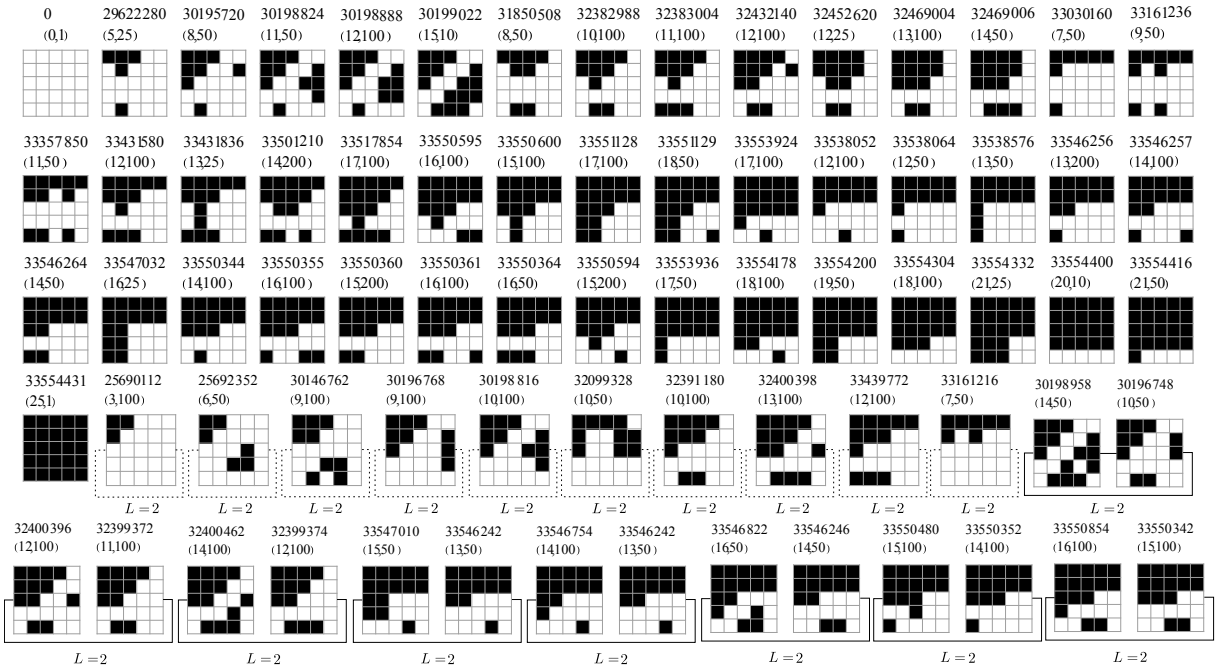

(d) Parameter region D

(e) Parameter region E

FIGURE D.8 (continued): *Equilibrium state diagrams for the ESPD with $C_5 \times C_5$ as underlying graph. The relevant parameter regions A–K of the phase plane are elucidated in Figure 6.3.*

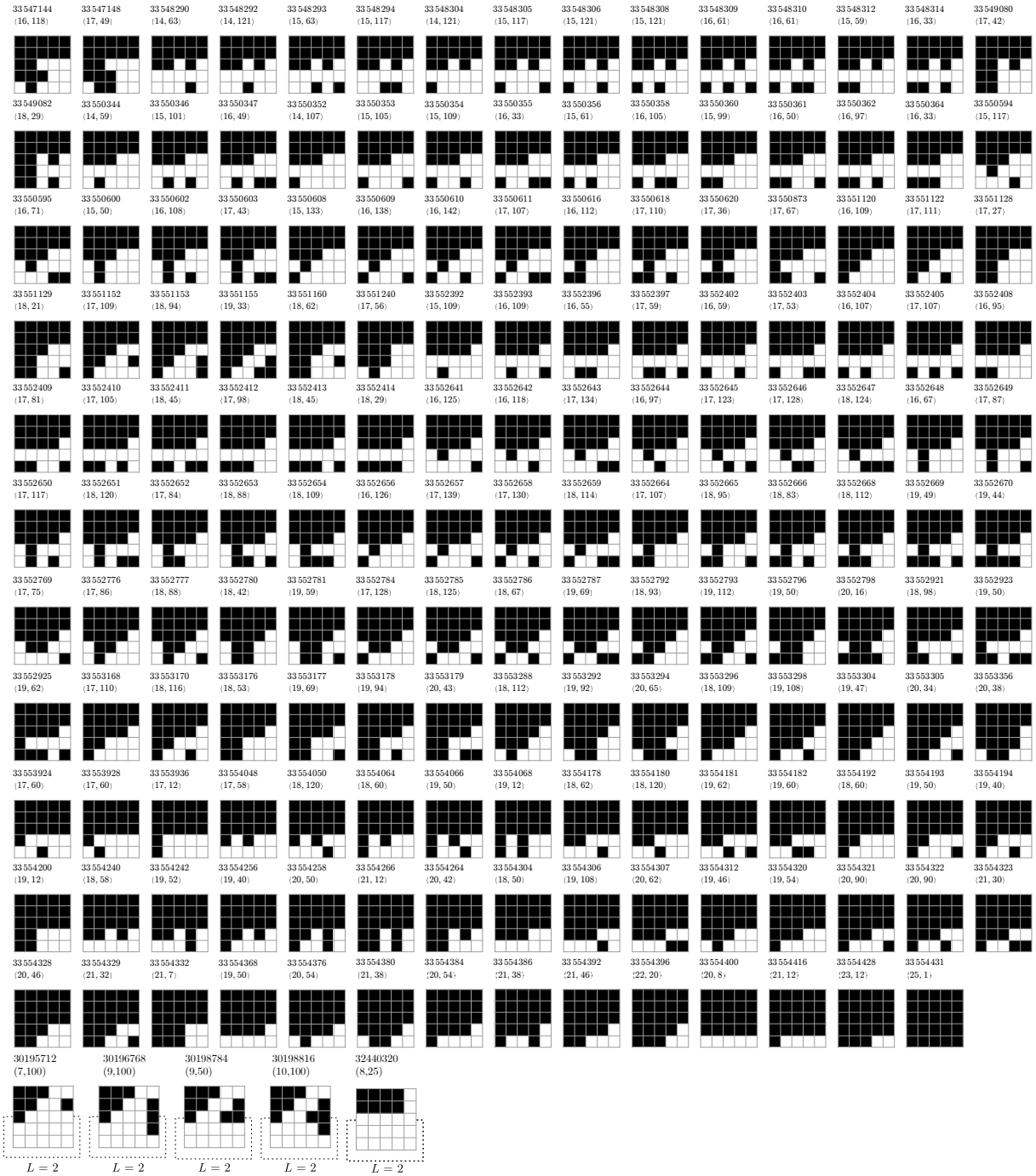

(e) Parameter region E (cont.)

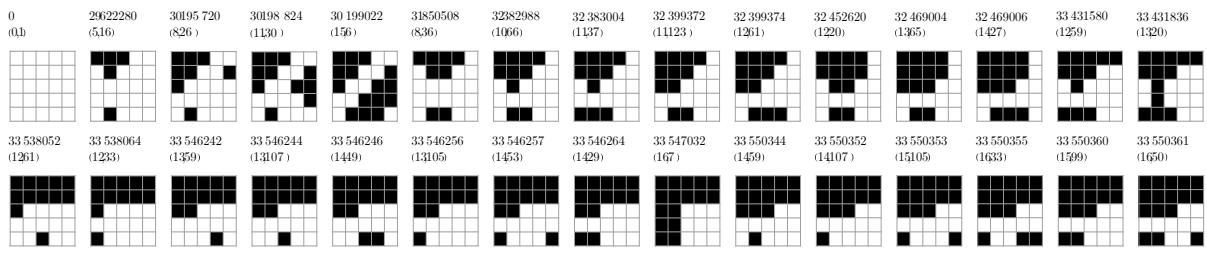

(f) Parameter region F

FIGURE D.8 (continued): *Equilibrium state diagrams for the ESPD with $C_5 \times C_5$ as underlying graph. The relevant parameter regions A–K of the phase plane are elucidated in Figure 6.3.*

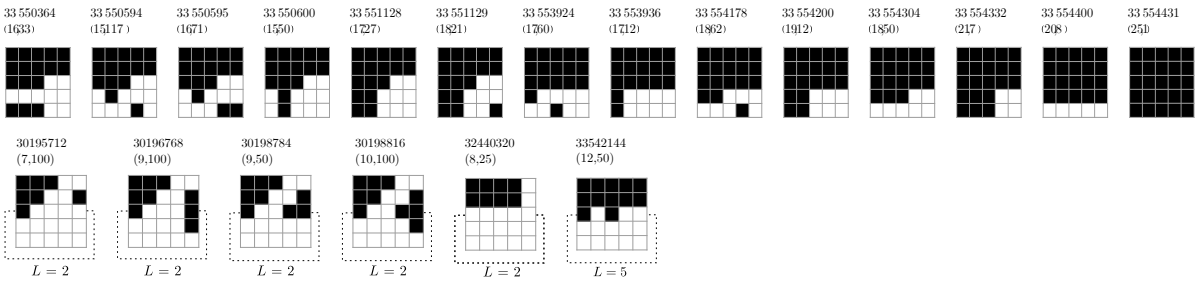

(f) Parameter region F (cont.)

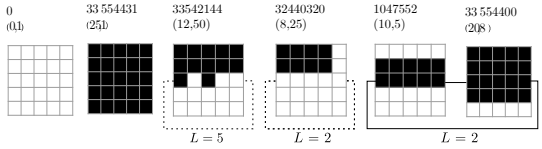

(g) Parameter region G

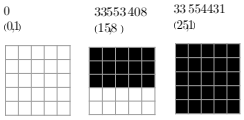

(h) Parameter region J

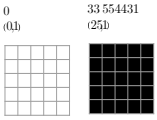

(i) Parameter region K

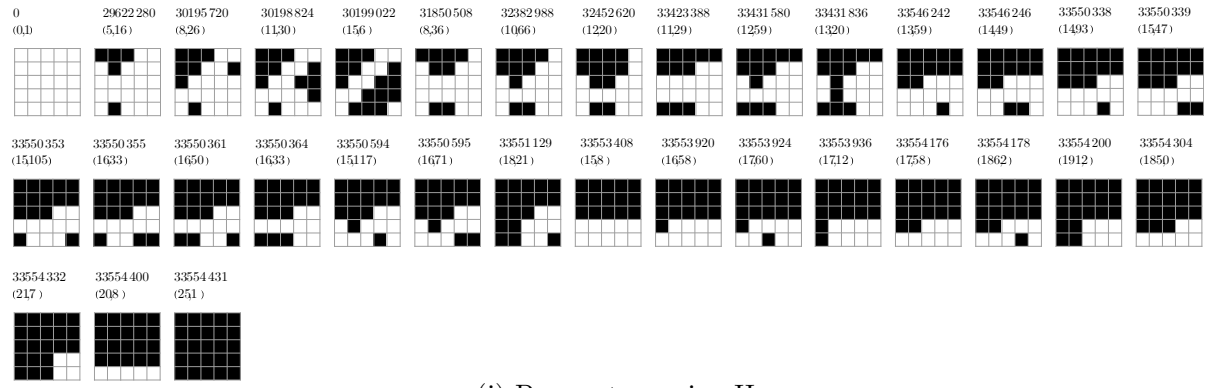

(j) Parameter region H

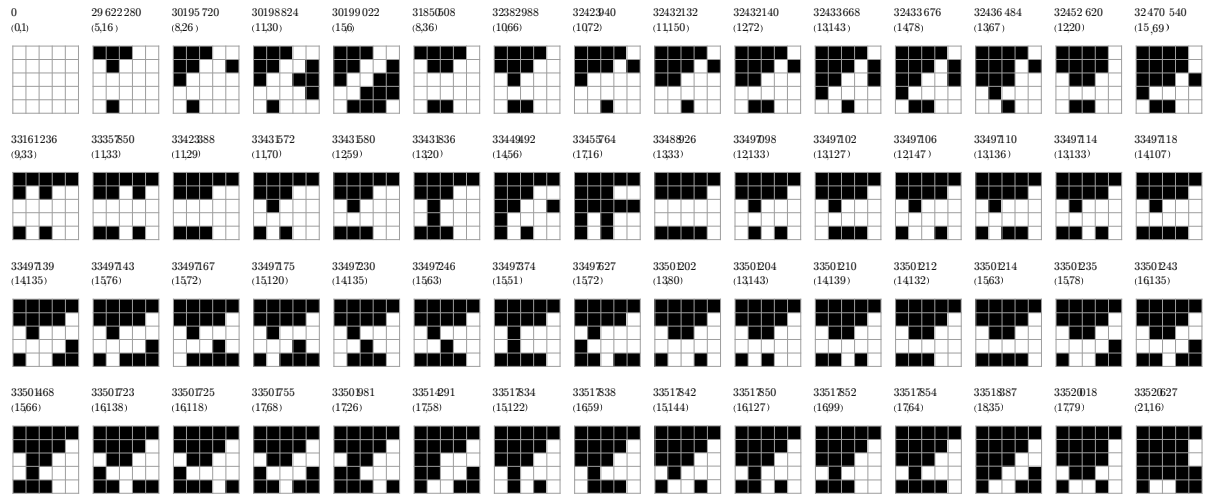

(k) Parameter region I

FIGURE D.8 (continued): *Equilibrium state diagrams for the ESPD with $C_5 \times C_5$ as underlying graph. The relevant parameter regions A–K of the phase plane are elucidated in Figure 6.3.*

(k) Parameter region I (cont.)

FIGURE D.8 (continued): *Equilibrium state diagrams for the ESPD with $C_5 \times C_5$ as underlying graph. The relevant parameter regions A–K of the phase plane are elucidated in Figure 6.3.*

(a) Parameter region A

FIGURE D.9: *Equilibrium state diagrams for the ESPD with $C_5 \times C_6$ as underlying graph. The relevant parameter regions A–K of the phase plane are elucidated in Figure 6.3.*

(a) Parameter region A (cont.)

FIGURE D.9 (continued): *Equilibrium state diagrams for the ESPD with $C_5 \times C_6$ as underlying graph. The relevant parameter regions A–K of the phase plane are elucidated in Figure 6.3.*

(b) Parameter region B

FIGURE D.9 (continued): *Equilibrium state diagrams for the ESPD with $C_5 \times C_6$ as underlying graph. The relevant parameter regions A–K of the phase plane are elucidated in Figure 6.3.*

(c) Parameter region C

FIGURE D.9 (continued): *Equilibrium state diagrams for the ESPD with $C_5 \times C_6$ as underlying graph. The relevant parameter regions A–K of the phase plane are elucidated in Figure 6.3.*

(c) Parameter region C (cont.)

FIGURE D.9 (continued): *Equilibrium state diagrams for the ESPD with $C_5 \times C_6$ as underlying graph. The relevant parameter regions A–K of the phase plane are elucidated in Figure 6.3.*

(d) Parameter region D

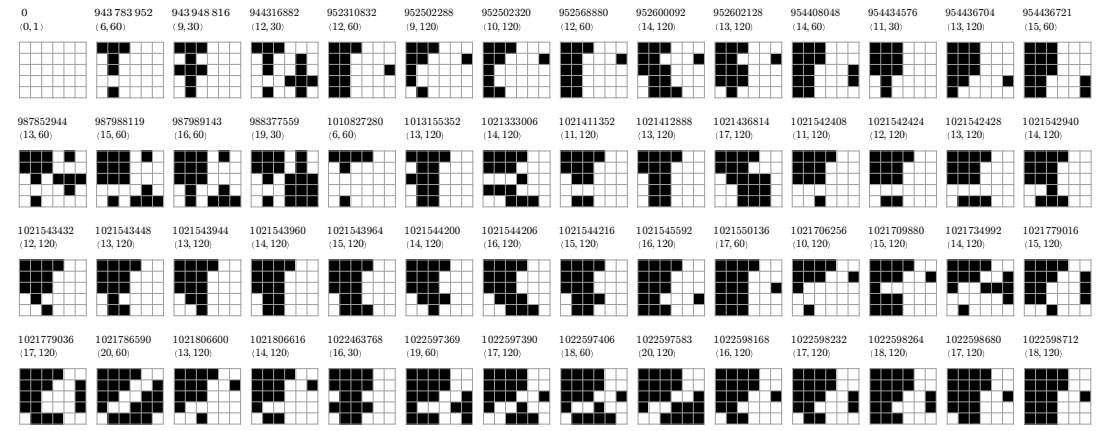

(e) Parameter region E

FIGURE D.9 (continued): *Equilibrium state diagrams for the ESPD with $C_5 \times C_6$ as underlying graph. The relevant parameter regions A–K of the phase plane are elucidated in Figure 6.3.*

(e) Parameter region E (cont.)

FIGURE D.9 (continued): *Equilibrium state diagrams for the ESPD with $C_5 \times C_6$ as underlying graph. The relevant parameter regions A–K of the phase plane are elucidated in Figure 6.3.*

(e) Parameter region E (cont.)

FIGURE D.9 (continued): *Equilibrium state diagrams for the ESPD with $C_5 \times C_6$ as underlying graph. The relevant parameter regions A–K of the phase plane are elucidated in Figure 6.3.*

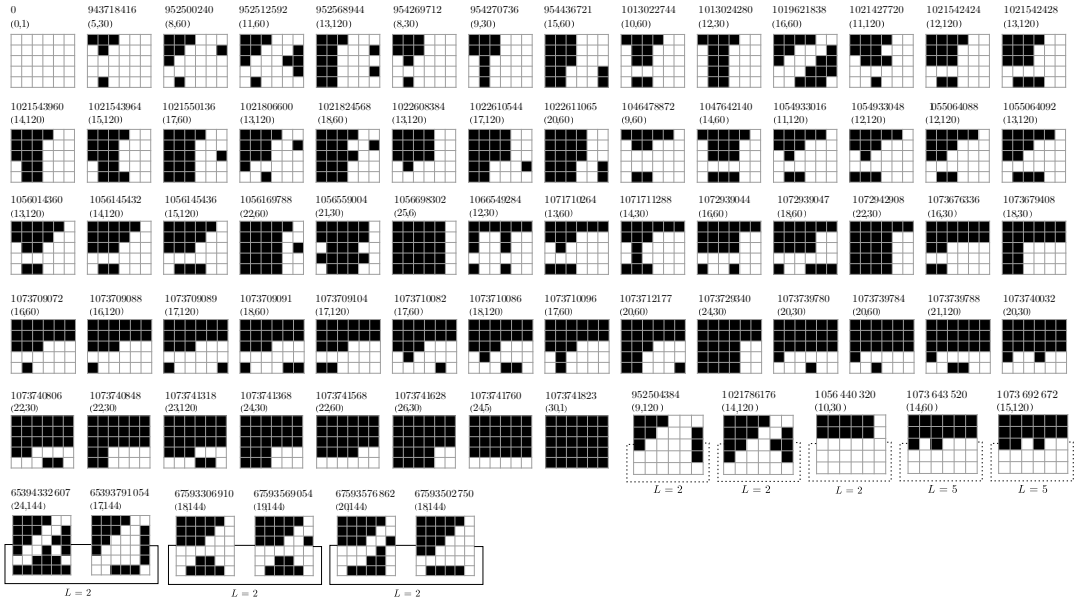

(f) Parameter region F

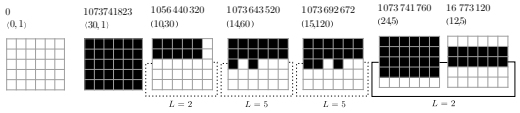

(g) Parameter region G

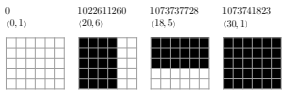

(h) Parameter region J

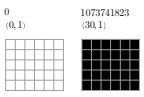

(i) Parameter region K

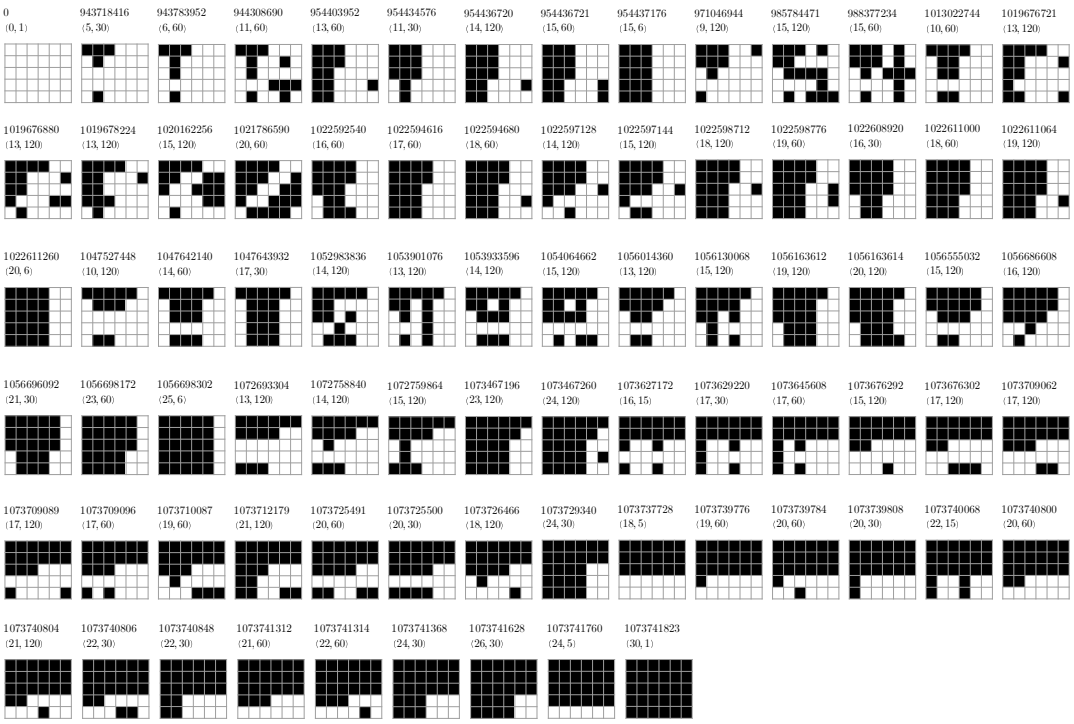

(j) Parameter region H

FIGURE D.9 (continued): *Equilibrium state diagrams for the ESPD with $C_5 \times C_6$ as underlying graph. The relevant parameter regions A–K of the phase plane are elucidated in Figure 6.3.*

(k) Parameter region I

FIGURE D.9 (continued): *Equilibrium state diagrams for the ESPD with $C_5 \times C_6$ as underlying graph. The relevant parameter regions A–K of the phase plane are elucidated in Figure 6.3.*

(k) Parameter region I (cont.)

FIGURE D.9 (continued): *Equilibrium state diagrams for the ESPD with $C_5 \times C_6$ as underlying graph. The relevant parameter regions A–K of the phase plane are elucidated in Figure 6.3.*

(a) Parameter region A

FIGURE D.10: *Equilibrium state diagrams for the ESPD with $C_6 \times C_6$ as underlying graph. The relevant parameter regions A–K of the phase plane are elucidated in Figure 6.3.*

(a) Parameter region A (cont.)

FIGURE D.10 (continued): *Equilibrium state diagrams for the ESPD with $C_6 \times C_6$ as underlying graph. The relevant parameter regions A–K of the phase plane are elucidated in Figure 6.3.*

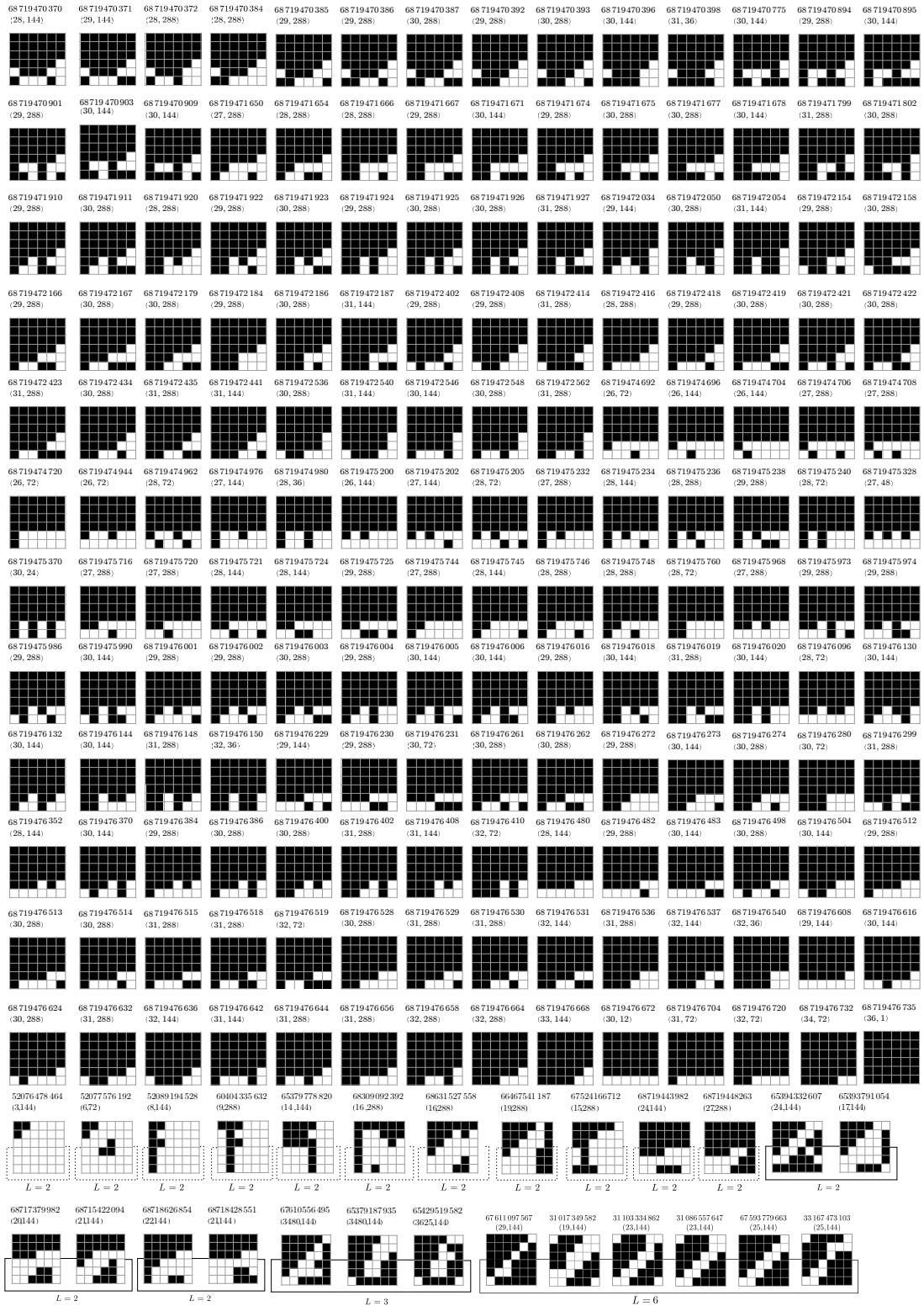

(a) Parameter region A (cont.)

FIGURE D.10 (continued): *Equilibrium state diagrams for the ESPD with $C_6 \times C_6$ as underlying graph. The relevant parameter regions A–K of the phase plane are elucidated in Figure 6.3.*

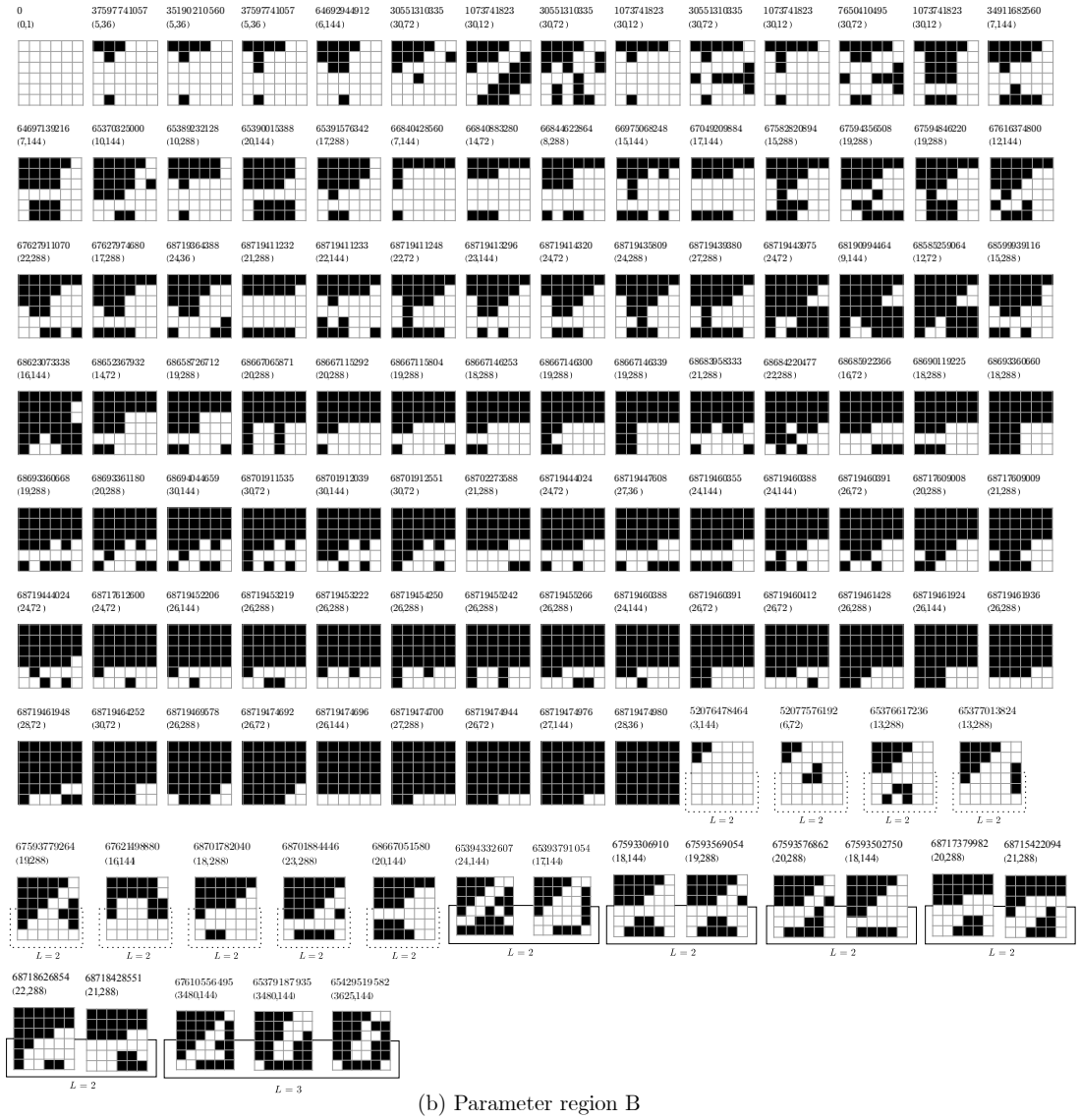

(b) Parameter region B

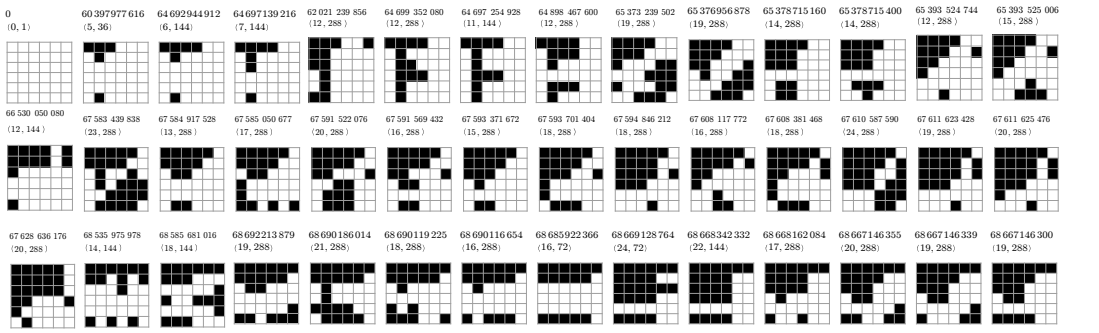

(c) Parameter region C

FIGURE D.10 (continued): *Equilibrium state diagrams for the ESPD with $C_6 \times C_6$ as underlying graph. The relevant parameter regions A–K of the phase plane are elucidated in Figure 6.3.*

(c) Parameter region C (cont.)

FIGURE D.10 (continued): *Equilibrium state diagrams for the ESPD with $C_6 \times C_6$ as underlying graph. The relevant parameter regions A–K of the phase plane are elucidated in Figure 6.3.*

(c) Parameter region C (cont.)

FIGURE D.10 (continued): *Equilibrium state diagrams for the ESPD with $C_6 \times C_6$ as underlying graph. The relevant parameter regions A–K of the phase plane are elucidated in Figure 6.3.*

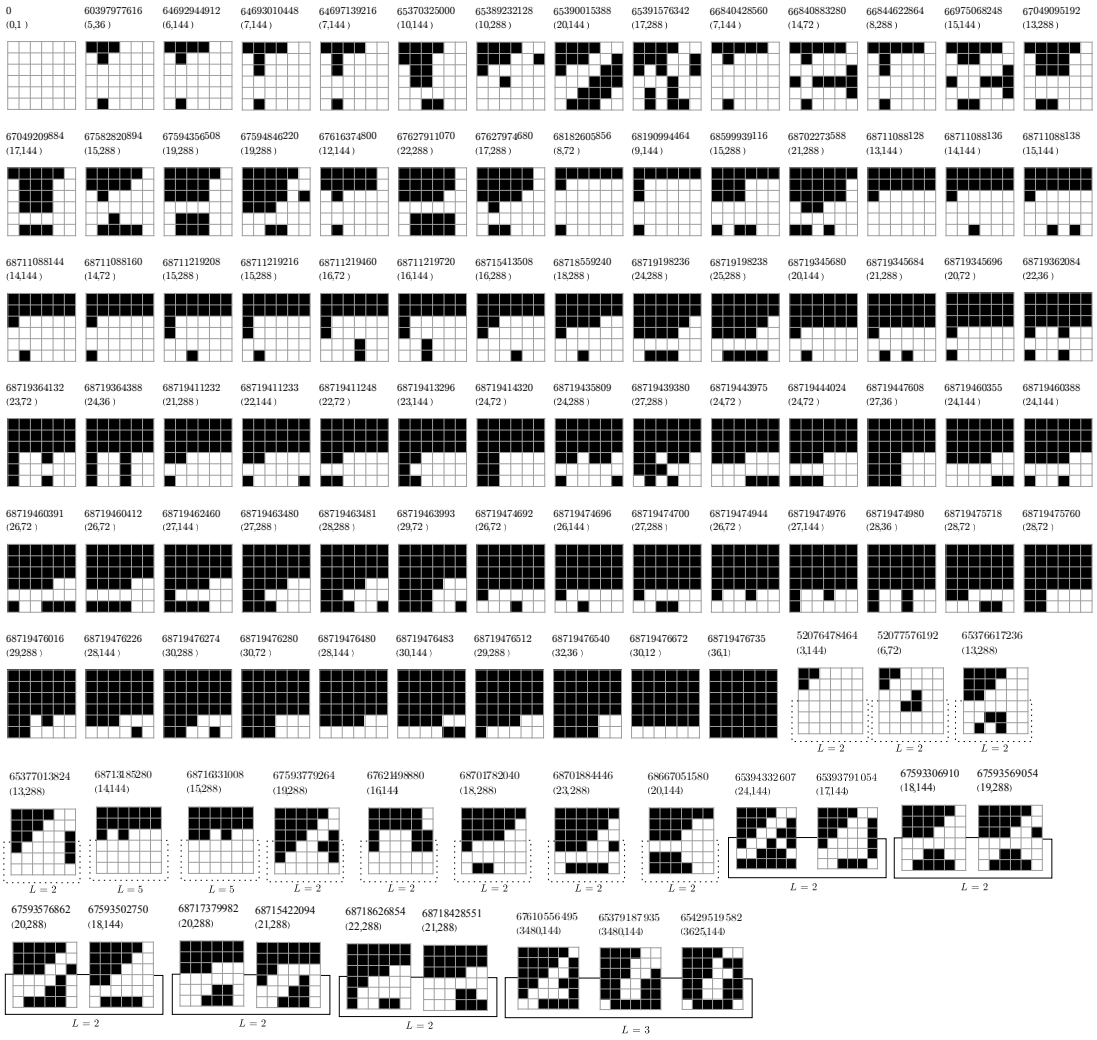

(d) Parameter region D

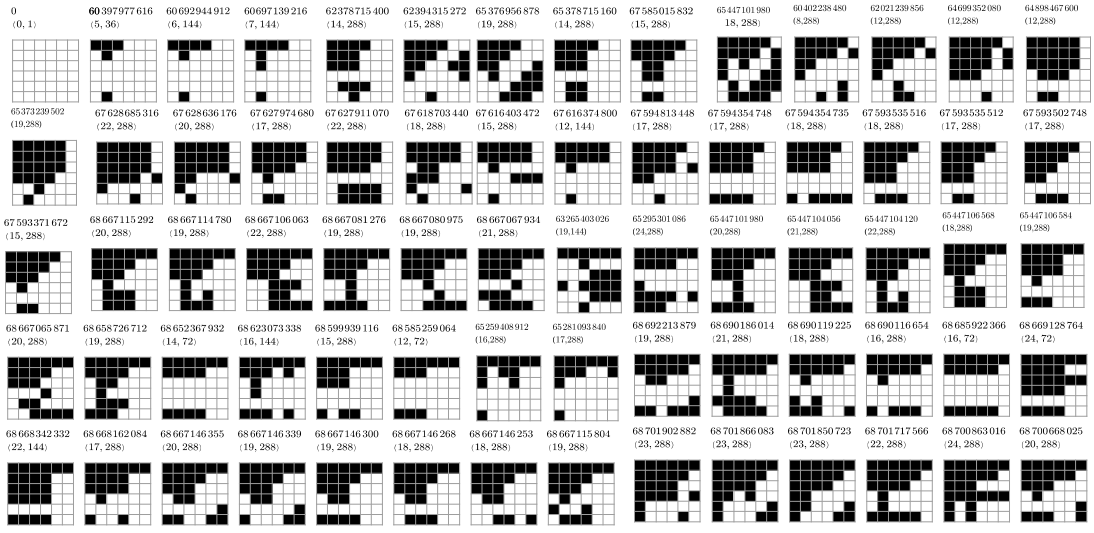

(e) Parameter region E

FIGURE D.10 (continued): *Equilibrium state diagrams for the ESPD with $C_6 \times C_6$ as underlying graph. The relevant parameter regions A–K of the phase plane are elucidated in Figure 6.3.*

(e) Parameter region E (cont.)

FIGURE D.10 (continued): *Equilibrium state diagrams for the ESPD with $C_6 \times C_6$ as underlying graph. The relevant parameter regions A–K of the phase plane are elucidated in Figure 6.3.*

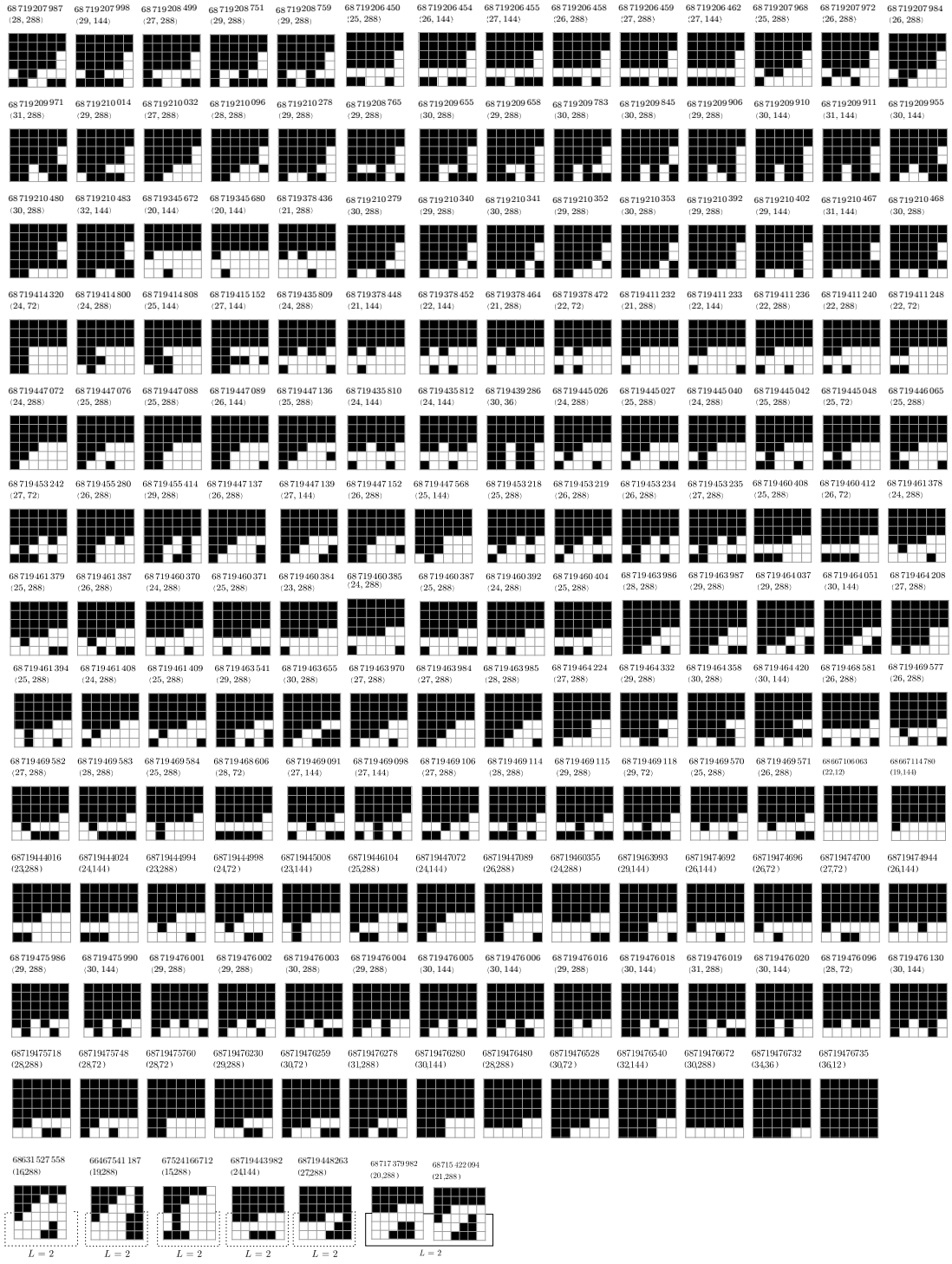

(e) Parameter region E (cont.)

FIGURE D.10 (continued): *Equilibrium state diagrams for the ESPD with $C_6 \times C_6$ as underlying graph. The relevant parameter regions A–K of the phase plane are elucidated in Figure 6.3.*

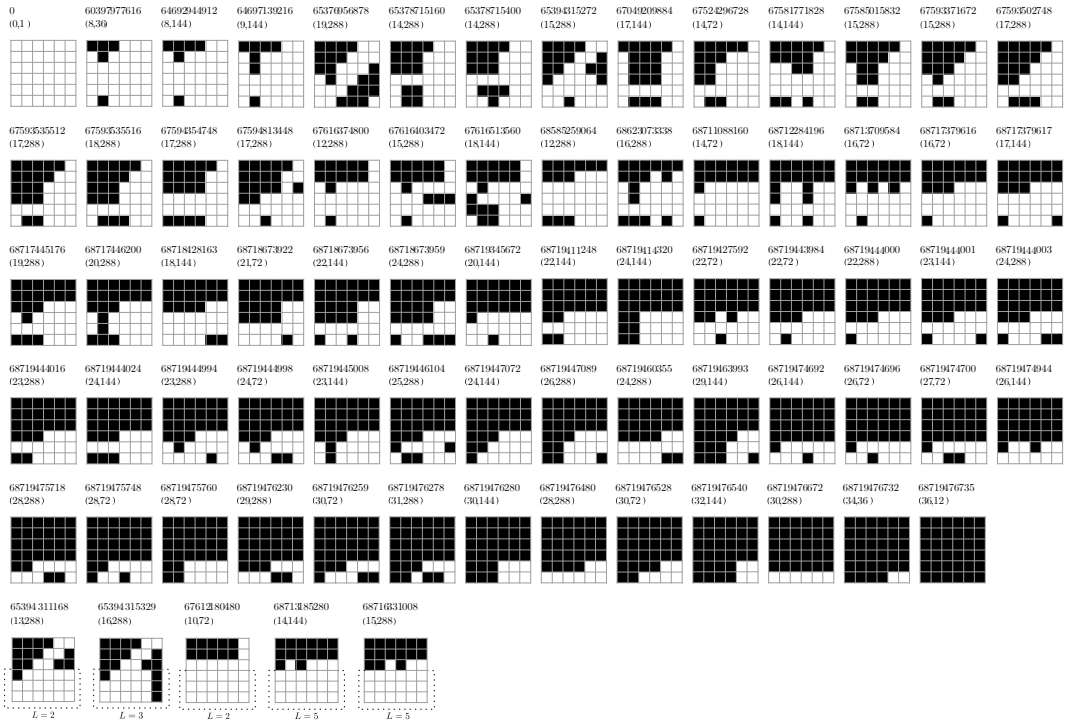

(f) Parameter region F

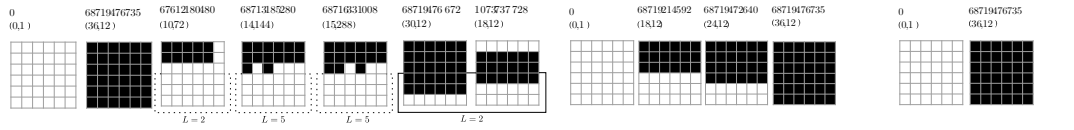

(g) Parameter region G (h) Parameter region J (i) Parameter region K

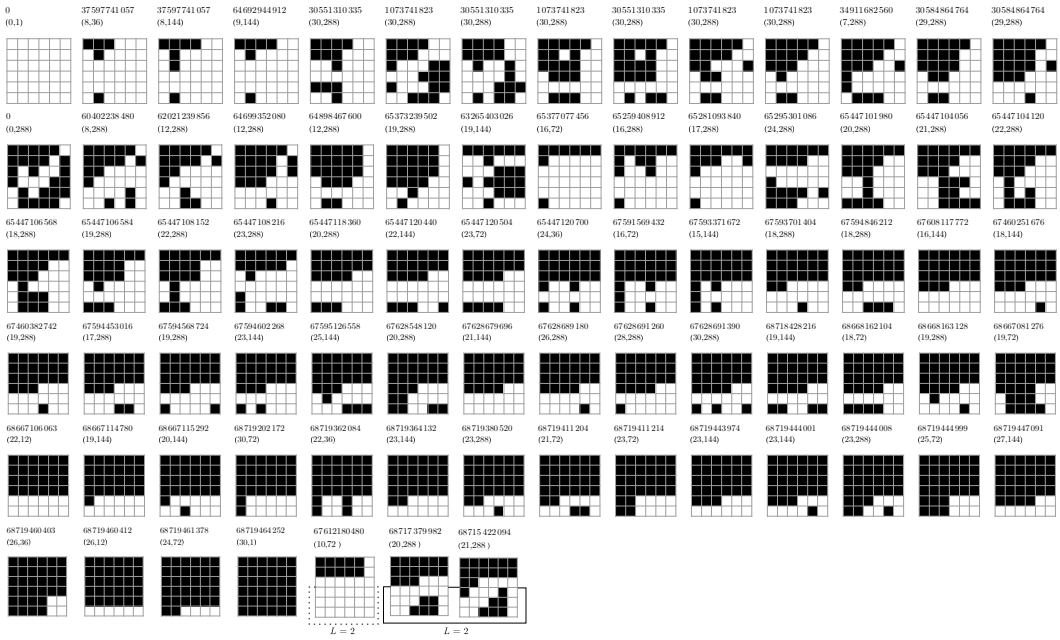

(j) Parameter region H

FIGURE D.10 (continued): *Equilibrium state diagrams for the ESPD with $C_6 \times C_6$ as underlying graph. The relevant parameter regions A–K of the phase plane are elucidated in Figure 6.3.*

(k) Parameter region I

FIGURE D.10 (continued): *Equilibrium state diagrams for the ESPD with $C_6 \times C_6$ as underlying graph. The relevant parameter regions A–K of the phase plane are elucidated in Figure 6.3.*

(k) Parameter region I (cont.)

FIGURE D.10 (continued): *Equilibrium state diagrams for the ESPD with $C_6 \times C_6$ as underlying graph. The relevant parameter regions A–K of the phase plane are elucidated in Figure 6.3.*